SJKFU

المجلة العلمية لجامعة الملك فيصل
Scientific Journal of King Faisal University

2024, 25, 2
العلوم الأساسية والتطبيقية
Basic and Applied Sciences

ISSN: 1658-0311, E-ISSN 1658-8371

In this issue
Potential of Honey Bee Propolis and Venom as Eco-friendly Control Agents in *Galleria mellonella* L.

وصف المجلة

المجلة العلمية لجامعة الملك فيصل: العلوم الأساسية والتطبيقية (ISSN: 1658-0311, E-ISSN: 1658-8371) مجلة علمية دولية محكمة، بدأ إصدارها منذ عام 1420هـ (2000م)، تصدرها جامعة الملك فيصل تحت إشراف المجلس العلمي للجامعة. تتبنى المجلة نهج الوصول المفتوح وتصدر في صورة مطبوعة وإلكترونيّة بدون تكاليف نشر. المجلة مفهرسة ضمن قاعده بيانات سكوبس (Scopus – CiteScore 2023 = 0.6). وتصدر بصورة نصف سنوية في شهريّ يونيو وديسمبر.

أول رئيس لهيئة التحرير أ.د. خالد سعد آل عبد السلام (12/4/1419هـ)، تلاه أ.د. عادل إبراهيم العفالق (12/6/1421هـ)، عقبه د. محمد سعد الوصالي (17/7/1432هـ)، وجاء بعده أ.د. غازي فيصل بسيوني (11/1/1433هـ)، وحالياً أ.د. عبدالرحمن عيسى الليلي (5/5/1441هـ).

رئيس الجامعة

عادل بن محمد أبوزناده ، جامعة الملك فيصل، السعودية

وكيل الجامعة للدراسات العليا والبحث العلمي

عبدالرحمن عيسى الليلي، جامعة الملك فيصل، السعودية

رئيس هيئة التحرير

عبدالرحمن عيسى الليلي، جامعة الملك فيصل، السعودية

نائب رئيس هيئة التحرير

بنا جويعد السبيعي، جامعة الملك فيصل، السعودية

المحررون الاستشاريون

عبدالله تاج الدين منصور علي منصور، جامعة الملك فيصل، السعودية
ديفيد إل ستولوف، جامعة ولاية كونيتيكت الشرقية، الولايات المتحدة الأمريكية
دوناتيلا بيرسيكو، المجلس الوطني للبحوث، إيطاليا
هوانسو لي، جامعة دانكوك، كوريا الجنوبية
أنطوانيلا ناجي، جامعة فاسيلي غولديس الغربية بأراد، رومانيا
كريستين باول، جامعة كاليفورنيا اللوثرية، الولايات المتحدة الأمريكية
وائل محمد أبو المكارم الديب، جامعة الملك فيصل، السعودية
محمد سانتالي، جامعة موريشيوس، موريشيوس
مايك جوي، جامعة وارويك، المملكة المتحدة
سي جون ميكر، جامعة أريزونا، الولايات المتحدة الأمريكية
بشيرة طعمة، جامعة روان، فرنسا
سام محمد، مدرسة إدارة الأعمال الدولية، هنغاريا
شاهر ربحي سعيد عليان، جامعة صحار، سلطنة عمان
فيصل قريشي، المركز الجامعي بأفلو الأغواط، الجزائر
محمود قنديل السيد قنديل، جامعة الملك فيصل، السعودية
ماريا كريستينا لوبيز دي لا مدريد، جامعة غوادالاخارا، المكسيك
نفيسة أفولاكي أديدوكون شيتو، جامعة فاونتن أوسوجبو، نيجيريا
أوبانغا سامبو، جامعة منغوليا الوطنية، منغوليا
كارولين مونتاجو، متقاعدة، المملكة المتحدة
علاء محمد صغير رفاعي، جامعة الملك فيصل، السعودية
راديم بادوسيك، جامعة أوسترافا، جمهورية التشيك
هيلين سارة فارلي ، جامعة جنوب كوينزلاند ، أستراليا
إيزابيلا إم فينتر ، جامعة ويسترن كيب ، جنوب إفريقيا
محمد علي محمد مرسي، جامعة الملك فيصل، السعودية
وصفي محمد الخزاعله، جامعة اليرموك، الأردن
سو جريجوري ، جامعة نيو إنجلاند ، أستراليا
محمد على عبداللطيف الحمادي، جامعة الملك فيصل، السعودية
جمال أحمد عباس، جامعه الكوفه، العراق
مصطفى محمد علي الحاروني، جامعة حلوان، مصر
ابراهيم محمد الفكي احمد، جامعة وادي النيل، السودان
بسام حسن زاهر، جامعة تشرين، سوريا
معن علي احمد الخطيب، جامعة فلسطين التقنية، فلسطين
عبدالرحمن صالح عبدالله الملحم، جامعة الملك فيصل، السعودية
يوسف يعقوب هلال، جامعة الموصل، العراق
منيرة سعد سلمان النويران، جامعة الملك فيصل، السعودية

مدير التحرير

الحسين حماده عبد العظيم، جامعة الملك فيصل، السعودية

مساعدو التحرير

فاضل محمد العامر، جامعة الملك فيصل، السعودية
عبد رب الأمير سلمان البوعلي، جامعة الملك فيصل، السعودية
حسين معتوق الهدلق، جامعة الملك فيصل، السعودية
إبراهيم جواد العبدالله، جامعة الملك فيصل، السعودية
صلاح عبدالعزيز المحيميد، جامعة الملك فيصل، السعودية

المراسلات العامة

رئيس هيئة التحرير، المجلة العلمية لجامعة الملك فيصل
ص. ب 400 الأحساء 31982، المملكة العربية السعودية
00966135895238، 00966135895237
scijkfu@kfu.edu.sa

Description

King Faisal University Journal: Basic and Applied Sciences (ISSN: 1658-0311, E-ISSN: 1658-8371) is an international, peer-reviewed scientific journal established in 1420 AH (2000 AD). Published by King Faisal University under the supervision of the University's Scientific Council, the journal is open access, offering both print and electronic formats with no publication fees. The journal is indexed in the Scopus database, with a CiteScore of 0.6 (2023), reflecting its commitment to quality research dissemination. It is published bi-annually, with issues released in June and December.

Prof. Khalid S. Al Abdulsalam (2000-2), Prof. Adel I. Al Afaleq (2002-14), Dr Muhammed S. Al Wasli (2014-15), Prof. Ghazi F. Basiouni (2015-2020) and Prof. Abdulrahman E. Al Lily (from 2020-present).

President of the University

Adel Mohammed Abuzenadah, King Faisal University, Saudi Arabia

Vice-Rector for Higher Studies and Scientific Research

Abdulrahman Essa Al Lily, King Faisal University, Saudi Arabia

Editor-in-Chief

Abdulrahman Essa Al Lily, King Faisal University, Saudi Arabia

Deputy Editor-in-Chief

Bana Jawid Al Subaiei, King Faisal University, Saudi Arabia

Consulting Editors

Abdallah Tageldein Mansour, King Faisal University, Saudi Arabia
David L. Stoloff, Eastern Connecticut State University, USA
Donatella Persico, National Research Council, Italy
Hwansoo Lee, Dankook University, South Korea
Antoanela Naaji, Vasile Goldis Western University of Arad, Romania
Christine Powell, California Lutheran University, USA
Wael Mohamed Abouelmakarem El-Deeb, King Faisal University, Saudi Arabia
Mohammad Santally, University of Mauritius, Mauritius
Mike Joy, University of Warwick, UK
C. June Maker, University of Arizona, USA
Bachira Tomeh, Université de Rouen, France
Sam Mohamad, International Business School (IBS), Hungary
Shaher Rebhi Said Elayyan, Sohar University, Oman
Korrichi Fayçal, University Center of Aflou Laghouat, Algeria
Mahmoud Kandeel Kandeel, King Faisal University, Saudi Arabia
María Cristina López de la Madrid, University of Guadalajara, Mexico
Nafisat Afolake Adedokun-Shittu, Fountain University Osogbo, Nigeria
Uyanga Sambuu, National University of Mongolia, Mongolia
Caroline Montagu, Retired, UK
Alaa Muhammad Sagheer Refaei, King Faisal University, Saudi Arabia
Radim Badosek, University of Ostrava, Czech Republic
Helen Sara Farley, University of Southern Queensland, Australia
Isabella M. Venter, University of the Western Cape, South Africa
Mohamed Aly Mohamed Morsy, King Faisal University, Saudi Arabia
Wasfi Mohammad Alkhazaleh, Yarmouk University, Jordan
Sue Gregory, University of New England, Australia
Mohammad Ali Alhammadi, King Faisal University, Saudi Arabia
Jamal Ahmed Abbass, University of Kufa, Iraq
Mostafa M Ali Elharony, Helwn University, Egypt
Ibrahim Mohamed Alfaki Ahmed, Nile Valley University, Sudan
Bassam Hassan Zaher, Tishreen University, Syria
Maan Ali Ahmad Alkhateeb, Palestine technical University, Palestine
Abdulrhman Saleh Almuhim, King Faisal University, Saudi Arabia
Yousif Yakoub Hilal, Mousul University, Iraq
Muneerah Saad AL Nuwairan, King Faisal University, Saudi Arabia

Managing Editor

Alhosein Hamada Abdelazeem, King Faisal University, Saudi Arabia

Editorial Assistants

Fadel Mohammad Al-Amer, King Faisal University, Saudi Arabia
Abd Rab Alameer S. Al-Boali, King Faisal University, Saudi Arabia
Husain Matouq Al-Hadlag, King Faisal University, Saudi Arabia
Ibrahim Jawad Al-Abdullah, King Faisal University, Saudi Arabia
Salah Abdulaziz Al-Mohameed, King Faisal University, Saudi Arabia

Correspondence

Editor-in-Chief, Scientific Journal of King Faisal University
P.O. Box 400 Al Ahsa, 31982, Saudi Arabia
00966135895238, 00966135895237
scijkfu@kfu.edu.sa

Table of Contents

جدول المحتويات

Scientific Journal of King Faisal University:
Basic and Applied Sciences

Study of the Nuclear Structure Properties in Strontium (^{90,92,94}Sr) Isotopes Using Nuclear Shell-model Calculations

Fatema Hameed Obeed and Ali Khalaf Hasan
Department of Physics, Faculty of Education for Girls, University of Kufa, Najaf, Iraq

LINK	RECEIVED	ACCEPTED	PUBLISHED ONLINE	ASSIGNED TO AN ISSUE
https://doi.org/10.37575/b/sci/240008	03/02/2024	14/07/2024	14/07/2024	01/12/2024
NO. OF WORDS	**NO. OF PAGES**	**YEAR**	**VOLUME**	**ISSUE**
3936	5	2024	25	2

ABSTRACT

In the current research, various nuclear properties energy spectrum, reduced electromagnetic transition probabilities, nuclear moments, and the distributions of both the nuclear charge and mass density as a function of radial distance from the nucleus center (r) were computed for^{90,92,94}Sr isotopes' using the NuShellX@MSU code. The Skyrme (SLy4) potential was utilized to compute the Strontium isotopes' wave functions with mass numbers 90, 92, and 94. By employing the Gloeckner interaction and bare G-matrix, the computed results showed good agreement with the available experimental information on the aforementioned nuclear features of all the above isotopes. Additionally, the spins and parities of energy levels were confirmed and determined in accordance with certain empirical values. Furthermore an acceptable agreement for transition strengths$B(E2; 2_1^+ \rightarrow 0_1^+)$ for ^{90,92,94}Sr , and the dipole magnetic moment of the ground state in the^{90}Sr isotope, was observed with the available experimental values. In these calculations, new values were predicted for the above nuclear properties, which had not been previously determined experimentally.

KEYWORDS:
energy spectra; gloeckner interaction; model space; nuShellX code; skyrme potential; transition strengths

CITATION
Obeed, F.H. and Hasan, A.K. (2024). Study of the nuclear structure properties in strontium (^{90,92,94}sr) isotopes using nuclear shell-model calculations. *Scientific Journal of King Faisal University: Basic and Applied Sciences*, **25**(2), 1–5. DOI:10.37575/b/sci/240008

1. Introduction

Nuclear shell-model calculations are essential for the theoretical framework used by both experimentalists and theoreticians to explain many nuclear structure properties (Salman and Hameed, 2022; Hasan *et al.*, 2021). This microscopic model of the atomic nucleus is one of the most fundamental nuclear models, presuming that nucleons occupy discrete energy levels and have specified angular momentum. In the ground state, an isotope's nucleons will be in the lowest possible energy state (Lawson, 1980). Isotopes in the mass region greater than or equal to 90 provide a rare opportunity to examine the effects of the proton subshell closure at 38 and the neutron shell closure at 50 on level arrangements. A substantial number of studies have recognized that the nuclear level arrangements in the mass region greater than or equal to 90 can be well defined within the shell-model framework. For instance, many nuclear properties of certain nuclei have been well identified within this framework. Heng et al. studied the level structure of the ^{90}Nb isotope using the NuShellX code (Heng *et al.*, 2019). N. S. Pattabiraman *et al.,* (2002) discussed the level structure of ^{92}Mo, considering proton subshell closure at 38 and neutron shell closure at 50. In their study, the configuration space included four proton orbits (from $f_{5/2}$to $g_{9/2}$) and six neutron orbits (from $p_{1/2}$ to $s_{1/2}$). Rainovski *et al.,* (2002) described the high-spin levels of the ^{90}Y nucleus, with computations carried out in the proton orbits ($0f_{5/2}$ to $0g_{9/2}$)and neutron orbits ($1p_{1/2}$,$0g_{9/2}$,$1d_{5/2}$), including an extended configuration with neutrons in the $0g_{7/2}$ orbital using Ritsschil code. The high levels of these isotopes arose from the configurations of a single $g_{9/2}$ neutron into the $d_{5/2}$ level through the neutron shell closure at 50. In particular, isotones with proton numbers equal to 38 in the mass number region of 90, 92, and 94 have been significant topics for examining the lasting interactions in shellmodel calculations and two-particle excitations.

The isotopes ^{90,92,94}Sr appear to be perfect candidates for such a study to better interpret the nuclear features of isotopes in the mass region greater than or equal to 90.

This research aims to perform shellmodel calculations using the NuShellX@MSU code to describe several nuclear properties of the ^{90,} ^{94,94}Sr isotopes.

2. Theory

Studying the transition probabilities B($E2$) can provide new and important information about the development of nuclear properties and the shell-model. The electromagnetic transition from an initial nuclear level (i), where the nucleus can be at rest, to a final nuclear level (f), results in the nucleus's momentum in state (f) and the emitted gamma ray being identical. The electromagnetic transition between them can only occur when the emitted photon carries away an amount of angular momentum (ℓ) such that $J_f = J_i + \ell$(Brown, 2005):

$$|J_i - J_f| \leq \ell \leq J_i + J_f, \quad (1)$$

Where ($J = |J|$).

The gamma transition rate is specified by E, the multipolarity(ΔE), the transition energy, and a factor that depends upon the details of the internal nuclear structure(Preetha and Kumar, 2017).The electromagnetic transition probabilities of $B(E2)$ and$B(M1)$of the transition between initial and final states J_i and J_f may be given according to the following formula (Aghahasani *et al.*, 2022; Obeed, 2021):

$$B(E2; J_i \rightarrow J_f) = \frac{e^2}{(2J_i+1)} \left|\langle J_f M_f | \hat{Q}_2 | J_i M_i \rangle\right|^2, \quad (2)$$

$$B(M1; J_i \rightarrow J_f) = \frac{{\mu_N}^2}{(2J_i+1)} \left|\langle J_f M_f | \hat{M}_1 | J_i M_i \rangle\right|^2, \quad (3)$$

where$\hat{Q}_2$and $\hat{M}_1$are operators of the nuclear moments.

Corresponding Author: Fatema Hameed Obeed 0096407817322815, fatimahh.alfatlawi@uokufa.edu.iq

Electric quadrupole moments are another essential quantity to characterize the nuclei's shapes, which are linked to the intrinsic quadrupole moments by the following relationship (Obeed, 2021):

$$Q_s(JK) = \frac{3K^2 - J(J+1)}{(2J+3).(J+1)} Q_o, \quad (4)$$

where K representsthe total angular momentum projection on the nuclear symmetry axis, J is the spin, and Q_0 is the intrinsic quadrupole moment.

Intrinsic quadrupole moments are defined according to the following relationship (Obeed and Hasan, 2021):

$$Q_o = \sqrt{\frac{16\pi}{5e^2}} . (B(E2))^{1/2}, \quad (5)$$

whereQ_s> 0 indicates the prolate deformation shape of nuclei,Q_s<0 designates the oblate deformation shape of the isotopes, and Q_s =0 indicates the spherical shape. The magnetic moments are given by the following formula (Carchidi *et al.*, 1986):

$$\mu(J=1) = \begin{bmatrix} J & 1 & J \\ -J & 0 & J \end{bmatrix} \times \frac{\sqrt{4\pi}}{3} \langle J \| \hat{O}\,(M1) \| J \rangle \mu_N, \quad (6)$$

where $\langle J \| \hat{O}\,(M1) \| J \rangle \mu_N$ represents the operator of the magnetic transition, $\mu_N = \frac{e\hbar}{2m_p c}$ =0.1051e.fm,$\mu_N$is the nuclear magnetons, and m_p is the proton mass.

Here, $\begin{bmatrix} J & 1 & J \\ -J & 0 & J \end{bmatrix}$ represents the $3j$ symbol for the angular momentum factor, the value of which is given by (Carchidi *et al.*, 1986):

$$\begin{bmatrix} J & 1 & J \\ -J & 0 & J \end{bmatrix} = \left[\frac{J(2J-1)}{(2J+1)(J+1)(2J+3)}\right]^{0.5}, \quad (7)$$

The calculations in Eq. (6) require knowing the values of the magnetic moments(g) factors: $g_l^p = 1, g_s^p = 5.585$ forprotons and $g_l^n = 0, g_s^n = -3.826$ for neutrons(Heyde and Irvine,1990).

In the calculations, the density distribution of a system containing A nucleons was calculated and given according to the following relationship (Roy and Nigam,1967):

$$\rho_o(r) = \sum_{i=1}^{A} |\varphi_i(\vec{r})|^2, \quad (8)$$

3. Results and Discussion

In this research, various nuclear characteristics of strontium isotopes (^{90,92,94}Sr) with neutrons (N = 52, 54 and 56) were calculated using the NuShellX@MSU code, which is a shell model code written by Bill Rae. This code can be used to determine the particular energies and eigenvectors of low states in shell-model Hamiltonian matrix computations, as well as the magnitude and beta decay, and radial wave functions were computed using Skyrme capabilities (SLy4) from the same code (Brown and Rae, 2014) with energetic charge nucleons and factor (g). The Gloeckner space model for the orbitals of the proton ($2p_{1/2}$, $1g_{9/2}$) and neutron ($3s_{1/2}$, $2d_{5/2}$) with the Gloeckner interaction and bare G-matrix was performed for the valence particles (two neutrons, four neutrons, and six neutrons) of the isotopes ^{90}Sr, ^{92}Sr, and ^{94}Sr, respectively, outside $^{88}_{38}$Sr, which is a closed core. Single-particle energies of a valence nucleon are represented by the values $\varepsilon_{2p1/2}(p)$=−7.124MeV, $\varepsilon_{1g9/2}(p)$=−6.248,$\varepsilon_{3s_{1l2}}(n)$ =−5.506 MeV and, $\varepsilon_{2d_{5l2}}(n)$ = −6.338 MeV. The calculations and results of each isotope are discussed in the following sections.

3.1. Energy levels:

The ***^{90}Sr isotope:*** This isotope has two neutrons scattered in orbits ($3s_{1/2}$, $2d_{5/2}$) over the $^{88}_{38}$Sr closed core. Figure 1 presents theoretical and experimental excitation spectra values for the ^{90}Sr isotope. An agreement was achieved for the ground state (0_1^+) of the calculated energy level, which was compared to the experimental energy level in the same ground state (0_1^+). An acceptable agreement was also found for theoretical energies values{0.941,1.543, 2.194, and 2.951}MeV associated with the states(total angular momentum and parity){$2_1^+, 4_1^+, 2_2^+,$ $and 0_2^+$ }, which were compared with the values of the experimental energies{ $0.831^{+4}_{-4}, 1.655^{+7}_{-7}, 1.892^{+4}_{-4}$, and $2.971^{+12}_{-12}\}$ MeV (Basu and McCutchan, 2020).Current calculations have suggested that the state associated with (3^-) with the experimental energy value 2.207^{+4}_{-4} MeV can be confirmed by the calculated theoretical state (3_1^+); this is due to the accepted agreement of the above energy value with the theoretical energy value of 2.210 MeV. It was noted that there are values of energies and their accompanying states {from 2.497±6;(2^+) to 2.927±7;4} MeV in the experimental data for which no corresponding values appeared in the calculations. The highest theoretical value for the energy2.951 MeV in the state $0_2^+$was obtained, while the experimental values are higher.

Figure1. Comparison between the calculated level energy values and the experimentaldataof the ^{90}Sr isotope(Basu and McCutchan, 2020)

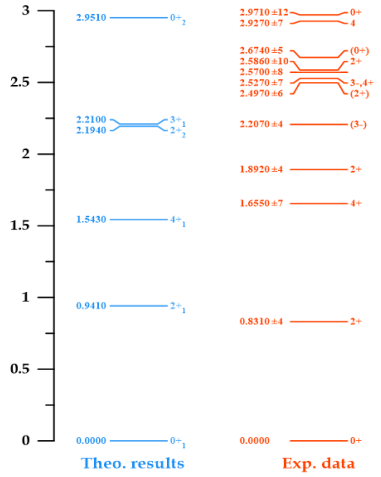

The ***^{92}Sr isotope*** has four nucleons (neutrons) dispersed in orbitals $3s_{1/2}$and $2d_{5/2}$ over the closed nucleus $^{88}_{38}$Sr. Figure 2 displays the experimental and theoretical excitation spectra values for the isotope ^{92}Sr as follows (Baglin, 2012):a complete agreement was found for the ground state(0_1^+) thatis compared to the ground state in experimental information.A certain extent of predictable agreement of theoretical energy values was also found (0.919 and 2.105)between the MeV of the states 2_1^+ and 1_1^+ and the experimental energy values($0.814^{+3}_{-3}$and 2.140^{+14}_{-14}MeV) in the same states. Through the calculated theoretical state (3_1^+), confirmation of the state associated(3^-) with the experimental energy level (2.185^{+4}_{-4} MeV) was obtained; this is due to the acceptable agreement of this level with the theoretical level(2.169MeV).A probable assertion of the spin only(4)at the experimental level value (1.673^{+4}_{-4} MeV)was found due to the acceptable compatibility of this energy value with the theoretical value(1.561MeV).The parity(+)was confirmed for the experimental energy value 1.778^{+12}_{-12} MeV associated with the spin (4), and the states($4_2^+, 0_2^+, 5_1^+$ and2^+_4)were identified .In terms of the experimental energy values($2.783^{+4}_{-4}, 2.849^{+6}_{-6}, 2.924^{+7}_{-7}$, and 3.014^{+6}_{-6}) these energies were compatible to an acceptable extent with the theoretical energy's values of 2.830, 2.871, 3.002, and 3.213MeV.New theoretical energy levels(2.179and 3.444 MeV)of the states 2_3^+ and 4^+_3were predicted in these calculations but still have no experimental energy value for comparison with. There are empirical energy values that have recently been observed: (1.384^{+9}_{-9} ,2^+), (2.053^{+6}_{-6}, (2^+), (2.088^{+17}_{-17} ,$0^{(+)}$), (2.527^{+4}_{-4}, 0^+), (2.765^{+5}_{-5}, (5^-)),

(2.783^{+4}_{-4},...),(2.820^{+18}_{-18},2(⁺),(1)),(3.128^{+7}_{-7},(6⁺)), and (3.558^{+7}_{-7},(6-,7-))which have no assessment with theoretical energies values. Through the current study, it was observed that the highest value of the theoretical energy was3.444MeV with the state 4^+_3, while higher values have been observed experimentally.

Figure2. Comparison between the calculated level energy values and the experimental data of the ^{92}Sr isotope (Baglin, 2012)

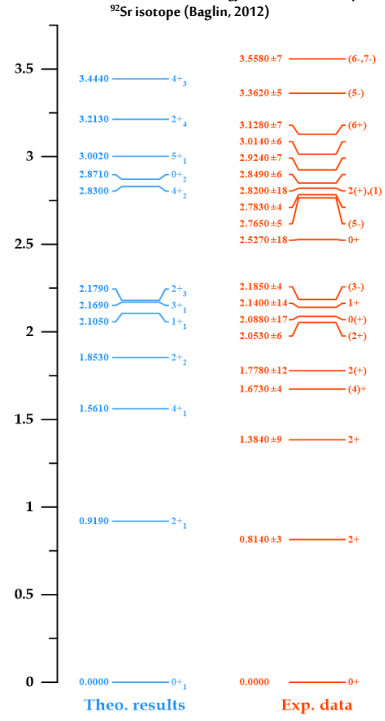

The***^{94}Sr isotope***: This isotope has six nucleons (neutrons) dispersed in the orbits $3s_{1/2}$, $2d_{5/2}$ over the $^{88}_{38}$Sr closed core. Figure 3 presents the theoretical and experimental excitation spectra values for the^{94}Sr isotope(Negretand and Sonzogni, 2011).Here , theoretically, the calculated energy level and its ground state(0^+_1) were in complete agreement with the experimental ground state(0^+), and there was a predictable confirmation of the states(3^-),(2^+), and (4^-) for experimental energy levels (1.926^{+14}_{-14}, 2.271^{+16}_{-16} and 2.603^{+14}_{-14}MeV).There was a largely appropriate agreement between these energies and the theoretical energies values (1.889 ,2.237and2.572 MeV). There are empirical energy values with the state (2.146^{+14}_{-14}, 4^+, and 2.414^{+18}_{-18}, (3^-)MeV)that have recently been observed and have no corresponding theoretical values.

Figure 3. Comparative between the calculated level energy values and the experimental data of the ^{94}Sr isotope (Negret and Sonzogni, 2011)

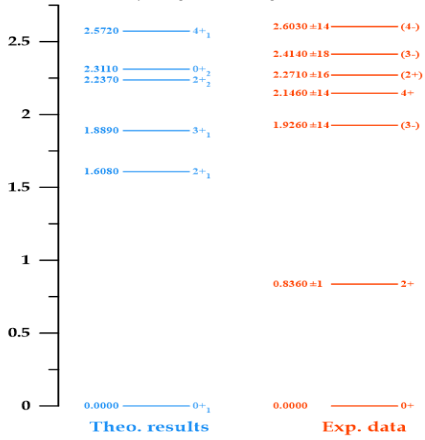

3.2. Electromagnetic transition probabilities B(E2), B(M1):

The results of electric quadrupole transition probabilities were calculated by selecting the effective nucleon charges of protons and neutrons as follows: (e_p=1.830e,e_n=1.66e),(e_p=1.772e ,e_n=1.544e), and (e_p=1.655e,e_n=1.31e),while the parameter values meters of the orbital and spin nucleon(g) factors $g_s(p)$, $g_s(n)$, $g_l(p)$ and $g_l(n)$were equal to(5.027, −3.443, 1.671, 0.671), (5.027 , −3.443, 1.02,0.02), and(5.027,−3.443,1.0), which , in turn, were used to correspondingly calculate the dipole magnetic *B(M1)* for^{90,92,94}Sr isotopes. The calculated values of reduced electromagnetic transition possibilities are listed in Tables 1, 2, and 3 for^{90,92,94}Sr isotopes. These tables display the *E2* and *M1* transition for the ^{90}Sr isotope. The computed *B(E2)* transition possibilities were in good agreement with the experimental data(Basu and McCutchan, 2020),specifically for the strong(*E2*)decays from 2^+_1 state to 0^+_1 stateat the value $B(E2;2^+_1 \rightarrow 0^+_1) = 203.6\pm^{33}_{19} e^2fm^4$, which perfectly agreed with the experimental data$(E2;2^+_1 \rightarrow 0^+_1) = 204.2\ e^2fm^4$. The calculated value for the*E2* and*M1*transition strength values$B(E2;3^+_1 \rightarrow 2^+_1) = 32.3e^2fm^4$ and $6.163 \times 10^{-2}\mu_N^2$ with transition strengths of $B(E2;3^+_1 \rightarrow 4^+_1) = 306.9e^2fm^4$ were not clearly categorized in the experimental data (*E1, M2,E1*) for the corresponding values.

In these calculations, the transition strength was predicted for *E2, M1*, and *E2*.The transition strengths *E2* and*M1* for the ^{92}Sr isotope are listed in Table2.This comparison displays that the calculated values in this study of the transition possibilities agreed with the empirical formation(Baglin, 2012), especially the(*E2*)transition strengths $B(E2;2^+_1 \rightarrow 0^+_1)$= 197.6 e^2fm^4 with the experimental value 197.3 $\pm\ ^3_3 e^2fm^4$ .In the calculations for*E2* and *M1*transition strengths of $1^+_1 \rightarrow 2^+_1$ of the values302.4 e^2fm^4 and5.13×10^{-2} μ_N^2 were found in comparison to the experimental values of $0.740\pm16\ e^2fm^4$ and$0.125\times10^{-2}\pm3\ \mu_N^2$ respectively. Lastly, Table 3 presents the comparison of the experimental (Negret and Sonzogni, 2011) and calculated (*E2* and *M1*) transition strength values for the ^{94}Sr isotope. These comparisons clarified that theforetold*E2* transition strength from $2^+_1 \rightarrow 0^+_1$; 203.8 e^2fm^4 well agreed with the experimental value $203.1 \pm\ ^4_4 e^2fm^4$.*E2*values and *M1*transition strengths were calculated for the transitions ($3^+_1 \rightarrow 2^+_1$ and $4^+_1 \rightarrow 3^+_1$) that created the values $9.498\times10^{12}\ e^2fm^4$, 0.521 μ_N^2, and $49.3e^2fm^4$. These values were unverified in multi-polarity(*E1* and *E1+M2*)in experimental data, but recent calculations have predicted*E2,M1, and E2*transition strengths. Anew electromagnetic transition of several *B(E2,↓)*and *B(M1,↓)*of ^{90,92,94}Sr isotopes was observed (as shown in Tables 1, 2, and 3), where there were no observations in the experimental data. More information on the theoretical knowledge of all isotopes regarding energy levels and electromagnetic transitions will be added.

Table 1. Theoretical comparison between the values of the electromagnetic transition probabilities for positive-parity spin states in the^{90}Sr isotope and empirical values (Basu and McCutchan, 2020).

$J_i \rightarrow J_f$	Theoretical Results			Experimental Results	
	$(BE2\downarrow)(e^2fm^4)$	$(BM1\downarrow)(\mu_N^2)$	multi-polarity	$(BE2\downarrow)(e^2fm^4)$	$(BM1\downarrow)(\mu_N^2)$
$2^+_1 \rightarrow 0^+_1$	204.2	-----	E2	$203.6\pm^{33}_{19}$	-----
$4^+_1 \rightarrow 2^+_1$	159.3	-----	E2	$124.5\pm^{11}_{7}$	-----
$3^+_1 \rightarrow 2^+_1$	32.36	6.163×10^{-2}	(E1,(M2))	$>2.87\times10^{-3}$	-----
$3^+_1 \rightarrow 4^+_1$	306.9	-----	(E1)	$>198.8\times10^{-5}$	-----

Table 2. Theoretical comparison between the electromagnetic transition probabilities for positive-parity spin states in the^{92}Sr isotope and experimental data (Baglin,2012)

$J_i \rightarrow J_f$	Theoretical Results		Experimental Results		
	$(BE2\downarrow)(e^2fm^4)$	$(BM1\downarrow)(\mu_N^2)$	multi-polarity	$(BE2\downarrow)(e^2fm^4)$	$(BM1\downarrow)(\mu_N^2)$
$2^+_1 \rightarrow 0^+_1$	197.6	-----	E2	$197.3\pm^{3}_{3}$	-----
$4^+_1 \rightarrow 2^+_1$	57.51	-----	E2	-----	-----
$1^+_1 \rightarrow 2^+_1$	302.4	5.13×10^{-2}	E2+M1	$0.740\pm^{16}_{16}$	$0.125\times10^{-2}\pm^{3}_{3}$
$3^+_1 \rightarrow 2^+_1$	37.72	3.49×10^{-2}	-----	-----	-----
$3^+_1 \rightarrow 4^+_1$	40.56	-----	-----	-----	-----
$3^+_1 \rightarrow 1^+_1$	41.04	-----	-----	-----	-----
$5^+_1 \rightarrow 4^+_1$	156.3	0.1584×10^{-2}	-----	-----	-----
$5^+_1 \rightarrow 3^+_1$	129.3	-----	-----	-----	-----

Table 3. Theoretical comparison between the electromagnetic transition probabilities for positive-parity spin states in the ^{94}Sr isotope and experimental data (Negret and Sonzogni, 2011)

$J_i \rightarrow J_f$	Theoretical Results		Experimental Results		
	$(BE2\downarrow)(e^2fm^4)$	$(BM1\downarrow)(\mu_N^2)$	multi-polarity	$(BE2\downarrow)(e^2fm^4)$	$(BM1\downarrow)(\mu_N^2)$
$2_1^+ \rightarrow 0_1^+$	203.8	-----	E2	$203.1 \pm \frac{4}{4}$	-----
$3_1^+ \rightarrow 2_1^+$	9.498×10^{-2}	0.5212	(E1)	-----	-----
$4_1^+ \rightarrow 2_1^+$	137.5	-----	E2	-----	-----
$4_1^+ \rightarrow 3_1^+$	149.3	-----	(M1+E2)	-----	-----

3.3. Electric quadrupole and magnetic dipole moments:

Nuclear shape is a fundamental property of the nucleus that describes nuclear structure and many nuclear properties. The current research contains the nuclear moments (Q_s) and (μ) of ^{90,92,94}Sr isotopes, which were calculated and are shown in Table4.The electric quadrupole moment was calculated for all isotopes using shell-model calculations, but there are, yet no observations in the experimental data. Through these calculations, it was observed that the quadrupole electrical moment of the ^{90}Sr isotope at the2_1^+, 4_1^+, and3_1^+states, as well as the states2_1^+, 3_1^+, and5_1^+in the ^{92}Sr isotope exhibited negative signs representing the dominance of the oblate shape. Moreover, the state 4_1^+in the ^{92}Sr isotope and the 2_1^+, 4_1^+, and3_1^+states of the ^{94}Sr isotope appeared with positive marks representing the prolate shape dominance of these states. Table 4 shows the calculated results of dipole magnetic (μ) moments of the ^{90}Sr isotope. This indicated that the $2_1^+$and 4_1^+states had values of 0.241μ_N and −0.608μ_N, which were predicted in reasonable agreement with the experimental data(Basu and McCutchan,2020) :−0.24 $\pm \frac{22}{22}\mu_N$ and −0.08 $\pm \frac{68}{68}\mu_N$ ofthe $2_1^+$and 4_1^+ states, respectively. In this study, the calculations yielded many values of dipole magnetic (μ) moments of ^{90,92,94}Sr isotopes, such as $(3_1^+, -2.102)\ \mu_N$ for the^{90}Sr isotope(2_1^+,-1.365) ,(4_1^+,-2.689),(3_1^+,-3.403),(1_1^+,-0.02) and (5_1^+,4.749) (μ_N) for the^{92}Sr isotope. Finally, 2_1^+ , 3_1^+, and 4_1^+ for the ^{94}Sr isotope were underestimated empirically, with values of −0.743, −3.443, and −2.754, respectively.

Table 4. Theoretical comparison between the values of the nuclear moments in ^{90,92,94}Srisotopes and empirical data using GI model space.

Isotopes	Theoretical Results			Experimental Results	
	J_i^π	(Q) (efm2) Sky29	$\mu(\mu_N)$	(Q) (efm2)	$\mu(\mu_N)$
^{90}Sr	2_1^+	−0.35	−0.241	-----	$-0.24\pm\frac{22}{22}$ (Basu and McCutchan, 2020)
	4_1^+	−21.05	−0.608	-----	$-0.08\pm\frac{68}{68}$ (Basu and McCutchan, 2020)
	3_1^+	−26.31	−2.102	-----	-----
^{92}Sr	2_1^+	−24.15	−1.365	-----	-----
	4_1^+	18.75	−2.689	-----	-----
	3_1^+	−1.57	−3.403	-----	-----
	1_1^+	0	0.02		
	5_1^+	−4.37	−4.749	-----	-----
^{94}Sr	2_1^+	28.81	−0.743	-----	-----
	3_1^+	20.86	−3.443	-----	-----
	4_1^+	16.68	−2.754	-----	-----

Q_i=2_1^+, 4_1^+, 3_1^+, 5_1^+

3.4. Density distributions of charge and mass in nuclei:

The nuclear charge and mass density distributions of ^{90,92,94}Sr isotopes were calculated and are shown in Figures 4, 5, and 6, respectively. These figures illustrate charge density distribution values of ^{90,92,94}Sr isotopes, which were centered at the nucleus midpoint with values of ρ_{ch}= {0.07981, 0.08165, and 0.08358} Ze/fm^{-3}remaining stable at the specified distance r=0.1fm. These values for^{90,92,94}Sr isotopes continued to decrease until they stabilized at zero at a distance r=7.9 fm. The mass density distribution in ^{90,92,94}Sr isotopes were in the nuclei midpoint at the value ρ_m= {0.1614,0.1642, and 0.1670} nuclei/fm^{-3}. These values remained stable at r = 0.1 fm. However, at a distance of r =0.2fm, these values increased to 0.1617,0.1645, and 0.1673 nuclei/fm^{-3}.These values continued to progressively increase up to the radial distancer =1.3,1.4, and 1.5 fm at the values0.1684,0.1718, and 0.1752 nuclei/fm^{-3}for ^{90,92,94}Sr isotopes, respectively. Subsequently, the mass density distributions of the studied isotopes started to decrease at distances of 1.4,1.5, and 1.6 fm, reaching values of 0.1683, 0.1716, and 0.1750nuclei/fm^{-3} for the ^{90,92,94}Sr isotopes. These values continued to decrease until stabilizing at zero at a radial distance of r = 7.9 fm for all isotopes under observation in the current study. There is, as yet, no experimental data for the distributions of the nuclear density of charge and mass for^{90,92,94}Sr isotopes for comparison with the present calculations.

Figure4. Density distributions of nuclear charge and mass as a function ofradial distance from the midpoint of the ^{90}Sr isotope

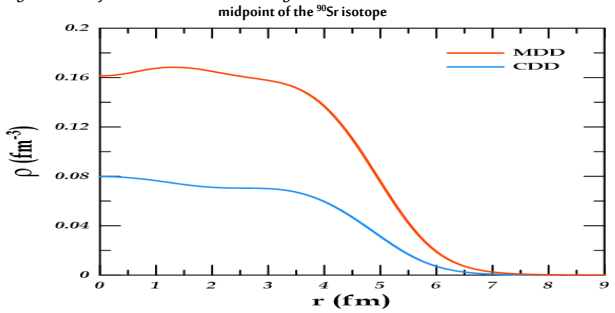

Figure 5. Density distributions of nuclear charge and mass contrary tothe radial distance from the center of the ^{92}Sr isotope

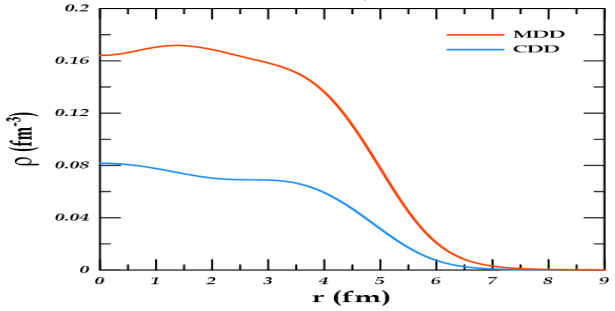

Figure6.Density distributions of nuclear charge and mass in contrast to the radial distance from the center of the ^{94}Sr isotope

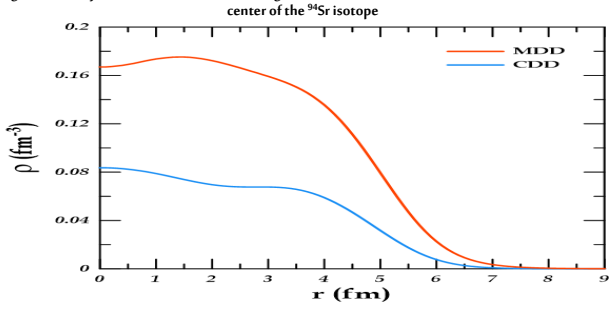

4. Conclusions

From the calculated results, the following can be concluded:

- Absolute agreement was observed between theoretical and experimental energy values, particularly for the ground state levels of ^{90,92,94}Sr isotopes.
- A positive parity of the ^{92}Sr isotopes was confirmed for one level of the empirical energy value.
- The states (total angular momentum and valence) of some levels in the ^{92}Sr isotope were determined for undetermined experimental energy levels.
- There was a strong agreement between the calculated quadrupole transitions and empirical data, especially evident in $B(E2\,; 2_1^+ \rightarrow 0_1^+)$of the ^{90,92,94}Sr isotopes.
- The current calculations revealed the electric quadrupole and dipole magnetic moments. It was predicted that the ground band energy states exhibit an oblate shape for^{90,92}Sr isotopes, except for one level in the ^{92}Sr isotope, which has a prolate shape. The shape of the^{94}Sr

isotope is expected to be prolate, which led to the conclusion that the shape of some regions of the nuclear striatum is affected by structural influences and could change from one isotope to another neighbor. In addition, it was found that the shape changes with the number of neutrons and can also change with the excitation energy or state within the same nucleus. These variances occur due to the rearrangement of the structure space of the valance particles or to the dynamic response.

- Density distributions for charge and mass in the isotopes $^{90.92,\ 94}$Sr were identified; the density distributions were found to be in the nucleus center for (Ze/fm^{-3}) and $\rho_0(\frac{nucleon}{fm^{-3}})$ and started decreasing until fixed at zero at specific values. In contrast to the charge density distributions, the mass density distributions showed contradictory behavior, starting to increase to certain values and decreasing until they stabilized at zero at certain values of radial distance.
- The Gl interaction and the Gl model space were used to calculate the aforementioned nuclear properties of the ^{90,92,94}Sr isotopes.

Biographies

Fatema Hameed Obeed

Department of Physics, Faculty of Education for Girls, University of Kufa, Najaf, Iraq, 0096407817322815, fatimahh.alfatlawi@uokufa.edu.iq

Prof. Obeed is an Iraqi who earned her master's degree in nuclear physics from Kufa University in Iraq in 2010. She achieved the title of professor in nuclear physics in 2022. Her primary research interests include theoretical studies in nuclear physics focusing on nuclear structure using Fortran and MATLAB programming codes. She has received training in teaching methods and computer education. Dr. Obeed has actively participated in numerous local and international scientific conferences and has published ten research papers in scientific journals indexed within the Scopus platform.

ORCID: 0000-0003-2076-0376.

Ali Khalaf Hasan

Department of Physics, Faculty of Education for Girls, University of Kufa, Najaf, Iraq, 0096407802461719, alikh.alsinayyid@uokufa.edu.iq

Prof. Hasan is an Iraqi who earned his Ph.D. in nuclear physics from the University of Basra, Iraq, in 2009. His primary research interests encompass quantum, theoretical, nuclear, and radiation physics. Dr. Hasan has actively participated in numerous local scientific conferences in Iraq. He has published approximately 50 papers in scientific journals within Iraq, including 23 papers in international Scopus-indexed journals such as the International Journal of Physical Sciences, Ukrainian Journal of Physics, International Journal of Current Research, and AIP Conference Proceedings.

ORCID: 0000-0002-8126-5179

References

Aghahasani, H., Mohammadi, S. and Sajjadi, Z. (2022). Study of high spin phenomena in even-even dysprosium isotopes by using projected shell model. *Iranian Journal of Physics Research*, **22**(3),141–51. DOI: 10.47176/ijpr.22.3.71276

Baglin, C.M. (2012). Nuclear data sheets for A=92. *Nuclear Data Sheets*,**113**(n/a), 2187–389. DOI: 10.1016/j.nds.2012.10.001

Basu, S.K. and McCutchan, E.A. (2020). Nuclear data sheets for A=90. *Nuclear Data Sheets*,**165**(n/a), 1–329. DOI: 10.1016/ j.nds .2020.04.001

Brown, B.A. (2005). *Lecture Notes in Nuclear Structure Physics National Super Conducting Cyclotron Laboratory and Department of Physics and Astronomy.* Michigan state university, USA: E Lansing, MI, 48824, 290.

Brown, B.A. and Rae, W.D.M. (2014). The shell model code nushellx@msu. *Nuclear Data Sheets*, **120**(n/a), 115–8. DOI: 10.1016/j .nds .2014.07.022.

Carchidi, M., Wildenthal, B.H. and Brown, B.A. (1986). Quadrupole moments of sd-shell nuclei. *Physical Review C*, **34**(6), 2280–97. DOI: 10.1103/PhysRevC.34.2280

Hasan, A.K., Obeed, F.H. and Rahim, A.N. (2021). Study of the electric quadrupole transitions in 50-51 Mn isotopes by using f742pn and f7cdpn interactions. *The Scientific Journal of King Faisal University: Basic and Applied Sciences,* **22**(2), 11–5. DOI: 10.37575/b/sci/0070

Heng, W.Y., Yang, D., Yan, M.K. and Wei, L.P. (2019). Investigation of the level structure of 90Nb nucleus using the shell-model. *Nukleonika*, **64**(4), 113–6. DOI: 10.2478/nuka-2019-0014

Heyde, K.L.G. and Irvine, J.M. (1990). *The Nuclear Shell-model.* Berlin, Heidelberg, Germany: Springer.

Lawson, R.D. (1980). *Theory of the Nuclear Shell-model.* Oxford, United Kingdom: Clarendon Press.

Negretand, A. and Sonzogni, A.A. (2011). Adopted levels, gammas for94sr isotope. *Nuclear Data Sheets*, **6**(n/a), n/a.

Obeed, F.H. (2021). Calculation of nuclear properties for 56–62Fe isotopes in the model space ho. *Ukrainian Journal of Physics,* **66**(8),643–52. DOI: 10.15407/ujpe66.8.643

Obeed, F.H. and Hasan, A.K. (2021). Calculation of quadrupole deformation parameter(β_2) from reduced transition probability B(E2)↑for transition ($0_1^+ \rightarrow 2_1^+$)at even-even 62-68zn isotopes. *Nuclear Physics and Atomic Energy*, **1**(22), 30–41. DOI: 10.15407/jnpae2021.01.030

Pattabiraman, N. S., Chintalapudi, S. N., Ghugre, S. S., Rao, B. T., Raju, M. L. N., Reddy, T. S. and Jain, H. C. (2002). Level structure of 92 Mo at high angular momentum: Evidence for Z= 38, N= 50 core excitation. *Physical Review C*, **65**(4), 044324. DOI:10 .11 03/Phys Rev C.65.044324

Preetha, P. and Kumar, S.S. (2017). Reduced transition probability B(E2) in even-even Ti isotopes. In: *62nd DAE-BRNS Symposium on Nuclear Physics*. Thapar University, Patiala, India, 20–24 /12/2017.

Rainovski, G., Schwengner, R., Schilling, K. D., Wagner, A., Jungclaus, A., Galindo, E. and Kröll, T. (2002). High-spin structure of the spherical nucleus 90 Y. *Physical Review C*, **65**(4), 044327. DOI: 10.1103 /PhysRevC.65.044327.

Roy, R. and Nigam, B. (1967). *Nuclear Physics. Theory and Experiment.* Hoboken, Jersey, New York: John Wiley and Sons Inc.

Salman, A.D. and Hameed, S.M. (2022). Study the nuclear structure of 6Li nuclei with the calculation of a large basis shell-model. In: *AIP Conference Proceedings, 3rd International Scientific Conference of Alkafeel University*. Alkafeel University, Najaf, Iraq, 22–23/3/2021.

Scientific Journal of King Faisal University:
Basic and Applied Sciences

Effects of Brassica Rapa on Dyslipidaemia and Oxidative Damage in Rats Consuming a Hyperlipidic Diet

Fatima Zohra El kadi[1], Karima Ould Yerou[2] and Hadj Mostefa Khelladi[3]

[1] Department of Biology, Faculty of Natural Sciences and Life, Djillali Liabés University, Sidi-Bel-Abbés, Algeria
[2] Department of Biology, Faculty of Sciences; Mustapha Stambouli University, Mascara, Algeria
[3] Department of Biology, Faculty of Natural Sciences and Life, Oran 1 Ahmed Benbella University, Oran, Algeria

LINK	RECEIVED	ACCEPTED	PUBLISHED ONLINE	ASSIGNED TO AN ISSUE
https://doi.org/10.37575/b/sci/230076	12/12/2023	03/08/2024	03/08/2024	01/12/2024
NO. OF WORDS	**NO. OF PAGES**	**YEAR**	**VOLUME**	**ISSUE**
3887	5	2024	25	2

ABSTRACT

This research investigated the influence of a hyperlipidic diet in Wistar rats and the therapeutic effect of Brassica rapa powder (BrP). A hyperlipidic diet was administered followed by oral supplementation of BrP (5%) for 28 days. The BrP supplementation caused a decrease in weight (- 41%), glycaemia (-12%), creatinemia (-51%), aspartate aminotransferase (AST) level (-80%), and cholesterolaemia (-25%) associated with an increase in HDLc level (+59%). However, the hepatic lipid profile showed a decrease in phospholipids (PL) (-59%) and total cholesterol (TC) (-67%). In addition, oxidative stress assessment showed a decrease in the serum (-22%), renal (-30%) and adipose (-8%) levels of TBARS. Furthermore, BrP supplementation boosted glutathione (GSH) protective activity in adipose tissue with a maximum of +49%. In conclusion, Brassica rapa enhances the serum and tissue balance of metabolic and antioxidant status.

KEYWORDS
Antioxidant, biomarkers, fat, in vivo, redox status, turnip

CITATION
El kadi, F.Z., Ould Yerou, K and Khelladi, H.M. (2024). Effects of Brassica rapa on dyslipidaemia and oxidative damage in rats consuming a hyperlipidic diet. *Scientific Journal of King Faisal University: Basic and Applied Sciences*, **25**(2), 6–10. DOI: 10.37575/b/sci/230076

1. Introduction

Hypercholesterolaemia is a disorder characterized by abnormal cholesterol secretion and absorption into the blood, which can lead to a variety of diseases, such as inflammation, atherosclerosis, renal failure, non-insulin-dependent diabetes, and aging (Kim *et al.*, 2014). Biomolecules with hypocholesterolaemic and phytotherapeutic potential are of great interest to the health community who can prevent and treat dyslipidaemic disorders, because the medical prescription of certain hypolipidaemic medicines, such as statins and fibrates, can cause many side effects or intolerances (Jung *et al.*, 2008). The enzymatic antioxidant defence is also compromised by hyperlipidaemia, namely the activities of glutathione peroxidase (GSH-Px), catalase (CAT), and superoxide dismutase (SOD). Analogously, hyperlipidaemia may have a cause in the redox imbalance. Similarly, antioxidants may be able to prevent the development of hyperlipidaemia by correcting the early events that lead to redox imbalance. The species *Brassica rapa* (Br) or "turnip" is an excellent source of antioxidants and secondary metabolites (Yerou *et al.*, 2022). This plant species has many therapeutic properties, including inhibition of oxidative stress, induction of detoxification enzymes, reduction of cancer cell proliferation, inhibition of carcinogenic mutations, protection of the human body against free radicals, treatment of hepatitis, jaundice, furuncle and sore throat, and it also has immunostimulant and anti-diabetic effects (Kapusta-Duch *et al.*, 2012). These biological functions are due to the abundance of various bioactive substances, including phenylpropanoid derivatives, sterol glucosides (glucosinolates), flavonoids (glycosides of isorhamnetin, kaempferol, and quercetin), and indole alkaloids. Also, due to the synergistic action of glucosinolates, polyphenols, and triterpenes, considered the main complexes in cruciferous, and the most studied regarding its structure, mechanism of action and the effects in human cells (Šamec and Salopek-Sondi, 2019). Several researchers have highlighted the impact of Brassicaceae on cardiovascular pathologies (including hypertension and stroke) and dyslipidaemia (Raiola *et al.*, 2018), obesity (López- Chillón *et al.*, 2019), metabolic syndrome (Al-Snafi, 2015), type 2 diabetes (Chen *et al.*, 2018), osteoporosis (Dias, 2019), cancer (Thomas-Charles and Fennell, 2019), and antimicrobial (reduced microbial colonization), anti-inflammatory, antifungal, anti-parasitic, and antiviral activities (Ramirez *et al.*, 2020). In light of this data, this research aims to study the effects of a hyperlipidic (atherogenic) diet induced in vivo and the action of Brassica powder (BrP) supplementation by estimating blood metabolic and redox status.

2. Materials and Methods

2.1. Plant Matter:

The edible portion of *Brassica rapa* (Br), also known as turnip and frequently consumed by Algerians, was considered when selecting the plant. The fresh Br rhizome was obtained in November 2022 from the Ghriss local market, which is 19 km from the Mascara province in Western Algeria (latitude: 35°23'47.90"N, longitude: 0° 08' 24.97" E). Br rhizomes were prepared in the laboratory and then dried for an entire day at 38°C. Following drying, the plant material was ground into a powder to produce *Brassica rapa* powder (BrP), which was then stored for later use in hermetic glass containers.

2.2. Experimental Design:

The general recommendations for using live animals in scientific research by the Pasteur Institute, Algiers, were followed; likewise, Mustapha Stambouli University approved all the experimental procedures used in this study. The experiment was conducted on 30 male *Wistar* rats, weighing approximately 200±10g at two months of age. Table 1 shows the distribution of animal groups (n = 10) and the constituents of the standard and experimental diets. *Ad libitum* access to food and water was provided, and the protocols for the care and handling of laboratory animals were followed. In animal husbandry, the following standards were maintained: ambient temperature of 24°C, relative humidity of 60%, and 12 light: 12 dark hours. The body weight (Bw) of the animals was recorded once a

Corresponding Author: Fatima Zohra El kadi 00213(0)5 57463123, elkadifatimazohra@yahoo.fr

week for 28 days, and their food intake was recorded every day.

Table 1: Composition of the standard and experimental diets (g/kg)

Composition	Standard diet	Experimental diet	
	CG	HFD	HFD-BrP (5%)
CAS	200	200	200
Sucrose	50	50	50
Corn starch	590	340	340
Cellulose	50	50	50
Vitamin mix	20	20	20
Mineral mix	40	40	40
Lipids (olive, nut, sunflower)	50	-	-
Lamb fat	-	300	300
BrP	-	-	50

CG: control group; HFD: High Fat Diet; HFD-BrP: High-Fat Diet supplemented with 5% of BrP

After a 12-hour fast on the 28th day of the experiment, the rats in each group were weighed and anesthetized via an intraperitoneal injection of a chloral solution (10%) at a rate of 3 ml/kg of Bw. An aortic puncture was conducted to obtain blood samples, which were then centrifuged at 1000 rpm for 20 min at 4°C (Sigma, 4K10 Bioblock Scientific, Germany). The serums were preserved in EDTA-Na2 (0.1%) (Merck, Germany). After twice successively washing and centrifuging the remaining pellet containing erythrocytes at 4000 rpm for 20 minutes at 4°C using NaCl (0.9%) (Merck, Germany), the cells were lysed by adding ice-cold water, incubated for 15 minutes in ice, and then recentrifuged. Kidneys, heart, liver, and adipose tissue were obtained, washed with an ice-cold NaCl (0.9%) solution, dried, and weighed; each organ was portioned and preserved at -80°C. All samples were stored until analysis.

2.3. Serum and Hepatic Biochemical Assays:

At sacrifice, a glucometer was used to measure the fasting blood glucose. Transaminase serums were estimated by the method of Reitman and Frankel (1957) using the Spinreact kit (Spain), serum total protein (Burtis and Ashwood, 1994) and serum albumin (Tietz et al., 1990) using the Chronolab kit (Switzerland). For the lipid balance, the Spinreact kit (Spain) was used: serum triglycerides (TG) (Burtis and Ashwood, 1994), serum total cholesterol (TC) (Richmond, 1973), and serum high-density lipoprotein (HDLc) (Lopes-Virella et al., 1977). The Friedwal formula was used to determine the serum low-density lipoprotein (LDLc): LDLc = TC- HDLc-(TG/5), serum creatinine (Schirmeister, 1964) and serum urea (Fawcett and Scott, 1960) using the Human kit (Germany), and serum uric acid (Friedewald et al., 1972) using the Biocon kit (Germany). All analyses were performed following the instructions of the kit supplier. A cold extraction of lipids on 1 g of sample was conducted in the presence of a chloroform/methanol mixture (Biochem chemopharma, UK), (4/1, V/V). The lipid extract was removed from the solvents under vacuum evaporation at 48°C (Büchi rotary evaporator, Germany). The total lipids were taken up in 10 ml of isopropanol for the analysis of various lipid fractions (Delsal, 1944). According to an enzymatic colorimetric method, total cholesterol (TC), triglycerides (TG) (Kit Spinreact, Girona Spain) and phospholipids (PL) (Kit Cypress, Belgium) were determined.

2.4. Oxidative Stress Status:

The method of Quintanilha et al. (1982) was used to determine the serum TBARS levels. First, 100 µl of the sample was diluted in 0.9 ml of NaCl (0.9%). After that, 20 µl of 2% butyl-hydroxy toluene (BHT) (Sigma-Aldrich Chemie, Germany) and 1 ml of TBA (15% TCA and 0.375% TBA in 0.5N HCl) were incorporated into this solution. Following 30 minutes of incubation at 100°C and ice cooling, the samples were centrifuged at 4000 x g for 10 minutes at 4°C. The measurement was made at 532 nm using spectrophotometry, and the results were presented as mmol/ml of serum. The protocol of Okawa et al. (1979) was followed to estimate the lipoperoxidation of the liver, heart, kidneys, and adipose tissue. We crushed 100 mg of tissue in 0.9 ml of 1.15% KCL. Likewise, 1.5 ml of acetic acid (20%, pH 3.5), 1.5 ml of tissue homogenate, 0.2 ml of a solution containing SDS (8.1%), and 1.5 ml of TBA (0.8%) constitute the reaction medium. After adding 4 ml of distilled water to adjust the final volume, the mixture was vortexed for 30 seconds and heated to 95°C for 1 hour. After adding 1 ml of distilled water and 5 ml of butanol, the tubes were agitated and centrifuged at 1000 x g for 10 minutes. Expressed as mmol/g tissue, the reading was obtained at 532 nm. The procedure described by Sedlak and Lindsay (1968) was used to analyse the reduced glutathione (GSH) in the tissue and erythrocyte samples. After preparing the homogenate in 0.1 M phosphate buffer (pH 6), 400 µl of cold distilled water, 100 µl of TCA 50%, and 500 µl of the sample (tissue homogenate, erythrocyte lysate) were mixed. After shaking, each sample was centrifuged at 1200 x g for 15 minutes. After centrifugation, 500 µl of supernatant was mixed with 100 µl of 0.01 M DTNB (5,5'-dithiobis (2-nitrobenzoic acid) and 400 µl of 0.4 M Tris buffer (pH 8.9). The absorbance at 412 nm was measured after 5 minutes of incubation. For erythrocytes and tissues, the results were expressed in µmol/ml and µmol/g, respectively.

2.5. Statistical Analysis:

Mean ± Standard Error (M±SE) with (n = 6) was used to express the results. In order to compare the means, students' tests were used (Statistica software, version 4.1, Statsoft, Tulsa, Oklahoma, USA), [a]CG vs HFD; [b]CG vs. HFD+BrP; [c] HFD vs HFD+BrP.

3. Results

3.1. Body and Organ Weight:

During the 28 days of experimentation, the two groups (CG and HFD) showed weight gain of 65.25 gr and 75.25 gr, respectively; however, after 28 days, we noted a stability in the weight of the HFD+BrP group with weight decreases of -41% and -27% comparatively with HFD ($p < 0.001$) and CG ($p < 0.01$), respectively (see Table 2).

Table 2: Weight evolution of experimental and control rats

Group	Day 0	Day 7	Day 14	Day 21	Day 28
CG	160.25±27	188.375±29	202.06±25^{a**}	215.5±20^{a**}	225.5±21^{a**,b**}
HFD	200.25±20	228.38±25	252.06±32 ^{a**,c**}	265.50±19^{a**,c**}	275.50±23^{a**,c***}
HFD +BrP	199.67±29	198.67±24	192.83±15^{c**}	198.67±21^{c**}	164.00±24^{c***,b**}

CG: Control group; HFD: High-fat diet; HFD-Br: High-fat diet supplemented with 5% of BrP; * $p < 0.05$; ** $p < 0.01$; *** $p < 0.001$.

The relative weight of the target organs is similar in all groups of rats (see Figure 1); the difference between the groups is statistically insignificant ($p > 0.05$).

Figure 1: Relative weights of organs of experimental and control rats

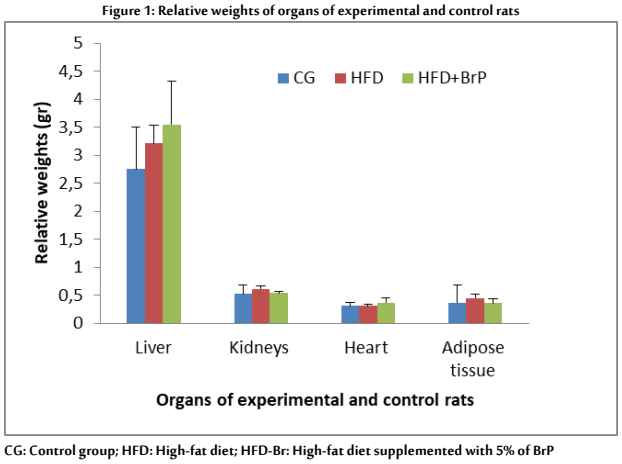

CG: Control group; HFD: High-fat diet; HFD-Br: High-fat diet supplemented with 5% of BrP

3.2. Serum and Hepatic Biochemistry:

The hyperlipidic diet caused hyperglycaemia, hyperuraemia, and hypercreatinemia with an augmentation in AST serum. In addition, a

disorder in the lipid profile was detected. BrP supplementation showed the following corrective actions: hypoglycaemia (-12%), hypocreatinemia (-51%), a strong decrease in AST serum level (-80%), hypochlesterolaemia (-25%), all of which are associated with an elevation in the HDLc serum level (+59%) (see Table 3).

Table 3: Effect of BrP on serum glucose, kidney/liver biomarkers and lipid profile following 28 days of oral exposure of hyperlipidaemic rats

Parameters	CG	HFD	HFD+ BrP
Blood glucose (mg/dl)	258.69±31^{a**}	345.48±17.5 ^{a**,c*}	305.40±11.8^{c*}
Kidney biomarkers			
Urea (mg/dl)	7.21±0.91^{b*}	6.82±0,81^{c*}	5.31±1.29 ^{b*,c*}
Creatinine (mg/dl)	0.64±0.31^{a**}	1.24±0.76 ^{a*,c*}	0.60±0.27^{c*}
Uric acid (mg/dl)	4.58±1.4	6.67±2.5	6.10±1.8
Liver biomarkers			
Total proteins (g/dl)	7.23±2	7.66±0.81	8.55±1.44
Albumin (g/dl)	2.35±0.96	2.92±0,36	2.94±0.72
AST (UI/l)	106.8±29 ^{a**,b**}	256.7±11.9 ^{a**,c***}	50.8±12 ^{b**,c***}
ALT (UI/l)	67.81±29	83.42±39	70.00±31
Lipid profile			
TG (mmol /L)	1.66 ±0.07^{b}	1.14 ± 0.04 ^{c}	0.65 ± 0.02^{b*,c*}
TC (mmol /L)	1.41 ± 0.41^{a}	2.54 ± 0.64^{a**,c*}	1.89 ±0.53^{c}
HDLc (mmol /L)	0.78±0.33^{a*}	0.35 ±0.13^{a*,c**}	0.84 ± 0.33^{c**}
LDLc (mmol /L)	1.22 ±0.60	1.64 ±0.13	1.47 ±0.63

CG: Control group; HFD: High-fat diet; HFD-Br: High-fat diet supplemented with 5% of BrP; AST: Aspartate aminotransferase; ALT: Alanine aminotransferase; TC: Total cholesterol; TG: Triglycerides; HDLc: High-density lipoprotein cholesterol; LDLc: Low-density lipoprotein cholesterol; * p < 0.05; ** p < 0.01; *** p < 0.01

The hepatic concentrations of PL, TC, and TG increased significantly in the HFD group, according to our findings. However, we also noticed that PL (-59%) and TC (-67%) levels decreased significantly in the BrP supplementation group compared to the HFD group (see Figure 2).

Figure 2: Effect of BrP on the hepatic lipid profile following 28 days of oral exposure in hyperlipidaemic rats

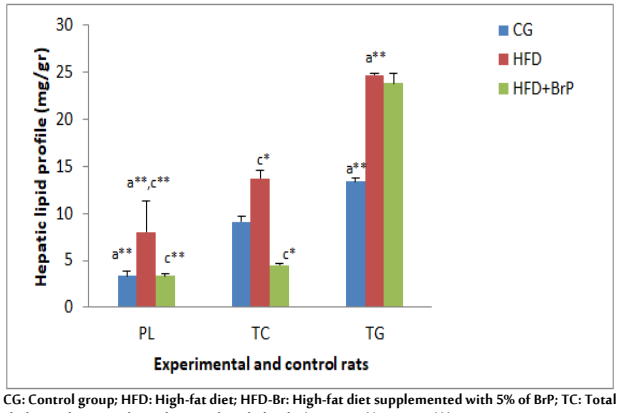

CG: Control group; HFD: High-fat diet; HFD-Br: High-fat diet supplemented with 5% of BrP; TC: Total cholesterol; TG: Triglycerides; PL: Phospholipids; * p < 0.05; ** p < 0.01; *** p < 0.001

3.3. Serum, Erythrocyte and Tissue Oxidative Stress Biomarkers:

According to the results in Table 4, the hyperlipidic diet caused a significant increase of TBARS in serum (+29%, p < 0.05) and renal tissue (+43%, p < 0.01) compared to HFD+BrP. Also, in adipocytes compared to CG (+32%, p < 0.01) and HFD+BrP (+9%, p < 0.05), the protective action of BrP decreased the amount of TBARS in serum (-22%, p < 0.05), renal (-30%, p < 0.01) and adipose tissue (-8%, p < 0.05) compared to HFD. In addition, BrP supplementation enhanced GSH protective activity in adipose, with an increase of +35% (p < 0.05) and +49% (p < 0.05) compared with HFD and CG, respectively.

Table 4: Effect of BrP on serum, erythrocyte and tissue oxidative stress biomarkers following 28 days of oral exposure in hyperlipidaemic rats

Parameters	CG	HFD	HFD+ BrP
Serum TBARS (µmol/l)	**5.7±0.9**	**6.7±1.9 ^{c*}**	**5.2± 0.6c***
Tissue TBARS (µmol/gr)			
Liver	115.38±24.43	131.05±18.5	114.67±24
Heart	86.16±10.06	90.33±4.9	95.07±28
Kidneys	116.08±37.1	121±22.3^{c**}	84.75±32.1^{c**}
Adipose tissue	113.30±9.89^{a**}	149.54±29.7 ^{a**,c*}	137.53±42.4^{c*}
Erythrocytic GSH (µmol/l)	0.58±0.12	0.66±0.35	0.70±0.29
Tissue GSH (µmol/l)			
Liver	49.72±9.87	50.15±6.51	48.04±1.82
Heart	51.22±1.18	60.88±3.04	66.56±2.50
Kidneys	53.38±2.45	59.63±1.53	59.21±1.77
Adipose tissue	52,88±7.77^{b*}	58.28±2.58^{c*}	78.71±1.340 ^{b*,c*}

CG: Control group; HFD: High-fat diet; HFD-Br: High-fat diet supplemented with 5% of BrP; TBARS: thiobarbituric acid reactive substances; GSH: Reduced glutathione; * p < 0.05; ** p < 0.01; *** p < 0.001

4. Discussion

The hyperlipidic diet in animals decreases the rate of satiety, induces increased weight gain, stimulates lipogenesis in visceral adipose tissue, and causes insulin resistance and lipid abnormalities. In this work, BrP supplementation appeared to decrease and stabilize the body weight of the animals. This indicates that BrP has a satiety effect that may boost the β3-adrenergic receptor in β3-AR-dependent lipolysis and limit the formation of lipids in fatty tissue cells (An *et al.*, 2010). In addition, a significant weight reduction was detected in the rats with fructose-induced metabolic syndrome supplemented with a hydroalcoholic extract of Br (400 mg/kg/day), with an elevation in hepatic glycogen concentration, compared to the reference group (metformin, 10 mg/kg/day) (Abo-youssef and Mohammed, 2013). The hyperglycaemia observed in our study following a hyperlipidic diet was due to a decrease in insulin excretion by the pancreas accompanied by polyuria and glycosuria (Ghasemi *et al.*, 2014), whose pathogenesis is characterized by insulin resistance, pancreatic β-cell dysfunction and apoptosis. In this context, the quantity and quality of dietary fat can modify glucose tolerance and insulin sensitivity. A high fat content in the diet leads to the deterioration of glucose tolerance through a number of mechanisms, including reduced insulin receptor binding, impaired glucose transport through reduced expression of transporter 4 (GLUT4), reduced glycogen synthase levels, and accumulation of triglycerides in skeletal muscle. The fatty acid composition of the diet influences the composition of tissue phospholipids, which can be linked to insulin action by altering membrane fluidity and insulin signalling. In addition, saturated fatty acids increase hepatic triglycerides, insulin resistance and harmful ceramides. Thus, it has been reported that the consumption of saturated fatty acids (SFAs) leads to a risk of developing type 2 diabetes (Micha and Mozaffarian, 2010). This increase of glycaemia was corrected by the administration of 5% BrP, which is in agreement with numerous studies confirming the antihyperglycemic effect of BrP in diabetic rats, as Br can boost insulin secretion and block intestinal glucose absorption (Amrita-Bhowmik *et al.*, 2009). Our data supports the pathogenic role of dyslipidaemia in the apparition and development of renal disease, which is explained by an increase in creatinine serum. According to Hattori *et al.* (1999), a high-fat diet causes an infiltration of macrophages in the kidneys, which leads to glomerulosclerosis. Administration of BrP normalized the creatinine level in hyperlipidic rats. This is consequent of the richness of Brassicaceae by anthocyanins, antioxidants and free radical scavengers.

A perturbation in liver enzyme activity is possibly an indication of liver injury or damage. However, triglyceride accumulation inside hepatocytes caused lipotoxicity due to oxidative stress inside the hepatocytes (Lim *et al.*, 2012). This correlates with our study in which an augmentation in AST was noted. BrP treatment caused a reduction in liver enzyme activity, which could be attributed to its ability to balance lipoperoxidation and cure lysed cells.

This investigation confirms the development of a lipid profile perturbation characterized by elevated triglyceride serum levels and total cholesterol and decreased HDLc. However, HDL prevents LDL from oxidation and prevents the development of atherosclerosis. Nevertheless, the hyperglycaemia previously detected in rats can causes HDL glycation and damages its protective functions, which can lead to atherosclerosis genesis. BrP administration improves metabolic disorder by inducing HDLc synthesis and blocking key enzymes of cholesterol and triglyceride synthesis because the high presence of flavonoids (quercetin), glucosinolates and coumarins actively participate to reduce hepatic fat and triglyceride levels (Soliman *et al.*, 2016).

Lipoperoxidation mainly attacks polyunsaturated fatty acids (PUFAs) of the biological membrane and perturbs the biological function of membrane proteins via receptor inactivation and protease enzyme activation, leading to an alteration in membrane permeability with cellular damage. Likewise, hyperglycaemia causes lipoperoxidation by stimulating the glycation and polyol pathways, which leads to the strong generation of free radicals. Our findings support previous research in rats with metabolic syndrome and diabetics treated with BrP, which shows that HFD elevates serum and tissue (renal and adipose) levels of TBARS, while treatment with BrP diminishes TBAR levels (Feillet-Coudray *et al.*, 2009). Moreover, Kim et al. (2006) reported that Br hydroalcoholic extract minimizes the damage caused by oxidative stress. The mechanism for these corrective actions can be attributed to quercetin, which is known to reduce TBAR levels via free radical-scavenging, inhibiting oxidative degradation, and metal-chelating. Furthermore, Brassica's antiradical activity is associated with the presence of a high concentration of secondary metabolites that can scavenge singlet and triplet oxygen or decomposing peroxides, which neutralize reactive oxygen species (ROS) (Fresco *et al.*, 2010). The natural non-enzymatic antioxidant system relies largely on glutathione, which protects cells from oxidative damage. The enzyme glutathione peroxidase functions primarily as a reducing agent and helps remove hydrogen peroxide. Our research confirms an enhancement of GSH activity in adipose tissue in the BrP-supplemented group, confirming the antiradical activity of BrP. Our results are consistent with those of Abo-youssef and Mohammed (2013), who confirmed an augmentation of GSH in rats with metabolic syndrome and treated with 70% ethanolic extract of Br.

Furthermore, this research has classic limitations. Due to the short duration of the study, it would be desirable to extend the duration of the investigation (subchronic exposure, more than 3 months). The route of administration by gavage for each animal would give greater exactitude and more reliability. The size of the sample was small; therefore, increasing the number of groups and doses will permit reproducibility. Finally, for a better understanding of the therapeutic effect of BrP, it would be preferable to study other parameters such as target organ histophysiology, rat neurobehavior and other biomarkers of oxidative stress.

5. Conclusion

Our results show that the hyperlipidic diet caused obesity and metabolic abnormalities associated with renal and adipose lipoperoxidation in the hyperlipidic rats. Moreover, these perturbations were corrected by *Brassica rapa* powder supplementation (significant antihyperglycaemic, antihyperlipidaemic, renoprotective, hepatoprotective and defensive effects). *Brassica rapa* contains promising molecules for the prevention and potentialisation of treatments for metabolic pathologies (obesity, diabetes, dyslipidaemia). In conclusion, these favourable biological actions associated with *Brassica rapa* in attenuating metabolic and oxidative disorders induced by a hyperlipidic diet may represent an interesting advance in the search for new therapeutic agents against this dyslipidaemia. We strongly suggest introducing *Brassica rapa* into the diet of patients with metabolic disorders as a food or dietary complement. Finally, we would like to point out that these results can only be extrapolated to humans after long-term studies on several animal species.

6. Acknowledgements

The authors would like to thank the Scientific Research Deanship, Department of Biology, Faculty of Sciences, Mustapha Stambouli University, Mascara, Algeria. Moreover, the authors express their appreciation to all the members of project No: D00L01UN220120230002.

Biographies

Fatima Zohra El kadi

Department of Biology, Faculty of Natural Sciences and Life, Djillali Liabés University, Sidi-Bel-Abbés, Algeria, 002135 57463123, elkadifatimazohra@yahoo.fr

El kadi is an Algerian associate professor, who received her Ph. D. from Djillali Liabes University, Algeria, in 2014. She has more than 20 international publications in indexed journals. Her research interests include oxidative status *in vivo*, bioactivity and pathology, phytopharmaceutical fields, and food toxicology. She is part of a national team focused on the concept of natural product valorisation and is a member of the International Journal of Minor Fruits, Medicinal and Aromatic plants.

ORCID: 0000-0002-9671-8505

Karima Ould Yerou

Department of Biology, Faculty of Sciences, Mustapha Stambouli University, Mascara, Algeria, +213(0) 663971364, ouldyeroukarima@gmail.com

Ould Yerou is an Algerian associate professor, who received her Ph. D. from Mustapha Stambouli University, Mascara, Algeria, in 2016. She has more than 10 international publications in indexed journals. Her research focuses on the different interactions between intestinal flora and the immune system, animal and human nutrition, food toxicology, immunochemical techniques, medicinal plants, oxidative stress, and biomolecules. She is a member of the national team focused on the natural product valorisation concept.

ORCID: 0000-0003-0124-4640

Hadj Mostefa Khelladi

Department of Biology, Faculty of Natural Sciences and Life, Oran 1 Ahmed Benbella University, Oran, Algeria, +213(0) 5 59224974, khmbiologie@gmail.com

Khelladi is an Algerian associate professor, who obtained his doctorate from the university of Oran 1 Ahmed Benbella, Algeria, in 2019. He has more than six international publications in indexed journals. His research interests include the *in vitro* and *in vivo* evaluation of bioactive compounds on nutrition-related pathologies such as high blood pressure and diabetes. He is a member of the Algerian Nutrition Society, which publishes original studies related to diet, nutrition and food sciences.

ORCID: 0000-0002-0092-4591

References

Abo-youssef, A.M. and Mohammed, R. (2013). Effects of Brassica rapa on fructose-induced metabolic syndrome in rats: a comparative study. *International Journal of Pharmaceutical Sciences Review and Research*, **21**(1), 1–5.

Al-Snafi, A.E. (2015). Therapeutic properties of medicinal plants: a review of their detoxification capacity and protective effects (part 1). *Asian Journal of Pharmaceutical Science and Technology*, **5**(4), 257–270.

Amrita-Bhowmik, A.B., Khan, L.A., Masfida Akhter, M.A. and Begum Rokeya, B.R. (2009). Studies on the antidiabetic effects of Mangifera indica stem-barks and leaves on nondiabetic, type 1 and type 2 diabetic model rats. Bangladesh Journal Pharmacol, **4**(2), 110–114. DOI:10.3329/bjp.v4i2.2488

An, S., Han, J.I., Kim, M.J., Park, J.S., Han, J.M., Baek, N.I. and Jeong, T.S. (2010). Ethanolic extracts of Brassica campestris spp. rapa roots prevent high-fat diet-induced obesity via β 3-adrenergic regulation of white adipocyte lipolytic activity. *Journal of Medicinal Food*, **13**(2), 406–414.DOI:10.1089/jmf.2009.1295

Burtis, C.A. and Ashwood, E.R. (1994). *Tietz textbook of clinical chemistry*.

Philadelphia, USA: Amer Assn for Clinical Chemistry.

Chen, G.C., Koh, W.P., Yuan, J.M., Qin, L.Q. and van Dam, R.M. (2018). Green leafy and cruciferous vegetable consumption and risk of type 2 diabetes: results from the Singapore Chinese Health Study and meta-analysis. *British Journal of Nutrition*, **119**(9), 1057–1067. DOI: 10.1017/S0007114518000119.

Delsal, J.L. (1944). New method of extraction of serum lipids by methylal. Application to micro-estimation of total cholesterol, phospho-aminolipins and proteins. *Bulletin de la Société de chimie Biologique*, **26**(n/a), 99–105.

Dias, J.S. (2019). Nutritional quality and effect on disease prevention of vegetables. In: *Nutrition in health and disease-our challenges now and forthcoming time*. London, UK: IntechOpen.

Fawcett, J. and Scott, J. (1960). A rapid and precise method for the determination of urea. *Journal of clinical pathology*, **13**(2), 156–159. DOI: 10.1136/jcp.13.2.156

Feillet-Coudray, C., Sutra, T., Fouret, G., Ramos, J., Wrutniak-Cabello, C., Cabello, G. and Coudray, C. (2009). Oxidative stress in rats fed a high-fat high-sucrose diet and preventive effect of polyphenols: Involvement of mitochondrial and NAD (P) H oxidase systems. *Free Radical Biology and Medicine*, **46**(5), 624–632. DOI: 10.1016/j.freeradbiomed.2008.11.020

Fresco, P., Borges, F., Marques, M.P.M. and Diniz, C. (2010). The anticancer properties of dietary polyphenols and its relation with apoptosis. *Current pharmaceutical design*, **16**(1), 114–134. DOI: 10.2174/138161210789941856

Friedewald, W.T., Levy, R.I. and Fredrickson, D.S. (1972). Estimation of the concentration of low-density lipoprotein cholesterol in plasma, without use of the preparative ultracentrifuge. *Clinical chemistry*, **18**(6), 499–502. DOI :10.1093/clinchem/18.6.499

Ghasemi, A., Khalifi, S. and Jedi, S. (2014). Streptozotocin-nicotinamide-induced rat model of type 2 diabetes. *Acta Physiologica Hungarica*, *101*(4), 408–420. DOI:10.1556/APhysiol.101.2014.4.2

Hattori, M., Nikolic-Paterson, D.J., Miyazaki, K., Isbel, N.M., Lan, H.Y., Atkins, R.C. and Ito, K. (1999). Mechanisms of glomerular macrophage infiltration in lipid-induced renal injury. *Kidney International*, **56**(n/a), S47–S50. DOI: 10.1046/j.1523-1755.1999.07112.x

Jung, U.J., Baek, N.I., Chung, H.G., Bang, M.H., Jeong, T.S., Lee, K.T. and Choi, M.S. (2008). Effects of the ethanol extract of the roots of Brassica rapa on glucose and lipid metabolism in C57BL/KsJ-db/db mice. *Clinical Nutrition*, **27**(1), 158–167. DOI: 10.1016/j.clnu.2007.09.009

Kapusta-Duch, J., Kopec, A., Piatkowska, E., Borczak, B. and Leszczynska, T. (2012). The beneficial effects of Brassica vegetables on human health. *Roczniki Państwowego Zakładu Higieny*, **63**(4), 389–95.

Kim, E.J., Kim, B.H., Seo, H.S., Lee, Y.J., Kim, H.H., Son, H.H. and Choi, M.H. (2014). Cholesterol-induced non-alcoholic fatty liver disease and atherosclerosis aggravated by systemic inflammation. *PloS one*, **9**(6), e97841. DOI:10.1371/journal.pone.0097841

Kim, Y.H., Kim, Y.W., Oh, Y.J., Back, N.I., Chung, S.A., Chung, H.G. and Lee, K.T. (2006). Protective effect of the ethanol extract of the roots of Brassica rapa on cisplatin-induced nephrotoxicity in LLC-PK1 cells and rats. *Biological and Pharmaceutical Bulletin*, **29**(12), 2436–2441. DOI: 10.1248/bpb.29.2436

Lim, S.S., Vos, T., Flaxman, A.D., Danaei, G., Shibuya, K., Adair-Rohani, H. and Pelizzari, P.M. (2012). A comparative risk assessment of burden of disease and injury attributable to 67 risk factors and risk factor clusters in 21 regions, 1990–2010: a systematic analysis for the Global Burden of Disease Study. *The lancet*, **380**(9859), 2224–2260. DOI: 10.1016/S0140-6736(12)61766-8.

Lopes-Virella, M.F., Stone, P., Ellis, S. and Colwell, J.A. (1977). Cholesterol determination in high-density lipoproteins separated by three different methods. *Clinical chemistry*, **23**(5), 882–884. DOI : 10.1093/clinchem/23.5.882

López-Chillón, M.T., Carazo-Díaz, C., Prieto-Merino, D., Zafrilla, P., Moreno, D.A. and Villaño, D. (2019). Effects of long-term consumption of broccoli sprouts on inflammatory markers in overweight subjects. *Clinical Nutrition*, **38**(2), 745–752. DOI :10.1016/j.clnu.2018.03.006

Micha, R. and Mozaffarian, D. (2010). Saturated fat and cardiometabolic risk factors, coronary heart disease, stroke, and diabetes: a fresh look at the evidence. *Lipids*, **45**(n/a), 893–905. DOI:10.1007/s11745-010-3393-4

Okawa, H., Ohishi, N. and Yagi, K. (1979). Assay for lipid peroxides in animal tissues by thiobarbituric acid reaction. *Anal Biochem*, **95**(2), 351–358. DOI:10.1016/0003-2697(79)90738-3

Quintanilha, A.T., Thomas, D.D. and Swanson, M. (1982). Protein-lipid interactions within purified and reconstituted cytochrome c reductase and oxidase. *Biophysical journal*, **37**(1), 68. DOI: 10.1016%2FS0006-3495(82)84603-1

Raiola, A., Errico, A., Petruk, G., Monti, D.M., Barone, A. and Rigano, M.M. (2017). Bioactive compounds in Brassicaceae vegetables with a role in the prevention of chronic diseases. *Molecules*, *23*(1), 15. DOI:10.3390/molecules23010015

Ramirez, D., Abellán-Victorio, A., Beretta, V., Camargo, A. and Moreno, D.A. (2020). Functional ingredients from Brassicaceae species: Overview and perspectives. *International journal of molecular sciences*, **21**(6), 1998. DOI :10.3390/ijms21061998

Reitman, S. and Frankel, S. (1957). A colorimetric method for the determination of serum glutamic oxalacetic and glutamic pyruvic transaminases. *American journal of clinical pathology*, **28**(1), 56–63. DOI: 10.1093/ajcp/28.1.56

Richmond, W. (1973). Preparation and properties of a cholesterol oxidase from Nocardia sp. and its application to the enzymatic assay of total cholesterol in serum. *Clinical chemistry*, **19**(12), 1350–1356. DOI: 10.1093/clinchem/19.12.1350

Šamec, D. and Salopek-Sondi, B. (2019). Cruciferous (brassicaceae) vegetables. In: *Nonvitamin and nonmineral nutritional supplements*. San Diego, California: Academic Press.

Schirmeister, J., Willmann, H. and Kiefer, H. (1964). Plasmakreatinin als grober Indikator der Nierenfunktion. *DMW-Deutsche Medizinische Wochenschrift*, **89**(21), 1018–1023. DOI: 10.1055/s-0028-1111251

Sedlak, J. and Lindsay, R.H. (1968). Estimation of total, protein-bound, and nonprotein sulfhydryl groups in tissue with Ellman's reagent. *Analytical biochemistry*, **25**(n/a), 192–205.

Soliman, A.M., Mohamed, A.S. and Marie, M.A.S. (2016). Effect of echinochrome on body weight, musculoskeletal system and lipid profile of male diabetic rats. *Austin J Endocrinol Diabetes*, **3**(2), 1045.

Thomas-Charles, C. and Fennell, H. (2019). Anti-prostate cancer activity of plant-derived bioactive compounds: A review. *Current Molecular Biology Reports*, **5**(n/a), 140–151. DOI:10.1007/s4061 0-019-00123-x

Tietz, N.W., Finley, P., Pruden, E. and Amerson, A. (1990). Clinical guide to laboratory tests Saunders 2nd Edition. Philadelphia, USA: WB Company.

Yerou, K.O., EL KADI, F.Z., Kanoun, K., Khelladi, H.M., Benzahia, H. and Bekhti, S. (2022). Preliminary phytochemical investigation and antioxidant potential of various extracts of dietary turnip (*Brassica rapa* L.). *Food and Environment Safety Journal*, **21**(1), 94–106. DOI: 10.4316/fens.2022.010

Scientific Journal of King Faisal University:
Basic and Applied Sciences

Applications of de Morton Mobility Index on the Middle-Aged Population—Post Cholecystectomy: A Preliminary Report

Saleh Abdulrahman Almulhim [1], Mounther Mohammed AlNaim [1], Abdullah Ahmed Alabdrabulridha [2], Renad Sunhat AlSubaie [2], Fatimah M. Alhubail [2], Abdulrahman Ahmed Alghamdi [2], Abdulmalek W. Alhithlool [2], Ahmed Hassan Kamal [2] and Abdulrahman Saleh Al-Mulhim [2]

[1] Department of Family Medicine, National Guard Hospital, Al-Ahsa, Saudi Arabia
[2] Surgery Department, College of Medicine, King Faisal University, Al-Ahsa, Saudi Arabia

LINK	RECEIVED	ACCEPTED	PUBLISHED ONLINE	ASSIGNED TO AN ISSUE
https://doi.org/10.37575/b/med/240010	20/02/2024	14/08/2024	14/08/2024	01/12/2024

NO. OF WORDS	NO. OF PAGES	YEAR	VOLUME	ISSUE
3586	4	2024	25	2

ABSTRACT

The aim of this paper is to determine the postoperative outcomes and mobility levels of patients by utilizing DEMMI scores. This is the first study addressing this score in laparoscopic cholecystectomy. This cohort study was conducted at the King Fahad Hospital Al Hofuf and the National Guard Hospital in the Kingdom of Saudi Arabia from January 2022 to January 2023 using a sample of old-age patients undergoing laparoscopic cholecystectomy (LC). The target population comprised of 75 patients aged 50 years and older. Seventy-five patients were included in the study; the median age was 55, with a minimum age of 50 and a maximum age of 72, resulting in a range of 22. The early DEMMI score has a median of 62, a minimum of 53, and a maximum of 100, yielding a range of 47. Regarding the DEMMI score at discharge, the median was 85, with a minimum of 74 and a maximum of 100, resulting in a range of 26. DEMMI scores are a good tool for assessing patients following laparoscopic cholecystectomy.

KEYWORDS

Assessment, complications, geriatric, surgery, movements, postoperative

CITATION

Almulhim, S. A., AlNaim, M. M., Alabdrabulridha, A. A., AlSubaie, R. S., Alhubail, F. M., Alghamdi, A. A., Alhithlool, A. W., Kamal, A. H. and Al-Mulhim, A. S. (2024). Applications of de Morton Mobility Index on the Middle-Aged Population—Post Cholecystectomy: A Preliminary Report. *Scientific Journal of King Faisal University: Basic and Applied Sciences*, **25**(2), 11–4. DOI: 10.37575/b/med/240010

1. Introduction

Gallbladder disease is a common surgical disorder, and the risk of developing cholecystitis and cholelithiasis linearly increases among old-age patients (Lo *et al.*, 1996; Bingener *et al.*, 2003). For such patients, laparoscopic cholecystectomy (LC) is the standard method of treatment (Kim *et al.*, 2018; Golden *et al.* 1996; Fried *et al.*, 1994).

In old-age patients, the preoperative risks factors (underlying health conditions), the decision between emergency and elective LC, and postoperative patient mobility levels are main factors affecting the risk of postoperative complications (Majeski, 2004).

In assessing postoperative outcomes, the de Morton Mobility Index (DEMMI) plays an essential role. It has been specifically developed and validated for older patients hospitalized in ward settings (de Morton *et al.*, 2008a). The independent mobility of this index is a key factor in predicting morbidity and determining hospital discharge readiness for older patients (de Morton, 2008b).

There are many published articles about utilization of the DEMMI for older medical and surgical patients (de Morton, 2008b). To the best of our knowledge, no studies have investigated the association between DEMMI and laparoscopic cholecystectomy.

Therefore, the objective of this study is to explore the DEMMI score of old-age patients following LC.

2. Methodology

This cohort study was conducted at King Fahad Hospital Hofuf and National Guard Hospital in the Kingdom of Saudi Arabia from January 2022 to January 2023 with a sample of middle-aged patients undergoing LC. The target population comprised of 75 patients aged 50 years and older who were scheduled for LC due to cholecystitis or cholelithiasis. Those with pre-existing mobility or cognitive impairments unrelated to the LC procedure or undergoing other major concurrent surgeries were excluded. Data collection encompassed demographic information (age, gender, BMI), clinical history (diabetes, hypertension, etc.), surgical details (type of surgery, operative time, anesthesia duration), and hospitalization duration. The primary outcome was mobility, assessed using the DEMMI. Secondary outcomes included length of hospital stay, rehospitalization rates, and patient-reported outcomes. Assessments of DEMMI scores were conducted early on postoperatively and at discharge.

3. Statistical Analysis

The data underwent analysis utilizing the Statistical Package for the Social Sciences (SPSS) version 26, developed by IBM Corp., Armonk, NY. Descriptive statistics involved the examination of categorical data through frequency tables and percentages, while continuous variables were evaluated using metrics such as median and range. Upon data exploration, it was determined that the distribution was not normal. Consequently, nonparametric tests were utilized for further investigation. The statistical tests, namely the Mann–Whitney U test and the Kruskal–Wallis test, along with post-hoc analysis for independent samples, were employed to examine associations between continuous and categorical variables. A p value of 0.05 for a 95% confidence interval was considered significant.

4. Results

Seventy-five patients were included in the study and the median age is 55, with a minimum of 50 and a maximum of 72, resulting in a range of 22. The early DEMMI score has a median of 62, a minimum of 53, and a maximum of 100, yielding a range of 47. Regarding the DEMMI score at discharge, the median was 85, with a minimum of 74 and a maximum of 100, resulting in a range of 26. The gender distribution reveals that females made up the sample's majority, constituting 77.3%, while males made up the remaining 22.7%. Body mass index (BMI) categories illustrate a diverse range, with the

Corresponding Author: Saleh Abdulrahman Almulhim 00966541318849, Saleh-1248@hotmail.com

majority of patients falling within the 35–40 range (57.3%) and the remainder having a BMI below 35 (14.7%) or above 40 (28.0%). A count of the number of attacks experienced prior to surgery shows a relatively balanced distribution, with 28.0% having fewer than three attacks, 44.0% reporting between three and ten attacks, and 28.0% experiencing more than ten attacks. Time from the first attack to surgery displays a spread across various intervals, with 30.7% undergoing surgery within three months, 36.0% within 3–12 months, and 33.3% after more than 12 months. The majority of surgeries were elective procedures (57.3%) as opposed to emergency surgeries (42.7%). Operative and anesthesia times show variability, with 62.7% of operations lasting over 90 minutes and an equivalent percentage of anesthesia durations exceeding 90 minutes.

Regarding length of hospital stay, 53.3% of participants remained hospitalized for more than 24 hours, while 32.0% were discharged within 24 hours and 13.3% within 12 hours. In terms of comorbidities, diabetes mellitus (DM) was present in 28.0% of participants, while 26.7% had hypertension (HTN), as shown in Table 1.

Table 1: The frequencies and percentages of the different patients' characteristics.

Variable		Frequency	Percent
Gender	F	58	77.3
	M	17	22.7
Body mass index	<35	11	14.7
	35-40	43	57.3
	>40	21	28
Number of attacks before surgery	<3	21	28
	3-10	33	44
	>10	21	28
Time from first attack to surgery	< 3 months	23	30.7
	3 – 12 months	27	36
	> 12 months	25	33.3
Type of surgery	Elective	43	57.3
	Emergency	32	42.7
Operative time	< 45 minutes	8	10.7
	45 – 90 minutes	20	26.7
	> 90 minutes	47	62.7
Anesthesia time	< 60 minutes	4	5.3
	60 – 90 minutes	24	32
	> 90 minutes	47	62.7
Hospital stay	< 12 hours	10	13.3
	< 24 hours	24	32
	> 24 hours	40	53.3
DM	N	54	72
	Y	21	28

The Kruskal–Wallis test indicated a noteworthy association between the number of attacks prior to surgery and early DEMMI scores ($\chi2(2) = 9.192$, $p = 0.01$). Patients experiencing fewer than 3 attacks displayed a significantly lower MR (28.07) compared to those who experienced 3 to 10 attacks (MR 45.64, $p = 0.003$). However, no significant association was observed with DEMMI scores at discharge ($\chi2(2) = 0.290$, $p = 0.865$) (Table 2) (Figures 1 and 2).

Furthermore, the Kruskal–Wallis test revealed a significant link between the time from the first attack to surgery and early DEMMI scores ($\chi2(2) = 6.266$, $p = 0.044$). Patients undergoing surgery within less than 3 months from the first attack demonstrated a lower MR (31.28) compared to those undergoing surgery within 3 to 12 months (MR 45.75, $p = 0.016$). However, no statistically significant association was found with DEMMI scores at discharge ($\chi2(2) = 0.502$, $p = 0.778$) (Table 2) (Figures 1 and 2).

Similarly, both early DEMMI scores ($\chi2(2) = 43.685$, $p < 0.001$) and DEMMI scores at discharge ($\chi2(2) = 23.184$, $p < 0.001$) showed significantly lower mean rank scores for operative times exceeding 90 minutes, anesthesia durations exceeding 90 minutes (early DEMMI: $\chi2(2) = 38.234$, $p < 0.001$; DEMMI at discharge: $\chi2(2) = 20.311$, $p < 0.001$), and hospital stays exceeding 24 hours (early DEMMI: $\chi2(2) = 13.234$, $p = 0.001$; DEMMI at discharge: $\chi2(2) = 6.424$, $p = 0.04$) (Table 2) (Figures 1 and 2).

In addition, patients undergoing emergency surgery exhibited significantly lower MR scores for both early DEMMI scores ($U = 1,339$, $p < 0.001$) and DEMMI scores at discharge ($U = 1,093$, $p < 0.001$) compared to those undergoing elective surgery, as revealed by the Mann–Whitney U test (Table 2) (Figures 1 and 2).

Table 2: The associations between the patients' variables and the early DEMMI score and DEMMI score at discharge using Mann–Whitney U and Kruskal–Wallis tests.

Variables	Early DEMMI score		DEMMI at discharge score	
	Test statistics (df)	p value	Test statistics (df)	p value
Number of attacks	$\chi2(2) = 9.192$	0.010	$\chi2(2)=0.290$	0.865
Time from first attack to surgery	$\chi2(2)= 6.266$	0.044	$\chi2(2)=0.502$	0.778
Type of surgery	U = 1,339	<0.001	U = 1,093	<0.001
Operative time	$\chi2(2) =43.685$	<0.001	$\chi2(2) = 23.184$	<0.001
Anesthesia duration	$\chi2(2) = 38.234$	<0.001	$\chi2(2) = 20.311$	<0.001
Hospital stay	$\chi2(2) = 13.234$	0.001	$\chi2(2) = 6.424$	0.040

$\chi2$ is Chi square and U is the test statistics for the Mann–Whitney test.

Figure 1: The graphical representations of the Mann–Whitney U and Kruskal–Wallis tests, which were used to test the association between patients' variables and early DEMMI scores.

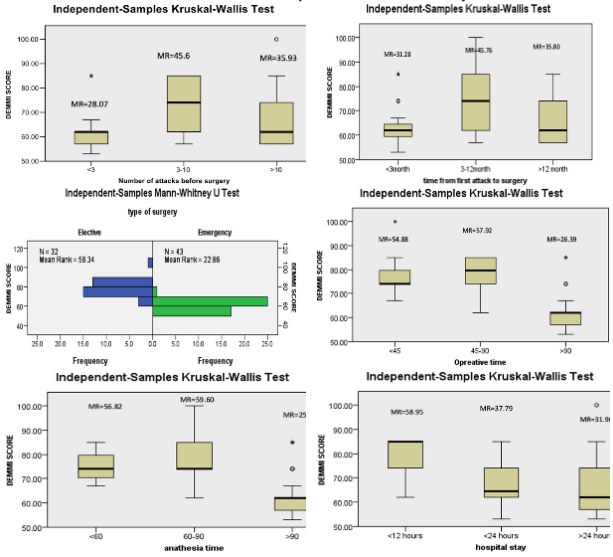

MR: Mean Rank

Figure 2: The graphical representations of the Mann–Whitney and Kruskal–Wallis tests, which were used to test the association between patients' variables and early DEMMI scores at discharge.

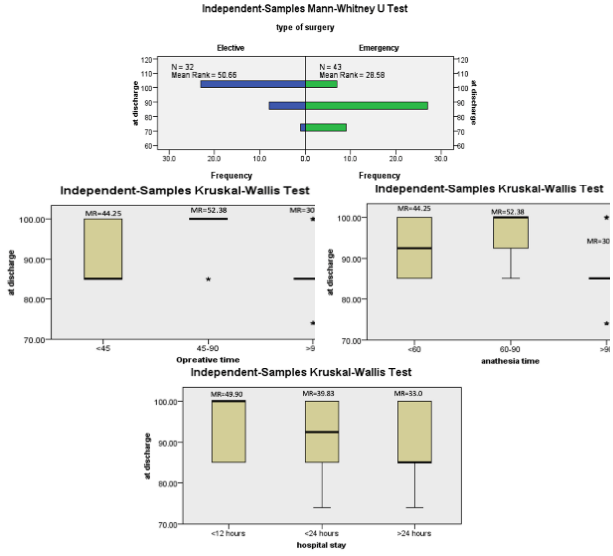

MR: Mean Rank

5. Discussion

The de Morton Mobility Index (DEMMI) was developed and validated through several reliability assessments. Studies examining the reliability of instruments confirm the DEMMI's outstanding reliability, with errors accounting for only around 9% of the scale width. This

indicates that, when applied to an older acute general medical population, the DEMMI demonstrates desirable dependability (de Morton *et al.*, 2008a). The study focused on evaluating the effectiveness of the DEMMI in examining five variables influenced by gender, BMI, DM, and HTN. This was done by comparing early DEMMI scores and DEMMI scores at discharge in older patients undergoing either elective or emergency LC. This cohort study involved 75 patients, predominantly female (77.3%), with a median age of 55. A notable 57.3% of these patients had a BMI between 35 and 40, highlighting high rates of obesity and overweight conditions in the group. Additionally, a significant number of patients had DM (28%) and HTN (26.7%). The study's findings were contrasted with another study indicating no significant differences in operative and postoperative outcomes due to obesity with regard to similar surgical procedures (Nassar *et al.*, 2022). This study identified a significant correlation between DEMMI scores and the frequency of attacks before surgery, revealing that fewer attacks led to higher scores. Additionally, a shorter interval between the first attacks and surgery correlated with increased scores. On the contrary, extended hospital stays over 24 hours resulted in lower scores both initially and at discharge. An additional report highlighted the benefits of early LC in acute cholecystitis, including safer procedures and potentially shorter hospital stays (Gurusamy *et al.*, 2013). However, diabetic patients had higher morbidity rates, though this did not affect surgery duration or hospitalization length (Bedirli *et al.*, 2001). Our study predominantly featured elective procedures (57.3%), highlighting their planned nature. Conversely, emergency surgeries correlated with lower mean rank scores and, thus, lower DEMMI scores both upon initial assessment and upon discharge compared to elective surgeries. Additionally, surgeries and anesthesia lasting over 90 minutes were significantly tied to lower DEMMI scores. Complementing this, another study discovered that aging was significantly related to increased complications in both elective and emergency LC, with the impact varying based on the urgency of the procedure (Kamarajah *et al.*, 2020). These results underscore the importance of considering surgical variables, the number of attacks, and the time before surgery when predicting early functional outcomes. Longer hospital stays, anesthesia durations, and surgical times were associated with poorer functional outcomes. Emergency procedures were linked to lower functional scores, highlighting the significance of careful consideration in such situations.

5.1. Limitations, Strengths, and Recommendations:

This study's limitations include its relatively small sample size and lack of analyses of social and demographic factors. Our study's strength is that it is the first study to evaluate DEMMI scores in patients undergoing LC, marking a significant contribution to the existing literature and expanding our knowledge in this area.

6. Conclusion

To our knowledge, this is the first study to investigate the efficacy of applying the DEMMI to a middle-aged population, although it has been applied to the geriatric population. It also focused on patients post LC. The limitation of the study may be its relatively low cohort. However, future studies with larger cohorts would be beneficial in highlighting the efficacy of applying this index to such patients.

Biographies

Saleh Abdulrahman Almulhim, MBBS

Department of Family Medicine, National Guard Hospital, Al-Ahsa, Saudi Arabia, 00966541318849, Saleh-1248@hotmail.com

Saleh is a family medicine resident at King Abdulaziz National Guard Hospital in Al-Ahsa. He graduated from King Faisal University in Al-Ahsa in 2021. He has a passion for increasing awareness among community members about healthy lifestyles and the importance of early screening, disease prevention, and health promotion. He has participated in many medical research projects that have improved community health. He also regularly participates in various voluntary activities that contribute to enhancing the health of community members.

ORCID: 0000-0002-7088-7693

Mounther Mohammed AlNaim, MBBS, SBFM, ABFM

Department of Family Medicine, National Guard Hospital, Al-Ahsa, Saudi Arabia, 00966582915666, Dr.monther.alnaim@gmail.com

Mounther is a family medicine physician who graduated from the Medicine and Surgery College and King Faisal University, Al-AhsaHe is on the Saudi Board of Family Medicine and the Arab Board of Family Medicine. He has worked as a consultant of family medicine and as a trainer for the Family Medicine Saudi Board Residency Program at King Abdulaziz Hospital for the National Guard of Health Affairs. He is a member of three societies ("walking and running association", the NAQAA Association, and the Association for Social Awareness and Rehabilitation).

ORCID: 0000-0002-6043-4869

Abdullah Ahmed Alabdrabulridha, MBBS

Surgery Department, College of Medicine, King Faisal University, Al-Ahsa, Saudi Arabia, 00966543229719, abdullah.a.alridha@gmail.com

Abdullah Alabdrabulridha is a highly motivated medical student at King Faisal University, demonstrating a robust academic journey and a burgeoning research portfolio. Abdullah's dedication to advancing healthcare knowledge is evident through his ongoing research pursuits and commitment to excellence in both academic and extracurricular activities. Abdullah Alabdrabulridha has participated in many academic activities inside and outside of the medical college of King Faisal University. He has also presented a surgical paper at a local scientific conference in Saudi Arabia. Abdullah Alabdrabulridha is a young and classic future Saudi physician.

ORCID: 0009-0006-1362-1764

Renad Sunhat AlSubaie, MBBS

College of Medicine, King Faisal University, Al-Ahsa, Saudi Arabia, 00966548641225, Subaierenad@gmail.com

Renad Alsubaie is a medical student at King Faisal University, demonstrating a robust academic journey and a burgeoning research portfolio. As an emerging scholar, she has contributed to the medical community through the publication of six articles, showcasing her commitment to advancing healthcare knowledge. Renad Alsubaie has participated in many academic activities inside and outside of the medical college of King Faisal University. She has also presented a surgical paper at a local scientific conference in Saudi Arabia. Renad Alsubaie is a young and classic future Saudi physician.

ORCID: 0009-0005-5528-704X

Fatimah M. Alhubail, MBBS

College of Medicine, King Faisal University, Al-Ahsa, Saudi Arabia, 00966568472883, fatimahalhubailmd@gmail.com

Fatimah Alhubail is a medical student at King Faisal University who strives for excellence both academically and in extracurricular activities. She has published two articles that have impacted the scientific community, as well as her general understanding and progression within her own community. She has participated in many academic activities inside and outside of the medical college of King Faisal University. She has also presented a surgical paper at a local scientific conference in Saudi Arabia. ORCID 0009-0005-2043-648X

Abdulrahman Ahmed Alghamdi, MBBS

College of Medicine, King Faisal University, Al-Ahsa, Saudi Arabia, 00996562243343, Abdg1144@gmail.com

Abdulrahman Alghamdi is a medical student at King Faisal University who has an excellent academic performance and an interesting in scientific research. He is looking forward to growing with his healthcare knowledge. He has participated in many academic activities inside and outside of the medical college of King Faisal University. He has also presented a surgical paper at a local scientific conference in Saudi Arabia. He is looking to specialize to become a prominent health provider and help patients globally.

ORCID: 0009-0004-7056-4781

Abdulmalek W. Alhithlool, MBBS

College of Medicine, King Faisal University, Al-Ahsa, Saudi Arabia, 00966538121511, AbdulmalekAlhithlool@gmail.com

Abdulmalek Alhithlool is a medical student at King Faisal University who has a strong academic background and a growing research portfolio. As a young academic, he has published two articles that have benefited the medical community, demonstrating his dedication to expanding our understanding of healthcare. Abdulmalek Alhithlool has participated in many academic activities inside and outside of the medical college of King Faisal University. He has also presented a surgical paper at a local scientific conference in Saudi Arabia. Abdulmalek Alhithlool is a young and classic future Saudi physician looking to specialize to become a prominent healthcare provider and help patients globally.

ORCID: 0009-0000-1598-0847

Ahmed Hassan Kamal, MBBS, MD

Surgery Department, Medical College, King Faisal University, Alhssa, Saudi Arabia, 00966536468476, aeltair@kfu.edu.sa

Kamal is an anatomist, orthopedic surgeon, and trauma surgeonwho currently serves as an assistant professor at the Faculty of Medicine, King Faisal University. He pursued his undergraduate studies at the University of Khartoum and did his postgraduate training at both the Sudanese Medical Specialization Board and the University of Khartoum. Previously, Dr. Kamal was privileged to be a secretary of training and research officer for the Sudan Association of Orthopedic Surgeons (SOSA). He has contributed to numerous studie and has presented several papers at international orthopedic conferences.

ORCID: 0000-0002-6031-8948.

Abdulrahman Saleh Al-Mulhim, FRCSI, FICS, FACS

Surgery Department, Medical College, King Faisal University, Al-Ahsa, Saudi Arabia, 00966504922399, asalmoulhem@kfu.edu.sa

Prof. Almulhim is a Saudi Professor, graduate from Royal College of Surgeon in Ireland- Dublin, a former vice-dean of research for the medical college, a present vice-dean of academic affairs, and editor-in-chief and board member for 12 international medical and surgical journals. He has published 65 ISI/Scopus-indexed articles with some of the largest publishers globally (Elsevier, Springer, Wiley). He has 6 surgical patents and 15 surgical filling from USA patent office. He is working as a senior consultant laparoscopic surgeon at hospitals in Saudi Arabia.

ORCID: 0000-0002-2525-9516

References

Bedirli, A., Sözüer, E.M., Yüksel, O. and Yilmaz, Z. (2001). Laparoscopic cholecystectomy for symptomatic gallstones in diabetic patients. *Journal of Laparoendoscopic and Advanced Surgical Techniques*, **11**(5), 281–284. DOI: 10.1089/109264201317054564

Bingener, J., Richards, M.L., Schwesinger, W.H., Strodel, W.E. and Sirinek, K.R. (2003). Laparoscopic cholecystectomy for elderly patients: gold standard for golden years? *Archives of surgery*, **138**(5), 531–536. DOI:10.1001/archsurg.138.5.531

de Morton, N.A., Davidson, M. and Keating, J.L. (2008 a). The de Morton Mobility Index (DEMMI): an essential health index for an ageing world. *Health and quality of life outcomes*, **6**(n/a), 1–15. DOI: 10.1186/1477-7525-6-63

de Morton, N.A., Keating, J.L. and Davidson, M. (2008 b). Rasch analysis of the barthel index in the assessment of hospitalized older patients after admission for an acute medical condition. *Archives of physical medicine and rehabilitation*, **89**(4), 641–647. DOI: 10.1016/j.apmr.2007.10.021

Fried, G.M., Clas, D. and Meakins, J.L. (1994). Minimally invasive surgery in the elderly patient. *Surgical Clinics of North America*, **74**(2), 375–387. PMID: 8165473

Golden, W.E., Cleves, M.A. and Johnston, J.C. (1996). Laparoscopic cholecystectomy in the geriatric population. Journal of the *American Geriatrics Society*, **44**(11), 1380–1383. DOI: 10.1111/j.1532-5415.1996.tb01412.x

Gurusamy, K.S., Davidson, C., Gluud, C. and Davidson, B.R. (2013). Early versus delayed laparoscopic cholecystectomy for people with acute cholecystitis. *Cochrane Database of Systematic Reviews*, **n/a**(6), CD005440. DOI: 10.1002/14651858.CD005440.pub3

Kamarajah, S.K., Karri, S., Bundred, J.R., Evans, R.P., Lin, A., Kew, T. and Griffiths, E.A. (2020). Perioperative outcomes after laparoscopic cholecystectomy in elderly patients: a systematic review and meta-analysis. *Surgical endoscopy*, **34**(n/a), 4727–4740. DOI:10.1007/s00464-020-07805-z

Kim, S.S. and Donahue, T.R. (2018). Laparoscopic cholecystectomy. *Jama*, **319**(17), 1834–1834. DOI: 10.1001/jama.2018.3438.

Lo, C.M., Lai, E.C., Fan, S.T., Liu, C.L. and Wong, J. (1996). Laparoscopic cholecystectomy for acute cholecystitis in the elderly. *World Journal of Surgery*, **20**(8), 983–987. DOI: 10.1007/s002689900148

Majeski J. (2004). Laparoscopic cholecystectomy in geriatric patients. *The American journal of surgery*. **187**(6), 747–50. DOI: 10.1016/j.amjsurg.2003.11.031

Nassar, A.H., Khan, K.S., Ng, H.J. and Sallam, M. (2022). Operative difficulty, morbidity and mortality are unrelated to obesity in elective or emergency laparoscopic cholecystectomy and bile duct exploration. *Journal of Gastrointestinal Surgery*, **26**(9), 1863–1872. DOI: 10.1007/s11605-022-05344-7

Thorsted, A.B., Thygesen, L.C., Jezek, A.H., Pedersen, M.M., Jorgensen, M.G., Vinding, K. and Pedersen, S.G. (2024). The De Morton Mobility Index (DEMMI) in hospitalized geriatric patients is associated with risk of readmission, mortality, and discharge to a post-acute care facility: A nationwide register-based cohort study. *Archives of Gerontology and Geriatrics*, **120**(n/a), 105325. DOI: 10.1016/j.archger.2024.105325

Scientific Journal of King Faisal University:
Basic and Applied Sciences

Familial Hypercholesterolaemia Patients with *LDLR* Mutation Among Asian Population in Southeast Asian Countries: Systematic Review

Nur Syahirah Shahuri, Noor Alicezah Mohd Kasim, Hapizah Md Nawawi, Yung-An Chua, Alyaa Al-Khateeb and Siti Hamimah Sheikh Abdul Kadir

Institute of Pathology, Laboratory and Forensic Medicine (I-PPerForM), Faculty of Medicine, Universiti Teknologi MARA, Sungai Buloh, Selangor, Malaysia

LINK	RECEIVED	ACCEPTED	PUBLISHED ONLINE	ASSIGNED TO AN ISSUE
https://doi.org/10.37575/b/med/240022	08/05/2024	01/09/2024	01/09/2024	01/12/2024
NO. OF WORDS	**NO. OF PAGES**	**YEAR**	**VOLUME**	**ISSUE**
7175	7	2024	25	2

ABSTRACT

Familial hypercholesterolaemia (FH) is a genetic disorder associated with premature cardiovascular diseases; however, the majority of patients remain undertreated. This systematic review aimed to determine the prevalence of FH patients with low-density lipoprotein receptor (*LDLR)* gene pathogenic variants (PV) among the Asian population in Southeast Asian countries. Our search yielded 1,120 citations, with 28 deemed possibly suitable based on title and abstract screening. However, only six studies that utilised the Dutch Lipid Clinic Network (DLCN) or Simon Broome (SB) criteria were eligible to be included. These studies provided prevalence figures for clinically diagnosed FH patients, with a total of 17.1% (n=1,005/5,874); this rate was represented by three Malaysian studies, which estimated that 36–76% of clinically diagnosed FH patients had *LDLR* PV. Most patients reported having pre-existing cardiovascular disease, a family history of premature coronary artery disease and tendon xanthomata. This study found that the prevalence of *LDLR* PV among genetically confirmed FH patients in Southeast Asia is 20.5% (n=286/5,874). Genetically confirmed FH patients are at a higher risk of developing premature coronary artery disease, requiring more aggressive lipid-lowering treatment. Therefore, identifying *LDLR* PV among the population is essential for early FH diagnosis and treatment.

KEYWORDS

Arterial disease, autosomal dominant, LDL receptor, *LDLR* prevalence, pathogenic variants, premature CAD, Undertreated

CITATION

Shahuri, N.S., Mohd Kasim, N.A, Md Nawawi, H., Chua, Y., Al-Khateeb, A. and Sheikh Abdul Kadir, S.H. (2024). Familial hypercholesterolemia patients with *LDLR* mutation among Asian population in southeast Asian countries: Systematic review. *Scientific Journal of King Faisal University: Basic and Applied Sciences*, **25**(2), 15–21.
DOI: 10.37575/b/med/240022

1. Introduction

Familial hypercholesterolaemia (FH) is an inherited metabolic disorder associated with an elevated level of low-density lipoprotein cholesterol (LDL-C or LDL cholesterol) and a greater risk of developing premature cardiovascular disease (PCAD) in both men and women (Bouhairie and Goldberg, 2015). LDL-C is a type of fat that circulates throughout the body and deposits within artery walls, where it is required for cell repair. Triglycerides and cholesterol, which are insoluble in water, must bind to proteins to pass through the hydrophilic blood (Hevonoja *et al.,* 2000). Early identification of FH, with subsequent effective LDL-C-lowering therapy, will lead to the prevention of coronary heart disease (CHD) and, eventually, early mortality among FH patients (Packard *et al.,* 2021).

FH is an autosomal dominant disorder caused by mutations in the LDL receptor (*LDLR)* or its ligand, apolipoprotein B 100 (*APOB)* (Pejic, 2014). LDL-C receptors are essential for LDL-C absorption from the blood into hepatocytes, while *APOB* is important for LDL-C structure maintenance and serves as a recognition site for the LDL-C receptors, which is required for receptor-mediated endocytosis. Mutations in the *LDLR* were reported to be the most common cause of FH, followed by *APOB* (Iacocca *et al.,* 2018). In rare situations, a gain-of-function variant in the proprotein convertase subtilisin-kexin type 9 gene (*PCSK9*) may be the cause (Vrablik *et al.,* 2020). In 85–90% of individuals with FH, over 1,600 gene variants in the *LDLR* were reported; these were followed by *APOB* mutations, where the most common one (Arg3500⟶Gln) affects approximately 10% of individuals with FH. *PCSK9* gene mutation accounts for less than 5% of FH cases. Furthermore, only severe *PCSK9* mutations cause FH (Pejic, 2014).

LDLR, a glycoprotein found in cell membranes, is involved in the binding and internalisation of lipoprotein particles in the bloodstream that carry cholesterol. *LDLR* is a widely expressed receptor that is essential for cholesterol homeostasis in humans (Goldstein and Brown, 1974). Many studies on how LDLR removes LDL, a significant cholesterol carrier in humans, have been conducted (Goldstein and Brown, 1973; Brown and Goldstein, 1974a; Brown and Goldstein, 1974b; Goldstein and Brown, 1974). Cultured fibroblasts from FH patients cannot remove serum LDL, resulting in higher serum LDL-C levels. Normal fibroblasts have a high cell surface binding affinity for LDL-C via *LDLR* (Brown and Goldstein, 1974a). Individuals with homozygotes for the *LDLR* mutation exhibit extensive deposition of cholesterol-mediated atheromatous plaques in their coronary arteries, aorta and aortic valves, and have blood LDL-C levels as high as 800 mg/dL (Brown and Goldstein, 1974b). Carriers with heterozygote *LDLR* mutations usually had a two-fold increased risk for coronary artery disease and a twice-elevated plasma LDL-C concentration compared to the general population. According to the majority of guidelines, patients with established coronary artery disease should have their LDL-C levels adjusted to below 70 mg/dL and 100 mg/dL, respectively, if they have two or more risk factors for the condition (Goldstein and Brown, 1973).

The exact prevalence of FH in Asian populations remains undetermined. Many studies have determined that the prevalence of FH in the general population ranges from 1:200 to 1:250 (Chua *et al.,* 2021). A meta-analysis of 11 million individuals from 104 studies estimated that the prevalence of heterozygous FH (HeFH) in the general population was 1 in 313 (Beheshti *et al.,* 2020). The European Atherosclerosis Society (EAS) Consensus Panel estimates that the prevalence of HeFH ranges from 1 in 200 to 1 in 500, but it could be as high as 1 in 31 in patients with atherosclerotic cardiovascular disease (ASCVD). Meanwhile, approximately 1:160,000 to 1:300,000 people have homozygous FH (HoFH) (Sun *et al.,* 2023). Both HoFH and HeFH induce a marked increase in LDL-C levelswhich often results in early cardiovascular disease (Marusic *et al.,* 2020). Globally, 90–95% of FH patients remain undiagnosed (EAS, 2018).

Multiple approaches are needed for screening, diagnosing and treating FH (Pang *et al.,* 2020). FH patients can be identified via clinical diagnosis, personal and family history and physical examination, with genetic

Corresponding Author: Siti Hamimah Sheikh Abdul Kadir 0060162128344, sitih587@uitm.edu.my

testing used to confirm the diagnosis (Migliara *et al.,* 2017). Physical manifestations of FH, such as tendon xanthomata and corneal arcus in patients under the age of 45, have been used to develop the most utilised diagnostic tools for the clinical diagnosis of FH (Rallidis *et al.,* 2020). For instance, Simon Broome's (SB) criteria are well-known clinical diagnostic measures for FH that are extensively used in the United Kingdom, (Humphries *et al.,* 2018). The Dutch Lipid Clinic Network (DLCN) criteria are commonly used in European nations (Gidding *et al.,* 2022), whereas the Make Early Diagnosis to Prevent Early Deaths (MEDPED) criteria are generally used in the United States (Maştaleru *et al.,* 2022). Each of these criteria has distinct features and standards for diagnosing FH. The MEDPED criteria are based solely on age- and family-relative-specific total cholesterol (TC) levels, while the DLCN and SB incorporate a variety of other comparable factors. However, there is no consensus on which diagnostic criteria should be used as standardised international tools for FH identification worldwide (Rallidis *et al.,* 2020).

As FH is an autosomal dominant disorder, a heterozygous individual has a 50% probability of transferring the gene to their offspring. If individuals with identical mutations in both alleles (homozygous), different pathogenic variants (PV) in both alleles of the same gene (compound heterozygotes) or PV in two different genes (double heterozygotes), they will have obligatory heterozygous offspring, as long as their partner does not have FH (McGowan *et al.,* 2019). Thus, cascade screening, which involves genetic testing on family members of a proband who have been previously diagnosed with FH, seems to be an effective strategy for FH screening (Vrablik *et al.,* 2020). Cascade screening is a low-cost method of identifying at-risk individuals that involves systematic family tracing (Migliara *et al.,* 2017).

There are several types of genetic tests, each with different approaches (Futema *et al.,* 2021). Targeted next-generation sequencing (NGS) technologies enabled comprehensive mutation identification, particularly loci of interest and simultaneous sequencing of several genes, resulting in genetic information in FH candidate genes, hypercholesterolaemia-associated genes and other lipid metabolism-related genes (Qin, 2019). However, it is uncertain whether including these additional genes in NGS panels enhances the number of FH patients who could be molecularly identified (Reeskamp *et al.,* 2020). FH, a reasonably common genetic condition, affects an estimated 20 million individuals worldwide, with over 90% of cases remaining untreated (Zubielienė *et al.,* 2022). In Asia Pacific, FH is a common hereditary disorder impacting at least 15 million people (Kalra *et al.,* 2021). The prevalence of FH in Asia was found to be 1:526 in a recent meta-analysis, which included four studies: two from Japan, one from Korea and one from China. In comparison, the FH prevalence in both North America (9 studies) and Europe was 1:313 (19 studies) (Beheshti *et al.,* 2020). Therefore, this systematic review aims to summarise the prevalence of FH patients with *LDLR* PV among the Asian population in Southeast Asian countries.

2. Method

This paper conducted a systematic review of observational studies that were carried out and published per the Preferred Reporting Items for Systematic Reviews and Meta-Analyses (PRISMA) criteria but without meta-analysis (Liberati *et al.,* 2009). The Condition, Context and Population (CoCoPop) framework was utilised to formulate the Population, Intervention, Comparator and Outcome (PICO) question (Munn *et al.,* 2015)

2.1. Search Strategy:

To retrieve potentially relevant reviews, we searched PubMed, SCOPUS and Web of Science using the keywords '(((Prevalence) OR (Incidence) OR (Frequency) OR (Occurrence) OR (Burden) OR (Commonness) OR (Frequentness) OR (Chronicity) OR (Continuousness) OR (Regularity) OR (Appearance) OR (Constancy)) AND ((Southeast Asian) OR (Brunei) OR (Cambodia) OR (Indonesia) OR (Laos) OR (Malaysia) OR (Myanmar) OR (Philippines) OR (Singapore) OR (Thailand) OR (Vietnam))) AND ((Familial Hypercholesterolaemia) OR (Familial Hypercholesterolaemia) OR (Hyperlipoproteinaemia) OR (Hyperlipidaemia) OR (HeFH) OR (HoFH) OR (FH))'. English language restrictions were applied to the search.

2.2. Inclusion Criteria:

2.2.1. Study Design

The review includes observational research such as cross-sectional, case-control and case series studies**.**

2.2.2. Scope of Study

The review criteria included studies or articles that: (1) contained information about adult patients (≥18 years old); (2) referred to settings located in Southeast Asia; (3) provided FH disease information; (4) reported on FH disease prevalence; and (5) discussed positive *LDLR* mutations in clinically diagnosed FH patients.

2.3. Outcome:

To determine the prevalence of FH patients with *LDLR* gene PV based on FH diagnostic criteria, study population and demographic profile (age and gender) as well as the frequency of *LDLR* PV in patients with FH within the Asian population in Southeast Asian countries.

2.4. Exclusion Criteria:

This review excluded articles for which full texts could not be obtained from the search; studies that lacked information on FH clinical diagnosis, personal and family history, physical examination or genetic testing; papers that did not include adult patients; or research that did not offer information on the prevalence or incidence of *LDLR* PV among FH patients. Moreover, this review rejected non-English research articles, conference proceedings, abstracts, book chapters and commentaries.

2.5. Study Selection and Data Extraction:

After the articles in the databases were identified, they were imported into the Mendeley version 2.79.0 software (Elsevier, UK). Duplicate articles were then removed. The studies were initially screened based on their titles/abstracts, and irrelevant publications were excluded (Table 1). The qualifying criteria were utilised to conduct the first-level screening of paper titles and abstracts. Systematic reviews and meta-analyses were omitted. Only full-text papers were searched to determine their suitability for additional screening and inclusion in the review. The full texts of the remaining publications were then analysed. A paper was classified as a general population study if the participants involved in the research were selected from the general population, as indicated by the authors. A data extraction form was used to extract the following data: age group of patients (adult or elderly), country of study, total number of FH patients who had *LDLR* mutations and the number of patients with diagnosed FH.

2.6. Strategy for Data Synthesis:

The review focused on narrative synthesis due to the small number of papers included and methodological discrepancies between the studies. Data were summarised using prevalence estimates of FH patients with *LDLR* PV among populations in Southeast Asian countries. If the prevalence was not directly available for data extraction, it was calculated based on the size of the total study cohort and the number of FH individuals with *LDLR* PV. Demographic data

(age, sex) and prevalence are reported as means with percentages (%).

3. Results

3.1. Study Selection:

Our search yielded 1,120 citations, with 28 deemed possibly relevant based on title and abstract screening. Following the application of the inclusion and exclusion criteria, publications were screened at the full-text level, with six papers being included in this review. Figure 1 depicts the flow of the included investigations.

3.2. Characteristics of the Included Studies:

The six included studies were published between 2005 and 2022 (basic details in Table 1). Four studies (Khoo *et al.,* 2000; Al-Khateeb *et al.,* 2011; Lye *et al.,* 2013; Razman *et al.,* 2022) were carried out in Malaysia, while the remaining two (Punzalan *et al.,* 2005; Pek *et al.,* 2018) were conducted in the Philippines and Singapore. All studies in this review used a cross-sectional study design. A total of 5,788 participants were involved in the studies, with the vast majority coming from a single research (Razman *et al.,* 2022). One study (Punzalan *et al.,* 2005) only included 60 participants. All six studies diagnosed FH as definite, probable or possible using either the DLCN or SB criteria.

Figure: 1. PRISMA flow diagram for selecting studies on FH in Southeast Asian countries

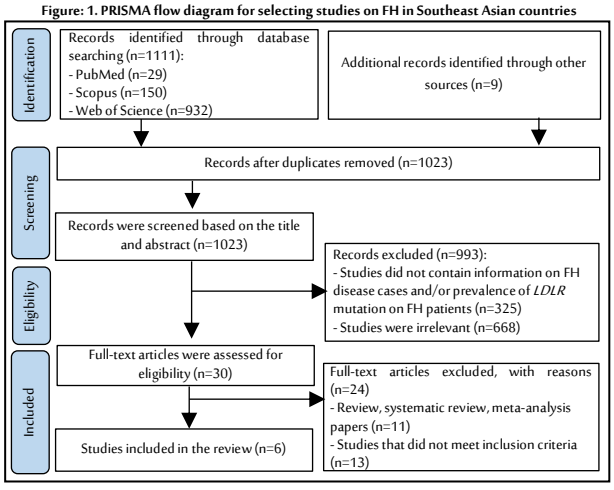

Table: 1. A summary of selected studies on FH in Southeast Asian countries

Study Author (publication year)	Country	Source	Diagnostic Criteria	Analysis Method	Sample Size	Mean Age Years	Sex, N	Outcome		
								Clinical Prevalence (clinically diagnosed FH), N (%)	FH Patients with PV, N (%)	Total *LDLR* PV Confirmed Prevalence, N (%)
Razman *et al.,* (2022)	Malaysia	Patients from hospital-based screening	DLCN	NGS	5,130	51.1	Male: 171 Female: 201	372/5,130 (7.3)	82/372 (22.0)	30/82 (36.6)
Al-Khateeb *et al.,* (2011)	Malaysia	Patients from hospital-based screening	SB	DHPLC	154	44.6	Male: 73 Female: 81	154/154 (100.0)	117/154 (76.0)	117/154 (76.0)
Pek *et al.,* (2018)	Singapore	PS	DLCN	NGS	192	33.5	Male: 77 Female: 115	192/192 (100.0)	54/192 (28.1)	50/192 (26.0)
Punzalan *et al.,* (2005)	Philippines	PS	DLCN	DHPLC	60	55	Male: 21 Female: 39	60/60 (100.0)	60/60 (100.0)	12/60 (20.0)
Lye *et al.,* (2013)	Malaysia	Patients from an outpatient clinic	DLCN	MLPA	252	46.8	Male: 73 Female: 68	141/252 (56.0)	108/141 (76.6)	55/141 (39.0)
Khoo *et al.,* (2000)	Southeast Asia	Patients from a lipid clinic	DLCN	DGGE and DNA-sequencing	86	54	Male: 41 Female: 45	86/86 (100.0)	22/86 (25.6)	22/86 (25.6)

PS: population study; PV: pathogenic variants; DLCN: Dutch Lipid Clinic Network; SB: Simon Broome; NGS: next-generation Sequencing; DHPLC: denaturing high-performance liquid chromatography; MLPA: multiplex-ligation dependent probe amplification; DGGE: denaturing gradient gel electrophoresis.

Table: 2. Publications on *LDLR* pathogenic variants and their associated clinical features and history among FH patients in Southeast Asian countries

Study	Country	Patients with LDLR PV, *n*	*LDLR* Gene Identified			Standard Clinical Presentation
			LDLR Variants	Total *LDLR* Variants, *n*	Total *LDLR* PV, *n* (%)	
Razman *et al.,* (2022)	Malaysia	30	c.241C>T, c.301G>A, c.580A>G, c.811G>A, c.833G>A, c.949G>A, c.1234A>C, c.1284C>G, *c.1289T>G, *c.1571T>G, *c.1774G>T, c.1820A>G, *c.2383C>G, c.2530G>A, c.1217G>A, c.1246C>T, c.1867A>G, c.1187-2A>G	18	18/18 (100.0)	This study found that patients with potential FH had higher proportions of existing personal CVD (13.8%), a family history of PCAD (34.5%), the presence of tendon xanthomata (10.3%) and premature corneal arcus (75.9%) as well as elevated LDL-C levels. Those with possible FH had lower proportions of these factors, with rates of 5.1% for CVD, 13.4% for family history of PCAD and 2.2% for the absence of tendon xanthomata and premature corneal arcus.
Al-Khateeb *et al.,* (2011)	Malaysia	117	c.81C>T, c.190+56G>A, c.190+58C>T, c.300C>T, c.910G>A, c.940+36G>A, c.1060+7T>C, c.1060+10G>C, c.1186+41T>A, c.1194C>T, c.1359-30C>T, c.1411A>G, c.1617C>T, c.1705+56C>T, c.1705+112C>G, c.1706-55A>C, c.1706-69G>T, c.1705+117T>G, c.1773C>T, c.1959T>C, c.2232A>G, *c.190+4A>T, *c.301G>A, *c.415G>C, *c.601G>A, *c.763T>A, *c.1706_1845, *c.2100C>G, *c.1996_2012del17	29	8/29 (27.6)	This study revealed that patients with PV had higher LDL-C levels (1.1%) compared to non-PV patients (0.8%). Also, patients with PV had a higher incidence of tendon xanthomata (66.7%) and CVD (88.1%), while non-PV patients had a lower incidence of tendon xanthomata (31.3%) and CVD (60.7%).
Pek *et al.,* (2018)	Singapore	50	c.232C>T, c.241C>T, c.532G>A, *c.632_634del, c.769C>T, c.985T>G, c.986G>A, c.1009G>A, c.1027G>A, *c.1060G>A, c.1061A>G, *c.1090del, *c.1091G>A, c.1171G>A, c.1217G>A, c.1222G>A, c.1241T>G, c.1247G>A, *c.1292C>T, *c.1420C>T, c.1474G>A, *c.1475A>T, *c.1514G>C, *c.1525A>G, c.1747C>T, c.1765G>A, c.1783C>T, c.1954_1955del, c.1963T>C, c.2054C>T, *c.2093G>A, *c.2108_2114dup, c.2230C>T, c.2291T>C, c.2383C>G, *c.2478del, c.313+1G>A, c.(67+1_68-1)_(2311+1_2312-1)del, c.(1586+1_1587-1)_(2140+1_2141-1)del, c.(2140+1_2141-1)_(2311+1_2312-1)del, c.(940+1_941-1)_1845+1_1846-1)dup	41	26/41 (63.4)	This study found that most patients with pathogenic mutations had a family history of premature CVD. Moreover, 7.4% of them had tendon xanthomata, 7.2% had experienced a CVD event and 6.3% had arcus cornealis.
Punzalan *et al.,* (2005)	Philippines	12	c.268G>A, c.986G>A, c.1747C>T, *p.G50R, *p.D147N, *c.1502C>A, *1602V, *c.190+4A>T, *c.1187-10G>A	9	9/9 (100.0)	This study revealed that patients exhibiting clinical features of FH were relatively young yet already had a high prevalence of CAD and CVD.
Lye et al., (2013)	Malaysia	55	c.940+775G>A	1	1/1 (100.0)	The FH patients recruited in this study were older. Age has been identified as a risk factor for age-related dyslipidaemia. The steady drop in LDL-C clearance as age increases is one of the reasons for age-related disturbance of lipid homeostasis.
Khoo *et al.,* (2000)	Southeast Asia	22	*c.-152G>T, *c.77delG>A, p.D69N, c.313+1G>A, p.R94H, p.R232W, p.E256K, *p.C308Y, *p.Q357X, *p.K372N, *p.L393R, p.I402T, p.N407K, p.G457R, p.D471N, *c.2108ins7bp, *p.A663T, *p.C675Y	18	18/18 (100.0)	This study found that patients with mutations had significantly higher LDL-C levels, a notably higher incidence of xanthomata (65%) and more than double the incidence of CHD (57%), in comparison to patients without the *LDLR* mutation who had xanthomata (41%) and CHD (26%).

LDLR: low-density lipoprotein receptor gene; PV: pathogenic variants; *novel pathogenic variant; CVD: cardiovascular disorder; CAD: coronary artery disease; FH: familial hypercholesterolaemia; LDL-C: low-density lipoprotein cholesterol.

Table 2 presents four studies in which most patients had personal CVD, a family history of PCAD and tendon xanthomata. One study found approximately 41 *LDLR* variants among 50 individuals with FH, of whom 26 had *LDLR* PV (Pek *et al.,* 2018). Moreover, two studies conducted in the same country detected eight *LDLR* PV among 117 patients with FH (Al-Khateeb *et al.,* 2011). Another research found 18 *LDLR* PV among 30 individuals with FH, of which four were novel variants (Razman *et al.,* 2022). In another investigation, nine *LDLR* PVs were discovered, six of which were novel variants identified in 12 patients with FH. Also, a single *LDLR* variant was found in 55 older FH patients, which is considered a rare case (Lye *et al.,* 2013). In a Southeast Asian study, approximately 18

LDLR distinct mutations were found (Khoo *et al.,* 2000); nine of these have been previously detected, while the other nine are novel mutations.

3.3. *LDLR* PV Prevalence Varies by Country:

The results showed that Singapore (Pek *et al.,* 2018), Southeast Asia (Khoo *et al.,* 2000) and the Philippines(Punzalan *et al.,* 2005) had a lower prevalence (26%, 25.6% and 20%, respectively) of *LDLR* mutations among clinically diagnosed FH patients compared to Malaysia (as indicated by three studies), where it was estimated that approximately 36—76% of patients had *LDLR* mutations (Al-Khateeb *et al.,* 2011; Lye *et al.,* 2013; Razman *et al.,* 2022).

3.4. Prevalence Varies Based on the Clinical Diagnostic Criteria:

Five studies (Khoo *et al.,* 2000; Punzalan *et al.,* 2005; Lye *et al.,* 2013; Pek *et al.,* 2018; Razman *et al.,* 2022) utilised DLCN, while only one research (Al-Khateeb *et al.,* 2011) used SB as a diagnostic tool to detect FH patients. The SB study had the highest frequency of *LDLR* PV, reaching 76%. Based on three studies that used DLCN, the prevalence of *LDLR* PV among FH patients was 22% in Malaysia (Razman *et al.,* 2022), 28.1% in Singapore (Pek *et al.,* 2018) and 25.6% in Southeast Asia (Khoo *et al.,* 2000).

3.5. Prevalence Varies Based on the Molecular Detection Technique:

NGS-based studies reported that 26% (Pek *et al.,* 2018) and 36.6% of FH subjects had *LD LR* PV (Razman *et al.,* 2022). Two studies that utilised the DHPLC analysis method found an approximate prevalence of 20% (Punzalan *et al.,* 2005), with Malaysian FH subjects having the highest prevalence of *LDLR* PV at 76% (Al-Khateeb *et al.,* 2011). Moreover, the MLPA method-based research revealed that about 39% of FH patients had *LDLR* PV (Lye *et al.,* 2013). In another study, DGGE and DNA sequencing revealed that around 25.6% of clinically diagnosed FH patients had *LDLR* PV (Khoo *et al.,* 2000).

4. Discussion

This paper is the first systematic review to identify the prevalence of *LDLR* PV among FH patients in Southeast Asian countries. This research included six studies, with a total of 5,788 participants. Approximately 1,005 patients were clinically diagnosed with FH, with 28.5% (n=286/1,005) having *LDLR* mutations; however, the vast majority of FH patients with *LDLR* PV were from a single study (Al-Khateeb *et al.,* 2011). The six studies reported that among the Asian population in Southeast Asian countries, there was a genetically confirmed prevalence of *LDLR* PV in FH patients at approximately 20.5%, with 13 out of 267 cases. In addition, another study discovered that the FH prevalence in the general population was 0.19% in Asia, compared to 0.32% in Europe and North America (Beheshti *et al.,* 2020).

This review found that FH with positive *LDLR* PV affects both men and women equally, and many patients had personal CVD. Over 85% of men and 50% of women with FH are expected to experience coronary events (Woodward, 2019). This increases the likelihood of FH going undetected in female as compared to male patients. However, because CAD usually manifests much later in life among women, most of them may be identified based on clinical criteria as they age (Garcia *et al.,* 2016). Notably, the literature lacks comprehensive investigation into the potential effects of delayed FH diagnosis in women with the presence of PV in the *LDLR*, as opposed to men; it is also uncertain as to whether such delays could lead to sub-optimal health outcomes. Nevertheless, understanding the gender-specific differences in FH with *LDLR* PV manifestation could enable earlier diagnosis of this condition, which is critical from a clinical standpoint.

In most countries, diagnosis is mostly based on DLCN criteria and less commonly on SB or MEDPED (EAS, 2018). The DLCN, SB and MEDPED criteria may yield different diagnostic outcomes even in the same population. This might compromise the accuracy of projected prevalence in various nations and diagnostic reliability in different groups (Hu *et al.,* 2020). Patients with PCAD and increased cholesterol had a greater frequency of *LDLR* PV, as seen in general population research (Beheshti *et al.,* 2020; Hu *et al.,* 2020). Thus, patients with PV require more aggressive lipid-lowering treatment than those without PV. According to a prior study, a significant percentage (>10%) of patients with acute coronary syndrome under the age of 60 were diagnosed with FH (Tanaka *et al.,* 2019). The five non-FH patients who were clinically diagnosed using the DLCN FH criteria were found to have FH. This is because the DLCN FH criteria have several advantages, such as reducing the likelihood of FH denial based on multiple clinical diagnostic elements, particularly the patient's clinical history of premature CAD and genetic diagnosis (Tada *et al.,* 2021). Since the DLCN FH criteria include extra categories (DLCN has four, while SB has three categories), utilising them instead of other criteria may improve sensitivity when accounting for those categories (Tada *et al.,* 2021).

The identification of a disease-causing pathogenic mutation equals a definitive FH diagnosis, making genetic screening the most accurate way to confirm FH (Cuchel *et al.,* 2014). In cascade screening, genetic testing is commonly used to confirm the origin of dyslipidaemia or establish the presence of a disease-causing gene mutation. First-degree relatives should be tested as part of standard clinic screening; it has been hypothesised that a strategy combining index cases and personal contact with family members by medical professionals may increase the number of tested people (Wald and Wald, 2018). According to the NICE recommendations for the diagnosis and treatment of FH, cascade screening, which combines genetic testing with LDL-C concentration measurement, must be used to identify affected relatives of index individuals with a clinical diagnosis of FH. This should include first-, second- and, if feasible, third-degree biological relations (DeMott, *et al.,* 2008; Ned and Sijbrands, 2011). However, genetic screening has its limitations, as it is expensive, time-consuming and needs access to healthcare facilities, making it less useful in less affluent regions of the world (Hu *et al.,* 2020). Furthermore, research utilising genetic screening yields low FH prevalence estimates, probably because not all FH-causing mutations have been found or included in diagnostic testing panels for FH (Medeiros and Bourbon, 2023). Most patients with a polygenic cause of elevated LDL-C are mutation-negative (Mickiewicz *et al.,* 2020). Polygenic hypercholesterolaemia is a common cause of elevated blood cholesterol. It represents the conditions in which serum triglyceride (TG) concentrations are within the recommended range but LDL-C levels are elevated. Polygenic hypercholesterolaemia may coexist with other conditions, such as metabolic syndrome or obesity, in certain people with mixed dyslipidaemias (elevations of both LDL-C and triglycerides). Clinically distinguishing FH from polygenic hypercholesterolaemia can be occasionally challenging.

FH prevalence tends to increase with age. Beheshti *et al.,* (2020) found that the frequency of FH was slightly lower among those aged 0—19 years (1 in 278; 95% CI; 1 in 345 to 1 in 222). Historically, older age has been seen as a risk factor for dyslipidaemia. Both cross-sectional and longitudinal investigations found that TC, LDL-C and TG concentrations were related to age (Cho *et al.,* 2020). Individuals with definite/probable FH who received cholesterol-lowering medication had 193% higher LDL-C levels than those who were unlikely to have FH

but were given cholesterol-lowering medication (Wang *et al.,* 2019). Factors contributing to the age-related disruption of lipid homeostasis and steady decline in LDL-C clearance include a progressively decreasing capacity to remove cholesterol by converting it to bile acids, a decreased activity of the enzyme that controls the rate of bile acid synthesis and a progressively declining growth hormone secretion. Growth hormone influences the expression of hepatic *LDLR*, which is critical for maintaining normal cholesterol levels (Pallottini and Trapani, 2010).

5. Study Limitation

Nevertheless, a multimodal strategy including clinical, biochemical, and genetic parameters is necessary to enhance the detection of FH and reduce CVD and mortality. New information on the prevalence of FH is revealed by these studies. However, certain significant restrictions should be considered. First, even though we used a thorough search approach, we only included peer-reviewed English language studies that were indexed in four online databases. It is still conceivable that other pertinent research was either not published or was indexed in other languages, print repositories, or grey literature. Furthermore, all studies included in this review were conducted on opportunistic samples and drawn from conveniently accessible sources. Thus, these findings could only be generalised to the sub-population from which the samples were collected and may not apply to the entire population.

6. Conclusions

In this systematic review, we concluded that the prevalence of *LDLR* mutations among genetically confirmed FH patients among the general population of Southeast Asians is 13:267 (286/5874), approximately 20.5% which is quite high, emphasising the need for genetic confirmation among index cases, as well as cascade screening from clinically diagnosed FH among Asian populations. There is a need for the identification of the prevalence of FH patients with *LDLR* mutations in Southeast Asian countries individually to determine the potential benefits of intensified FH screening in certain population subgroups and to further investigate potential biases and inequalities in current FH diagnostic criteria and screening programmes.

Biographies

Nur Syahirah Shahuri

Institute of Pathology, Laboratory and Forensic Medicine (I-PPerForM), Faculty of Medicine, Universiti Teknologi MARA, Sungai Buloh, Selangor, Malaysia, 60134217506, syahirahshahuri@gmail.com

Nur Syahirah is a graduate research assistant. She is an active committee member postgraduate association in Faculty of Medicine, Universiti Teknologi MARA. She was selected as a finalist for a moderated poster presentation at the International Congress on Lipid and Atherosclerosis (ICoLA) and Asian-Pacific Society of Atherosclerosis and Vascular Diseases (APSAVD) in 2022. She had represented Malaysia for an oral presentation at the APSAVD Congress 2021.

ORCID: 0009-0003-6934-4055

Noor Alicezah Mohd Kasim

Institute of Pathology, Laboratory and Forensic Medicine (I-PPerForM), Faculty of Medicine, Universiti Teknologi MARA, Sungai Buloh, Selangor, Malaysia, 60172001140, noor202@uitm.edu.my

Noor Alicezah is a consultant chemical pathologist at Hospital Al Sultan Abdullah UiTM and professor in laboratory medicine at Faculty of Medicine UiTM Sg Buloh. She has been actively engaged in cardiovascular research for over a decade, focusing on Familial Hypercholestrolaemia, atherosclerosis, dyslipidemia and the study of natural products. She has received numerous research grants and has published over 40 indexed publications, along with more than 100 of other types of publications. She has successfully guided several Master and Clinical Master students to completion. She is currently supervising two Ph.D. students, four Master's students and 1 Clinical Master's students.

ORCID: 0000-0003-3855-5768

Hapizah Md Nawawi

Institute of Pathology, Laboratory and Forensic Medicine (I-PPerForM), Faculty of Medicine, Universiti Teknologi MARA, Sungai Buloh, Selangor, Malaysia, 60123838075, hapizah.nawawi@gmail.com

Dr. Hapizah is a professor at UiTM Sungai Buloh and an expert in chemical pathology and metabolic medicine, dyslipidemia and atherosclerosis. She received numerous research grants; completed four international grants, 73 national grants and with 19 active national grants. She has published more than 160 indexed publications and 400 of other publications. She has successfully supervised three Ph.D. and 18 Master students to completion, while ongoing supervisor for another 3 Ph.D. and 2 Master students.

ORCID: 0000-0003-4462-8484

Yung-An Chua

Institute of Pathology, Laboratory and Forensic Medicine (I-PPerForM), Faculty of Medicine, Universiti Teknologi MARA, Sungai Buloh, Selangor, Malaysia, 60129647410, yungan.chua@gmail.com

Yung-An Chua is a University Sains Malaysia graduate, a former postdoctoral researcher at Institute of Pathology, Laboratory and Forensic Medicine (I-PPerForM), Faculty of Medicine, UiTM Sungai Buloh, and currently appointed as a senior lecturer at UiTM Sungai Buloh. He has three active national grants. He has published five indexed publications and nine of other publications. He is currently supervising one Master student. He is an active researcher in molecular aspect of familial hypercholesterolemia.

ORCID: 0000-0003-2387-0087

Alyaa Al-Khateeb

Institute of Pathology, Laboratory and Forensic Medicine (I-PPerForM), Faculty of Medicine, Universiti Teknologi MARA, Sungai Buloh, Selangor, Malaysia, 60129545014, alyaa@uitm.edu.my

Alyaa is an associate professor in Faculty of Medicine , Universiti Teknologi MARA who obtained her PhD from University Sains Malaysia , she is an expert in molecular medicine and clinical chemistry. She plays a role as a researcher in 15 grants. She also has published 36publications. She has successfully supervised two Ph.D. and two Master students to completion, and currently supervising another one active Ph.D. student.

ORCID: 0000-0002-4263-2191

Siti Hamimah Sheikh Abdul Kadir

Institute of Pathology, Laboratory and Forensic Medicine (I-PPerForM), Faculty of Medicine, Universiti Teknologi MARA, Sungai Buloh, Selangor, Malaysia, 60162128344, sitih587@uitm.edu.my

Siti Hamimah is an associate professor in Faculty of Medicine, Universiti Teknologi MARA who obtained her PhD from Imperial College of London, and has been actively engaged in cell-to-cell interaction field. She has successfully secured international and national research grants. She has published 76 indexed publications and 117 of other publications. She has supervised 9 Ph.D. and 9 Master students till completion. Currently, she is supervising another 5 Ph.D. and 7 Master students.

ORCID: 0000-0002-1671-4839

Acknowledgement

The authors gratefully acknowledge the financial support granted by the Malaysian Ministry of Education (MOE) [MOE/UiTM Grant Ref: 100-TNCPI/GOV 16/6/2 (002/2020)] and the United Kingdom's Medical Research Council (MRC) [MRC Grant Ref: MR/T017384/1] under the Newton-Ungku Omar Fund (NUOF): UK-Malaysia Joint Partnership Call on Non-communicable Diseases programme.

References

Al-Khateeb, A., Zahri, M.K., Mohamed, M.S., Sasongko, T.H., Ibrahim, S., Yusof, Z. and Zilfalil, B.A. (2011). Analysis of sequence variations in low-density lipoprotein receptor gene among Malaysian patients with familial hypercholesterolemia. *BMC Medical Genetics*, **12**(n/a), 1–11. DOI: 10.1186/1471-2350-12-40

Beheshti, S.O., Madsen, C.M., Varbo, A. and Nordestgaard, B.G. (2020). Worldwide prevalence of familial hypercholesterolemia: meta-analyses of 11 million subjects. *Journal of the American College of Cardiology*, **75**(20), 2553–66. DOI: 10.1016/j.jacc.2020.03.057

Birnbaum, R.A., Horton, B.H., Gidding, S.S., Brenman, L.M., Macapinlac, B.A. and Avins, A.L. (2021). Closing the gap: identification and management of familial hypercholesterolemia in an integrated healthcare delivery system. *Journal of Clinical Lipidology*, **15**(2), 347–57. DOI: 10.1016/j.jacl.2021.01.008

Bouhairie, V.E. and Goldberg, A.C. (2015). Familial hypercholesterolemia. *Cardiology Clinics*, **33**(2), 169–79. DOI: 10.1016/j.ccl.2015.01.001

Brown, M.S. and Goldstein, J.L. (1974a). Expression of the familial hypercholesterolemia gene in heterozygotes: mechanism for a dominant disorder in man. *Science*, **185**(4145), 61–3. DOI: 10.1126/science.185.4145.61

Brown, M.S. and Goldstein, J.L. (1974b). Familial hypercholesterolemia: defective binding of lipoproteins to cultured fibroblasts associated with impaired regulation of 3-hydroxy-3-methylglutaryl coenzyme A reductase activity. *Proceedings of the National Academy of Sciences*, **71**(3), 788–92. DOI: 10.1073/pnas.71.3.788

Cho, S.M.J., Lee, H.J., Shim, J.S., Song, B.M. and Kim, H.C. (2020). Associations between age and dyslipidemia are differed by education level: The Cardiovascular and Metabolic Diseases Etiology Research Center (CMERC) cohort. *Lipids in Health and Disease*, **19**(n/a), 1–12. DOI: 10.1186/s12944-020-1189-y

Chua, Y.A., Razman, A.Z., Ramli, A.S., Kasim, N.A.M. and Nawawi, H. (2021). Familial hypercholesterolaemia in the Malaysian community: prevalence, under-detection and under-treatment. *Journal of Atherosclerosis and Thrombosis*, **28**(10), 1095–107. DOI: 10.5551/jat.57026

Cuchel, M., Bruckert, E., Ginsberg, H.N., Raal, F.J., Santos, R.D., Hegele, R.A. and Wiklund, O. (2014). Homozygous familial hypercholesterolaemia: New insights and guidance for clinicians to improve detection and clinical management. A position paper from the Consensus Panel on Familial Hypercholesterolaemia of the European Atherosclerosis Society. *European Heart Journal*, **35**(32), 2146–57. DOI: 10.1093/eurheartj/ehu274

EAS Familial Hypercholesterolaemia Studies Collaboration. (2018). Overview of the current status of familial hypercholesterolaemia care in over 60 countries-the EAS Familial Hypercholesterolaemia Studies Collaboration (FHSC). *Atherosclerosis*, **277**(n/a), 234–55. DOI: 10.1016/j.atherosclerosis.2018.08.051

Futema, M., Taylor-Beadling, A., Williams, M. and Humphries, S.E. (2021). Genetic testing for familial hypercholesterolemia—past, present, and future. *Journal of Lipid Research*, **62**(n/a), n/a. DOI: 10.1016/J.JLR.2021.100139

Garcia, M., Mulvagh, S.L., Bairey Merz, C.N., Buring, J.E. and Manson, J.E. (2016). Cardiovascular disease in women: Clinical perspectives. *Circulation Research*, **118**(8), 1273–93. DOI: 10.1161/CIRCRESAHA.116.307547

Goldstein, J.L. and Brown, M.S. (1973). Familial hypercholesterolemia: identification of a defect in the regulation of 3-hydroxy-3-methylglutaryl coenzyme A reductase activity associated with overproduction of cholesterol. *Proceedings of the National Academy of Sciences*, **70**(10), 2804–8. DOI: 10.1073/pnas.70.10.2804

Goldstein, J.L. and Brown, M.S. (1974). Binding and degradation of low-density lipoproteins by cultured human fibroblasts: comparison of cells from a normal subject and from a patient with homozygous familial hypercholesterolemia. *Journal of Biological Chemistry*, **249**(16), 5153–62. DOI: 10.1016/s0021-9258(19)42341-7

Hevonoja, T., Pentikäinen, M.O., Hyvönen, M.T., Kovanen, P.T. and Ala-Korpela, M. (2000). Structure of low-density lipoprotein (LDL) particles: basis for understanding molecular changes in modified LDL. *Biochimica et Biophysica Acta (BBA)-Molecular and Cell Biology of Lipids*, **1488**(3), 189–210. DOI: 10.1016/s1388-1981(00)00123-2

Hu, P., Dharmayat, K.I., Stevens, C.A., Sharabiani, M.T., Jones, R.S., Watts, G.F. and Vallejo-Vaz, A.J. (2020). Prevalence of familial hypercholesterolemia among the general population and patients with atherosclerotic cardiovascular disease: A systematic review and meta-analysis. *Circulation*, **141**(22), 1742–59. DOI: 10.1161/CIRCULATIONAHA.119.044795

Iacocca, M.A., Chora, J.R., Carrié, A., Freiberger, T., Leigh, S.E., Defesche, J.C. and ClinGen FH Variant Curation Expert Panel. (2018). ClinVar database of global familial hypercholesterolemia-associated DNA variants. *Human Mutation*, **39**(11), 1631–1640. DOI: 10.1002/humu.23634

Kalra, S., Chen, Z., Deerochanawong, C., Shyu, K.G., San Tan, R., Tomlinson, B. and Yeh, H.I. (2021). Familial hypercholesterolemia in Asia Pacific: a review of epidemiology, diagnosis, and management in the region. *Journal of Atherosclerosis and Thrombosis*, **28**(5), 417–34. DOI: 10.5551/jat.56762

Khoo, K.L., Van Acker, P., Defesche, J.C., Tan, H., Van de Kerkhof, L., Heijnen-van Eijk, S. and Deslypere, J.P. (2000). Low-density lipoprotein receptor gene mutations in a Southeast Asian population with familial hypercholesterolemia. *Clinical Genetics*, **58**(2), 98–105. DOI: 10.1034/j.1399-0004.2000.580202.x

Liberati, A., Altman, D.G., Tetzlaff, J., Mulrow, C., Gøtzsche, P.C., Ioannidis, J.P. and Moher, D. (2009). The PRISMA statement for reporting systematic reviews and meta-analyses of studies that evaluate health care interventions: explanation and elaboration. *Annals of Internal Medicine*, **151**(4), W-65. DOI: 10.1371/journal.pmed.1000100

Lye, S.H., Chahil, J.K., Bagali, P., Alex, L., Vadivelu, J., Ahmad, W.A.W. and Mohamed, R. (2013). Genetic polymorphisms in LDLR, APOB, PCSK9 and other lipid related genes associated with familial hypercholesterolemia in Malaysia. *PloS One*, **8**(4), e60729. DOI: 10.1371/journal.pone.0060729

Marusic, T., Sustar, U., Sadiq, F., Kotori, V., Mlinaric, M., Kovac, J. and Groselj, U. (2020). Genetic and clinical characteristics of patients with homozygous and compound heterozygous familial hypercholesterolemia from three different populations: Case series. *Frontiers in Genetics*, **11**(n/a), 572176. DOI: 10.3389/fgene.2020.572176

McGowan, M.P., Hosseini Dehkordi, S.H., Moriarty, P.M. and Duell, P.B. (2019). Diagnosis and treatment of heterozygous familial hypercholesterolemia. *Journal of the American Heart Association*, **8**(24), e013225. DOI: 10.1161/JAHA.119.013225

Medeiros, A.M. and Bourbon, M. (2023). Genetic testing in familial hypercholesterolemia: is it for everyone?. *Current Atherosclerosis Reports*, **25**(4), 127–32. DOI: 10.1007/s11883-023-01091-5

Mickiewicz, A., Futema, M., Ćwiklinska, A., Kuchta, A., Jankowski, M., Kaszubowski, M. and Gruchała, M. (2020). Higher Responsiveness to Rosuvastatin in Polygenic versus Monogenic Hypercholesterolemia: A Propensity Score Analysis. *Life*, **10**(5), 73. DOI: 10.3390/life10050073

Migliara, G., Baccolini, V., Rosso, A., D'Andrea, E., Massimi, A., Villari, P. and De Vito, C. (2017). Familial hypercholesterolemia: a systematic review of guidelines on genetic testing and patient management. *Frontiers in Public Health*, **5**(n/a), 252. DOI: 10.3389/fpubh.2017.00252

Munn, Z., Moola, S., Lisy, K., Riitano, D. and Tufanaru, C. (2015). Methodological guidance for systematic reviews of observational epidemiological studies reporting prevalence and cumulative incidence data. *JBI Evidence Implementation*, **13**(3), 147–53. DOI: 10.1097/XEB.0000000000000054

Nordestgaard, B.G., Chapman, M.J., Humphries, S.E., Ginsberg, H.N., Masana, L., Descamps, O.S. and European Atherosclerosis Society Consensus Panel. (2013). Familial hypercholesterolaemia is underdiagnosed and undertreated in the general population: guidance for clinicians to prevent coronary heart disease: consensus statement of the European Atherosclerosis Society. *European Heart Journal*, **34**(45), 3478–90. DOI: n10.1093/eurheartj/eht273

Packard, C., Chapman, M.J., Sibartie, M., Laufs, U. and Masana, L. (2021). Intensive low-density lipoprotein cholesterol lowering in

cardiovascular disease prevention: opportunities and challenges. *Heart*, **107**(17), 1369–75.

Pek, S.L.T., Dissanayake, S., Fong, J.C.W., Lin, M.X., Chan, E.Z.L., Justin, I. and Tavintharan, S. (2018). Spectrum of mutations in index patients with familial hypercholesterolemia in Singapore: single center study. *Atherosclerosis*, **269**(n/a), 106–16. DOI: 10.1016/j.atherosclerosis.2017.12.028

Punzalan, F.E.R., Sy, R.G., Santos, R.S., Cutiongco, E.M., Gosiengfiao, S., Fadriguilan, E. and Laurie, A. (2005). Low Density Lipoprotein–Receptor (LDL-R) Gene Mutations among Filipinos with Familial Hypercholesterolemia. *Journal of Atherosclerosis and Thrombosis*, **12**(5), 276–83. DOI: 10.5551/jat.12.276

Qin, D. (2019). Next-generation sequencing and its clinical application. *Cancer Biology and Medicine*, **16**(1), 4. DOI: 10.20892/j.issn.2095-3941.2018.0055

Rallidis, L.S., Iordanidis, D. and Iliodromitis, E. (2020). The value of physical signs in identifying patients with familial hypercholesterolemia in the era of genetic testing. *Journal of Cardiology*, **76**(6), 568–72. DOI: 10.1016/j.jjcc.2020.07.005

Razman, A.Z., Chua, Y.A., Mohd Kasim, N.A., Al-Khateeb, A., Sheikh Abdul Kadir, S.H., Jusoh, S.A. and Nawawi, H. (2022). Genetic spectrum of familial hypercholesterolaemia in the Malaysian community: Identification of pathogenic gene variants using targeted next-generation sequencing. *International Journal of Molecular Sciences*, **23**(23), 14971. DOI: 10.3390/ijms232314971

Sharifi, M., Futema, M., Nair, D. and Humphries, S.E. (2019). Polygenic hypercholesterolemia and cardiovascular disease risk. *Current Cardiology Reports*, **21**(n/a), 1–6. DOI: 10.1007/s11886-019-1130-z

Tada, H., Okada, H., Nomura, A., Usui, S., Sakata, K., Nohara, A. and Kawashiri, M.A. (2021). Clinical Diagnostic Criteria of Familial Hypercholesterolemia- A Comparison of the Japan Atherosclerosis Society and Dutch Lipid Clinic Network Criteria. *Circulation Journal*, **85**(6), 891–7. DOI: 10.1253/circj.CJ-20-0901

Tanaka, N., Teramoto, T. and Yokoyama, S. (2019). Application of the Japanese guidelines for the diagnosis of familial hypercholesterolemia in general practice: It is to be validated in international harmonization. *Journal of Atherosclerosis and Thrombosis*, **26**(1), 93–8. DOI: 10.5551/jat.46979

Trapani, L. and Pallottini, V. (2010). Age-related hypercholesterolemia and HMG-CoA reductase dysregulation: Sex does matter (a gender perspective). *Current Gerontology and Geriatrics Research*, **2010**(1), 420139. DOI: 10.1155/2010/420139

Vrablik, M., Tichý, L., Freiberger, T., Blaha, V., Satny, M. and Hubacek, J.A. (2020). Genetics of familial hypercholesterolemia: new insights. *Frontiers in Genetics*, **11**(n/a), 574474. DOI: 10.3389/fgene.2020.574474

Wald, D.S. and Wald, N.J. (2019). Integration of child–parent screening and cascade testing for familial hypercholesterolaemia. *Journal of Medical Screening*, **26**(2), 71–5. DOI: 10.1177/0969141318796856

Wang, Y., Li, Y., Liu, X., Tu, R., Zhang, H., Qian, X. and Wang, C. (2019). The prevalence and related factors of familial hypercholesterolemia in rural population of China using Chinese modified Dutch Lipid Clinic Network definition. *BMC Public Health*, **19**(n/a), 1–7. DOI: 10.1186/s12889-019-7212-4

Woodward, M. (2019). Cardiovascular disease and the female disadvantage. *International Journal of Environmental Research and Public Health*, **16**(7), 1165. DOI: 10.3390/ijerph16071165

Zubielienė, K., Valterytė, G., Jonaitienė, N., Žaliaduonytė, D. and Zabiela, V. (2022). Familial hypercholesterolemia and its current diagnostics and treatment possibilities: a literature analysis. *Medicina*, **58**(11), 1665. DOI: 10.3390/medicina58111665

Scientific Journal of King Faisal University:
Basic and Applied Sciences

Using Machine Learning to Analyze Emotions in Arabic and Dialectical Texts

Dina Abdelnaser Hamed [1], Ben Bella Said Tawfik [2] and Mohamed Abdullah Makhlouf [2]

[1] Department of Information Technology, Faculty of Information Technology and Computer Science, Sinai University, Arish, Egypt.
[2] Department of information systems, Faculty of computers and informatics and computer science, Suez Canal university, Ismailia, Egypt.

LINK	RECEIVED	ACCEPTED	PUBLISHED ONLINE	ASSIGNED TO AN ISSUE
https://doi.org/10.37575/b/sci/240014	21/03/2024	01/10/2024	01/10/2024	01/12/2024

NO. OF WORDS	NO. OF PAGES	YEAR	VOLUME	ISSUE
7690	9	2024	25	2

ABSTRACT

Social media is an imperative necessity in contemporary life. People can easily express their emotions and share moments on social media by writing a few words. Organizations approach Twitter as a rich data source that may be used to study emotions, but while many efforts have focused on sentiment analysis from text, emotion classification has received less attention. Emotion analysis usually provides a more in-depth assessment of the author's feelings, and in this research, we propose a dialectal Arabic text emotion classification architecture that accurately classifies the expressions into four emotions (anger, joy, fear, and sadness). Considering the improvements in natural language processing (NLP), we investigated the Bidirectional encoder representations from transformers (BERT) model. We implemented our proposed ensemble model via a majority voting technique that merges the best three versions of the pre-trained BERT models that are considered state-of-the-art in the classification field. We compared the results of our model with eight other machine learning classifiers and ten versions of the BERT model. The proposed ensemble approach accomplished around 84%, however the highest accuracy of the other investigated models was 76%. The presented experiments were examined on the Arabic tweets' dataset for the EI-OC task provided by SemiEval, which contains 5600 tweets.

KEYWORDS

text classification, fine-tuning, voting technique, naive bayes, augmentation, transformers

CITATION

Hamed, D.A., Tawfik, B.B.S. and Makhlouf, M.A. (2024). Using machine learning to analyze emotions in Arabic and dialectical texts. *Scientific Journal of King Faisal University: Basic and Applied Sciences*, **25**(2), 22–30. DOI: 10.37575/b/sci/240014

1. Introduction

In our daily life, we use a variety of facial expressions, vocal activities, and written material to express our emotions, prompting researchers to conduct emotion analysis. The majority of recently presented studies concentrate on sentiment analysis as positive and negative (Medhat *et al.*, 2014), but few go deeper to extract emotions from written text. In this work, we focus on emotion analysis from written text. A large number of researchers have introduced various new techniques and methods for emotion analysis in several languages such as English, Chinese and Persian, but very few have looked at the Arabic language and dialects.

Arabic ranks as the fifth most spoken language in the world and is the official language of more than 27 countries. More than 456 million Arabs speak the language, and Arabic Social Networks are the fastest-growing social networking sites in terms of languages used. Over the last five years, more than 237 million Arabs have used social media (Istizada, 2023). Emotion significantly impacts human cognitive processes, such as perception, focus, memory retention, logical thinking, and problem-solving. It has a significant effect on attention, while stimulating behavior and activity. Emotion analysis is an important field of study faces many challenges because of how complicated natural languages are, and because it is difficult to comprehend and measure how people express their feelings mathematically. Studies are in continuous development to prove that emotion analysis is an extremely useful and powerful marketing tool that helps product managers understand customers' emotions and opinions. It is important to improve a promotion's success, product acceptance, and customer satisfaction.

Organizations are also trying to analyze posts, comments, and discussions to extract all possible information about whether or not they are interested in a particular topic (Storey & O'Leary, 2024) and the level of user satisfaction toward a specific product or service. They focused on emotional marketing by trying to stimulate people's emotions to buy products or services. On the other hand, emotion analysis can indicate the success or failure of some governmental or non-governmental institutions in some of the tasks assigned to them, such as safety, stability, and good performance. It can also be used as a special code between members of the same organization as a kind of privacy and to facilitate the workflow with high efficiency.

The novelty of this paper lies in proposing a robust adaptive model to accurately classify Arabic text into four emotions: anger, joy, fear, and sadness. Taking advantage of advances in natural language processing (Wolf *et al.*, 2020), we explored the BERT model and implemented a group approach that integrated the three best versions of the pre-trained BERT model via the majority voting technique. Our proposed approach competes with the state of the art classification.

We compared the performance of our approach to eight other machine learning classifiers and ten versions of the BERT model. The proposed classification method achieved an accuracy of about 84%, outperforming the highest accuracy of 76% achieved by other models. We conducted experiments on a dataset of Arabic tweets for the EI-OC mission provided by SemiEval, which included about 5,600 tweets. Our findings demonstrate the effectiveness of the proposed group approach in accurately categorizing emotions in the Arabic script.

The remainder of this work is organized as follows: Relevant works are shown in Section 2, background information is shown in Section 3, methodology and our model are presented in Section 4, experiments and results analysis are presented in Section 5, and the conclusion is presented in Section 6.

2. Related Work

In recent years, research connected to emotion analysis has made efforts to employ machine learning approaches. This section covers a number of studies that employ machine learning algorithms to analyze user opinions, sentiments, and product evaluations found in web material.

A. Singh *et al.* (2016) compared algorithms for supervised machine

Corresponding Author: Dina Abdelnaser Hamed 00201015668988, dina.hamed@su.edu.eg

learning classifications that were designed to classify data based on prior knowledge; analyze the accuracy, learning speed, complexity, and risk of overfitting; measure the effectiveness of supervised machine learning algorithms; and compare them broadly with several machine learning techniques. According to Abdullah and Shaikh (2018), the UNCC technology examines tweets in English and Arabic to determine emotions. They presented the identical design in both languages for each of the five challenges. The system's main input is a set of psycholinguistic characteristics and a mix of word2vec and doc2vec embeddings (for example, Affective Tweets from the Weka-package). They acquire much higher Spearman correlation scores when they use a fully connected neural network design.

Daood *et al.* (2017) focused on Arabic emotion categorization. They collected a set of Arabic tweets from the Levant and marked them with their desired sentiments and employed a number of ways to categorize user text messages in order to ascertain their emotional states. They analyzed the results of multiple machine learning algorithms, taking numerous factors into consideration to reach the best emotion recognition result. According to Mohammad *et al.* (2018), they are the results of the SemEval-2018 Task, which comprises numerous subtasks on extrapolating a person's level of productivity from their tweets. They generated tagged data from tweets in English, Arabic, and Spanish for each assignment. The separate tasks were Emotion Classification, Emotion Intensity Ordinal Classification, Emotion Intensity Regression, and Valence (Sentiment) Regression. They presented an overview of the techniques, resources, and tools employed by the participating organizations, focusing on the most beneficial. They also looked at the underpinnings of a trustworthy proclivity for a certain race or gender.

Context-aware Geted Recurrent Units(C-GRU) were introduced by A. E. Samy *et al.* (2018), which assessed the context (themes) of tweets and utilized them as an extra layer to infer the thoughts that the tweet was attempting to communicate. By determining the weights that each sub-modal contributed to the predictions (from subjects and sentences), the multi-modal model combined the two learned outputs.

Abdullah *et al.* (2020) developed an approach for recognizing and categorizing emotions in Arabic tweets by employing anger, sadness, pleasure, and disgust. The results of the studies demonstrated the usefulness of the suggested models, which enhanced the state of the art for categorizing Arabic tweets using support vector machines (SVM) and naive Bayes (NB), which produced the best results.

Alswaidan and Menai (2020) developed three models for emotion identification in Arabic text: a deep feature-based (DF) model, a human-engineered feature-based (HEF) model, and a combination model (HEF+DF). Comparing the performances of the suggested models on each emotion label allowed them to determine how well they performed on the IAEDS, AETD, and SemEval-2018 datasets. He also compared the model's results to those of other cutting-edge models. The results show that the HEF+DF model outperformed the DF and HEF models across all datasets.

Elnagar *et al.* (2020) thoroughly analyzed several deep learning models for categorizing Arabic text to see how well they performed and investigated the influence of using word2vec embedding models to improve classification task performance.

Khalil *et al.* (2021) created a Bi-LSTM deep learning model to categorize emotions (EC) in shared Arabic tweets for the SemEval-2018 competition. They have consolidated the dataset files into a single file to be used in the cross-validation technique. Aravec with CBOW was used in the word embedding stage. According to their statistics, Jaccard Accuracy was 0.498, Precision was 0.695, Recall was 0.551, and F1 Score was 0.615.

Kamila *et al.* (2022) used a multi-task framework to create four emotion labels (anger, joy, fear, and sorrow) with intensity values and three temporal orientation labels (past, present, and future) from user tweets. The detected tweets for each user were pooled to determine the user's temporal orientation and sentiment. They explored how users' emotional states and temporal orientations interact with one another. According to this research, anger and happiness are associated with future orientation, but sorrow and fear are associated with historical orientation.

Alzanin *et al.* (2022) recently assessed three classifiers, Support Vector Machine (SVM), Gaussian Naive Bayes (GNB), and Random Forest (RF), to classify Arabic text tweets into five groups based on linguistic features and content. They also looked at two alternative textual representations: term frequency-inverse document frequency and word embedding with Word2vec. In our review of related works, we highlighted several studies that addressed emotion classification in Arabic text using various machine learning algorithms. While these studies provided valuable insights into different methodologies and techniques, they often lacked comprehensive evaluations that directly compare the effectiveness and performance metrics of the proposed approaches. Singh *et al.* (2016), for instance, compared supervised machine learning classifiers across accuracy, learning speed, and complexity but did not benchmark against a unified dataset or standard evaluation metrics. Similarly, Abdullah and Shaikh (2018) and Daood *et al.* (2017) focused on emotion detection in Arabic tweets using specific models like SVM and neural networks, yet their evaluations primarily emphasized individual model performance rather than comparative analysis against other state-of-the-art methods. Our work addresses this gap by systematically evaluating our ensemble pretrained BERT model against a diverse set of baseline classifiers, demonstrating significant improvements in accuracy and robustness across emotion categories, and provides a clearer perspective on the advancements and impact of our proposed methodology in the field of Arabic emotion classification.

3. Background

In this section, we will present a brief review of the transformer architecture and the main classification algorithms.

3.1. Transformer Architecture:

The transformer architecture is a deep learning model designed for natural language processing (NLP) introduced in 2017 that utilizes self-attention to capture long-range dependencies within input sequences (Vaswani *et al.* 2017). The transformer architecture has transformed the field of NLP by enabling models to attend to different parts of the input sequence and generate more accurate outputs. The transformer architecture consists of an encoder-decoder framework, with the encoder generating hidden representations of the input sequence and the decoder generating the output sequence. The self-attention mechanism computes attention weights for each input token, determining the level of attention each token should receive when computing the next hidden representation. This architecture has been widely used in NLP tasks, and pre-trained transformer models such as BERT and GPT-2 (Qian *et al.* 2022) have achieved state-of-the-art performance on many benchmarks (Yagi *et al.* 2023).

As seen in Figure 1, computers cannot understand words, thus in the word embedding stage, they take the input text and turn the words into vectors of numbers. The positional vector, which provides context based on the location of each word in the sentence, is then added to provide word embedding with context information in a vector of numbers. The transformer architecture consists of the

encoder, decoder, and final linear layer. The linear layer takes the decoder's output as input and outputs it.

3.1.1. Encoder Layer

Each multi-head attention block (with padding mask) at the encoder layer receives three inputs: Q as question, V as value, and K as key. These are processed through linear (dense) layers before the multi-head attention function, which entails determining which portion of the input to focus on by creating distinct attention vectors and calculating the weighted average attention vector for each word in the phrase. The feed-for-word step is a basic feed-for-word neural network that is applied to each attention vector to make it more digestible so that it may be put to the next decoder block or linear layer based on its position.

3.1.2. Decoder Layer

The decoder module takes the output of the encoder as input and generates the output sequence, the masked multi-head attention (input should be masked) at the decoder layer displays as a vector of weighted values to show how strongly each word is connected to the other word in the same phrase. There is also multi-head attention (with padding mask) because Q receives the decoder's first attention block output, V and K receive the encoder output as inputs, and the attention weights describe the priority given to the decoder's input depending on the encoder's output. In other words, the decoder anticipates the next token by seeing the encoder output and self-attending to it. Point-wise feed-forward networks provide the same function as the encoder layer's equivalent step.

Figure 1. Transformers Architectures

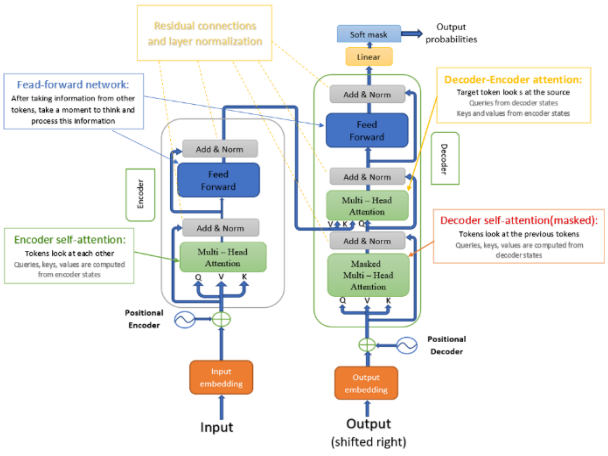

3.2. The Main Classification Algorithms:

3.2.1. Support Vector Machine Algorithm (SVM)

The Support Vector Machine is one of the most extensively used supervised learning algorithms for classification and regression problems (Ye *et al.* 2009). The goal of the SVM method is to find the optimal line or decision boundary that divides n-dimensional space into classes, allowing us to simply categorise new data points in the future. This ideal decision boundary is referred to as a hyperplane. In SVM, we employ two alternative classifiers (Support Vector classifier (SVC) and Linear Support Vector classifier (Linear SVC). The main distinction is that Linear SVC minimises squared hinge loss, whereas SVC minimises regular hinge loss. Linear SVC allows you to manually draw a 'hinge' string for loss parameters.

3.2.2. Naive Bayes Algorithm (NB)

NB is a classification approach that is based on the Bayes Theorem and the concept of predictor independence (Venkatesh *et al.* 2020). To put it simply, a Naive Bayes classifier believes that the existence of one feature in a class has nothing to do with the presence of any other feature. It organizes critical information and anticipates the target or dependent variable values generated by an independent or predictor variable. In NB, we employ two distinct algorithms (Multinomial NB and Bernoulli NB). Multinomial NB is concerned with counts for several features that occur, whereas Bernoulli NB is concerned with counts for a single feature that occurs as well as counts for the same feature that does not occur.

3.2.3. Stochastic Gradient Descent Algorithm (SGD)

SGD is a prominent and widely used method in Machine Learning algorithms (Yousaf *et al.* 2020). Gradient simply refers to the slope or tilt of a surface. To get to the lowest point on the surface, one must descend a slope.

3.2.4. Decision Tree Algorithm

The Decision Tree (DT) function generates a classification structure that resembles a tree (Mendonça *et al.* 2007). It divides the main facts into classes and predicts the values of the target or dependent variable that is constructed using an independent or predictor variable.

3.2.5. Random Forest Algorithm

Random Forest is a common data science technique for obtaining judgments based on random trees (Breiman, 2001). It is made up of several separate decision trees that work together as a single unit. The successful prediction model is the class that earns the most votes from all of the trees in the random forest.

3.2.6. K Neighbors Algorithm

K Neighbors Algorithm is a machine learning algorithm that is built on the Euclidean distance between instance (Kadhim, 2019). It predicts class labels for each instance and discovers the Nearest k examples by computing the smallest Euclidean distance between each instance and the others.

4. Methodology

In this stage, we will provide the dataset used in the research as well as our proposed approach for analyzing emotions from Arabic tweets using multiple machine learning classification algorithms and comparing the trials to determine the best methodology that can be applied in this sector. Using the Python programming language, we implement these models and assess the outcomes.

4.1. Data Set:

4.1.1. Original Dataset

In our research, we utilized a standard dataset of Arabic tweets given by SemiEval for the EI-OC task 1 [8]. This dataset contained 5600 tweets, 60% of the data, with 3,376 tweets for the training set divided into 889 for joy, 882 for anger, 877 for fear, and 728 for sadness. The testing and validation sets made up 40%, with 1,563 tweets for the test set divided into 448 for joy, 373 for anger, 372 for fear, and 370 for sadness, and 661 tweets for the development set divided into 224 for joy, 150 for anger, 146 for fear, and 141 for sadness. Each set contained the specified emotional labels: anger, fear, joy, and sadness.

4.1.2. Augmented Dataset

To expand the dataset, we used the contextual word embedding augmentation technique to take some sentences and replace words with other words with the same meaning as predicted by a label-conditioned bi-directional language model. For example, " مبجبش عشان لو حتى التهديد مبجبش" was replaced with "مصلحتي في لو حتى التهديد" and "شعرت باللامبالاة أثناء الاجتماع الطويل" was replaced with " مصلحتي شعرت بالملل أثناء الاجتماع الطويل", and then we appended the new sentence to the dataset. This step was only performed on the training

set, which increased the number of tweets from 3,376 to 4,215.

4.2. Data preprocessing:

Text preprocessing is important in creating any word embedding model because it can greatly impact the outcomes. Given that our dataset was in Arabic, we performed a specific preprocessing to identify the most effective pattern. The primary preprocessing steps used are outlined in the following subsections:

4.2.1. Tokenization

The preprocessing module starts here. separates the textual input into words or tokens, each separated by a delimiter (such as a space or a punctuation mark). The tokenization procedure produces a list of terms (Grefenstette ,1999).

We used the Arabic-specific tokenization tools provided by libraries such as the Natural Language Toolkit (NLTK) or custom tokenization scripts tailored for our specific dataset. These tools ensure that the tokenization process preserves linguistic nuances and handles Arabic script complexities effectively. Each token typically represents a word or a sub-word and serves as the basic building block for further text processing tasks like sentiment analysis and emotion classification. For example:

Original Text: "أحب القراءة والكتابة في وقت الفراغ."

Word Tokenization Output: ['أحب', 'القراءة', 'والكتابة', 'في', 'وقت', 'الفراغ', '.']

Sub-word Tokenization Output: ['أحب', 'القراء', 'ة', 'والكتاب', 'ة', 'في', 'وقت', 'الفراغ", '.']

4.2.2. Normalization

It is necessary to preprocess the text to remove noise and normalize some letters to make Arabic text clearer and more helpful in enhancing classification, so we clean the data as follows:

a) Replace various characters, which can be written in a variety of ways, with the normal form as "أ","آ" replaced with "ا" .
b) Remove links and mentions.
c) Remove all diacritical marks as indicated in Table 1.
d) Remove the elongation 'tatweel' character '_', which is used to expand words (for example, the word 'خطيـر' may convert to the normal form).
e) Remove all punctuation marks like periods, question marks, exclamation points, commas, colons, semicolons, dashes, hyphens, brackets, braces, parentheses, apostrophes, quotation marks, and ellipses.
f) Remove numbers.
g) Remove Latin characters (Aa, Zz).
h) Remove repeated characters. When describing an action, such as laughing" هيهيهيهه ", users frequently purposefully repeat a character in a word: awe-inspiring" واااااااو indignant, indignant"لاااااااااااا", etc. Every other repeating character was removed since we reasoned that a word could only have two repetitions.
i) We Replace emojis with their meaning in words, as shown in Table 2 (Singh *et al.* 2019), because emojis are common in social media and have great importance in enhancing the meaning of the sentence and expressing the writer's feelings, so we cannot ignore them.

Table 1. Diacritics

Diacritical marks التشكيل				
Tanween with Shaddah	Tanween تنوين	Short vowels with Shaddah شدة	Short vowels	Pronunciation
ـًّ	ـً	ـَّ	ـَ	fatHah فتحة
ـٍّ	ـٍ	ـِّ	ـِ	Kasrah كسرة
ـٌّ	ـٌ	ـُّ	ـُ	DHammah ضمة
		ـّ	ـْ	Sukuun سكون

Table 2. Emojis and their textual description

Emoji	Description
😂	Face with tears of joy
😘	Face blowing a kiss
😄	Grinning face with smiling eyes
😌	Relieved face
😝	Squinting face with tongue
😥	Sad but relieved face
😡	Angry face
😭	Loudly crying face
😓	Downcast face with sweat
😰	Anxious face with sweat

4.2.3. NLP Approach

In this approach, we use the transformer learning technique [19], where an NLP model trained on a very large dataset such as the Common Crawl and Wikipedia Corpus performs. Similar tasks on another dataset can be fine-tuned for specific tasks, which calls for a pre-trained model that adopts the mechanism of self-attention (Dai *et al.* 2020). It is like recurrent neural networks (RNNs) (Bullinaria, 2013) in processing sequential input data, but it works in parallel and inputs all at once, unlike other neural networks, so the attention mechanism provides context for every position in the input sequence.

4.2.4. Proposed Ensemble Model

BERT and GPT-2 are the most important transformer-based models. In this work, we will focus on a pre-trained BERT model and learn how to compare its various models and work on them to perform text classification. Figure 2 illustrates the overall architecture of our system, which consists of four steps: text preprocessing, pretrained BERT fine-tuning, prediction, and voting.

Figure 2. Proposed ensemble model flowchart

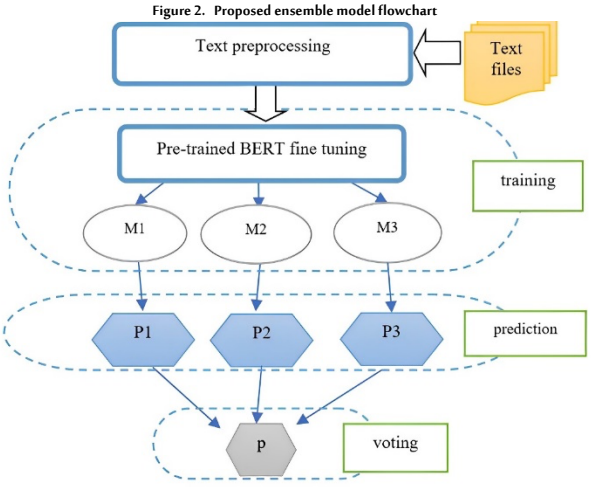

4.2.5. Pretrained BERT Fine-tuning

In this step, we work on the pre-trained BERT and fine-tune it for our Arabic data set. To do that, we connect the BERT outputs to an additional layer involving the SoftMax classifier after the fine-tuning to predict the text label. In the beginning, we tokenize every sentence into N tokens and add the [CLS] token at its beginning, the [CLS] token is a special token added to the beginning of each input sentence during tokenization. It stands for 'classification' and is utilized in tasks where the model needs to make a prediction based on the entire input sequence. The final hidden state corresponding to the [CLS] token after processing by BERT serves as the aggregated representation of the entire input sequence, which is then used as input to subsequent

classification layers, such as the SoftMax classifier, to predict the text label.

After that, for each token i, we create an input representation called Ei by adding its vector embeddings. Then, we feed the Ei vectors into BERT and fine-tune its parameters using the corpus labelled data. As shown in Figure 3, We put h for the special [CLS] token's final hidden vector and Ti for the i-th input token's final hidden vector. Finally, to obtain the probability distribution for the projected output category, we use the final hidden state h as the representation of the entire text as an input for the feed-forward layer with the SoftMax classifier (Sun *et al.* 2019).

$$P(c/h) = Softmax(Mh) \quad (1)$$

Equation (1) represents a way to calculate the probability of a target variable c, given a context or condition h. The equation uses a vector of scores Mh, which calculates the probability of each possible value of c given h. The Softmax function is applied to this vector to obtain a probability distribution over the possible values of c, where M is our task-specific parameter matrix. During fine-tuning, all parameters from BERT and M are trained jointly to maximize the log-probability of the correct category.

Figure 3. The fine-tuned BERT diagram

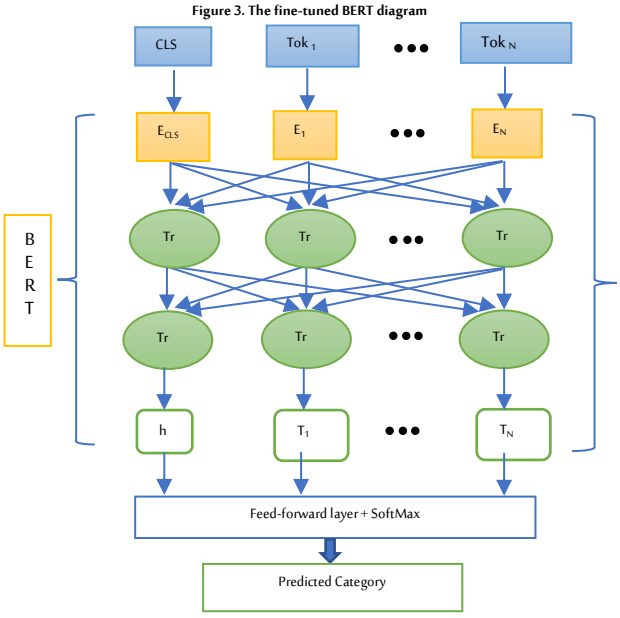

4.2.6. Voting Technique

We use a voting technique to reduce the complexity of ensemble models (Tiwari *et al.* 2024). In this step, each member of the ensemble model makes an equal contribution in parallel by giving a vote based on their predictions (Mohammed & Kora, 2022). There are two strategies of voting technique: soft voting by taking the average of the predicted results, or hard voting, that were adopted in our research, as shown in Figure 4. We take the best prediction by aggregating the scores of each predicted label for the three models and taking the highest score for the different results. We can see that if two or three make the same decision, we will take the top rating. If each model predicts a different answer, we will take the prediction that has the highest score.

If all opinions of all models have the same scores, then the prediction in this case will be the class that not only received the same score from all models, but also received the highest overall score across all models with the scores for each predicted label across all three models.

Figure 4. Hard voting technique

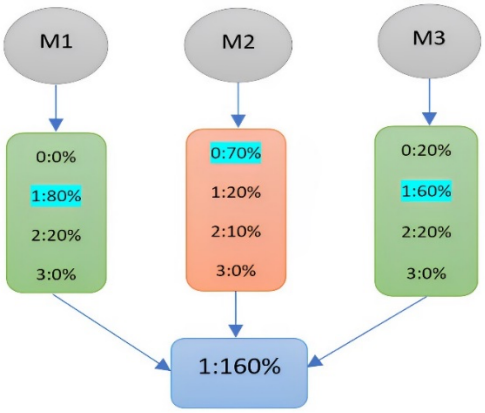

4.3. Machine Learning Approach:

In this approach, we applied eight supervised ML algorithms such as (linear SVC, SVC, multinomial NB, Bernoulli NB, SGD classifier, random forest classifier, decision tree classifier, and K Neighbors classifier. We show the ML architecture in a simple diagram in Figure 5 that shows the steps we followed for classifying the emotions of Arabic text into four emotion classes: anger, fear, joy, and sadness.

In the second phase, feature extraction and selection are carried out once the text has been prepared for processing. This section involves deleting irrelevant, redundant, and noisy data to obtain the best features that enhance the sentiment analysis procedure.

Figure. 5. Machine learning classification diagram

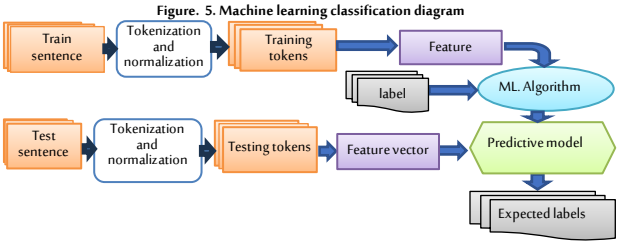

4.3.1. Features Selection

Many text features have been exploited in Sentiment Analysis (SA) research. The most popular ones are negation, n-grams, part of speech (POS), and term frequency. In our work, we use n-gram. The n-gram is a continuous string of n words taken from a prescribed sequence of text.

4.3.2. Features Extraction

In this phase, a piece of text is transformed into a feature with a specific weight to create each feature. There are various weighting methods, such as Boolean, Term Frequency (TF), and Term Frequency-Inverse Document Frequency (TF-IDF) (Rajaraman & Ullman, 2011). It uses the TF-IDF Vectorizer, a simple technique to vectorize text documents that transform sentences into a feature vector of numbers to be compatible with classifiers in the classification stage.

4.3.3. Machine Learning Classification

After getting, reading, preprocessing, and vectorizing the dataset by the TF-IDF Vectorizer, we proposed an adaptive emotion classification model for Arabic text into four emotional classes: anger, joy, fear, and sadness, using a broad, comprehensive set of machine learning classifiers. This model works on eight supervised ML algorithms such as linear SVC, SVC, multinomial NB, Bernoulli NB, decision tree classifier, SGD classifier, random forest classifier, and K-Neighbors classifier. Each algorithm is described in detail in this section.

5. Experiments and Results

In this paper, we work on several experiments to achieve the proposed model for Arabic text classification. We use the BERT model for Arabic text (Antoun *et al.* 2020), which has been pre-trained on 200 million phrases in Arabic, about 8.2 billion words, or 77 GB of text content. It features 512 maximum sequence lengths, 12 attention heads, 12 encoder blocks, 768 hidden dimensions, and 110 M parameters. We examine 10 new versions of this model and select the best three models to build our proposed ensemble model: bert-base-arabertv2, bert-medium-Arabic, and bert-large-arabertv02-twitter. We evaluate our proposed ensemble BERT model against other machine learning algorithms.

5.1. Analysis of Different BERT Models for Arabic Text Classification:

We trained ten different transformer models (Alammary, 2022) and evaluated their performance based on the training loss, validation loss, and F1-score. From these evaluations, we selected the three models that performed the best, which were the bert-base-arabertv2, bert-medium-Arabic, and bert-large-arabertv02-twitter models. Table 3 shows the results of the last epoch for each of the ten models, including their training loss, validation loss, and F1-score. The bert-base-arabertv2, bert-medium-Arabic, and bert-large-arabertv02-twitter models had the lowest training and validation losses and the highest F1-score, indicating that they performed the best overall. Therefore, we used these three models in the validation and test phases of our proposed ensemble model.

Table 3. Results of last epoch in each BERT model

Transformers model name	Training Loss	Validation Loss	F1-score
aubmindlab/bert-base-arabertv2	0.817400	0.972181	0.711044
aubmindlab/bert-large-arabertv2	1.403100	1.390501	0.220877
asafaya/bert-mini-Arabic	0.935900	1.096127	0.562784
asafaya/bert-medium-Arabic	0.710900	1.110692	0.692890
asafaya/bert-large-Arabic	1.400800	1.421856	0.226929
Distilbert-base-multilingual-cased	0.856100	1.223140	0.614221
nlptown/bert-base-multilingual-uncased-sentiment	0.816600	1.338099	0.594554
bert-large-arabertv02-twitter	0.664000	0.760911	0.757943
xlm-roberta -base	1.002700	1.036626	0.630862
xlm-roberta-large	1.392200	1.418853	0.220877

5.2. Evaluation Experiments:

As demonstrated in this experiment, we made a comparison between training the three selected models on the original data set and the augmented data set after appending the augmented sentences.

The results presented in Table 4 show the performance of the three selected BERT models of the last epoch in the training step, namely bert-base-arabertv2, bert-medium-Arabic, and bert-large-arabertv02-twitter, on both the original and augmented datasets. The models were evaluated based on their training loss, validation loss, and F1 score.

The bert-large-arabertv02-twitter model achieved the highest F1-score of 0.757943 on the original dataset and 0.753404 on the augmented dataset, followed by the bert-base-arabertv2 with an F1-score of 0.715582 on the original dataset and 0.670197 on the augmented dataset, and the bert-medium-Arabic with an F1-score of 0.694402 on the original dataset and 0.682300 on the augmented dataset.

Overall, the results suggest that the performance of the models varied depending on the quality of the dataset, with models performing better on the original dataset than the augmented dataset, which means that adding synonyms significantly confuses the results.

Table 4. Results of last epoch in the 3 best BERT models we used in our proposed model

Model	Faze	Training Loss	Validation Loss	F1-Score
bert-base-arabertv2	original	0.781600	0.896417	0.715582
	augmented	0.578800	1.106806	0.670197
bert-medium-Arabic	original	0.780700	0.910520	0.694402
	augmented	0.574400	1.196405	0.682300
bert-large-arabertv02-twitter	original	0.664000	0.760911	0.757943
	augmented	0.548300	0.914224	0.753404

We performed the voting step using the three best-performing models (bert-base-arabertv2, bert-medium-Arabic, and bert-large-arabertv02-twitter) and found that the F1-score increased by 9%. We then validated our ensemble model on a new dataset that included augmented sentences and compared the results with those obtained from the original dataset. However, we found that the results obtained using the augmented dataset were worse than those obtained using the original dataset, as shown in Table 5. The results suggest that the proposed ensemble model did not perform better on the augmented dataset, contrary to the researchers' expectations, due to the complexity of the Arabic language and the fact that a word carries more than one meaning depending on its presence in the sentence and its relationship to the words next to it. The augmentation process caused dispersion in the model used and led to worse results than using the original database.

Table 5. Classification report

	Dev (validation set)-original			Test-original		
emotion	precision	recall	f1-score	precision	recall	f1-score
anger	0.82	0.7	0.76	0.8	0.79	0.8
fear	0.8	0.86	0.83	0.86	0.84	0.85
joy	0.9	0.93	0.92	0.91	0.92	0.92
sadness	0.66	0.71	0.69	0.77	0.79	0.78
accuracy			0.82			0.84
	Dev-augmented			Test-augmented		
emotion	precision	recall	f1-score	precision	recall	f1-score
anger	0.84	0.63	0.72	0.85	0.69	0.76
fear	0.81	0.91	0.86	0.80	0.86	0.83
joy	0.91	0.9	0.9	0.92	0.92	0.92
sadness	0.6	0.75	0.66	0.71	0.80	0.75
accuracy			**0.81**			**0.82**

In our research paper, we analyzed the results obtained from our emotion classification model and used a confusion matrix to clearly visualize the performance of the model on both the original dataset and the augmented dataset. Figure 6 (a) displays the confusion matrix for the validation results on the original dataset, representing the true prediction labels and the missed ones for each of the four classes. The diagonal line of the confusion matrix shows the number of predictions where the classifier correctly predicted the emotion label, while the other numbers indicate the missed predictions. Similarly, Figure 6 (b) displays the results of the test step on the original dataset.

To further evaluate the effectiveness of our model, we also analyzed the performance on the augmented dataset. Figure 6 (c) represents the validation results on the augmented dataset, and Figure 6 (d) displays the results of the test step on the augmented dataset. By comparing the results from the original and augmented datasets, we can observe a clear difference in the number of missed predictions between different emotions. Specifically, we found that the highest number of missed predictions was between anger and sadness. These findings suggest that our model may need further improvement to better distinguish between these two emotions. Overall, our analysis of the confusion matrix provides a comprehensive understanding of the performance of our emotion classification model and highlights areas for potential improvement.

Figure 6. Confusion matrices for dev. and test results on original and augmented datasets

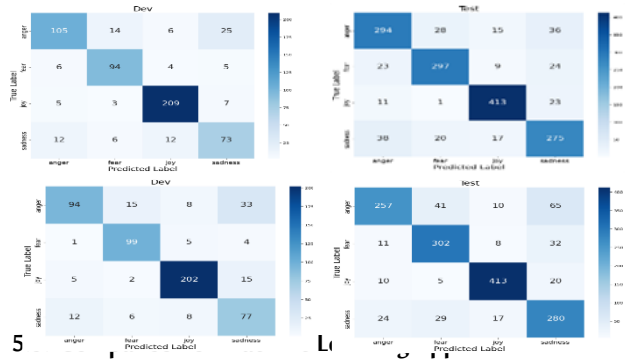

5 [illegible]

Our research aimed to compare the performance of eight machine learning algorithms with three n-grams (uni-gram, bi-gram, tri-gram) in text classification (Wynne & Wint, 2019) (Euna *et al.* 2023). We evaluated the performance of each algorithm by calculating accuracy, precision, recall, and f1-score, and summarized the results in Table 6. Our findings indicate that the uni-gram approach provided the best results across all algorithms tested. In addition, we observed that the linear support vector classifier (SVC) achieved the highest accuracy, with a F1-score of 59.8%.

However, we also developed a proposed ensemble model and compared its performance with that of the eight machine learning algorithms tested. Our experimental results showed that our proposed ensemble model achieved a significant improvement in accuracy, with an F1-score of 84%, compared to the 60% accuracy obtained by the linear SVC model.

These findings demonstrate that our proposed ensemble model offers a promising approach to improving the accuracy and reliability of text classification tasks and has important implications for the field of natural language processing. By using a combination of several machine learning techniques, our ensemble model was able to outperform the individual models, highlighting the value of ensemble techniques in improving text classification performance. F1-score is the harmonic mean of a system's precision and recall values. It can be calculated by the following formula (Yacouby & Axman, 2020) to make a clear comparison with the same measure. By calculating the F1-score for the classifiers, the linear SVC classifier achieved the best result with 59.8%.

$$F1 - score = 2 * (precision * recall)/(precision + recall) \quad (2)$$

Table 6. results of ML classifiers

Algorithm	gram	accuracy	precision	Recall
Linear SVC	1	0.601	0.598	0.601
	2	0.600	0.598	0.600
	3	0.596	0.595	0.596
SVC	1	0.560	0.612	0.560
	2	0.486	0.607	0.486
	3	0.440	0.630	0.440
MultinomialNB	1	0.581	0.628	0.581
	2	0.568	0.624	0.568
	3	0.561	0.622	0.561
Bernoulli-NB	1	0.511	0.615	0.511
	2	0.375	0.640	0.375
	3	0.316	0.682	0.316
SGD Classifier	1	0.585	0.580	0.585
	2	0.589	0.589	0.589
	3	0.587	0.585	0.587
Decision Tree	1	0.289	0.318	0.289
	2	0.289	0.318	0.289
	3	0.289	0.318	0.289
Random Forest	1	0.239	0.362	0.239
	2	0.237	0.278	0.237
	3	0.235	0.056	0.235
K-neighbors	1	0.432	0.517	0.432
	2	0.423	0.513	0.423
	3	0.419	0.502	0.419

5.4. Comparison With Previous Works:

Our research focused on evaluating the performance of our proposed ensemble BERT model compared to previous related work that used the same dataset. Our objective was to determine the effectiveness of our approach in tackling the SemEval 2018 EL-OC task1 dataset, a challenging task in the field. Our experimental results showed that our ensemble BERT model achieved the best results in accuracy, with an improvement of +8.5% compared to the previous best-performing model.

To compare the performance of our proposed model with previous work, we tested our results over the SemEval 2018 EL-OC task1 dataset and compared them with the results published in previous publications. Specifically, we compared our results with those obtained by Kamila *et al.* (2022). Our proposed model achieved an F1-score of 0.83 and an accuracy of 0.84, which represents a significant improvement over the results achieved by Kamila *et al.* (2022), who achieved an F1-score of 0.731 and an accuracy of 0.753.

Overall, our results demonstrate that our proposed ensemble BERT model is highly effective in addressing the SemEval 2018 EL-OC task1 dataset, outperforming the previous state-of-the-art models. These findings have important implications for the field of natural language processing, as they offer a promising approach for improving the accuracy and reliability of text classification tasks.

6. Conclusion

This work represented an ensemble pretrained BERT model that provides emotion classification for Arabic text in four classes (anger, joy, fear, and sadness) using a voting technique between the best three models in the Transformers library, which is a powerful, modern state-of-art model that has improved the accuracy of results from 76% to 84%. We merged these models and compared the results with other experiments on eight machine learning classifiers: linear SVC, SVC, multinomial NB, Bernoulli NB, SGD classifier, decision tree classifier, random forest classifier, and K-Neighbors classifier, implemented using three different n-grams with the TF-IDF feature values technique, using the Arabic tweets dataset given by the SemiEval competition for the EI-oc task. Our method produced excellent performance with 82% validation accuracy and 84% testing accuracy.

In the future, we aim to apply the model we proposed to a larger dataset, work on the NLP technique to resolve natural language issues like the sarcasm detection issue and assess its impact on the results of emotion detection.

While this work has demonstrated potential approaches to emotion classification for Arabic text, the Arabic inflectional system, or the so-called Eraab, can be used to broaden the scope of this research, which has already shown some promising methods for sentiment categorization for Arabic text. We think that including the Eraab system in the framework for emotion analysis may enhance the results.

Biographies

Dina Abdelnaser Hamed

Department of Information Technology, Faculty of Information Technology and Computer Science, Sinai University, Arish, Egypt, Mobile +201015668988, Email dina.hamed@su.edu.eg

Dina is an Egyptian Teaching Assistant in the faculty of information technology and computer science at Sinai University. She has over ten years of experience in teaching and academic field and received her bachelor's degree in information technology at Sinai University, Egypt. She teaches programming, artificial intelligence, computer graphics, and logic subjects, and she is proficient in programming

languages such as c++, c sharp, python, and mat lap. Her research interests include machine learning, data mining, and text classification.

ORCID: 0000-0003-1430-2010

Ben Bella Said Tawfik

Department of information systems, Faculty of computers and informatics and computer science, Suez Canal university, Ismailia, Egypt, Mobile +201223761595, Email benbellat@ci.suez.edu.eg

Prof. Ben Bella is an Egyptian professor in the faculty of computers and information at Suez Canal University with over 30 years of experience in the computer science field. He received his Ph. D. degree from the military technical college in 1986 and 1990 and from Colorado State University in 1998, respectively. He has published 20 ISI/Scopus-indexed articles with the largest global publishers including Elsevier, IJECE, Symmetry, IEEE. His research fields are related to computer networks, image processing, information systems, pattern recognition, and wireless sensor networks.

ORCID: 0000-0001-9352-7538.

Mohamed Abdullah Makhlouf

Department of information systems, Faculty of computers and informatics and computer science, Suez Canal university, Ismailia, Egypt, Mobile +201001263049, Email m.abdallah@ci.suez.edu.eg

Prof. Makhlouf is an Egyptian Professor in faculty of computers and information, Suez Canal university. He received his Ph. D. degree from Faculty of Science, Zagazig University. He got the post-doctoral studies in Computer science from Granada University Spain in 2016. He has published 14 ISI/Scopus-indexed articles in (IEEE Access, Symmetry, Journal of King Saud University, IJCSNS) His research interests: Machine learning, data mining, intelligent Bioinformatics, Decision support systems and predictive models.

ORCID: 0000-0002-8854-4912

References

Abdullah, M. and Shaikh, S. (2018). Teamuncc at SemEval-2018 Task 1: Emotion detection in English and Arabic tweets using deep learning. *In Proceedings of the 12th International Workshop on Semantic Evaluation*, **n/a**(n/a), 350–7. DOI**:** 10.18653/v1/S18-1

Abdullah, M., AlMasawa, M., Makki, I., Alsolmi, M. and Mahrous, S. (2020). Emotions extraction from Arabic tweets. *International Journal of Computers and Applications*, **42**(7), 661–75. DOI: 10.1080/1206212X.2018.1482395

Alammary, A.S. (2022). BERT models for Arabic text classification: A systematic review. *Applied Sciences*, **12**(11), 5720. DOI: 10.3390/app12115720

Alswaidan, N. and Menai, M.E.B. (2020). Hybrid feature model for emotion recognition in Arabic text. *IEEE Access*, **8**(n/a), 37843–54. DOI: 10.1109/ACCESS.2020.2975906

Alzanin, S.M., Azmi, A.M. and Aboalsamh, H.A. (2022). Short text classification for Arabic social media tweets. *Journal of King Saud University-Computer and Information Sciences*, **34**(9), 6595–604. DOI: 10.1016/j.jksuci.2022.03.020

Antoun, W., Baly, F. and Hajj, H. (2020). Arabert: Transformer-based model for arabic language understanding. *ArXiv Preprint ArXiv:2003.00104*. **n/a**(n/a), 9–15. DOI: 10.48550/arXiv.2003.00104

Breiman, L. (2001). Random forests. *Machine Learning*, **45**(1), 5–32. DOI: 10.1023/A:1010933404324

Bullinaria, J.A. (2013). Recurrent neural networks. *Neural Computation: Lecture*, **12**(n/a), 1–20.

Dai, B., Li, J. and Xu, R. (2020). Multiple positional self-attention network for text classification. *In Proceedings of the AAAI Conference on Artificial Intelligence*, **34**(5), 7610–7. DOI: 10.1609/aaai.v34i05.6261

Daood, A., Salman, I. and Ghneim, N. (2017). Comparison study of automatic classifiers performance in emotion recognition of Arabic social media users. *Journal of Theoretical and Applied Information Technology*, **95**(19), n/a.

Elnagar, A., Al-Debsi, R. and Einea, O. (2020). Arabic text classification using deep learning models. *Information Processing and Management*, **57**(1), 102121. DOI: 10.1016/j.ipm.2019.102121

Euna, N.J., Hossain, S.M.M., Anwar, M.M. and Sarker, I.H. (2023). Content-based spam email detection using an N-gram machine learning approach. In: S. Nazmul , S.A. Mohammad , M Shamim , K. ASM (eds) *Applied Intelligence for Industry 4.0*. England, Oxon, Chapman and Hall.

Grefenstette, G. (1999). Tokenization. In: van Halteren, H. (eds) *Syntactic Wordclass Tagging. Text, Speech and Language Technology, vol 9*. Springer, Dordrecht. DOI: 10.1007/978-94-015-9273-4_9

Istizada (2023). *Complete List of Arabic Speaking Countries*. Available at: https://istizada.com/complete-list-of-arabic-speaking-countries/ (assessed on 15/8/2024)

Kadhim, A. I. (2019). Survey on supervised machine learning techniques for automatic text classification. *Artificial Intelligence Review*, **52**(1), 273–92. DOI: 10.1007/s10462-018-09677-1

Kamila, S., Hasanuzzaman, M., Ekbal, A. and Bhattacharyya, P. (2022). Investigating the impact of emotion on temporal orientation in a deep multitask setting. *Scientific Reports*, **12**(1), 493. DOI: 10.1038/s41598-021-04331-3

Khalil, E.A.H., Houby, E.M.E. and Mohamed, H.K. (2021). Deep learning for emotion analysis in Arabic tweets. *Journal of Big Data*, **8**(1), 136. DOI: 10.1186/s40537-021-00523-w

Medhat, W., Hassan, A. and Korashy, H. (2014). Sentiment analysis algorithms and applications: A survey. *Ain Shams Engineering Journal*, **5**(4), 1093–113. DOI: 10.1016/j.asej.2014.04.011

Mendonça, L.F., Vieira, S.M. and Sousa, J.M.C. (2007). Decision tree search methods in fuzzy modeling and classification. *International Journal of Approximate Reasoning*, **44**(2), 106–23. DOI: 10.1016/j.ijar.2006.07.004

Mohammad, S., Bravo-Marquez, F., Salameh, M. and Kiritchenko, S. (2018). Semeval-2018 task 1: Affect in tweets. In: *Proceedings of the 12th International Workshop on Semantic Evaluation*, **n/a**(n/a), 1–17. DOI: 10.18653/v1/S18-1001

Mohammed, A. and Kora, R. (2022). An effective ensemble deep learning framework for text classification. *Journal of King Saud University-Computer and Information Sciences*, **34**(10), 8825–37. DOI: 10.1016/j.jksuci.2021.11.001

Qian, T., Xie, A. and Bruckmann, C. (2022). Sensitivity analysis on transferred neural architectures of bert and gpt-2 for financial sentiment analysis. *arXiv preprint arXiv:2207.03037*. DOI: 10.48550/arXiv.2207.03037

Rajaraman, A. and Ullman, J.D. (2011). *Mining of massive datasets*. 2nd edition. Stanford University, California, USA: Cambridge University Press. DOI: 10.1017/CBO9781139924801

Samy, A.E., El-Beltagy, S.R. and Hassanien, E. (2018). A context integrated model for multi-label emotion detection. *Procedia Computer Science*, **142**(n/a), 61–71. DOI: 10.1016/j.procs.2018.10.461

Singh, A., Blanco, E. and Jin, W. (2019). Incorporating emoji descriptions improves tweet classification. In: *Proceedings of the 2019 Conference of the North American Chapter of the Association for Computational Linguistics: Human Language Technologies*, **1** (n/a), 2096–101. DOI: 10.18653/v1/N19-1214

Singh, A., Thakur, N. and Sharma, A. (2016). A review of supervised machine learning algorithms. In**:** *3rd International Conference on Computing for Sustainable Global Development (INDIACom)*, New Delhi, India, 16–18 /3/ 2016.

Storey, V.C. and O'Leary, D.E. (2024). Text analysis of evolving emotions and sentiments in COVID-19 Twitter communication. *Cognitive Computation*, **16**(4), 1834–57. DOI: 10.1007/s12559-022-10025-3

Sun, C., Qiu, X., Xu, Y. and Huang, X. (2019). How to fine-tune bert for text classification?. In: *Chinese Computational linguistics: 18th China National Conference, CCL 2019,* Kunming, China, 18-20/10/2019. DOI: 10.48550/arXiv.1905.05583

Tiwari, D., Nagpal, B., Bhati, B.S., Gupta, M., Suanpang, P., Butdisuwan, S. and Nanthaamornphong, A. (2024). SPSO-EFVM: A Particle Swarm Optimization-Based Ensemble Fusion Voting Model for Sentence-Level Sentiment Analysis. *IEEE Access*, **12**(n/a), 23707–24. DOI: 10.1109/ACCESS.2024.3363158.

Vaswani, A., Shazeer, N., Parmar, N., Uszkoreit, J., Jones, L., Gomez, A.N. and Polosukhin, I. (2017). Attention is all you need. Advances in neural information processing systems. In: *31st Conference on Neural Information Processing Systems (NIPS 2017),* Long Beach, CA, USA. 04-09/12/2017.

Venkatesh, R., K.V., Ranjitha and Venkatesh Prasad, B.S. (2020). Optimization scheme for text classification using machine learning Naïve Bayes classifier. In: *ICDSMLA 2019: Proceedings of the 1st*

International Conference on Data Science, Machine Learning and Applications, **n/a**(n/a), 576–86. DOI: 10.1007/978-981-15-1420-3_61

Wolf, T., Debut, L., Sanh, V., Chaumond, J., Delangue, C., Moi, A. and Rush, A.M. (2020). Transformers: State-of-the-art natural language processing. In: *Proceedings of the 2020 Conference on Empirical Methods in Natural Language Processing: System Demonstrations*, **n/a**(n/a), 38–45. DOI: 10.18653/v1/2020.emnlp-demos.6

Wynne, H.E. and Wint, Z.Z. (2019). Content-based fake news detection using n-gram models. In: *Proceedings of the 21st International Conference on Information Integration and Web-based Applications and Services*, **n/a**(n/a), 669–73. DOI: 10.1145/3366030.3366116

Yacouby, R. and Axman, D. (2020). Probabilistic extension of precision, recall, and F1 score for more thorough evaluation of classification models. *In Proceedings of the First Workshop on Evaluation and Comparison of NLP Systems*, **n/a**(n/a), 79–91. DOI: 10.18653/v1/2020.eval4nlp-1.9

Yagi, S., Elnagar, A. and Fareh, S. (2023). A benchmark for evaluating Arabic word embedding models. *Natural Language Engineering*, **29**(4), 978–1003. DOI: 10.1017/S1351324922000444

Ye, Q., Zhang, Z. and Law, R. (2009). Sentiment classification of online reviews to travel destinations by supervised machine learning approaches. *Expert Systems with Applications*, **36**(3), 6527–35. DOI: 10.1016/j.eswa.2008.07.035

Yousaf, A., Umer, M., Sadiq, S., Ullah, S., Mirjalili, S., Rupapara, V. and Nappi, M. (2020). Emotion recognition by textual tweets classification using voting classifier (LR-SGD). *IEEE Access*, **9**(n/a), 6286–95. DOI: 10.1109/ACCESS.2020.3047831

Scientific Journal of King Faisal University:
Basic and Applied Sciences

Phytochemical Analysis, Total Phenolic Content, Hemolytic and Anti-hemolytic Activities of *Centaurea iberica* (Asteraceae)

Ruba Joujeh[1], Salim Zaid [1] and Sobhi Mona [2]

[1] Department of Plant Biology, Faculty of Science, University of Damascus, Damascus, Syria
[2] Department of Plant Protection, Faculty of Agriculture, University of Aleppo, Aleppo, Syria

LINK	ACCEPTED	PUBLISHED ONLINE	ASSIGNED TO AN ISSUE
https://doi.org/10.37575/b/sci/242068	27/10/2024	27/10/2024	01/12/2024

NO. OF WORDS	NO. OF PAGES	YEAR	VOLUME	ISSUE
3872	5	2024	25	2

ABSTRACT

Several plants contain chemical substances that have various biological activities, but they also probably cause harmful effects on cellular membranes. This work deals with the *Centaurea iberica* (Iberian starthistle) plant. The objective of this study is to identify the main chemical groups in the methanolic extract 80% of the plant, determine its total phenolic content, evaluate its toxic effect on human erythrocytes, and also assess its activity in the protection of normal and glucose-6-phosphate dehydrogenase (G6PD) enzyme-deficient human erythrocytes membranes against oxidative hemolysis. Phytochemical analysis revealed that *C. iberica* extract contains several bioactive compounds. The results also showed that the plant extract contained good level of total phenolic compounds. The extract exhibited a low hemolytic effect. It also showed excellent activity in the protection of normal and G6PD-deficient human erythrocytes against oxidative hemolysis.

KEYWORDS
Erythrocytes, G6PD, Iberian starthistle, methanolic extract, toxic effect, oxidative hemolysis

CITATION
Joujeh, R., Zaid, S. and Mona, S. (2024). Phytochemical analysis, total phenolic content, hemolytic and anti-hemolytic activities of *Centaurea iberica* (Asteraceae). *Scientific Journal of King Faisal University: Basic and Applied Sciences*, **25**(2), 31–35. DOI: 10.37575/b/sci/242068

1. Introduction

Since ancient time, plants are used as source of shelter and food for human (Kalita *et al.*, 2011). Plants contain different components which are used in traditional medicine, and several modern drugs have natural origin (Lohith *et al.*, 2013).

Although Syria is not a big country, it is rich in animal and plant diversity. This is due to its climatic and topographic diversity. More than 3500 species belonging to 131 plant families have been found in this country, hundreds of which might have medicinal importance (Alachkar *et al.*, 2011). *Centaurea* genus is in the family Asteraceae, comprising about 400 to 700 species (Kilic, 2013). Their purple, blue, yellow, or orange flower heads are color spots in many Mediterranean habitats and are appreciated photo subjects by many travelers (Hilpold, 2011). Members of the *Centaurea* genus are used as ornamentals such as *Centaurea cyanus* (Tomar, 2017) and *Centaurea cineraria*. Some *Centaurea* species are used in folk medicine and this is due to the secondary compounds they contain (Hilpold, 2011). The term "Novel Weapons Hypothesis" was proposed to describe the general effects of *Centaurea* species (Khammar and Djeddi., 2012). *Centaurea iberica* is an annual or biennial herb (20-80 cm), with pale pink, flowers (Davis, 1975). It contains many phytochemical compounds. Previously, flavones, fatty acids, steroids, volatile constituents, and sesquiterpene lactones have been reported from this plant (Khan *et al.*, 2011). It was known for its uses in folk medicine for the cure of peptic ulcer, malaria, stomach upset, common cold, abdominal pain, and herpes infections, and suggested against inflammatory situations such as asthma and abscesses (Khammar and Djeddi., 2012). On the other hand, Previous investigations on different extracts of this plant have shown cytotoxic activity (Dumlu and Gürkan., 2006).

The cytotoxic effect of many plants on human erythrocytes has previously been tested. The extract of *Allium strachey*i Baker prepared using butanol as a solvent, was reported to have a high cytotoxic effect (100%) on human erythrocytes, at the concentration of (500 µg/ml) (Mukherjee and Rajasekaran., 2010). In another study, the extract of *Bridellia Ferruginea* prepared using hexane as a solvent, was reported to have a hemolytic effect (92%) at the concentration (80 ng/ml) (Vinjamuri *et al.*, 2015).

This study investigated the phytochemical components in *C. iberica* extract, evaluated its total phenolic content, its hemolytic effect, and anti-hemolytic activity through the inhibition of induced oxidative hemolysis. This research forms part of our detailed study on some *Centaurea* species (doctoral thesis).

2. Materials and Methods

2.1. Plant Material Collection:

Arial parts of *C. iberica* were collected from the countryside of Aleppo city (Al Sfera). The plant material was authenticated and air-dried. Then, it was ground well to powder.

2.2. Preparation of the Hydro Alcoholic Extract:

50 g of plant powder was mixed with 250 ml of aqueous methanol 80% in a sealed container. Then the container was put in an ultrasonic waves bath (Hwashin Technology, Korea) for 25 min (30 kHz, 25^{O}C). The extract obtained was filtered using the Whatman-No.-1 filter paper in the sintered glass Büchner funnel under low pressure. The crude extract was obtained by evaporating the solvent in a rotary evaporator (Heidolph Instruments, Germany) under reduced pressure at 40 ^{O}C and kept in a desiccator. The extract was weighed to calculate the percentage of the extraction yield (Sangeetha and Vidhya, 2016).

2.3. Qualitative Analysis of *C. iberica* Extract:

Phytochemical screening of the aerial parts of *C. iberica* was conducted. Few amount of *C. iberica* extract was dissolved in distilled water and then filtered. Phytochemical constituents screening was performed using the filtrate.

2.3.1. Saponins

Few amount of filtrate (10 ml) was shaken vigorously. The presence of saponins was indicative if foam appeared and persisted for 10 minutes (Mojab *et al.*, 2003).

Corresponding Author: Ruba Joujeh 00963991184213, rubajoujeh3@gmail.com

2.3.2. Phenolic compounds

Few amount (3 ml) of lead acetate solution (10%) was added to 5 ml of filtrate. The presence of phenolic compounds was indicative if bulky white precipitate developed (Sangeetha and Vidhya, 2016).

2.3.3. Tannins

Few drops of ferric chloride solution (5%) were added to the filtrate. The presence of tannins was indicative if green color appeared (Shwetha *et al.*, 2016).

For Gelatin test, 1% gelatin solution containing 10% sodium chloride was prepared, then few drops of this solution were added to the filtrate, the presence of tannins was indicative if white precipitate developed (Pandey and Tripathi, 2014).

2.3.4. Flavonoids

Little amount of the filtrate (5 ml) was treated with few magnesium turnings and drops of concentrated hydrochloride acid HCl. The presence of flavonoids was indicative if pink color developed (Mojab *et al.*, 2003).

2.3.5. Carbohydrates

Few drops of methanolic alpha-naphthol (1%) were added to the filtrate (5 ml), and shaked well. Then concentrated Sulfuric Acid was added to the tube, and the presence of carbohydrates was indicative if a violet ring appeared at the junction (Wani *et al.*, 2012).

2.4. Determination of Total Phenolic Content (TPC):

TPC in the hydromethanolic extract of *C. iberica* was determined by the Folin–Ciocalteu method as described by (Alhafez *et al.*, 2014): To 1ml of the extract, 4.8 ml of distilled water was added, followed by the addition of 4 ml of sodium carbonate Na_2CO_3 (2%) and 200 µl of Folin–Ciocalteu reagent. The mixture was incubated for 60 minutes at 25°C. Then, the absorbance of the mixture was measured at 760 nm using a spectrophotometer. A blank sample was prepared using distilled water instead of *C. iberica* extract. The TPC of the extract was determined in four replicates. Gallic acid solutions (50-450 mg/L) were used as standard. TPC in the dry extract was quantified from the standard calibration curve of gallic acid solutions, and expressed as milligrams of gallic acid equivalents per gram of dry extract.

2.5. Cytotoxic effect on human erythrocytes (hemolytic effect assessment) (Sahu *et al.*, 2014):

1 ml of different concentrations of *C. iberica* extract (100-250-500-1000-2000-3000 µg/ml) was transferred by micropipette to test tubes containing a fixed volume (1 ml) of red blood cell suspension (10%). Test tubes were incubated for thirty minutes in a water bath at 37°C. Then, tubes were centrifuged by laboratory centrifuge for ten minutes at 2500 rpm (Heraeus Megafuge, Germany), and the absorbance was determined spectrophotometrically at 540 nm (Shimadzu, Japan). The hemolytic effect of the extract was evaluated by comparison with the positive control (distilled water) and negative control (PBS). The hemolysis percentage was calculated using the equation:

Percentage hemolysis = $[(Abs_s-Abs_p) / (Abs_d-Abs_p)] *100$

Abs_s- Absorbance of sample.

Abs_p- Absorbance of PBS.

Abs_d- Absorbance of distilled water.

Note: the erythrocytes suspension and the concentrations of the *C. iberica* extract were prepared in phosphate buffer saline (PBS) [KH_2PO_4 (0.24 g), NaCl (8 g), Na_2HPO_4 (1.44 g), KCl (0.2 g) dissolved in 1 liter of distilled water, pH=7.4] (Kuhlmann, 2006).

2.6. Inhibition of H_2O_2-induced hemolysis (anti-hemolytic activity) (Kavitha and Lena, 2014):

The human erythrocyte hemolysis was performed with hydrogen peroxide (H_2O_2) as a free radical initiator. 0.5ml of erythrocytes suspension (10%) was added to 1ml of *C. iberica* extract of different concentrations (100-250-500-1000-2000-3000 µg/ml), and the tubes were incubated for five minutes at room temperature. To each tube, 0.5 ml of H_2O_2 (in PBS pH 7.4) was added (the concentration of H_2O_2 was prepared to obtain about 90% hemolysis after 4 h incubation). Likewise, the erythrocytes were treated with 1 ml of PBS and 0.5 ml H_2O_2 and without plant extract to obtain complete hemolysis (blank). Test tubes were incubated at 37°C for four hours. Then, centrifuged at 2500 rpm for 10 min. Finally, the absorbance (abs) of the supernatants was measured spectrophotometrically at 540 nm. The inhibitory effect of the extract was compared with positive control (standard antioxidant Ascorbic acid) and negative control (PBS). The 50% inhibitory concentration (IC50) values were calculated as the antioxidant concentration required for the inhibition of 50% of hemolysis.

The percentage of protection was determined by the equation:

Protection%= 100 – [(Abs of test sample / Abs of control) *100]

The same procedure was done to investigate the activity of the extract in the protection of G6PD enzyme-deficient human erythrocytes against oxidative hemolysis. In this test, three concentrations of plant extract were chosen (1000-2000-3000) µg/ml. These concentrations were selected because they showed the highest activities in the previous test on the normal erythrocytes.

3. Results

3.1. Yield Extraction and Phytochemical Analysis:

After extraction, *C. iberica* extract resulted in 15.46% yield. The extract was characterized by a yellowish-green color and a pleasant grassy smell.

Phytochemical screening revealed that *C. iberica* extract contains several bioactive compounds which display several pharmacological and biological activities. It revealed the presence of saponins, phenolic compounds, flavonoids, tannins and carbohydrates.

3.2. Total Phenolic Content (TPC):

TPC in *C. iberica* aerial parts extract was determined by the Folin-Ciocalteu method. Total phenolics determination was based on the absorbance value of the extract solution (0.01 g/ml) that reacted with the Folin-Ciocalteu reagent, followed by a reference to the standard calibration curve of gallic acid (figure 1), according to the following equation: $y = 0.0036x + 0.2257$, $R^2 = 0.9961$

The Result implied that *C. iberica* aerial parts hydromethanolic extract contains good phenolic content with a value of 40.09± 0.52 mg gallic acid equivalent/g of extract (mg GAE/g).

Figure 1. The standard calibration curve of gallic acid equivalents (mg GAE/L)

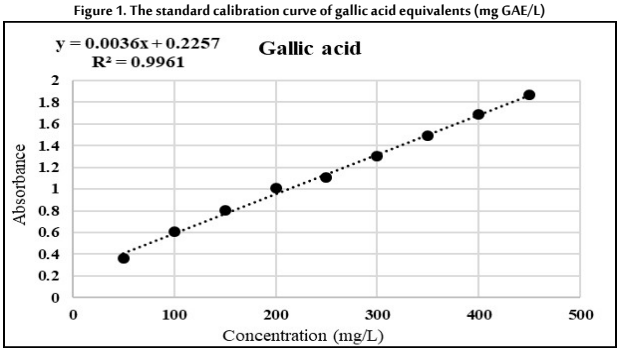

3.3. Cytotoxic Effect on Human Erythrocytes:

C. iberica hydromethanolic extract exhibited a low hemolytic effect on human erythrocytes in comparison to negative control, so it is probably considered safe for human erythrocytes at low concentrations. The absorbance value was increased gradually with an increase in plant extract concentration (Table 1). Significant differences between extract and negative control were noticed at the range of concentrations (500-3000 µg/ml).

Table 1. The percentages of hemolytic activity by *C. iberica* extract

concentration (µg/ml)	*C. iberica* Hemolysis%
100	1.32 ± 1.6
250	2.09 ± 2.3
500	4.83* ± 2.9
1000	6.71* ± 2.0
2000	9.06* ± 0.9
3000	10.05* ± 1.1

All values are represented as mean ± SD
*Correlation is significant at the 0.05 level

3.4. Inhibition of H_2O_2 Induced Hemolysis (Anti-hemolytic Activity):

When red blood cells were incubated with the standard antioxidant (Ascorbic acid) and H_2O_2, a marked reduction in hemolysis was noticed at the range of concentrations of (250-3000 µg/ml), while at the highest concentration (3000 µg/ml) hemolysis was found to be increased as well as the protection was decreased (table 2, figure 2). The IC50 value of Ascorbic acid was 230.9 µg/ml (figure 3).

Table 2. The percentages of hemolysis and protection by Ascorbic acid and *C. iberica* against oxidative hemolysis

Concentration (µg /ml)	Ascorbic acid		IC50 (µg /ml)
	Hemolysis%	Protection%	
100	79.7475	20.25±1.5	230.9
250	43.9875	56.01±3.9	
500	23.8775	76.12±3.6	
1000	9.9575	90.04±1.7	
2000	5.3775	94.62±2.1	
3000	21.65	78.35±2.6	
Concentration (µg /ml)	*C. iberica*		IC50 (µg /ml)
	Hemolysis%	Protection%	
100	85.81	14.19*±2.77	623.41
250	79.738	20.26*±1.72	
500	61.262	38.74*±2.03	
1000	41.52	58.48*±2.02	
2000	15.452	84.55*±3.43	
3000	10.27	89.73*±2.24	

Protection values are represented as mean ± SD
*Correlation is significant at the 0.05 level

Figure 2. Anti-hemolytic activity of Ascorbic acid against oxidative hemolysis

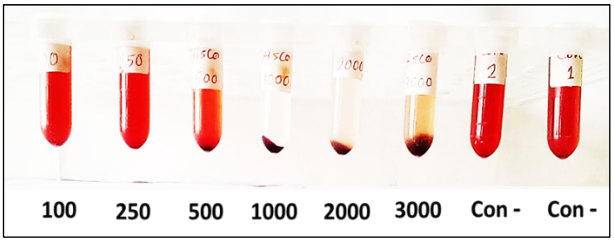

Figure 3. Anti-hemolytic activity of Ascorbic acid IC50 (µg/ml)

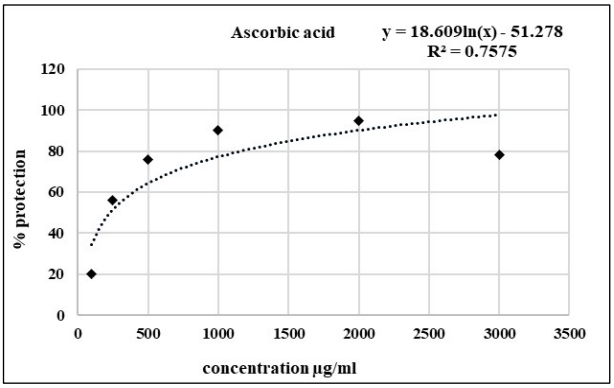

For normal erythrocytes, *C. iberica* extract showed an anti-hemolytic effect in a concentration-dependent manner. It provided notable activity at concentrations range of (2000-3000 µg/ml), in comparison to Ascorbic acid as a positive control, in terms of percentage inhibiting activity which ranged from 84.55% to 89.73% (table 2, figure 4). The IC50 value of *C. iberica* extract was 623.41µg/ml (figure 5). The lower the IC50 the more protection offered against hemolysis. Significant differences ($p<0.001$) between extract and Ascorbic acid were noticed at all tested concentrations.

Figure 4. The anti-hemolytic activity of *C. iberica* extract in comparison to Ascorbic acid

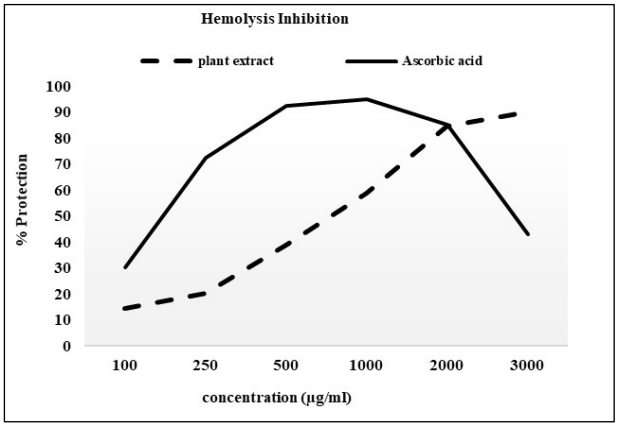

Figure 5. The anti-hemolytic activity of *C. iberica* IC50 (µg/ml)

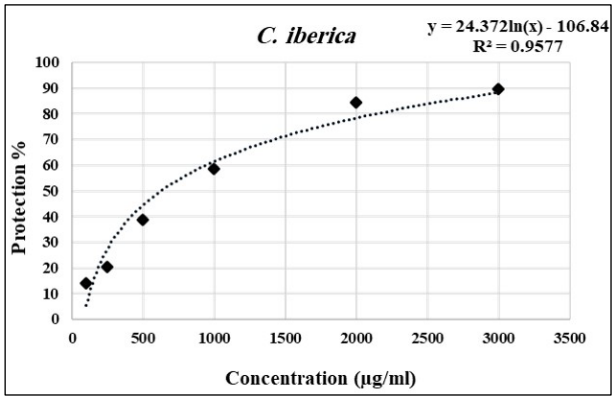

In the case of G6PD-deficient erythrocytes, the extract also provided excellent activity with a maximum protection value of (92.72%) at the concentration (3000 µg/ml) (table 3).

Table 3. The protective effect of *C. iberica* extract for G6PD enzyme-deficient human erythrocytes

C. iberica		
Concentration (µg /ml)	Hemolysis%	Protection%
1000	10.28	89.72±0.9
2000	9.39	90.61±1.13
3000	7.28	92.72±1.3

Protection values are represented as mean ± SD

4. Discussion

In comparison with a previous study that used ultrasound-assisted extraction and was conducted in Turkey, the extraction yield of *C. iberica* using different solvents (chloroform, methanol, n-Hexane) was (1.46%, 7.04%, 1.14%), respectively. The difference in yield can be explained by different environmental factors (Erel *et al.*, 2014). In our study, the ultrasound-assisted extraction technique was used. As per to previous study (Albayrak *et al.*, 2017), ultrasonic extraction gave a better extract with a larger amount of extractive substances and stronger antioxidant and antimicrobial activities than the extracts prepared using other techniques (Soxhlet extraction, Maceration).

The result implied that *C. iberica* aerial parts hydromethanolic extract contains good phenolic content. Phenolic compounds are widely

found in plant products, and they are found to have antioxidant activities (Nabavi *et al.*, 2010), these activities due to their general structure which consists of hydroxyl group attach to the aromatic ring which is capable donating electron and stabilizing free radicals (Afsar *et al.*, 2016).

The increase in toxicity values with an increase in plant extract concentration is due to the quantity of chemical compounds contained in the extract. *C. iberica* aerial parts extract contains saponins as demonstrated by the results of the chemical analysis, which were known for their hemolytic effect (Noudeh *et al.*, 2010). With consideration that the color of the extract in high concentrations increases the absorbance value versus the colorless PBS solution.

The principle of this assay is that hydrogen peroxide generates radicals that attack the erythrocyte membrane and thus induce the chain oxidation of lipids and proteins, and cause hemolysis (Joshan and Rawal, 2012). Ascorbic acid was used in this test as positive control because it is well-known antioxidant agent, it may scavenge radicals and thus inhibit cytotoxicity prompted by oxidants (Boonkasem *et al.*, 2015). Our results are in agreement with the previous study which reported that low concentrations of Ascorbic acid provided good antioxidant activity, while high concentrations caused hemolysis (Ibrahim *et al.*, 2006). Our results suggest that *C. iberica* aerial parts extract is a good anti-hemolytic agent and offeres biological action compared with the standard used. This result reflects the antioxidant capacity of the extract which has been reported to be highly correlated with the content of phenolic compounds (Sariburun *et al.*, 2010). In this context, the inhibitory effect of the plant extract may be due to its phenolic compounds which can quench the radicals generated by H_2O_2, before these radicals attack the erythrocytes membrane and cause oxidative hemolysis.

5. Conclusion

According to the literature survey, this is the first report of the hemolytic and anti-hemolytic effects of *C. iberica*. The current study concluded that *C. iberica* aerial parts extract contains good levels of total phenolic compounds and also many bioactive constituents. The results demonstrated that *C. iberica* has a low hemolytic effect, and also showed appropriate anti-hemolytic activity against hydrogen peroxide-induced hemolysis. Therefore, it can be suggested that *C. iberica* aerial parts extract may have a beneficial effect in the treatment of oxidative stress-related diseases. Additional studies are wanted to support these results.

Biographies

Ruba joujeh

Department of Plant Biology, Faculty of Science, University of Damascus, Damascus, Syria. +963 991184213, rubajoujeh3@gmail.com

Ruba, Syrian nationality. Ph.D. student in Plant Sciences, her interests include Phyto-chemistry, plants' essential oils, Phyto-medicine, plant anatomy, and taxonomy of higher and lower plants. She worked as a lecturer at the Faculty of Agricultural Engineering, University of Aleppo. She has published over 18 research manuscripts in both local and international journals, many of which are available online. She has 10 years of teaching and research experience.

ORCID: 0000-0002-3425-8793.

Salim Zaid

Department of Plant Biology, Faculty of Science, University of Damascus, Damascus, Syria. +963 933124729, szaid60@yahoo.com

Prof. Salim Zaid, Syrian nationality. Ph.D. in Plant Biology. Professor of Plant Biology, Faculty of Science, University of Damascus, Syria. Salim Zaid, works at the Department of Botany at the Faculty of Science, University of Damascus. He obtained his Ph.D. in Biology (Plant Development) from Germany and has numerous research publications in both local and international journals, many of which are available online, in the field of plant biology, plant morphology, plant tissue culture, and plant physiology. He has over 30 years of teaching and research experience.

Sobhi Mona

Department of Plant Protection, Faculty of Agriculture, University of Aleppo, Aleppo, Syria. +963 945774236, dr.sobhi52@gmail.com

Prof. Sobhi Mona, Syrian nationality, Professor of Plant Protection, Faculty of Agriculture, University of Aleppo, Syria. Ph.D. in Natural Sciences from Joseph Fourier University (Grenoble I) in France, focusing on the cellular effects of herbicides from the carbamate family. He has numerous research publications in both local and international journals, many of which are available online, in the field of plant protection (weed control), plant biology, and plant nutrition. He has over 35 years of teaching and research experience.

Acknowledgments

The authors are grateful to Damascus University for financial assistance and research facilities, and to Agriculture Faculty Laboratories, and Pharmacy Faculty Laboratories (University of Aleppo).

References

Afsar, T., Razak, S., Khan, M.R., Mawash, S., Almajwal, A., Shabir, M. and Haq, I.U. (2016). Evaluation of antioxidant, anti-hemolytic and anticancer activity of various solvent extracts of Acacia hydaspica R. Parker aerial parts. *BMC Complementary and Alternative Medicine*, **16**(n/a), 1–16. DOI:10.1186/s12906-016-1240-8.

Wani, S.A., Shah, K.W. and Ahmad, M.A. (2012). Preliminary phytochemical investigation and thin layer chromatography of Rheum emodi. *International Research Journal of Pharmacy*, **3**(4), 176–7.

Alachkar, A., Jaddouh, A., Elsheikh, M.S., Bilia, A.R. and Vincieri, F.F. (2011). Traditional medicine in Syria: Folk Medicine in aleppo governorate. *Natural Product Communications*, **6**(1), 79–84. DOI:10.1177/1934578X1100600119.

Albayrak, S., Atasagun, B. and Aksoy, A. (2017). Comparison of phenolic components and biological activities of two *Centaurea* sp. obtained by three extraction techniques. *Asian Pacific Journal of Tropical Medicine*, **10**(6), 599–606. DOI:10.1016/j.apjtm.2017.06.010.

Alhafez, M., Kheder, F. and AlJoubbeh, M. (2014). Polyphenols, flavonoids and (-)-epigallocatechin gallate in tea leaves and in their infusions under various conditions. *Nutrition and Food Science*, **44**(5), 455–63. DOI:10.1108/NFS-10-2013-0119.

Boonkasem, P., Sricharoen, P., Techawongstein, S. and Chanthai, S. (2015). Determination of Ascorbic acid and total phenolics related to the antioxidant activity of some local tomato (*Solanum lycopersicum*) varieties. *Der Pharma Chemica*, **7**(4), 66–70.

Davis, P.H. (1975). *Flora of Turkey and the east Aegean islands*. Edinburgh, Scotland: Edinburgh University Press.

Dumlu, M.U. and Gürkan, E. (2006). A new active compound from *Centaurea* species. *Zeitschrift für Naturforschung C*, **61**(1-2), 44–6. DOI: 10.1515/znc-2006-1-208.

Erel, S. B., Demir, S., Nalbantsoy, A., Ballar, P., Khan, S.H., Yavasoglu N. and Karaalp C. (2014). Bioactivity screening of five *Centaurea* species and in vivo anti-inflammatory activity of *C. athoa*. *Pharmaceutical Biology*, **52**(6), 775–81. DOI: 10.3109/13880209.2013.868493.

Hilpold, A. (2011). *Evolution of Centaurea Acrolophus sub group*, Ph.D. Thesis, Universitat DE Barcelona, Barcelona, Spain.

Ibrahim, I.H., Sallam, S.M., Omar, H. and Rizk, M. (2006). Oxidative hemolysis of erythrocytes induced by various vitamins. *International Journal of Biomedical Science: IJBS*, **2**(3), 295. DOI: 10.59566/IJBS.2006.2295.

Joshan, D.S. and Rawal, S. (2012). Comparative evaluation of antioxidant and antihemolytic capacities of plants of indian origin using multiple antioxidant assays. *International Journal of*

Phytopharmacy, **2**(n/a), 107–15. DOI: 10.7439/ijpp.v2i4.691.

Kalita, S., Kumar, G., Karthik, L. and Rao, K.V.B. (2011). Phytochemical Composition and in vitro hemolytic activity of *Lantana Camara* L. (Verbenaceae) leaves. *Pharmacologyonline*, **1**(n/a), 59–67.

Kavitha, G. and lena, J. (2014). Evaluation of Antihemolytic capacities of *Lippia citridora* with in vitro models. *International Journal of Ethnomedicine and Pharmacological Research,* **2**(1), 11–7.

Khammar, A. and Djeddi, S. (2012). Pharmacological and biological properties of some *Centaurea* species. *European Journal of Scientific Research*, **84**(3), 398–416.

Khan, A.N., Fatima, I., Abdul Khaliq, U., Malik, A., Miana, G.A., Qureshi, Z. and Rasheed, H. (2011). Potent anti-platelet constituents from *Centaurea iberica*. *Molecules,* **16**(3), 2053–64. DOI: 10.3390/molecules16032053.

Kilic, O., (2013). Essential oil compounds of three *Centaurea* L. taxa from Turkey and their chemotaxonomy. *Journal of Medicinal Plants Research*, **7**(19), 1344–50. DOI: 10.5897/JMPR12.1233.

Kuhlmann, W.D. (2006). *Buffer Solutions*. Available at: https://www.kuhlmann-biomed.de/en/buffer-solutions/ (accessed on 03/09/2024).

Lohith, K., Vijay, R., Pushpalatha, K.C., and Chandrashekar, G.J. (2013). In-vitro Cytotoxic Study of *Moullava spicata (dalz.)* Nicolson Leaf Extract. *International Research Journal of Pharmaceutical and Applied Sciences* (IRJPAS), **3**(2), 38–42.

Mojab, F., Kamalinejad, M., Ghaderi, N. and Vahidipour, H.R. (2003). Phytochemical screening of some species of iranian plants, *Iranian Journal of Pharmaceutical Research*, **2**(2), 77–82. DOI: 10.22037/IJPR.2010.16.

Mukherjee, A., and Rajasekaran, C. (2010). *In-vitro* hemolytic activity of *Allium stracheyi* Baker, *Journal of Pharmacy Research*, **3**(5), 1160–1162.

Nabavi, S.F., Nabavi, S.M. and Ebrahimzadeh, M.A. (2010). In vitro antioxidant and antihemolytic activities of grain bran, *Pharmacologyonline*, **3**(n/a), 52–9.

Noudeh, G.D., Sharififar, F., Khatib, M., Behravan, E. and Afzadi, M.A. (2010). Study of Aqueous extract of three medicinal plants on cell membrane–permeabilizing and their surface properties. *African Journal of Biotechnology*, **9**(1), 110–6.

Pandey, A. and Tripathi, S. (2014). Concept of standardization, extraction and pre phytochemical screening strategies for herbal drug, *Journal of Pharmacognosy and Phytochemistry*, **2**(5), 115–9.

Sahu, P., Gupta, S., Banerjee, M., Priya, C.L. and Rao, K.V. (2014). Phytochemical composition, antimicrobial, hemolytic activity and HPLC analysis of ethanolic extract of *Cleome viscosa* linn. Stems. *Research Journal of Pharmacy and Technology*, **7**(10), 1140–4.

Sangeetha, G. and Vidhya, R. (2016). In vitro anti-inflammatory activity of different parts of *Pedalium murex* (L.), *International Journal of Herbal Medicine*, **4**(3), 31–36.

Sariburun, E., Sahin, S., Demir, C., Turkben, C. and Uylaser, V. (2010). Phenolic content and antioxidant activity of raspberry and blackberry cultivars, *Journal of Food Science*, **75**(4), 328–35. DOI: 10.1111/j.1750-3841.2010.01571.x.

Shwetha, R.J., Tahareen, S. and Myrene, R.D. (2016). Antioxidant and Anti-Inflammatory activity of tinospora cordifolia using in vitro models, *Journal of Chemical, Biological and Physical Science,* **6**(62), 497–512.

Tomar, A. (2017). Medicinal use of *Centaurea cyanus* Linn. To cure ophthalmia. *Journal of Pharmacognosy and Phytochemistry*, **6**(5), 232–3.

Vinjamuri, S., Shanker, D., Ramesh, R. and Nagarajan, S. (2015). In vitro evaluation of hemolytic activity and cell viability assay of hexanoic extracts of bridelia ferruginea benth. *World Journal of Pharmacy and Pharmaceutical Sciences*, **4**(7), 1263–8.

Scientific Journal of King Faisal University:
Basic and Applied Sciences

Histological Study and Chemical Composition of *Apium graveolens*: In Vivo Antimicrobial Activity

Imane Abdelsadok [1], Karima Ouldyerou [1], Boumediene Meddah [1], and Pascal Sonnet [2]

[1] Bioconversion, Microbiological Engineering, and Health Safety Laboratory, Department of Biology, Faculty of Nature and Life Sciences, Mustapha Stambouli University, Mascara, Algeria
[2] Infectious Agents, Resistance and Chemotherapy Laboratory UR 4294, Faculty of Pharmacy, University of Picardie Jules Verne, Amiens, France

LINK	RECEIVED	ACCEPTED	PUBLISHED ONLINE	ASSIGNED TO AN ISSUE
https://doi.org/10.37575/b/sci/240033	01/08/2024	18/11/2024	18/11/2024	01/12/2024

NO. OF WORDS	NO. OF PAGES	YEAR	VOLUME	ISSUE
5449	6	2024	25	2

ABSTRACT

The purpose of the current investigation is to evaluate the methanolic extract from *Apium graveolens* seeds for chemical composition and in vivo antimicrobial activity, supported by a histological study. The chemical profile of the methanolic extract was identified using high-performance liquid chromatography diode array detector analysis. The toxicity and antimicrobial effects of the methanolic extract were examined through in vivo experiments on rats weighing 220 ± 5 g. The histological study was conducted using the rats' ileum. The methanolic extract (80%) contained sinapic acid (49.9%), ascorbic acid (25.4%), butylated hydroxyanisole acid (6.1%), and quercetin (8.2%), with a yield ratio of 11.74%. The dose of 50 mg/kg of the methanolic extract did not lead to animal lethality or toxicity symptoms. Two days after treatment, the blood cultures of all females treated with the methanolic extract at 50 mg/kg showed sterility (100%). The same result appeared on the fifth day after treatment in all males of the same group. Histopathological examination revealed normal and well-preserved architecture of the ileum in both sexes. The study concludes that the methanolic extract of *Apium graveolens* possesses significant antimicrobial capacity.

KEYWORDS

Anatomopathology, celery, chemical compounds, enteric infection, HPLC, rats

CITATION

Abdelsadok, I., Ouldyerou, K., Meddah, B., and Sonnet, P. (2024). Histological study and chemical composition of *Apium graveolens*: In vivo antimicrobial activity. *Scientific Journal of King Faisal University: Basic and Applied Sciences*, **25**(2), 36–41. DOI:10.37575/b/sci/240033

1. Introduction

Enteric infections are a growing public health problem, posing a critical threat across the world.

One particular international public health concern is the struggle against *Escherichia coli* (*E. coli*) infections, which cause intestinal diseases and bleeding. Such bacteria, which can be found in food and drinking water, can cause acute intestinal inflammation and chronic diarrhea (Pokharel *et al.*, 2023 and Xiao *et al.*, 2022). *E. coli* is the most common gram-negative bacterium associated with bloodstream infections (Kolesnichenko *et al.*, 2021). Such infections are thought to be responsible for more than 2 million deaths per year (Cheng et al., 2024). The use of antibiotherapy has been crucial in preventing microbial infections. Nevertheless, the global expansion of antibiotic resistance highlights the need for novel therapies.

A new supply of natural antimicrobial substances is provided by medicinal plants, which are important in addressing basic health demands. Furthermore, several natural materials, including essential oils originating from edible and medicinal plants, spices, and herbs have been declared to possess antimicrobial potency and perform as natural antimicrobials against a variety of pathogenic microbes, as well as food spoilage (Khalil *et al.*, 2015). *Apium graveolens*, popularly known as celery, belongs to the family Apiaceae, which primarily consists of aromatic plants, including the genus Apium. These plants are grown worldwide for their petioles, bulbous roots, seeds, and green leaves (Mezeyova *et al.*, 2018 and Roslon *et al.*, 2010) and possess in vitro antimicrobial properties (Salehi et al., 2019). Indeed, in some investigations, *A. graveolens* has shown modest antibacterial efficacy against multi-drug-resistant *Salmonella typhi* (Al-Aboody, 2021; Rani and Khullar, 2004). Other studies have reported that methanol is the best solvent for extracting antimicrobial compounds from Apium plants (Edziri *et al.*, 2012 and Penna *et al.*, 2001). Moreover, recent research has revealed positive antibacterial effects of these plants against methicillin-resistant *Staphylococcus aureus* in vitro and in vivo (Prakoso *et al.*, 2020).

According to the literature, however, no in vivo studies have been conducted on the antimicrobial activity of the methanolic extract of *A. graveolens* seeds from the Mascara region in western Algeria. The objective of this investigation is to study the polyphenolic profile of the methanolic extract of *A. graveolens* seeds, evaluate its in vivo antimicrobial activity against intestinal infection induced by the pathogen *E. coli*, and conduct a histological study.

2. Materials and Methods

2.1. Sampling:

For the present investigation, *Apium graveolens* seeds (Figure 1) were collected in May 2021from El Maarif in the Tighennif plain, which extends over an area of 108 km^2 and is located 20.70 km from Mascara in western Algeria (latitude 35°24′55.56 N; longitude 0°19′46.72 E) (Figure 2). The plant materials were authenticated by experts for the present research.

Figure 1: Seeds of *Apium graveolens*

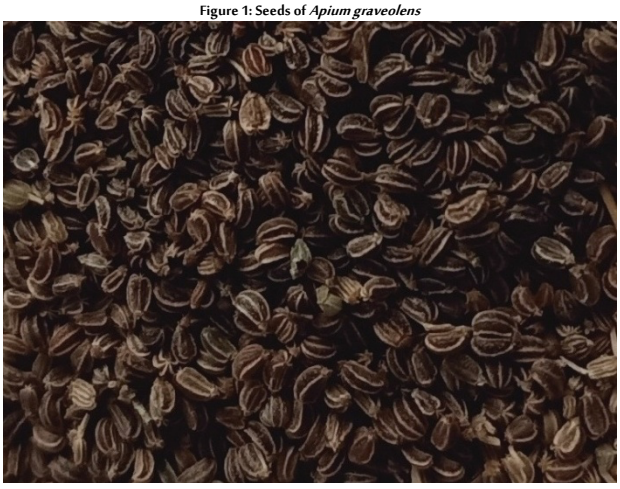

Corresponding Author: Imane Abdelsadok 00213777568478, imane.abdelsadouk@univ-mascara.dz

Figure 2: Location of the Tighennif plain

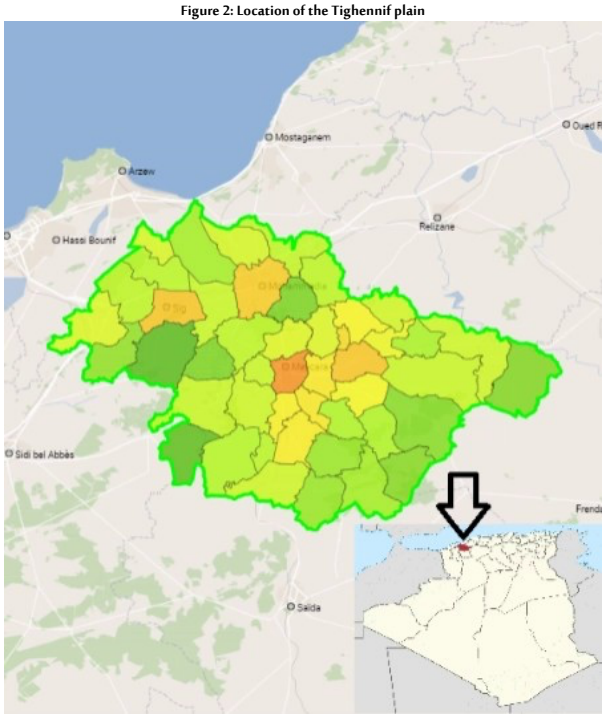

2.2. Bacterial Strains:

The pathogenic agent *Escherichia coli* (*E. coli* ATCC 25922) utilized in this investigation was acquired from the Faculty of Nature and Life Sciences at the University of Mostaganem, Algeria. To validate the test microorganism and test its susceptibility, the VITEK microbial identification system adapted by bioMérieux (bioMérieux, France) was chosen.

2.3. Extraction and Preparation of Plant Sample:

The dried plant materials were macerated with 500 ml of methanol (80%) for 24 h at room temperature. The extract was filtered and dried at a temperature of 40 °C under reduced pressure (Chouikh *et al.*, 2020). The crude extract was lyophilized and maintained at 4 °C for further analysis (ElNaker *et al.*, 2021).

2.4. High Performance Liquid Chromatography Diode Array Detector (HPLC-DAD) Analysis:

Following the aim of evaluating the polyphenolic profile of the tested extract, the analysis was performed using HPLC identification with the YL9100 HPLC system (Young Lin, Anyang, Korea). The HPLC instrument was supplied with a C18 column and diode array detector. The mobile phase consisted of acidified water at 1% formic acid/acetonitrile, and methanol was applied as a solvent. The extract concentration was 5 mg/ml, and the composites were detected at 254 nm under a flow rate of 1 ml/min with a gradient mode; injection volumes were then set at 20 µl. The identification and quantification of phytochemical constituents were assessed by comparison with standards. The quantity of each phytocomponent was expressed based on peak area without correction factors.

2.5. Experimental Animals:

The experimental animals utilized in this research were Wistar rats of both sexes weighing 220 ± 5g. These test rats were raised in the Animal Care Facility of the Faculty of Nature and Life Sciences, Mustapha Stambouli University, Mascara, Algeria.

Animals were housed under optimal standard conditions of temperature (25 ± 2 °C) and relative humidity (60%–70%) with a nychthemeral rhythm (12 h light/dark cycle); standard food and water were given adlibitum. All experimental studies were performed following an overnight fast, but free water access was available. The test animals were assigned at random to several groups to conduct the different experiments.

All experimental processes and approaches adopted in this investigation were conducted according to the ethical standards of the Organization for Economic Cooperation and Development and in compliance with Algerian Law Number 12-235/2012, which is crucial for safeguarding animals used in scientific research.

2.6. Acute Toxicity:

The study aimed to investigate the toxic effects of the methanolic extract acquired from *A. graveolens* seeds in Wistar rats (weighing 220 ± 5g) based on the criteria established by the Organization for Economic Cooperation and Development (OECD, 2008).Two groups were used: The first group (n = 6) received normal saline (9%) orally (p.o.) and served as a control group (CG), whose behavior was to be compared to that of rats from the other group. The second group (n = 6) received individual doses of the methanolic extract of *A. graveolens* seeds (AGM) (50 mg/kg) p.o. (AGMG).

After treatment, the animals were fasted for 2 hours, after which food was made available. To conduct this experiment, the test animals were selected at random. They were observed over 7 days for mortality, changes in skin color, membranes, and pupils, body posture, movement, rearing, tremors, and absorption, as well as the effects of the dose on pain, touch sensitivity, righting reflex, and dietary behavior.

2.7. In Vivo Antimicrobial Activity:

The methanolic extract was tested for its antimicrobial properties on an *E. coli*-induced intestinal infection model. A total of 18 rats were divided randomly into three groups (n = 6), which were designated as follows: The negative control group (NCG) received sterile normal saline (9%); the positive control group (PCG) was treated with a standard antibiotic (4 mg/kg of amoxicillin and clavulanic acid) administered p.o.; and the tested group (CSAG) was administered a dose of 50 mg/kg body weight of *A. graveolens* seed methanolic extract (AGM) p.o.

Forty eight hours before the administration of treatment, all animals were given 1ml of saline solution containing 10^8cfu/ml of *E. coli* in the exponential phase intraperitoneally and then placed in various cages. After 24 hours, blood cultures were conducted to ensure that the animals were infected. After 72 hours, blood cultures were conducted for all groups. This process was carried out regularly after 48, 72, and 144 hours (Yunana *et al.*, 2018). This investigation was conducted under aseptic conditions.

2.8. Histological Study and Preparation of Samples:

After 7 days of experiment, a histological evaluation was conducted on all experimental animals. They were anesthetized, then sacrificed, and the ileum of each was removed. The ileum was kept in a 10% formalin buffer solution. Samples were dehydrated with increasing alcohol percentages from 50% to 99.6% and cleared in xylene; they were then embedded in paraffin using an embedding machine.

After this, blocks of paraffin-embedded samples were sectioned using a rotary ultramicrotome, distributed onto glass slides, and dried overnight. They were stained with hematoxylin and eosin for further microscopic analysis. Microphotography was conducted using Leica Microsystems (Leica Microsystems, Wetzlar, Germany).

3. Results and Discussion

3.1. Yield and AGM Chemical Composition:

The yield value of AGM was 11.74%, higher than the 8.4% obtained by Minaiyan et al. (2021). Seasonal and geographical variables and the postharvest procedure, as well as the extraction solvent, affect the yield percentage (Burdejova *et al.*, 2023). The HPLC analysis of the AGM revealed many phytochemicals, of which the most significant were sinapic acid (49.9%), ascorbic acid (25.4%), quercetin (8.2%), and butylated hydroxyanisole acid (6.1%). This chemical composition is not present in the celery seed ethanol extract and celery seed ethyl acetate fraction identified by gas chromatography-mass selective detector (Kim *et al.*, 2021). However, sinapic acid and quercetin were found in *A.graveolens* seed extract as profiled by Ghoname *et al.* (2023). The phytochemistry of *A. graveolens* is known to be impacted by various factors, including the plant parts (leaves, stem, or seeds), climatic conditions, geographic location, agronomic applications, time and stage of harvest, and postharvest treatment (Chaudhry *et al.*, 2022; Malhotra, 2006 and Sorour *et al.*, 2015) (Table 1, Figure 3).

Table 1: Chemical composition of the methanolic extract of *A. graveolens* seeds.

Peak	Retention Time (min)	Area (%)	Compound Name
1	3.093	49.9	Sinapic acid
2	3.820	25.4	Ascorbic acid
3	19.567	6.1	Butylated hydroxyanisole acid
4	26.777	7.6	Unknown
5	27.300	2.6	Unknown
6	29.540	8.2	Quercetin
7	34.817	0.2	Unknown
	Total	100.0	

Figure 3. High performance liquid chromatography chromatogram of the methanolic extract of *A. graveolens* seeds.

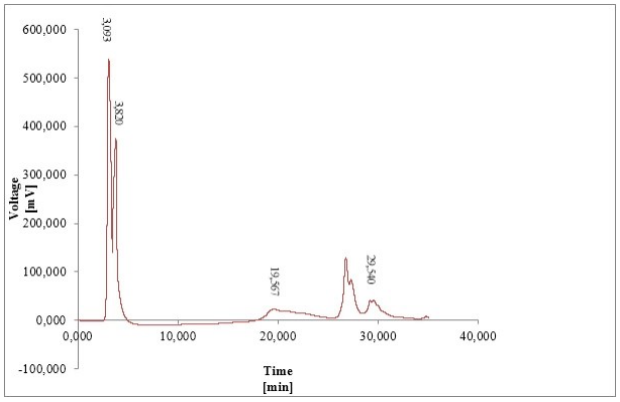

3.2. Acute Toxicity:

Our findings indicated that the dose of 50 mg/kg of AGM did not result in any animal death or signs of toxicity throughout the experimentation period (Table 2).

Table 2: Extract effect on acute toxicity.

Parameters	CG	AGMG
Alertness	usual	usual
Restlessness	usual	usual
Grooming	usual	usual
Touch response	usual	usual
Pain response	usual	usual
Tremors	usual	usual
Writhing reflux	usual	usual
Salivation	usual	usual
Pupils	usual	usual
Urination	usual	usual
Food intake	usual	usual
Water intake	usual	usual
Convulsion	usual	usual
Writhing	usual	usual
Gripping	usual	usual
Skin color	usual	usual
Fur shedding/density	usual	usual
Corneal reflex	usual	usual
Mortality	no mortality	no mortality

CG: control group; AGMG: group received the methanolic extract of *A.graveolens* seeds.

3.3. Antimicrobial Activity Evaluation:

Blood cultures of the NCG (males and females) revealed an intense bacterial culture during the first four samples, followed by a slight decrease in the last sample. However, blood cultures of the PCG showed an intense bacterial culture in males and a slightly less intense bacterial culture in females on day D'0. A continuous decrease in bacterial intensity was observed in all specimens of the PCG across the rest of the experiment.

Observation of the blood cultures of the CSAG indicated an intense bacterial culture in both sexes in the first sample. In the males of this group, a significant decrease in the number of bacterial colonies was detected in the two subsequent blood samples (D'3 and D'5). In D'6 and D'7, the blood cultures were sterile. In the females of the group, blood cultures showed sterility from the second blood sample onward. The sterility of the blood cultures carried out for the CSAG from the second sample for females and the fourth sample for males suggests, when compared to the PCG, that the components of AGM are more powerful than the tested antibiotic (Table 3).

Numerous epidemiological investigations have demonstrated that the genus Apium contributes significantly to avoiding microbial proliferation thanks to its antibacterial and antifungal properties (Kooti and Daraei, 2017). The crude extracts of *A. graveolens* show notable bactericidal activity against several gram-positive, -negative, and fungal strains. It has been demonstrated that plant extracts' potency and their bioactive components, especially flavonoids, have antimicrobial properties (Al-Aboody, 2021).

Indeed, the outcomes seen here accord with those of Uddin et al.(2015), performed in vitro, which demonstrated that *A. graveolens* extracts had strong antimicrobial effects and exhibited good efficacy against *E. coli*, *S. aureus*, *S. typhi*, *B. subtilis*, and *P. aeruginosa*. Flavonoids, alkaloids, and saponins are phytoconstituents of *A.graveolens* extract that contribute to its antibacterial activity. Flavonoids' antibacterial effects can be attributed to a number of processes, including energy metabolism suppression, nucleic acid production, and cytoplasmic membrane function, while bacterial cell membrane permeability is correlated with saponins (Khotimah *et al.*, 2020).

Due to its hydroxyl group's action on bacterial membranes, quercetin is a flavonoid that demonstrates antibacterial activity against a variety of gram-positive and gram-negative bacteria. Quercetin was found to be a potent antibacterial agent in vitro against isolates of *E. coli* that produced OXA-48 β-lactamase by lowering the minimum inhibitory concentrations of imipenem and piperacillin when used in combination (Majumdar and Mandal, 2024). By modulating the activity of adenosine triphosphate, this phytocomposite inhibits the growth of *E. coli* (Qi *et al.*, 2022).

Moreover, the structural integrity of the bacterial cell wall and cell membrane was compromised by quercetin, which made these more permeable. The cell's endochylema contents were discharged, which altered adenosine triphosphate activity. In fact, quercetin impacted protein expression in the cell, reduced bacterial protein production, and ultimately caused cell lysis and death (Wang et al., 2018). In addition, quercetin breaks or modifies plasma membranes, prevents population intervention pathways, stops bacterial adhesion, and inhibits efflux pumps, which interrupt the synthesis of nucleic acids (Qi *et al.*, 2022).

Studies conducted in vitro and in vivo have revealed that vitamin C works against clinical isolates of *E. coli* as an antibacterial and anti-biofilm agent (Hassuna *et al.*, 2023).

The antibacterial action of sinapic acid against *E. coli* and *S. aureus* is substantial. It contributes to the suppression of the NorA efflux pump,

since it has the highest affinity for the protein NorA and forms meaningful interactions, including hydrogen bonds with tyrosine (Singh *et al.*, 2022).

Table 3: Detection of *E. coli* in blood cultures.

Group	Sex	D'0	D'3	D'5	D'6	D'7
NCG	Male	++++	++++	++++	++++	+++
	Female	++++	++++	++++	++++	+++
PCG	Male	++++	++	++	+	–
	Female	+++	++	++	+	–
CSAG	Male	++++	+	+	–	–
	Female	++++	–	–	–	–

++++: too numerous to count; +++: numerous; ++: moderate; +: low; –: sterile.
NCG: negative control group (infected); PCG: positive control group (infected; treated with antibiotics); CSAG: infected group treated with the methanolic extract of *A.graveolens* seeds.

3.4. Histological Study:

The anatomopathological study of the ilea of the NCG in males and females indicated intense inflammation marked by an inflammatory infiltrate containing eosinophilic polynuclear leukocytes and lymphocytes, vascular congestion, and remodeling of lymph nodes, which reflects ileitis; this was probably a consequence of the induced intestinal infection. This could then be expected, through bacterial invasion, to translocate to target organs, such as the liver, spleen, and general blood circulation.

Microscopic examination of the ileum in rats from the PCG revealed an inflammatory infiltrate and vascular congestion in both sexes. In addition, the histological architecture of this group was modified by a well-marked cellular necrosis of the villi. These results show that the antibiotic had an oxidative effect, causing cell necrosis. Subsequently, it caused a modification in the architecture of the ileum by affecting the intestinal microbial flora and the immune system of the ileum in general, resulting in an imbalance and the persistence of inflammation. This led to other complications and pathologies.

Ileum histology of the CSAG, however, showed a normal and well-preserved morphological appearance similar to that of the neutral control group, with normal mucosa and epithelial tissue and well-preserved architecture and relief of the villi, as well as a normal chorion, seat of a slight infiltrate, which is normal in males, and no visible vascular congestion or necrotic remodeling in males or females, representing no inflammation. This appearance was more conspicuous than that of the PCG, which suggests, firstly, that the extract treated the infection and, secondly, that it protected the organ against lesions, destruction, and cellular necrosis. Indeed, it stimulated its functioning and its microbial flora by improving the immune system, fighting against the pathogen, treating inflammation, and fighting cellular oxidation (Figure 4).

Recent research has examined the anti-inflammatory potential of chemicals extracted from Apium plants (Al-Asmari *et al.*, 2017; Powanda and Rainsford, 2011; Vahidi *et al.*, 2019 and Ziyan *et al.*, 2007). One of these chemicals is quercetin, whose anti-inflammatory effect was demonstrated by its decreasing the production of inflammatory molecules such as nuclear factor-kappa B (NF-ĸB), reactive C-protein, activator protein 1, mitogen-activated protein kinase, reactive nitric oxide synthase, and cyclooxygenase-2 (Aghababaei and Hadidi, 2023).

Moreover, due to the presence of vitamins, including vitamin C and vitamin A, *A. graveolens* can positively affect the immune system (Sowbhagya, 2014). A recent study demonstrated the antioxidant and anti-inflammatory qualities of ascorbic acid in treating urinary tract infections induced by *E. coli*, with significant increases in antioxidants (glutathione and total antioxidant capacity) and decreases in inflammatory mediators (malondialdehyde and NF-ĸB) (Hassuna *et al.*, 2023). Furthermore, sinapic acid suppresses the signaling of activating transcription factor 2 protein and NF-ĸB by targeting transforming growth factor beta-activated kinase 1 (Jang *et al.*, 2023).

These findings also align with the histological results obtained in the CSAG, where ileitis, the inflammation of the ileum, was not visible.

Plants of the genus Apium are rich in flavonoids and phenolic components, which are principally responsible for antioxidant activity. Numerous studies have been performed to demonstrate that the seeds, roots, and leaves of Apium plants possess antioxidant capacities both in vitro and in vivo (Al-Asmari *et al.*, 2017; Liu *et al.*, 2020). Recent investigations have revealed that celery leaves, as compared to petioles, are an excellent source of natural antioxidants and free radical scavengers (Liu et al., 2020). Flavonoids and phenolic chemicals found in celery extract prevent reactive oxygen species (ROS) from being produced during inflammation (Hussain *et al.*, 2016).

Quercetin is the most potent natural antioxidant. It has been shown that quercetin exhibits antioxidant properties as an ROS scavenger (Aghababaei and Hadidi, 2023). By controlling glutathione levels, it can strengthen the body's antioxidant systems (Qi *et al.*, 2022). Furthermore, quercetin can reduce oxidative stress in A549 cells by modifying the expression of genes linked to antioxidants (Qi *et al.*, 2022).

In addition to ascorbic acid, a reducing agent that may decrease and neutralize ROS, including hydrogen peroxide, sinapic acid is a promising antioxidant that efficiently reduces oxidative stress indicators in plasma and tissues while increasing non-enzymatic antioxidants in plasma (Nithya and Subramanian, 2017).

Such data explain the absence of cellular necrosis, the preservation of the villus structure, and the well-maintained architecture of the ileum in the CSAG. They thus confirm the antioxidant effect of this extract.

Figure 4: Histopathological sections of ileum.

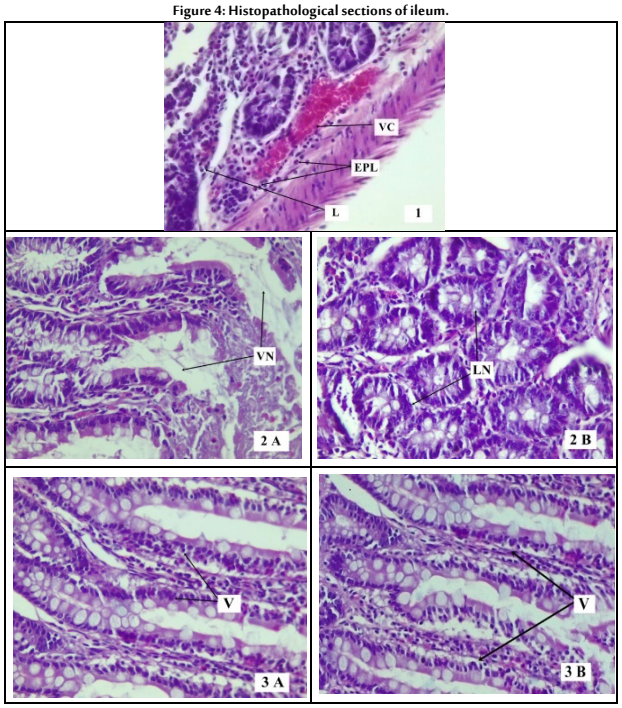

(1) Negative control group (infected); (2) positive control group (infected; treated with antibiotics), (A) male; (B) female; (3) infected group treated with the methanolic extract of *A. graveolens* seeds, (A) male; (B) female (Hematoxylin and eosin staining x 100). VC: vascular congestion; L: lymphocytes; EPL: eosinophilic polynuclear leukocytes; VN: villi necrosis; V: villi; LN: lymphatic nodes.

4. Conclusion

This study revealed that the methanolic extract of *A.graveolens* seeds was a rich source of various bioactive molecules (sinapic acid

[49.9%], ascorbic acid [25.4%], butylated hydroxyanisole acid [6.1%], and quercetin [8.2%]). *A. graveolens* seed extract harvested from western Algeria was found to be completely safe and non-toxic at the dose of 50 mg/kg. Furthermore, the in vivo study showed that this extract was 100% effective in treating *E. coli*-induced intestinal infection in the treated animals.

The efficiency of this extract could be associated with the various phytochemicals found in the plant. This result is confirmed and validated by the application of this plant in treating various microbial infections in traditional medicine. *Apium graveolens* is an antimicrobial agent that could be used as an antibiotic or a natural antimicrobial ingredient in the antibiotic industry. This plant also possesses anti-inflammatory and antioxidant properties, which qualify it as an excellent therapeutic substance.

This study suggests that future research should be designed to investigate the effect of other extraction solvents and techniques on the phytocomposition of this plant and evaluate its antimicrobial activity in vitro and in vivo in treating infections and combating antibiotic resistance. Additionally, clinical trials should be devised with large sample numbers and extended follow-up periods to explore the extract's applicability and acquire relevant clinical data, including toxicity, to evaluate its specific therapeutic dosage and improve its application in patients.

Biographies

Imane Abdelsadok

Bioconversion, Microbiological Engineering, and Health Safety Laboratory, Department of Biology, Faculty of Nature and Life Sciences, Mustapha Stambouli University, Mascara, Algeria, 00213777568478, imane.abdelsadouk@univ-mascara.dz

Imane is an Algerian PhD student in the field of Biological Sciences in the Bioconversion, Microbiological Engineering, and Health Safety Laboratory, Department of Biology, Faculty of Nature and Life Sciences, Mustapha Stambouli University, Mascara. She is a biological engineer who graduated from Abdelhamid Ibn Badis University of Mostaganem, Algeria, and earned her master's degree in Pharmacognosy and Phytotherapy from the same university in 2017. Her research interests include natural substances and biological activities.

ORCID ID: 0009-0005-9362-5687.

Karima Ouldyerou

Bioconversion, Microbiological Engineering, and Health Safety Laboratory, Department of Biology, Faculty of Nature and Life Sciences, Mustapha Stambouli University, Mascara, Algeria, 213663971364, *mhanine11@yahoo.fr*

Dr. Ouldyerou is an Algerian lecturer who obtained her Ph.D. in Biology from Mustapha Stambouli University, Mascara, Algeria, in 2016. She has been a member of the research staff of the Laboratory of Bioconversion, Microbiological Engineering, and Health Safety at Mascara University since 2012. Her research focuses on medicinal plants. She has published many articles in highly regarded journals and has participated in conferences in several countries, including Morocco, Tunisia, Spain, and Algeria.

ORCID ID: 0000-0003-0431-603X.

Boumediene Meddah

Bioconversion, Microbiological Engineering, and Health Safety Laboratory, Department of Biology, Faculty of Nature and Life Sciences, Mustapha Stambouli University, Mascara, Algeria, 213771757063, meddah19@yahoo.fr

Prof. Meddah earned his Ph.D. in Clinical Chemistry in the Faculty of Pharmacy at the University of Picardie Jules Verne, France. In 1999, he started as an Assistant in Clinical Pharmacy at the same university. He was recruited as a Professor of Biochemistry at the University of Mascara, Algeria, in 2000, a post he still occupies. Since 2011, he has led the research team at the Bioconversion, Microbiological Engineering, and Health Safety Laboratory. His research focuses on the valorization of natural substances and their therapeutic formulation.

ORCID ID: 0000-0002-6837-3458.

Pascal Sonnet

Infectious Agents, Resistance, and Chemotherapy Laboratory UR 4294, Faculty of Pharmacy, University of Picardie Jules Verne, Amiens, France, 033322827478, pascal.sonnet@u-picardie.fr

Prof. Sonnet graduated from Caen University in 1997 with a Ph.D. in Medicinal Chemistry. From 1997 to 1998, he worked as a Postdoctoral Research Assistant in Synthetic Organic Chemistry at Montreal University. In 1998, he started as an Assistant Professor of Medicinal Chemistry at the UPJV Faculty of Pharmacy. In 2004, he was promoted to professor. He has led the AGIR research team since 2018. His research area is the development of antibacterial and antimalarial medicines.

ORCID ID: 0000-0003-0118-9151.

Acknowledgements

The authors wish to thank all the individuals and institutions who made this study possible.

References

Aghababaei, F. and Hadidi, M. (2023). Recent advances in potential health benefits of quercetin. *Pharmaceuticals*, **16**(7), 1020. DOI: 10.3390/ph16071020

Al-Aboody, M.S. (2021). Cytotoxic, antioxidant, and antimicrobial activities of Celery (Apium graveolens L.). *Bioinformation*, **17**(1), 147.DOI:10.6026/97320630017147

Al-Asmari, A.K., Athar, M.T. and Kadasah, S.G. (2017). An updated phytopharmacological review on medicinal plant of Arab region: Apium graveolens linn. *Pharmacognosy Reviews*, **11**(21), 13. DOI: 10.4103/phrev.phrev_35_16

Chouikh, A., Rebiai, A., Aref, M., Heded, M., Adjal, E.H. and Alia, F. (2020). Effects of extraction methods on total polyphenols, free radical scavenging and antibacterial activity of crude extracts of Cleome arabica L. growing in Oued Souf region. *Algerian Journal of Biosciences*, **1**(1), 14–7. DOI: 10.5281/zenodo.4051407

Burdejova, L., Tobolkova, B., Polovka, M. and Neugebauerova, J. (2023). Differentiation of medicinal plants according to solvents, processing, origin, and season by means of multivariate analysis of spectroscopic and liquid chromatography data. *Molecules*, **28**(10), 4075. DOI: 10.3390/molecules28104075

Chaudhry, F., Ahmad, M.L., Hayat, Z., Ranjha, M.M.A.N., Chaudhry, K., Elboughdiri, N. and Uddin, J. (2022). Extraction and evaluation of the antimicrobial activity of polyphenols from banana peels employing different extraction techniques. *Separations*, **9**(7), 165. DOI : 10.3390/separations9070165

Cheng, J., Liu, Y., Li, S., Pu, K., Yang, L. and Tan, L. (2024). Incidence of and Risk Factors for Third-Generation Cephalosporin-Resistant Escherichia coli Bloodstream Infections in Children. *Infection and Drug Resistance*,**17**(n/a), 543–50. DOI: 10.2147/IDR.S449731

Edziri, H., Ammar, S., Souad, L., Mahjoub, M.A., Mastouri, M., Aouni, M. and Verschaeve, L. (2012). In vitro evaluation of antimicrobial and antioxidant activities of some Tunisian vegetables. *South African Journal of Botany*, **78**(n/a), 252–6. DOI:10.1016/j.sajb.2011.09.012

ElNaker, N.A., Daou, M., Ochsenkühn, M.A., Amin, S.A., Yousef, A.F. and Yousef, L.F. (2021). A metabolomics approach to evaluate the effect of lyophilization versus oven drying on the chemical composition of plant extracts. *Scientific Reports*, **11**(1), 22679. DOI: 10.1038/s41598-021-02158-6

Ghoname, E.S.A., Hassan, D. and Hammad, E.M. (2023). Antimicrobial Activity of Dill Seeds and Celery Seeds on Beef Burger. *European Journal of Nutrition and Food Safety*, **15**(9), 106–17. DOI:10.9734/ejnfs/2023/v15i91339

Hassuna, N.A., Rabie, E.M., Mahd, W.K.M., Refaie, M.M., Yousef, R.K.M. and Abdelraheem, W.M. (2023). Antibacterial effect of vitamin C against uropathogenic E. coli in vitro and in vivo. *BMC*

Microbiology, **23**(1), 112. DOI:10.1186/s12866-023-02856-3

Hussain, T., Tan, B., Yin, Y., Blachier, F., Tossou, M.C. and Rahu, N. (2016). Oxidative stress and inflammation: What polyphenols can do for us?. *Oxidative Medicine and Cellular Longevity*, **2016**(1), 7432797. DOI:10.1155/2016/7432797

Jang, S., Kim, S., So, B.R., Kim, Y., Kim, C.K., Lee, J.J. and Jung, S.K. (2023). Sinapic acid alleviates inflammatory bowel disease (IBD) through localization of tight junction proteins by direct binding to TAK1 and improves intestinal microbiota. *Frontiers in Pharmacology*, **14**(n/a), 1217111.DOI:10.3389/fphar.2023.1217111

Khalil, A., Nawaz, H., Ghania, J.B., Rehman, R.and Nadeem, F. (2015). Value added products, chemical constituents and medicinal uses of celery (Apium graveolens L.)—A review. *International Journal of Chemical and Biochemical Sciences*, **8**(2015), 40–8.

Khotimah, H., Diyantoro, D.W.I. and Sundari, A.S. (2020). Screening in vitro antimicrobial activity of celery (Apium graveolens) against Staphylococcus Sp. *Malays. J. Med. Health Sci*, **16**(n/a), 72–7.

Kim, M.A., Lee, H.J., Bae, H.G., Yang, S.O., Lee, H.J. and Kim, M.J. (2021). Metabolite analysis and anti-obesity effects of celery seed in 3T3-L1 adipocytes. *Food Science and Biotechnology*, **30**(n/a), 277–86. DOI:10.1007/s10068-020-00866-9

Kolesnichenko, S.I., Lavrinenko, A.V. and Akhmaltdinova, L.L. (2021). Bloodstream infection etiology among children and adults. *International Journal of Microbiology*, **2021**(1), 6657134. DOI:10.1155/2021/6657134

Kooti, W. and Daraei, N. (2017). A review of the antioxidant activity of celery (Apium graveolens L). *Journal of Evidence-Based Complementary &Alternative Medicine*, **22**(4), 1029–34. DOI:10.1177/2156587217717415

Liu, D.K., Xu, C.C., Zhang, L., Ma, H., Chen, X.J., Sui, Y.C. and Zhang, H.Z. (2020). Evaluation of bioactive components and antioxidant capacity of four celery (Apium graveolens L.) leaves and petioles. *International Journal of Food Properties*, **23**(1), 1097–109. DOI:10.1080/10942912.2020.1778027

Majumdar, G. and Mandal, S. (2024). Evaluation of broad-spectrum antibacterial efficacy of quercetin by molecular docking, molecular dynamics simulation and in vitro studies. *Chemical Physics Impact*, **8**(n/a), 100501. DOI: 10.1016/j.chphi.2024.100501

Malhotra, S.K. (2006). *Celery*. In Handbook of Herbs and Spices, 3rd ed., Elsevier, Amsterdam, The Netherlands.

Malhotra, S.K. (2012). *Celery*. In Handbook of Herbs and Spices, 2nd ed., Sawston, UK.

Mezeyova, I., Hegedűsová, A., Mezey, J., Šlosár, M. and Farkaš, J. (2018). Evaluation of quantitative and qualitative characteristics of selected celery (Apium graveolens var. dulce) varieties in the context of juices production. *Potravinarstvo*, **12**(1), 173–9. DOI: 10.5219/883

Minaiyan, M., Ghanadian, S.M. and Hossaini, M. (2021). Protective effect of Apium graveolens L.(Celery) seeds extracts and luteolin on acetic acid-induced colitis in rats. *International Journal of Preventive Medicine*, **12**(1), 100. DOI:10.4103/ijpvm.IJPVM_651_20

Nithya, R. and Subramanian, S. (2017). Antioxidant properties of sinapic acid: In vitro and in vivo approach. *Asian Journal of Pharmaceutical and Clinical Research*, **10**(6), 255. DOI:10.22159/ajpcr.2017.v10i6.18263

Organization for Economic Cooperation and Development (OECD) (2008). *Repeated Dose Oral Toxicity Test Method*. OECD Guidelines for Testing of Chemicals. Paris, France: OECD.

Penna, C., Marino, S., Vivot, E., Cruañes, M.C., Muñoz, J.D.D., Cruañes, J. and Martino, V. (2001). Antimicrobial activity of Argentine plants used in the treatment of infectious diseases. Isolation of active compounds from Sebastianiabrasiliensis. *Journal of Ethnopharmacology*, **77**(1), 37–40. DOI: 10.1016/s0378-8741(01)00266-5

Pokharel, P., Dhakal, S. and Dozois, C.M. (2023). The diversity of *Escherichia coli* pathotypes andvaccination strategies against this versatile bacterial pathogen. *Microorganisms.*, **11**(2), 344.DOI: 10.3390/microorganisms11020344

Powanda, M.C. and Rainsford, K.D. (2011). A toxicological investigation of a celery seed extract having anti-inflammatory activity. *Inflammopharmacology*, **19**(4), 227–33. DOI:10.1007/s10787-010-0049-1

Prakoso, Y.A., Rini, C.S., Rahayu, A., Sigit, M. and Widhowati, D. (2020). Celery (Apium graveolens) as a potential antibacterial agent and its effect on cytokeratin-17 and other healing promoters in skin wounds infected with methicillin-resistant Staphylococcus aureus. *Veterinary World*, **13**(5), 865. DOI: 10.14202/vetworld.2020.865-871

Qi, W., Qi, W., Xiong, D. and Long, M. (2022). Quercetin: Its antioxidant mechanism, antibacterial properties and potential application in prevention and control of toxipathy. *Molecules*, **27**(19), 6545. DOI: 10.3390/molecules27196545

Rani, P. and Khullar, N. (2004). Antimicrobial evaluation of some medicinal plants for their anti-enteric potential against multi-drug resistant salmonella typhi. *Phytotherapy Research: An International Journal Devoted to Pharmacological and Toxicological Evaluation of Natural Product Derivatives*, **18**(8), 670–3. DOI: 10.1002/ptr.1522

Roslon, W., Osinska, E. and Gajc-Wolska, J. (2009, April). The influence of raw material stabilization on the quality of celery (Apium graveolens L.) leaves. In *VI International Postharvest Symposium* **877**(n/a), 201–8. DOI:10.17660/ActaHortic.2010.877.20

Salehi, B., Venditti, A., Frezza, C., Yücetepe, A., Altuntaş, Ü., Uluata, S. and Sharifi-Rad, J. (2019). Apium plants: Beyond simple food and phytopharmacological applications. *Applied Sciences*, **9**(17), 3547. DOI: 10.3390/app9173547

Singh, K., Coopoosamy, R.M., Gumede, N.J. and Sabiu, S. (2022). Computational insights and in vitro validation of antibacterial potential of shikimate pathway-derived phenolic acids as NorA efflux pump inhibitors. *Molecules*, **27**(8), 2601. DOI: 10.3390/molecules27082601

Sorour, M.A., Hassanen, N.H. and Ahmed, M.H. (2015). Natural antioxidant changes in fresh and dried celery (Apium graveolens). *Am. J. Energy Eng*, **3**(2-1), 12–6. DOI:10.11648/j.ajee.s.2015030201.13

Sowbhagya, H.B. (2014). Chemistry, technology, and nutraceutical functions of celery (Apium graveolens L.): An overview. *Critical Reviews in Food Science and Nutrition*, **54**(3), 389–98. DOI:10.1080/10408398.2011.586740

Uddin, Z., Shad, A.A., Bakht, J., Ullah, I. and Jan, S. (2015). In vitro antimicrobial, antioxidant activity and phytochemical screening of Apium graveolens. *Pakistan Journal of Pharmaceutical Sciences*, **28**(5). 1699–704.

Vahidi, A., Ebrahim Rezvani, M., Ramezani, V., Boroumand, M. and Jahani, Y. (2019). Evaluation of anti-nociceptive and anti-inflammatory activities of Apium graveolens L. roots extract in mice. *Research Journal of Pharmacognosy*, **6**(3), 69–75. DOI:10.22127/rjp.2019.89467

Wang, S., Yao, J., Zhou, B., Yang, J., Chaudry, M.T., Wang, M. and Yin, W. (2018). Bacteriostatic effect of quercetin as an antibiotic alternative in vivo and its antibacterial mechanism in vitro. *Journal of Food Protection*, **81**(1), 68–78. DOI: 10.4315/0362-028X.JFP-17-214

Xiao, S., Tang, C., Zeng, Q., Xue, Y., Chen, Q., Chen, E. and Han, L. (2022). Antimicrobial resistance and molecular epidemiology of Escherichia coli from bloodstream infection in Shanghai, China, 2016–2019. *Frontiers in Medicine*, **8**(n/a), 803837. DOI: 10.3389/fmed.2021.803837

Yunana, B.T., Guiyi, J.C. and Bukar, B.B. (2018). In vitro and in vivo evaluation of antibacterial activity of Bridelia ferrugine extracts on some clinical isolates. *The Journal of Phytopharmacolog.*, **7**(4), 392–8. DOI: 10.31254/phyto.2018.7407

Ziyan, L., Yongmei, Z., Nan, Z., Ning, T. and Baolin, L. (2007). Evaluation of the anti-inflammatory activity of luteolin in experimental animal models. *Planta Medica*, **73**(3), 221–6. DOI:10.1055/s-2007-967122

Scientific Journal of King Faisal University:
Basic and Applied Sciences

Performance Optimisation of a Wind Turbine Simulator with Transverse Cracked Blades using Taguchi-Based Grey Relational Analysis

Abdulhamed Hamdan Al-Hinai, Karu Clement Varaprasad and V. Vinod Kumar
Department of Mechanical and Mechatronic Engineering, Sohar University, Sohar, Oman

LINK	RECEIVED	ACCEPTED	PUBLISHED ONLINE	ASSIGNED TO AN ISSUE
https://doi.org/10.37575/b/eng/240044	24/09/2024	20/11/2024	20/11/2024	01/12/2024
NO. OF WORDS	**NO. OF PAGES**	**YEAR**	**VOLUME**	**ISSUE**
8039	8	2024	25	2

ABSTRACT

The presence of blade surface cracks creates chances for vibration propagation that affects wind turbine performance. This study examines the effects of transverse cracks on the vibration levels and power output of wind turbine systems. Multiple regression models are developed as predictive tools to highlight the impact of transverse crack sizes and variations in rotational speed on vibration levels and power generation. Grey relational analysis is used as an optimisation technique to identify optimal settings for maximum power output and minimum vibration levels. By modelling and analysing these factors, the study reveals a significant correlation between increased crack size and elevated vibration levels, which can compromise structural integrity. Additionally, while higher rotational speeds initially boost power output, they also lead to exponential increases in vibration, exacerbating the risks associated with blade defects. The findings emphasise the critical need for a balanced approach in optimising turbine performance, introducing a novel approach to speed management and vibration control, which is employed in this study. The research suggests potential avenues for future exploration, including the development of advanced materials and design innovations aimed at mitigating these risks, enabling safer and more efficient turbine operation.

KEYWORDS
Defect, optimal settings, power, rotational speed, regression, vibration

CITATION
Al-Hinai, A. H., Varaprasad, K. C. and Vinod Kumar, V. (2024). Performance optimisation of wind turbine simulator with transverse cracked blades using Taguchi-based grey relational analysis. *Scientific Journal of King Faisal University: Basic and Applied Sciences*, **25**(2), 42– 9. DOI: 10.37575/b/eng/240044

1. Introduction

Wind energy has rapidly gained prominence as a key renewable energy source, motivated by global implementation of energy efficiency and reliability (Wagner, 2015). The evolution of the wind energy sector from constant-speed wind turbine systems to more advanced systems reflects industrial innovation (Polinder, 2011). Direct-drive wind turbine systems are particularly valued for their reliability in wind turbine applications, especially as wind power is increasingly integrated into the grid (Blaabjerg and Ma, 2017).

Wind turbines are complex machines that convert wind energy into electrical power and are composed of key components such as blades, rotors and generators (Al-Hinai *et al.,* 2024). Horizontal-axis turbines are a more popular type and feature three blades and high-speed asynchronous generators (Lubosny, 2003). These systems rely on the dynamic wind pressure exerted on the blades to be converted into electrical energy. The efficiency of this process depends on the durability of the blades, which must withstand significant mechanical and environmental stresses (Pacheco *et al.*, 2024). However, blade defects remain a challenge, impacting turbine performance and longevity and leading to increased maintenance, downtime and safety risks (Liu *et al.*, 2015). Fatigue-related failures are common, particularly in blades and joints, with transverse fracture faults being a significant issue, as shown in Figure 1 (Sutherland, 1999). Crack formation in blades typically occurs in three steps: crack initiation, stable crack extension and eventual fracture. The total fatigue life of a blade can be expressed as the sum of crack initiation life and crack propagation life:

$$N_{total} = N_{initiation} + N_{propogation}$$

Wind turbine vibrations present significant challenges to the system's performance and longevity, originating from aerodynamic forces, mechanical imbalances and structural defects (Xie and Aly, 2020). Various control and vibration monitoring techniques are employed to detect and mitigate these issues (Barszcz, 2019). Experimental setups and simulations are vital for studying these vibrations and optimising turbine performance (Tibaldi *et al.*, 2016). Additionally, regression modelling and optimisation techniques are widely used in wind energy research to predict performance metrics in order to enhance efficiency (Balasubramanian *et al.*, 2020).

Figure 1: Transverse defects on wind turbine blades (Wang *et al.*, 2022)

This research seeks to optimise the wind turbine performance while minimising vibration levels. This involves an innovative analysis of a wind turbine simulation system with transversely defective blades operating at various rotational speeds. The study identifies the optimal settings that enhance power output while reducing vibration levels, making proactive maintenance through condition monitoring increasingly essential as wind turbines continue to grow in capacity (Koulocheris *et al.*, 2013). The structure of this paper is as follows: Section 2 reviews the existing literature on wind turbine technology and vibration challenges; Section 3 outlines the methodology used, including the simulation setup and data analysis techniques; Section 4 presents the results, focusing on the optimisation of power output and vibration reduction; and finally, Section 5 concludes with the study's contributions and suggestions for future research.

Corresponding Author: Abdulhamed Hamdan Al-Hinai 00968 99883473, 223306@students.su.edu.om

2. Literature Review

In recent years, wind energy has gained importance as a critical source of renewable energy. With advancements in wind turbine technology, the status of effective condition monitoring and vibration analysis has increased to ensure optimal performance and operational safety. As wind turbines become larger and are deployed in remote areas, condition monitoring becomes vital (Yang *et al.*, 2009).

Wind turbine blades are susceptible to various forms of damage and wear over time, leading to increased vibrations and decreased performance. Research has identified numerous technologies and methods to mitigate these vibrations and enhance wind turbine efficiency. Integrated approaches and optimisation algorithms have been explored extensively for vibration control and performance optimisation. Skrimpas *et al.* (2016) proposed an algorithm for effective along-wind vibration control of large wind turbines, demonstrating the potential of algorithmic solutions for dynamic response issues (Skrimpas *et al.*, 2016). Similarly, Sarkar and Chakraborty (2018) investigated optimal designs for long-wind vibration control, showcasing the synergy of advanced control algorithms and passive vibration control devices (Sarkar and Chakraborty, 2018).

Machine learning algorithms have also shown promise in structural health monitoring, as highlighted by Flah *et al.* (2020), who conducted a systematic review on the subject (Flah *et al.*, 2020). Conversely, Sheng (2012) focused on vibration analysis in the 'Wind Turbine Gearbox Condition Monitoring Round Robin Study', providing insights into the specific challenges and requirements of monitoring turbine gearboxes (Sheng, 2012). Liu *et al.* (2020) examined fault diagnosis of industrial wind turbine blade bearings using acoustic emission analysis, demonstrating its effectiveness in harsh conditions and slow-speed operations (Liu *et al.*, 2020).

Innovative methods continue to emerge. Joshuva and Sugumaran (2017) introduced a new blade condition monitoring technique based on the transmissibility of frequency response functions, utilising signals from multiple sensors for both damage detection and location (Joshuva and Sugumaran 2017). Ou *et al.* (2017) proposed a novel intelligent icing detection method for blades using SCADA data, addressing the significant issue of ice accretion (Ou *et al.*, 2017). Yang *et al.* (2015) emphasised the critical role of structural health monitoring and condition monitoring in assessing wind turbine components, while Antoniadou *et al.* (2015) discussed the complexities of damage detection in offshore wind turbines, highlighting the need for effective structural health monitoring and condition monitoring strategies (Yang *et al.*, 2015). Liu *et al.* (2019) explored non-contact methods such as thermography for blade icing detection, offering insights into subsurface damage detection (Liu et al., 2019). Florian and Sørensen (2015) stressed the need for reliable remote monitoring systems and proposed a blade lifetime assessment model for preventive maintenance planning (Florian and Sørensen 2015). Kusnick *et al.* (2015) focused on intelligent condition monitoring systems for rotor imbalance detection (Kusnick *et al.*, 2015).

Vibration analysis remains a cornerstone of wind turbine monitoring. Dong *et al.* (2018) studied structural vibration monitoring and operational modal analysis of offshore wind turbines, enhancing the understanding of vibration characteristics (Dong *et al.*, 2018). Liu *et al.* (2020) introduced an empirical wavelet thresholding method for blade-bearing fault detection, while Teng *et al.* (2019) proposed a novel vibration model for diagnosing compound faults in gearboxes (Liu *et al.*, 2020 and Teng *et al.*, 2019). He *et al.* (2016) developed an innovative order-tracking method for planetary gearbox vibration analysis (He *et al.*, 2016).

Blade defects significantly impact turbine performance and reliability. Manufacturing flaws are a primary cause of blade repairs and failures. Computational fluid dynamics can effectively analyse faults in vertical axis wind turbines, with defects affecting torque output. Researchers have developed probabilistic models to assess blade reliability, treating defects as uncertainty variables (Riddle *et al.*, 2018). Monte Carlo simulations describe failure probabilities, offering more accurate reliability assessments and potential reductions in design conservatism.

Despite extensive research on vibration analysis and condition monitoring, comprehensive studies on the performance of turbines with defective blades are lacking. Castorrini *et al.* (2019) conducted a computational analysis of performance deterioration due to environmental erosion, but more research is needed on defective blades' impact on overall performance (Castorrini *et al.*, 2019). Research focused on the aerodynamic shape optimisation of blades using advanced computational models and the development of novel optimisation algorithms, such as the artificial bee colony algorithm for shape optimisation (Derakhshan *et al.*, 2015). Non-stationary signal processing techniques applied to vibration analysis and the use of vibration and power curve analysis for detecting icing on blades represent potential areas for future research (Maheswari and Umamaheswari, 2017). As the wind energy industry expands, reducing operation and maintenance costs while improving reliability remains a priority (Tchakoua *et al.*, 2014).

3. Methods and Materials

To investigate the performance of a wind turbine simulator (WTS), real wind speed data from the town of Sohar in Oman was used as a hypothetical operating range of shaft rotational speed using WTS conversion. The WTS model employed in this research work was the SpectraQuest (SQ) type that used a VibraQuest (VQ) simulation software and data acquisition system. This investigation aimed to reduce the generated average of the vibration waveform range. This is basically the difference between the average of (m) positive peaks and the average of (n) negative peaks, as shown in Figure 2. When the vibration level was reduced, the WTS performance increased. The following equations were used to calculate the average of positive peaks, the average of negative peaks and the vibration level:

$$\text{Average of positive peaks} = \frac{\sum_{i=1}^{m}(\text{positive vibration peaks})}{m}$$

$$\text{Average of negative peaks} = \frac{\sum_{i=1}^{n}(\text{negative vibration peaks})}{n}$$

$$\text{Vibration level} = \text{average of positive peaks} - \text{average of negative peaks}$$

This section involved 1) an experimental setup of the SQ WTS; 2) the Taguchi design of the experiment (DoE); 3) experimental testing of the WTS as per DoE; 4) analysing the generated vibration waveform and power output; 5) analysing Taguchi response; 6) regression modelling of vibration level and power output; and finally 7) optimising the multi-responses using grey relational analysis (GRA) and sensitivity analysis.

Figure 2: Research concept

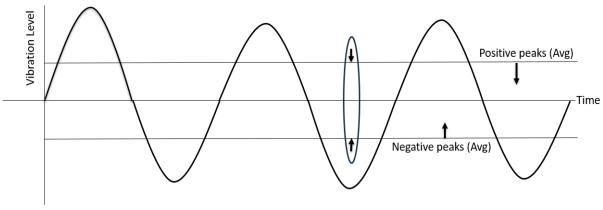

Experimental setup: The SQ WTS used in this research was of a three-blade type horizontal-axis wind turbine, as shown in Figure 3. The base dimensions were 2.991 m × 2.438 m, the centreline height was 2.369 m, the swept blade diameter was 3.3 m, and the weight was 222.7 kg. A tachometer and an accelerometer were mounted on the rotational shaft to measure the rotational speed and vibration level in one direction of vibrational excitation, respectively (Koulocheris *et al.*, 2013). A data acquisition system read the signals from these sensors and sent them to the VQ simulation software for analysis and to generate vibration reports, as shown in Figure 4. The three transversely defective blades used in this research work are shown in Figure 5.

Figure 3: SQ WTS

Figure 4: VQ analysis software

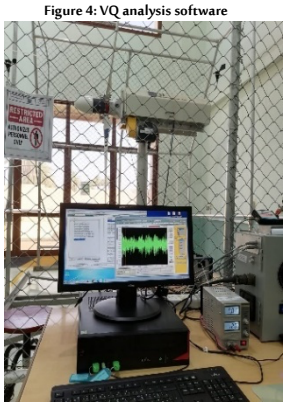

Figure 5: Three transversely defective blades (three crack levels)

Taguchi design of experiments: The experimental work was planned by Taguchi design of experiments (DoE) with two main independent parameters; namely A: crack size and B: shaft rotational speed. The transverse crack size varied from 33.4 mm to 74.0 mm, and finally to 98.8 mm, while the shaft rotational speed varied from 50 rpm to 100 rpm, and finally to 150 rpm, as a hypothetical operating range of Sohar wind speed using WTS conversion ratio. The total number of experimental tests performed was L9 (nine tests as per the DoE). The responses were the generated vibration level (average of positive peaks and average of negative peaks) and power output.

Experimental testing of the WTS as per DoE: This involved a systematic replacement of one of the three blades with transversely defective blades. The defective blades had crack sizes of 33.4 mm, 74.0 mm and 98.8 mm, respectively. The testing started with the first defective blade of 33.4 mm under a shaft rotational speed of 50 rpm, then 100 rpm, and finally 150 rpm. The same testing was repeated for defective blades of 74.0 mm and 98.8 mm, respectively.

Vibration waveform and power output analysis: The accelerometer read the vibration signals and sent them to the data acquisition system that transferred them to the VQ software to generate the vibration report in MS Excel format. The generated report showed a defined set of 10,000 vibration waves (positive and negative waveform peaks) for each test that were used later for vibration analysis. The WTS had a three-phase field-controlled alternator to produce the power output (voltage and current). The control interface of the WTS displayed both voltage and current that indicated the amount of field power output.

Regression modelling: The regression modelling for vibration levels and power output was performed to develop the following regression models; linear, linear and squared, linear and interaction, and finally the full model. The regression models were compared for the best fit with respect to the R-squared values for each response.

Optimisation of multi-responses using GRA: This research work aimed to optimise the performance of wind turbine systems while mitigating the vibration that occurs. For the average of negative vibration peaks and power output, the higher-the-better criterion was used, while for positive vibration peaks, the lower-the-better criterion was used. The normalisation of the original sequence of each response was calculated as follows:

For higher-the-better criterion: $$Y_{ij} = \frac{X_{ij} - min(X_{ij})}{max(X_{ij}) - min(X_{ij})}$$

For lower-the-better criterion: $$Y_{ij} = \frac{max(X_{ij}) - X_{ij}}{max(X_{ij}) - min(X_{ij})}$$

where x_{ij} is the measured response, $min(x_{ij})$ is the minimum of x_{ij} and $max(x_{ij})$ is the maximum of x_{ij}, i is the response variables and j is the experiment number. The deviation sequence (distinguishing coefficient) Δ_{ij} was calculated as follows:

$$\Delta_{ij} = max(Y_{ij}) - Y_{ij}$$

where $max(Y_{ij})$ is the expected sequence, Y_{ij} is the comparability sequence and Δ_{ij} is the deviation sequence of $max(Y_{ij})$ and Y_{ij}. The grey relational coefficient ξ_{ij} was calculated as follows:

$$\xi_{ij} = \frac{min(\Delta_{ij}) + \zeta \times max(\Delta_{ij})}{\Delta_{ij} + \zeta \times max(\Delta_{ij})}$$

where ζ is the differentiating coefficient, $0 \leq \zeta \leq 1$, and 0.5 is the widely accepted value. The grey relational grade (GRG) (γ_j) for each experiment was computed as follows, for n number of responses:

$$\gamma_j = \frac{\sum_{i=1}^{n} \xi_{ij}}{n}$$

If larger γ_j is obtained, then the equivalent set of process parameters is nearer to the most favourable optimal setting.

4. Results and Discussion

The generated vibration reports by the VQ software are discussed in this section, with regression analysis, optimisation and sensitivity analysis.

4.1. Initial Observations:

During the initial setup phase, preliminary observations were made to understand the baseline performance of the WTS with both healthy and defective blades. The presence of a transverse defect in one blade led to increased vibration levels and fluctuations in power output. These observations were important for this research work, as they showed the impact of blade defects under varying conditions:

- For healthy blade performance: The simulator with three healthy blades exhibited stable operational characteristics with minimal vibration levels. Power output increased consistently and within expected ranges for the given rotational speeds. The vibration waveforms recorded were smooth and showed almost no signs of irregularities, indicating the balanced and proper functioning of the blades.
- For defective blade performance: Replacing one healthy blade with a transversely defective blade resulted in noticeable changes. Increased vibration levels were immediately observed. There was a significant impact of the defect on the turbine's dynamic behaviour. The vibration waveforms displayed irregularities and higher peaks compared to the healthy blade setup, indicating the potential for structural instabilities. The power output was observed to fluctuate more with the defective blade. This reflected the impact of increased vibrations and possible energy losses.

4.2. Waveform Analysis Results:

The vibration signals were analysed and recorded using VQ software.

This software provides a detailed time-domain waveform for each test scenario. Figure 6 illustrates the vibration waveforms generated by VQ software. The vibration levels increased as the rotational speed increased.

Figure 6: Vibration waveforms: a) at 50 rpm (crack size = 33.4 mm), b) at 100 rpm (crack size = 33.4 mm), c) at 150 rpm (crack size = 33.4 mm), d) at 50 rpm (crack size = 74.0 mm), e) at 100 rpm (crack size = 74.0 mm), f) at 150 rpm (crack size = 74.0 mm), g) at 50 rpm (crack size = 98.8 mm), h) at 100 rpm (crack size = 98.8 mm), and i) at 150 rpm (crack size = 98.8 mm)

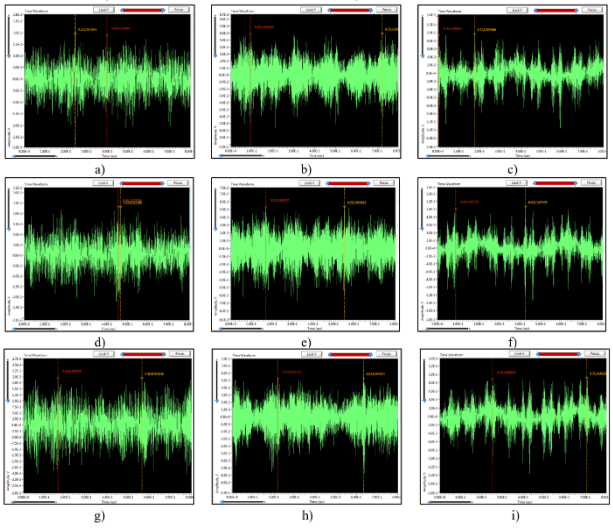

The detailed performance of the experimental work was performed for nine tests, considering the Taguchi design of the experiment. In each test, the VQ software generated a waveform report of a set of 10,000 vibration waves with positive and negative peaks. At the same time, the three-phase field-controlled alternator produced the power output (voltage and current) displayed on the control interface of the WTS. Table 1 shows the measured responses of the experimental work.

Table 1: Measured responses from experimental tests

	Input Parameters		Responses			
Tests	Crack Size, A (mm)	Rot Spd., B (rpm)	Avg. (negative peaks) (m/s^2)	Avg. (positive peaks) (m/s^2)	Vibration Level (m/s^2)	Power output (W)
1	33.4	50	-1.361	1.384	2.745	1.804
2	33.4	100	-4.990	4.647	9.637	9.912
3	33.4	150	-5.940	5.757	11.697	23.622
4	74.0	50	-1.337	1.470	2.807	1.539
5	74.0	100	-5.173	4.646	9.820	9.632
6	74.0	150	-6.105	6.116	12.221	23.331
7	98.8	50	-1.390	1.464	2.855	1.478
8	98.8	100	-5.171	4.750	9.921	9.475
9	98.8	150	-6.087	6.125	12.212	23.037

4.3. Taguchi Response Analysis:

Taguchi's response analysis focuses on optimising performance metrics through the design of experiments and the minimisation of variability. The experimental investigations on WTS with a transverse cracked blade were analysed using Taguchi's response analysis, response for means and response for signal-to-noise ratios (SNR). The influence of selected input process parameters on various performance measures such as average of peaks (negative and positive), vibration level and power output are detailed.

4.3.1. Taguchi's Response Analysis for the Average of Negative Peaks

In this case, the process parameters, crack size (A) and rotational speed (B), were analysed for their effects on the average of the negative side of vibration waveform peaks. In Table 2, the mean and SNR values illustrated how changes in each factor (A or B) impact the system's performance. Considering the higher-the-better criterion, the best possible set of process parameters observed from the analysis was A1B1, which means a crack size of 33.4 mm and a rotational speed of 50 rpm.

Table 2: Response table for the average of negative peaks

Level	Means		Signal-to-Noise Ratios	
	A	B	A	B
1	5.903	8.637	14.97	18.73
2	5.795	4.889	14.75	13.78
3	5.784	3.956	14.74	11.94
Delta	0.119	4.681	0.22	6.78
Rank	2	1	2	1

4.3.2. Influence of Process Parameters on the Average of Negative Peaks

Focusing on the average of negative peaks of the vibration waveform, it was observed that varying crack sizes had a small impact on the negative peak values. The mean values increased slightly from level 1 to level 3. This indicated that larger cracks resulted in slight increases in negative peak amplitudes. However, the variation in negative peaks associated with increasing the rotational speed is far more pronounced. As the rotational speed escalated from level 1 to level 3, negative peak values decreased significantly. This reflected a substantial negative correlation between higher rotational speeds and the average of negative peaks. The delta value of 4.681 further emphasised that rotational speed is considerably more influential on this response than the size of the crack.

4.3.3. Taguchi's Response Analysis for the Average of Positive Peaks

In this instance, the average of the positive side of the vibration waveform peaks was examined in relation to the process parameters of crack size (A) and rotating speed (B). The performance of the WTS was impacted by changes in each factor (A or B), as seen by the mean and SNR in Table 3. The optimal set of process parameters found in the analysis, while taking into account the lower-the-better criterion, was A1B1 also, which corresponded to a crack size of 33.4 mm and a rotational speed of 50 rpm.

Table 3: Response table for the average of positive peaks

Level	Means		Signal-to-Noise Ratios	
	A	B	A	B
1	3.930	1.440	-10.458	-3.162
2	4.078	4.681	-10.807	-13.407
3	4.113	5.999	-10.863	-15.558
Delta	0.184	4.560	0.406	12.396
Rank	2	1	2	1

4.3.4. Influence of Process Parameters on the Average of Positive Peaks

Examining the average of positive peaks of the vibration waveform, there was found to be a similar trend. The means showed a gradual increase from level 1 to level 3 as crack size increased. This suggested that larger cracks can lead to elevated positive peak amplitudes. However, the impact of rotational speed was once again more dramatic. The SNR declined steeply from level 1 to level 3. This indicated that higher rotational speeds correlate with significantly reduced positive peaks. The noticeable delta of 4.560 underscored how rotational speed influenced this parameter more strongly than crack size did, drawing parallels to the observed effects on negative peaks.

4.3.5. Taguchi's Response Analysis for the Vibration Level

The present study also examined the impact of two process parameters, namely crack size (A) and rotating speed (B), on the vibration waveform level. Table 4 shows how variations in each factor (A or B) affected the system's performance. Based on the lower-the-better criterion, A1B1, which indicated a crack size of 33.4 mm and a rotational speed of 50 rpm, was likewise the best feasible set of process parameters found in the analysis.

Table 4: Response table for vibration level

Level	Means		Signal-to-Noise Ratios	
	A	B	A	B
1	8.026	2.802	-16.604	-8.949
2	8.283	9.793	-16.850	-19.817
3	8.329	12.043	-16.926	-21.613
Delta	0.303	9.241	0.322	12.664
Rank	2	1	2	1

4.3.6. Influence Of Process Parameters on the Vibration Level

The vibration level analysis further reinforced the conclusion regarding the dominant role of rotational speed. As crack size increased, the average vibration level also rose. This suggested that larger cracks contributed to a wider level of vibration. The delta value of 0.303 indicated a consistent effect, but the influence of rotational speed was markedly more significant. With a delta of 9.241, the widening of the vibration level at higher speeds (from 2.802 to 12.043) highlighted that the increased rotational speeds led to substantial enhancements in the vibration profile, which correlated with the turbine's operational dynamics.

4.3.7. Taguchi's Response Analysis for the Power Output

The present study tested the impact of the two process parameters on the power output. The performance of the system was impacted by changes in each factor (A or B), as shown by the mean and signal-to-noise ratios values in Table 5. Considering the higher-the-better criterion, A1B3, which indicated a fracture size of 33.4 mm and a rotational speed of 150 rpm, was the best feasible set of process parameters found in the analysis.

Table 5: Response table for power output

Level	Means		Signal-to-Noise Ratios	
	A	B	A	B
1	11.779	1.607	17.505	4.088
2	11.501	9.673	16.925	19.710
3	11.330	23.330	16.725	27.358
Delta	0.449	21.723	0.779	23.270
Rank	2	1	2	1

4.3.8. Influence Of Process Parameters on The Power Output

When examining the generated power output, the effects of both parameters became even clearer. Here, as crack size increased, the power output consistently decreased. This indicated that larger cracks adversely impact energy production capability, which was illustrated by a delta of 0.449. In stark contrast, the influence of rotational speed was overwhelmingly positive. As rotational speeds rose, the mean power output surged dramatically, from 1.607 at level 1 to an impressive 23.330 at level 3, with a delta value of 21.723.

4.4. Analysis of Variance for Measured Performance:

Analysis of variance (ANOVA) is a statistical tool used to compare the means of input parameters to determine the significant differences between them. It assesses the observed variations in data due to real differences between input parameters. The ANOVA for the measured performance in WTS showed the significance of the input parameters, crack size (A) and rotational speed (B), on the system's responses. ANOVA was used on the performance measures at 95% confidence level and was computed using Minitab statistical software. In this context, ANOVA was likely to reveal that rotational speed (B) was the more dominant factor influencing both the vibration level and power output. Conversely, crack size (A) showed a statistically secondary role effect.

- For the average of negative peaks, the analysis revealed that crack size (A) had 2 degrees of freedom (DF) with an adjusted sum of squares (Adj SS) of 0.0261 and an adjusted mean square (Adj MS) of 0.0130. This yielded an F-value of 3.73 and a P-value of 0.122. In contrast, rotational speed (B) had 2 DF, an Adj SS of 36.8381, an Adj MS of 18.4190, an F-value of 5,270.03 and a significant P-value of 0.000. The error term was attributed to 4 DF and contributed an Adj SS of 0.0140 and an Adj MS of 0.0035. This brought the total Adj SS to 36.8781.
- For the average of positive peaks, crack size (A) also had 2 DF with an Adj SS of 0.0569 and an Adj MS of 0.0284. This resulted in an F-value of 2.65 and a P-value of 0.185. Rotational speed (B) exhibited a much larger effect, with 2 DF, an Adj SS of 33.0363, an Adj MS of 16.5181, an F-value of 1,538.58 and a P-value of 0.000. The error component again had 4 DF, yielding an Adj SS of 0.0429 and an Adj MS of 0.0107. This culminated in a total Adj SS of 33.1361.
- In the case of vibration range, crack size (A) was characterised by 2 DF, an Adj SS of 0.160 and an Adj MS of 0.0798. This led to an F-value of 4.69 and a P-value of 0.089. Rotational speed (B) highlighted a more substantial impact. It reflected in its 2 DF, an Adj SS of 139.328 and an Adj MS of 69.6642, which produced an F-value of 4,096.79 and a P-value of 0.000. The error term had 4 DF with an Adj SS of 0.068 and an Adj MS of 0.0170. This resulted in a total of 139.556 for the Adj SS.
- Lastly, for power output, crack size (A) held 2 DF with an Adj SS of 0.308 and an Adj MS of 0.154. This resulted in a significant F-value of 30.03 and a P-value of 0.004. Rotational speed (B)demonstrated an even stronger statistical significance, with 2 DF, an Adj SS of 723.471, an Adj MS of 361.736, an F-value of 70,470.46 and a P-value of 0.000. The error component contributed 4 DF with an Adj SS of 0.021 and an Adj MS of 0.005. This led to a total Adj SS of 723.800.

The ANOVA results demonstrated that rotational speed (B) was the higher significant factor influencing all the performance measures in the wind turbine simulator, with consistently high F-values and very low P-values across the board. While crack size (A) showed less influence, on the vibration level, it was mostly significant and, on the power output, it was more significant. However, its significance is considerable if the WTS run for a longer time.

4.5. Multi-Regression Modelling Results:

Regression is an effective statistical method used to model the relationship between dependent variables and independent variables. It helps to predict the dependent variable's value based on the known values of the independent variables. In this section, a regression analysis was conducted to quantify the relationship between crack size (A) and shaft rotational speed (B) as predictors and the average of negative peaks, average of positive peaks, vibration level and power output as responses. Using Minitab software in the regression analysis, four types of regression models were developed to determine the best model fit for WTS performance.

- The first model is a linear regression model that incorporates two input variables: crack size (A) and rotational speed (B).
- The second model, termed linear plus squared, not only includes the same linear input variables, A and B, but also adds squared terms for crack size (A^2) and rotational speed (B^2).
- The third model is a linear regression model with interaction, which includes the linear variables A and B alongside an interaction term that represents the product of crack size and rotational speed ($A \times B$).
- Lastly, the fourth model (full quadratic model) encompasses all the components of the previous models, integrating the linear variables A and B, their squared terms A^2 and B^2 and the interaction term $A \times B$. This comprehensive approach allows for a detailed exploration of how these variables collectively influence vibration range and power output.

The R-squared values of the developed models were compared to determine the best-fit model. The regression models analysed in the study yielded various R^2 values, which reflect the proportion of variance explained by the models across the outcomes:

- For the first model (linear regression model), the R^2 values were 89.203% for the average of negative peaks (in m/s^2), 94.279% for the average of positive peaks, 91.896% for the vibration range and 97.838% for power output.
- The second model (linear and squared) demonstrated a significant improvement, achieving R^2 values of 99.962% for average negative peaks, 99.870% for average positive peaks, 99.951% for vibration range and 99.997% for power output.
- The third model (linear and interaction) showed the R^2 values slightly lower but still substantial, with 89.217% for average negative peaks, 94.350% for average positive peaks, 91.931% for vibration range and 97.840% for power output.
- Finally, the fourth model (full quadratic), which incorporated linear, squared and interaction terms, attained R^2 values of 99.975% for average negative peaks, 99.941% for average positive peaks, 99.986% for vibration range and an impressive 99.999% for power output.

From the developed regression models, the full quadratic model showed the best fit. The regression equations for the responses are:

$$\text{Average of negative peaks} = 5.30860287 - 0.0042579A - 0.1580261B + 3.4165 \times 10^{-5}A^2 + 0.00056322B^2 - 2.082 \times 10^{-5}A \times B$$

$$\text{Average of positive peaks} = -3.7228 + 0.00262453A + 0.1193637B - 3.365 \times 10^{-5}A^2 - 0.0003848B^2 + 4.632 \times 10^{-5}A \times B$$

$$\text{Vibration level} = -9.0314029 + 0.00688248A + 0.27738983B - 6.781 \times 10^{-5}A^2 - 0.000948B^2 + 6.7141 \times 10^{-5}A \times B$$

$$\text{Power output} = -0.6459295 - 0.0032357A - 0.0039085B - 2.9461 \times 10^{-8}A^2 - 0.00111891B^2 - 3.634 \times 10^{-5}A \times B$$

4.6. Optimisation:

The objective of this research was to optimise the performance of the wind turbine system by balancing the power output and minimising vibration levels. The optimisation process utilised GRA in conjunction with a full factorial design in Minitab software. The optimisation process resulted in defining the optimal settings of process parameters. The GRA focused on two primary criteria: maximising the power output (higher-the-better) and minimising the vibration level (lower-the-better). In this case, the vibration level is the level between average of positive peaks and average of negative peaks. This means that only vibration level and power output responses are considered in the optimisation process. By applying these criteria, a grey relational grade (GRG) was computed for each experimental test.

- The first test received a Grade Relational Coefficient (GRC) of 1.000 and a GRG of 0.668, ranking it second overall.
- The second test reported a GRC of 0.407 and a GRG of 0.427, resulting in a seventh-place ranking.
- The third test, notable for its strong performance, achieved a GRC of 0.346 and a GRG of 0.673, earning the top rank of one.
- The fourth test recorded a GRC of 0.987 and a GRG of 0.661, securing the third rank.
- The fifth test had a GRC of 0.401 and a GRG of 0.421, placing it in eighth position.
- The sixth test yielded a GRC of 0.333 and a GRG of 0.654, ranking fifth overall.
- The seventh test obtained a GRC of 0.977 and a GRG of 0.655, which put it in fourth place.
- The eighth test had a GRC of 0.398 and a GRG of 0.418, finishing ninth.
- Finally, the ninth test achieved a GRC of 0.334 and a GRG of 0.642, resulting in a sixth-place ranking.

The GRG combined the GRCs into a single performance score. The third test (A1B3) showed the highest GRG (0.673), giving it the top rank, which means crack size = 33.4 mm and rotational speed = 150 rpm. This indicated the best overall performance. With higher GRG achieved, the third test was the best balance between vibration control and power output, making it a more optimal scenario. The confirmation of the results is shown in Table 6. The regression equation for GRG is:

$$\text{GRG} = 1.3724 + 2.3 \times 10^{-5}A - 0.018779B - 9.236 \times 10^{-8}A^2 + 9.46 \times 10^{-5}B^2 - 2.812 \times 10^{-6}A \times B$$

Table 6: Initial and optimal setting for WTS performance analysis

	Initial setting	Optimal setting
Parameters and levels	A1B1	A1B3
Average of negative peaks (m/s²)	-1.361	-5.940
Average of positive peaks (m/s²)	1.384	5.757
Vibration level (m/s²)	2.745	11.697
Power output (W)	1.804	23.622
Grey relational grade	0.668	0.673

4.7. Sensitivity Analysis:

To illustrate how the values of independent variables, the crack size and rotational speed, can affect the dependent variables, the vibration levels and power output, the analysis can be extended using theoretical frameworks grounded in the observed trends and relationships derived from the tested scenarios. Assumptions can be made as follows: 1) the relationship between independent variables and dependent variables can be approximated linearly in the feasible operational range; 2) crack size will vary between 0 mm (no defect) to 100 mm (severe defect), while rotational speed will vary from 0 rpm to 200 rpm, capturing both healthy operation and increasing operational stress; and finally, 3) vibration levels should be expected to increase with crack size and rotational speed, while power output should ideally increase with rotational speed but may decrease as crack size increases.

Based on observed data, a hypothetical model can be defined using the following generalised equations capturing the relationships between the variables:

$$Vibration\ level = c + (k1 \times crack\ size) + (k2 \times rotational\ speed)$$

$$Power\ output = d + (m1 \times rotational\ speed) - (m2 \times crack\ size)$$

Where k1, k2, m1 and m2 are coefficients representing the sensitivity of the respective dependent variables to the independent variables, and c and d are constants representing baseline vibration levels and power output under ideal conditions (e.g. no defect and no rotational speed). The differing signs in the equations captured the nuanced effects of each variable on the system's performance.

For simulated scenarios, to explore how the values of crack size and rotational speed affect vibration levels and power output, the following hypothetical values were considered:

- Crack size (mm): 0, 33.4, 50, 74, 98.8, 100
- Rotational speed (rpm): 50, 100, 150, 200

The following hypothetical coefficients were assumed based on the given data:

- k1 = 0.1 (increase of 0.1 m/s² for every mm of crack size)
- k2 = 0.05 (increase of 0.05 m/s² for every rpm of speed)
- m1 = 0.15 (increase of 0.15 W for every rpm of speed)
- m2 = 0.02 (decrease of 0.02 W for every mm of crack size)
- c = 1.5 (baseline vibration level with no defect)
- d = 5 (baseline power output with no defect)

Using these values, the vibration levels and power output were calculated. At a crack size of 0 mm and a rotational speed of 50 rpm, the vibration level measured 4 m/s², and the power output was recorded at 12.5 W. When the crack size increased to 33.4 mm and the rotational speed was set at 100 rpm, the vibration level rose significantly to 9.84 m/s², with the power output reaching 19.332 W. As the crack size continued to grow to 50 mm and the rotational speed increased to 150 rpm, the vibration level further escalated to 14 m/s², while the power output increased to 26.5 W. At a crack size of 74 mm and a rotational speed of 200 rpm, the vibration level was measured at 18.9 m/s², producing a power output of 33.52 W. Conversely, at a crack size of 98.8 mm and a rotational speed of 100 rpm, the vibration level recorded was 16.38 m/s², accompanied by a power output of 18.024 W. Finally, at a crack size of 100 mm with a rotational speed of 200 rpm, the vibration level peaked at 21.5 m/s², while the power output reached 33 W. These results illustrate the relationship between crack size, rotational speed, vibration levels and power output, highlighting the trends in performance as conditions change.

From the calculations in this simulated scenario, the relationship between independent and dependent variables can be observed clearly: as crack size increased, and/or as rotational speed increased, the average vibration levels tended to rise, and the power output initially increased with higher rotational speeds but was negatively influenced by increasing crack sizes. Thus, while higher speeds can enhance power generation, larger defect sizes could lead to a reduction in the overall power output. This theoretical exploration

allowed for anticipating the operational behaviour of the WTS under configurations, beyond those specifically tested, aiding in optimisation and fault management strategies.

4.8. Study's Limitations:

The use of wind speed data from Sohar, Oman, may restrict the generalisability of the results to other regions with different wind patterns. Additionally, the WTS may not fully capture the complexity of real-world turbine operations, which potentially affects the accuracy of vibration and power output measurements. The research focuses specifically on transverse blade defects and a limited range of parameters, such as crack size and shaft rotational speed. Other variables, such as wind turbulence and material fatigue, may be considered, which could influence the performance.

5. Conclusions

This research investigated the effects of input parameters such as crack size and rotational speed on the performance of a WTS system using vibration analysis, including regression analysis and the Taguchi design of experiments. The findings underscore the influence of blade defects on operational stability and power generation capabilities.

The experimental data revealed that the presence of defects significantly altered the vibration profile of the WTS. Specifically, the average of negative peaks increased from -1.361 m/s² for a healthy blade at 50 rpm to -5.940 m/s² when the crack size increased to 33.4 mm at 150 rpm. The average power output changed dramatically in tandem with these vibrations. This demonstrated increased fluctuations: the power output rose from 1.804 W (healthy blade at 50 rpm) to 23.622 W (transversely defective blade at 150 rpm).

Regression analysis yielded R^2 values of 99.999% for power output in the full quadratic model, the highest among all fitted models. This indicated an excellent fit and suggested that both crack size and rotational speed substantially contributed to the variance in performance metrics.

The optimisation process was undertaken using GRA, indicating that the optimal settings for enhanced performance were achieved with a crack size of 33.4 mm and a rotational speed of 150 rpm. This resulted in the best GRG of 0.673. These conditions effectively balance the power output (23.622 W) while maintaining a manageable vibration level (11.697 m/s²).

The sensitivity analysis demonstrated that both increasing crack size and rotational speed escalated vibration levels. At a crack size of 100 mm combined with a rotational speed of 200 rpm, vibration levels surged to 21.5 m/s², while power output was only marginally affected. This suggested operational strain could lead to mechanical failure over time.

This study lays a strong foundation for future research aimed at developing predictive maintenance strategies and improving the understanding of WTS under real-world conditions. Continuous monitoring and modelling of key parameters are essential for ensuring the reliability and efficiency of wind energy systems, reducing downtimes and optimising energy output in practical applications. Future research should focus on exploring advanced materials and design modifications to mitigate the adverse effects of cracks and enhance safe operation at higher speeds. Additionally, expanding on specific recommendations and addressing potential challenges in implementing these solutions will be critical for advancing the field.

6. Declarations

Ethical approval - The ethical approval declaration is not applicable.

Consent for publication - The authors consent to the publication of this manuscript.

Acknowledgement - The authors thank the Faculty of Engineering at Sohar University for their guidance.

Authors' contributions - A. H. A. designed the framework of this paper and was a major contributor to writing the manuscript. K. C. V. was a major contributor in revising and improving sections 1, 2 and 3. V. V. K. was also a major contributor to revising the manuscript and improving sections 4 and 5. All authors read and approved the final manuscript.

Conflicting interests - The authors declare that they have no competing interests relevant to this research paper.

Funding - This work did not receive any specific grant from funding agencies in the public, commercial or not-for-profit sectors.

Availability of data and materials - Materials used in this study are available upon reasonable request from the corresponding author.

Biographies

Abdulhamed Hamdan Al-Hinai

Department of Mechanical and Mechatronic Engineering, Sohar University, Sohar, Oman, +968 99883473 223306@students.su.edu.om

Al-Hinai was born in Oman, he received BSc in Mechanical Engineering from Sultan Qaboos University in Oman and M.Sc. in Thermal Power (Gas Turbine Technology) from Cranfield University in England. He is currently a Ph.D. research scholar at Sohar University in Oman. Abdulhamid has academic and administrative experience of more than 24 years. His research areas are Renewable energy Technologies, Wind Energy, Thermodynamics, and Solar Power. He attended and participated in many workshops, seminars, training courses and conferences.

ORCID ID: 0009-0005-5354-2895

Karu Clement Varaprasad

Department of Mechanical and Mechatronic Engineering, Sohar University, Sohar, Oman, +968 99808146, CKaru@su.edu.om

Varaprasad is an Indian associate professor in the Faculty of Engineering at Sohar University in Oman earned his Ph.D. in Mechanical Engineering from Jawaharlal Nehru Technological University, India in 2011. With over 20 years of teaching experience at various engineering colleges. Additionally, he is a member of the review team for the American Journal of Mechanical and Materials Engineering and serves on the editorial board of an international journal of mechanical, computational, and manufacturing research. He has contributed to over 23 reputable international journals.

ORCID ID: 0000-0002-8182-804X

V. Vinod Kumar

Department of Mechanical and Mechatronic Engineering, Sohar University, Sohar, Oman, +968 95979577, VKumar@su.edu.om

Vinod Kumar has been serving as an assistant professor and Program Coordinator of Mechanical and Mechatronic Engineering at Sohar University in Oman since 2009. He earned his Ph.D. in Mechanical Engineering from Nagpur University, India. With over 20 years of experience in academia, he has authored numerous research articles in internationally renowned journals and has also worked as a reviewer for various international journals. His research interests revolve around Passive Cooling, Energy Conservation, and Renewable Energy Technologies.

ORCID ID: 0000-0001-5420-4584

References

Al-Hinai, A., Varaprasad, K.C. and Kumar, V.V. (2024, June). Analytical Simulation Approach to Evaluate the Ambient Humidity Effects on the Performance of a Wind Accelerator. In *IOP Conference Series: Earth and Environmental Science*, **1365**(1), 012006. DOI: 10.1088/1755-1315/1365/1/012006

Balasubramanian, K., Thanikanti, S.B., Subramaniam, U., Sudhakar, N. and Sichilalu, S. (2020). A novel review on optimization techniques used in wind farm modelling. *Renewable Energy Focus*, **35**(n/a), 84–96. DOI: 10.1016/j.ref.2020.09.001

Barszcz, T. (2019). Standard Vibration Analysis Methods. In: T. Barszcz (eds.) *Vibration-Based Condition Monitoring of Wind Turbines. Applied Condition Monitoring*, Switzerland, Springer Nature Springer, DOI:10.1007/978-3-030-05971-2_2

Blaabjerg, F. and Ma, K. (2017). Wind energy systems. *IEEE*, **105**(11), 2116–31. DOI: 10.1109/JPROC.2017.2695485

Castorrini, A., Greco, E. and Sicilian, M. (2019). Computational analysis of performance deterioration of a wind turbine blade strip subjected to environmental erosion. *Computational Mechanics*, **64**(n/a), 1133–53. DOI: 10.1007/s00466-019-01697-0

Derakhshan, S., Tavaziani, A. and Kasaeian, N. (2015). Numerical shape optimization of a wind turbine blades using artificial bee colony algorithm. *Journal of Energy Resources Technology*, **137**(5), 051210. DOI: 10.1115/1.4031043

Dong, X., Lian, J., Wang, H., Yu, T. and Zhao, Y. (2018). Structural vibration monitoring and operational modal analysis of offshore wind turbine structure. *Ocean Engineering*, **150**(n/a), 280–97. DOI: 10.1016/J.OCEANENG.2017.12.052

Flah, M., Nunez, I., Ben Chaabene, W. and Nehdi, M.L. (2021). Machine learning algorithms in civil structural health monitoring: A systematic review. *Archives of Computational Methods in Engineering*, **28**(4), 2621–43. DOI: 10.1007/s11831-020-09471-9

Florian, M. and Dalsgaard Sørensen, J. (2015). Wind turbine blade life-time assessment model for preventive planning of operation and maintenance. *Journal of Marine Science and Engineering*, **3**(3), 1027–40. DOI: 10.3390/JMSE3031027

He, G., Ding, K., Li, W. and Jiao, X. (2016). A novel order tracking method for wind turbine planetary gearbox vibration analysis based on discrete spectrum correction technique. *Renewable Energy*, **87**(n/a), 364–75. DOI: 10.1016/J.RENENE.2015.10.036

Joshuva, A. and Sugumaran, V. (2017). A data driven approach for condition monitoring of wind turbine blade using vibration signals through best-first tree algorithm and functional trees algorithm: A comparative study. *ISA transactions*, **67**(n/a), 160–72. DOI: 10.1016/j.isatra.2017.02.002

Koulocheris, D., Gyparakis, G., Stathis, A. and Costopoulos, T. (2013). Vibration signals and condition monitoring for wind turbines. *Engineering*, **5**(12), 948. DOI: 10.4236/eng.2013.512116

Kusnick, J., Adams, D.E. and Griffith, D.T. (2015). Wind turbine rotor imbalance detection using nacelle and blade measurements. *Wind Energy*, **18**(2), 267–76. DOI: 10.1002/we.1696

Liu, X., Lu, C., Liang, S., Godbole, A. and Chen, Y. (2015). Influence of the vibration of large-scale wind turbine blade on the aerodynamic load. *Energy Procedia*, **75**(n/a), 873–9. DOI: 10.1016/j.egypro.2015.07.196

Liu, Y., Cheng, H., Kong, X., Wang, Q. and Cui, H. (2019). Intelligent wind turbine blade icing detection using supervisory control and data acquisition data and ensemble deep learning. *Energy Science & Engineering*, **7**(6), 2633–45. DOI: 10.1002/ese3.449

Liu, Z., Wang, X. and Zhang, L. (2020). Fault diagnosis of industrial wind turbine blade bearing using acoustic emission analysis. *IEEE Transactions on Instrumentation and Measurement*, **69**(9), 6630–9. DOI: 10.1109/TIM.2020.2969062

Lubosny, Z. (2003). Wind Turbine Generator Systems. In*: Z. Lubosny (eds.) Wind Turbine Operation in Electric Power Systems. Power Systems,* Berlin, Germany, Springer. DOI: 10.1007/978-3-662-10944-1_2

Maheswari, R.U. and Umamaheswari, R. (2017). Trends in non-stationary signal processing techniques applied to vibration analysis of wind turbine drive train–A contemporary survey. *Mechanical Systems and Signal Processing*, **85**(n/a), 296–311. DOI: 10.1016/J.YMSSP.2016.07.046

Ou, Y., Chatzi, E.N., Dertimanis, V.K. and Spiridonakos, M.D. (2017). Vibration-based experimental damage detection of a small-scale wind turbine blade. *Structural Health Monitoring*, **16**(1), 79–96. DOI: 10.1177/1475921716663876

Pacheco, J., Pimenta, F., Guimarães, S., Castro, G., Cunha, Á., Matos, J.C. and Magalhães, F. (2024). Experimental evaluation of fatigue in wind turbine blades with wake effects. *Engineering Structures*, **300**(n/a), 117140. DOI: 10.1016/j.engstruct.2023.117140

Polinder, H. (2011). Overview of and trends in wind turbine generator systems. In*: IEEE Power and Energy Society General Meeting*, Detroit, MI, USA, 24–28/07/2011. DOI: 10.1109/PES.2011.6039342

Riddle, T.W., Nelson, J.W. and Cairns, D.S. (2018). Effects of defects in composite wind turbine blades–Part 3: A framework for treating defects as uncertainty variables for blade analysis. *Wind Energy Science*, **3**(1), 107–20. DOI: 10.5194/wes-3-107-2018

Sarkar, S. and Chakraborty, A. (2018). Optimal design of semiactive MR-TLCD for along-wind vibration control of horizontal axis wind turbine tower. *Structural Control and Health Monitoring*, **25**(2), e2083. DOI: 10.1002/stc.2083

Sheng, S. (2012). *Wind turbine gearbox condition monitoring round robin study-vibration analysis* (No. NREL/TP-5000-54530). National Renewable Energy Lab. (NREL), Golden, CO (United States). DOI: 10.2172/1048981

Skrimpas, G.A., Kleani, K., Mijatovic, N., Sweeney, C.W., Jensen, B.B. and Holboell, J. (2016). Detection of icing on wind turbine blades by means of vibration and power curve analysis. *Wind Energy*, **19**(10), 1819–32. DOI: 10.2172/9460

Tchakoua, P., Wamkeue, R., Ouhrouche, M., Slaoui-Hasnaoui, F., Tameghe, T.A. and Ekemb, G. (2014). Wind turbine condition monitoring: State-of-the-art review, new trends, and future challenges. *Energies*, **7**(4), 2595–630. DOI: 10.3390/EN7042595

Teng, W., Ding, X., Cheng, H., Han, C., Liu, Y. and Mu, H. (2019). Compound faults diagnosis and analysis for a wind turbine gearbox via a novel vibration model and empirical wavelet transform. *Renewable Energy*, **136**(n/a), 393–402. DOI: 10.1016/j.renene.2018.12.094

Tibaldi, C., Kim, T., Larsen, T.J., Rasmussen, F., Rocca Serra, R.D. and Sanz, F. (2016). An investigation on wind turbine resonant vibrations. *Wind energy*, **19**(5), 847–59. DOI: 10.1002/WE.1869

Wagner, H. (2015). Introduction to wind energy systems. *EPJ Web of Conferences*, **98**(n/a), n/a. DOI: 10.1051/epjconf/20159804002

Wang, J., Zhang, L., Huang, X., Zhang, J. and Yuan, C. (2022). Initiation mechanism of transverse cracks in wind turbine blade trailing edge. *Energy Eng*, **119**(1), 407–18. DOI: 10.32604/ee.2022.016439

Xie, F. and Aly, A.M. (2020). Structural control and vibration issues in wind turbines: A review. *Engineering Structures*, **210**(n/a), 110087. DOI: 10.1016/j.engstruct.2019.110087

Yang, W., Lang, Z. and Tian, W. (2015). Condition monitoring and damage location of wind turbine blades by frequency response transmissibility analysis. *IEEE Transactions on Industrial Electronics*, **62**(10), 6558–64. DOI: 10.1109/TIE.2015.2418738

Yang, W., Tavner, P.J., Crabtree, C.J. and Wilkinson, M. (2009). Cost-effective condition monitoring for wind turbines. *IEEE Transactions on Industrial Electronics*, **57**(1), 263–71. DOI: 10.1109/TIE.2009.2032202

Scientific Journal of King Faisal University:
Basic and Applied Sciences

Potential of Honey Bee Propolis and Venom as Eco-friendly Control Agents in *Galleria mellonella* L.

Amro Ahmed Taha [1,2], Mohamed Samir Younis [2], Heba A. Al-Ghanam [3] and Doaa Abd El-Maksoud Abou El-Atta [3]

[1] Research and Training Station, King Faisal University, Al-Ahsa, Saudia Arabia
[2] Bee Research Department, Plant Protection Research Institute, Agricultural Research Center, Giza, Egypt
[3] Plant Protection Research Institute, Agricultural Research Center, Dokki, Giza, Egypt

LINK	RECEIVED	ACCEPTED	PUBLISHED ONLINE	ASSIGNED TO AN ISSUE
https://doi.org/10.37575/b/sci/240041	02/09/2024	21/11/2024	21/11/2024	01/12/2024
NO. OF WORDS	**NO. OF PAGES**	**YEAR**	**VOLUME**	**ISSUE**
6,966	7	2024	25	2

ABSTRACT

The study was conducted to determine the toxicity approach of four honey bee propolis and venom concentrations, 500, 1,000, 2,000 and 3,000 ppm, regarding the biological aspects of the wax moth larvae *Galleria mellonella* L. Using 2,000 and 3,000 ppm propolis concentrations gave a 100% reduction percentage on wax moth larvae after spraying the treatment for 72 and 48 hours consistently. Applying 3,000 ppm of bee venom resulted in a 100% mortality percentage for the three test times of 24, 48 and 72 hours. The lowest period of larval development was observed when propolis was used at a concentration of 3,000 ppm, with an average of 7.66±0.33 days. At the 3,000 and 2,000 ppm concentrations of propolis, the pupal stage was unable to develop for adults of the insect, as all the individuals died. For bee venom, at concentrations of 3,000 and 2,000 ppm, none of the larvae have succeeded in the development of pupa or adult insects. Bee venom was the most effective substance against wax moth larvae, followed by propolis; LC50 values were 272.62 and 3,166.42 ppm, respectively. These results clarified the need for more research to affirm their effect in the field and on honey bees.

KEYWORDS

Biological aspects, mortality rate, natural substances, suppression materials, toxicity, wax moths

CITATION

Taha, A.A., Younis, M.S., Al-Ghanam, H.A. and Abou El-Atta, D.A. (2024). Potential of honey bee propolis and venom as eco-friendly control agents in *Galleria mellonella* L. *Scientific Journal of King Faisal University: Basic and Applied Sciences*, **25**(2), 50–6. DOI: 10.37575/b/sci/240041

1. Introduction

Beekeeping is an important part of modern agriculture because it pollinates the country's main crops, makes honey for the food industry and produces beeswax for use in many other industries. For this reason, it is important to keep an eye on the health and productivity of honey bee colonies (Bradbear, 2004). Honey bees are often attached by *Galleria mellonella*, *Achroia grisella* and the new species of wax moths, *Galleria similes* (Ellis *et al.,* 2013). It is thought that the damage done by *G. mellonella* larvae is one reason why wild and solitary honey bee numbers are declining (Kong *et al.,* 2019). This insect breaks down beeswax, which is a valuable product that can bring in a lot of money, along with honey (Bradbear, 2004). Additionally, both adult and larval wax moth stages can spread pathogens that cause serious bee diseases, like foulbrood (Owayss and Abd-Elgayed, 2007). A variety of physical techniques have been used to control *G. mellonella* L. (James, 2011). A wide range of biological control agents (Ellis *et al.,* 2013) and the sterile insect technique have been assessed for their efficacy against this parasite (El-Kholy and Mikhaiel, 2008). Furthermore, numerous insect hormone analogues and insect growth regulators have been evaluated for their effectiveness against *G. mellonella L.* (Amany *et al.,* 2021). However, chemicals are still needed to get rid of this pest. It is easy and efficient to use these chemicals, but we should think about whether they are safe and will contaminate bee products (Naqqash *et al.,* 2016). Accordingly, a thorough assessment of viable non-chemical wax moth control strategies in dry environments might be a crucial task for bettering living circumstances, as it would help beekeepers combat this pest and boost their yield. The study objectives are to assess and validate some proposed bee products as agents for controlling wax moths and identify a possible preventive strategy for the study region.

2. Materials and Methods

2.1. Study Area and Honey Bee Colonies:

Field experiments for collecting and producing honey bee propolis and venom were evaluated in 2023 at the Research and Training Station Apiary, King Faisal University, Al-Ahsa Province, Eastern Region, Kingdom of Saudi Arabia. Local honey bee colonies (*Apis mellifera yemenitica*) with nearly equal strength in bees, brood and food were used.

2.2. Propolis Samples Collection and Extraction:

Propolis resin was obtained by scraping propolis off frame rests and edges, bottom boards and the insides of hive boxes. Propolis was refined with an ethanol solvent. Propolis was minced after being stored overnight in a deep freezer at -20°C. A propolis sample was weighed, then a 70% ethanol solvent (1:30 w:v) was added, and the mixture was left at room temperature for 24 hours. The propolis suspension was subjected to an ultrasonic bath for 20 minutes at a temperature of 20°C. The filter paper was employed to separate the resultant suspension at ambient temperature. The operation was subsequently repeated with the portion of the suspension that was retained in the filter. The residue was subsequently extracted again under identical circumstances (Popova, *et al.*, 2004). For forthcoming research, the extracted material (the stock) will undergo evaporation for drying (Netíková *et al.,* 2013).

2.3. Bee Venom Collection and Extraction:

Bee venom was harvested using the Bee Venom Collector Device for 20 minutes every 15 days. The device was set aside the third comb from the entrance to the hive. After the collection was finished, the dried venom was scraped off with a sharp blade and placed into a dark container and kept in a cool and dry place. Bee venom extracts are made with a water solvent (Kosuge, 1969). The stock extracts,

Corresponding Author: Amro Ahmed Taha 00966558054186, aaismail@kfu.edu.sa

Ethanol Extraction of Propolis (EEP) and Water Extraction of Venom (WEV), were tested against the fifth instar of the wax moth larvae *Galleria mellonella*. Four concentrations (500, 1,000, 2,000 and 3,000 ppm) were prepared and tested from each extract by spraying over the larvae.

2.4. Preparation of *G. mellonella* L. Larvae Culture:

Local strains of *G. mellonella* L. larvae were procured from the Plant Protection Research Institute, Pest Physiology Department, ARC, Egypt. The collected larvae were placed in glass rearing jars (8 x 8 x 20 cm) and artificially raised using a medium that was created by following Wiesner's guidelines (1993). The media included bee honey (75 mL), glycerol (75 mL), rice cerelac (100 g), wheat bran (100 g), dry yeast (1 g), nipagen as an antimicrobial (0.15 g), vitamins and minerals (2 capsules; 500 mg) and water (50 mL). The collected larvae were transferred to a glass rearing jar, which was filled with 50 freshly hatched larvae per jar, 100 g of the medium and a metal cover with holes for ventilation. The jar was then sealed and kept in an incubator set at 25°C with fresh food supplied three times a week. To start a new generation, pieces of wax were put into the pupal stages' jars to facilitate their transition into moths and encourage them to deposit eggs on them (Figure 1).

Figure1. Shows adult (a), eggs (b), larva and pupa (c) and symptoms of damage (d) (the author took all photos)

2.5. Biochemical Studies:

2.5.1. Toxicity and Biological Aspects of Bee Propolis and Venom Extracts Against *G. mellonella* Larvae

Under laboratory settings, 500, 1,000, 2,000 and 3,000 ppm concentrations were prepared from the stock solutions (100%) of propolis and bee venom extracts. These tested materials were then used as liquid formulations for EEP and WEV extraction and placed onto plastic plates (10 cm) containing the required media. Ten larvae of *G. mellonella* fifth instar were put together with 10 g of tiny artificial medium fragments in each Petri plate. One millilitre of each concentration was sprayed above the wax moth larvae. Then, the larvae and medium were covered with a muslin cloth and fastened with elastic bands to keep the larvae from fleeing. The number of dead larvae was counted by daily observations. Every treatment was carried out three times. Every day, the examined larvae were inspected to count and remove any dead ones. After 24, 48 and 72 hours of treatment, mortality percentages were computed.

2.5.2. Preparation of Homogenate Samples

To homogenise the samples, all dead *G. mellonella* larvae were collected for each treatment, placed in the freezer and placed on the centrifuge device, and then a sample was taken for an analysis representative of each treatment. After homogenising the samples in distilled water, the BECKMAN GS-6R Centrifuge was used to centrifuge the mixture for 10 minutes at 5°C at 6,000 rpm. Following centrifugation, the fluid supernatant was separated into tiny aliquots (0.5 mL) and kept cold until the primary constituents were analysed. Each biochemical determination was done in three replicates (Assar *et al.*, 2016).

2.5.3. Total Carbohydrate Content Determination

Using an anthron reagent, the technique outlined by Singh and Sinha (1977) was used to calculate the total amount of carbs. (A) Anthron reagent preparation: 28 mL of H_2O, 50 mg of anthron and 72.0 mL of concentrated H_2SO_4 (98%) were combined, and the mixture was vigorously shaken. (B) Method: 100 µL of the insect homogenate sample solution was diluted to one millilitre using distilled water, and then five millilitres of anthron reagent were added. In a test tube, 1.1 mL of water and 5 mL of anthron reagent were used as a blank. After 10 minutes of being submerged in boiling water, each tube was allowed to cool for 15 minutes at room temperature. At 620 nm, the absorbance was measured. The carbohydrate content was given as milligrams per gram of body weight.

2.5.4. Total Protein Content Determination

Following centrifugation, the fluid supernatant was separated into tiny aliquots (0.5 mL) and kept cold until the primary constituents were analysed. Each biochemical determination was done in three duplicates. The Bradford (1976) technique was employed to quantify the total proteins by utilising bovine serum albumin as a reference standard. (A) Protein reagent preparation: 50 millilitres of 95% ethanol was used to dissolve 100 milligrams of Coomassie Brilliant Blue G-250. Then, 100 mL of 85% (w/v) phosphoric acid was added to this solution. One litre was the final volume at which the resultant solution was diluted. (B) Protein assay: 50 µL of pupal homogenate were pipetted into a test tube with 50 µL of phosphate buffer (pH 6.6). The test tube's contents were then vortexed after the protein reagent (5 mL) was added. After two minutes, the absorbance at 595 nm was measured in comparison to a blank made with five millilitres of protein reagent and 0.1 millilitres of phosphate buffer (pH 6.6). The protein content was calculated in milligrams per gram of body weight.

2.5.5. Total Lipid Content Determination

Phosphovanillin reagent and standard curve were used to quantify the content of total lipids in the insect homogenate following Joseph *et al.,* (1972). Following centrifugation, the fluid supernatant was separated into tiny aliquots (0.5 mL) and kept cold until the primary constituents were analysed. Each biochemical determination was done in three duplicates. (a) Preparation of the phosphovanillin reagent: 10 mL of 100% ethanol was used to dissolve 0.6 g of pure vanillin, which was then added to 100 mL of distilled water. After adding 400 mL of concentrated phosphoric acid, the mixture was kept at room temperature in a dark glass bottle. (b) Procedure: In a test tube, 250 µL of insect homogenate sample solution was combined with 5 mL of concentrated sulfuric acid, and the mixture was heated in a boiling water bath for 10 minutes. Then, 500 µl of the digest was added to the 6.0 mL phosphovanillin reagent after it cooled to room temperature. Following a 45-minute dark incubation period, the colour generated was quantified at 525 nm in comparison to a reagent blank made with 6.0 mL of phosphovanillin reagent and 500 µl of distilled water. The lipid content was given as milligrams per gram of body weight. (c) Lipid standard curve preparation: To create the standard curve, serial concentrations of a combination of palmitic and oleic acids (7:3) ranging from 0.5 to 5 mg/mL were produced in 100% ethanol and handled similarly to the unknown. Optical density was used to blot the standard curve against concentration.

2.6. Analytical Statistics:

Probit analysis was used to calculate analytical statistics and LC_{50} values, which were given in ppm units. ANOVA was used to assess the mortality data (Snedecor and Cochran, 1980). Using the Costate (version 6.204) statistical software programme, CoHort Software (CoStat Software, 2004), the least significant difference (LSD) was performed to assess the means differences at $p \leqslant 0.05$.

3. Results and Discussion

3.1. Toxicity Tests of the Bee Propolis and Venom Against Wax Moth Larvae:

Table 1 indicated that bee venom was the most potent applied compound against wax moth larvae followed by propolis. LC_{50} values were 272.62 and 3,166.42 ppm, respectively.

Table1. LC50 and LC90 values of the tested bee propolis and venom on wax moth larvae *G. mellonella*

Treatment	LC_{50} (ppm)	LC_{90} (ppm)	Upper lower value	Slope± S.E.
Propolis	3,166.42	15,419.54	2,526.15 4,518.34	1.68±0.28
Bee venom	272.62	1,569.80	128.56 403.03	1.68±0.30

S.E. = Standard Error

According to Mahgoub *et al.,* (2018), third-instar larvae were given topical applications of crude honey bee venom at doses of 0, 6.25, 12.5, 25 and 50 µg. At the lower concentration, the calculated death percentages for all treatments were 8%, and at the high concentration, 52%. The determined fatal median concentration (LC_{50}) was 38.27 µg/µl. The result of Ghoneim (2020) indicated that 3,428.9 ppm was determined to be the LC_{50}. In terms of growth and development, the larvae's somatic weight gain decreased somewhat in proportion to the concentration.

Garedew *et al.,* (2004) mentioned that propolis is toxic at high concentrations and an insect growth regulator at lower ones. In addition, using propolis on the fifth larval instar caused a very high mass-specific metabolic rate and cuticle thinner and more fragile, allowing the free transit of nonpolar toxic substances from the surroundings after being easily disrupted by propolis components.

3.2. Effect of Bee Propolis and Venom on the Larval Stage of *G. mellonella*:

Table 2 and Figure 2 present the mean mortality and reduction percentage of wax moth larvae when applied to four concentrations of propolis 500, 1,000, 2,000 and 3,000 ppm. Propolis recorded the highest mortality number for concentrations of 2,000 and 3,000 ppm after treatment for 72 hours. The mean mortality values were 10 for both concentrations, followed by propolis concentrations of 2,000 and 3,000 ppm after 48 hours with mean mortality values of 7.66±0.33 and 9.6±0.33, respectively. The lowest percentages of the mortality rate for using a propolis concentration was observed for 500 ppm after 24 hours of treatment: 0.0% and 6.6%, respectively. Using 2,000 and 3,000 ppm of propolis concentrations gave a 100% reduction percentage after treatment for 72 hours, followed by using the propolis after 48 hours, which led to the percentage of mortality being 76.6% and 96%, respectively. According to Shimanuki and Knox (1997), honey, pollen, wax combs and the skins of bee larvae are the main foods for wax moth larvae. A statistical analysis indicated that significant differences in the mortality rate of the wax moth among all treatments were observed. According to Hussein *et al.,* (2022), depending on the concentration and length of exposure, there are substantial changes in the percentage of killing between propolis extract concentrations at a probability threshold of 5%. During the initial therapeutic period, the mortality percentage observed at a concentration of 2% was 53.3%. For one week, the interaction resulted in the highest death rate of 76.6% when the concentration was 3%. In contrast, the comparator medication did not cause any mortality. The experiment also revealed the initial larval stage's susceptibility to compounds extracted from propolis and cinnamon plants. The results showed that there were considerable variations in the proportion of organisms killed based on the concentration and duration of exposure to the extracts. As an illustration, the maximum mortality rate observed at the given concentration was 3%, which increased to 76.6% during one week of treatment. Conversely, the minimum mortality rate at the same dose was 2%, reaching 53.3% on the first day of the experiment. Sanad and Mohany (2015) indicated that mortality percentages went up by increasing the time after application. The highest percentages of late instar larvae were obtained after 72 hours of treatment of all tested materials, except for the mint treatment. Mint oil recorded the highest accumulative mortality percentage after the three days at 4%, giving 70%, pursued by 4% Chinese propolis and 4% cinnamon, which gave 60%, while 4% clove gave 50%, and 4% of Egyptian propolis gave only 40%. These results agree with Izhar-ul-Haq *et al.,* 2008.

Table 2. Mean mortality and percentages of the late wax moth stage treated with propolis

Propolis concentrations(ppm)	24 hours	%	48 hours	%	72 hours	%
500	0.0b	-	0.66d±0.33	6.6	1.66c±0.881	16.6
1,000	0.66b±0.33	6.6	2.33c±0.66	23.3	5.66b±0.33	56.6
2,000	3.66a±0.33	36.6	7.66b±0.33	76.6	10.0a	100
3,000	3.0a±0.57	30	9.6a±0.33	96.0	10.0a	100
Control	0.0b	-	0.0d	-	0.0d	-
$LSD_{5\%}$	1.050		1.242		1.328	
F	7.3		121.214		10.187	
P	.0000***		.0000***		.0000***	

Figure 2. Mortality percentages of the wax moth larvae stage treated with propolis

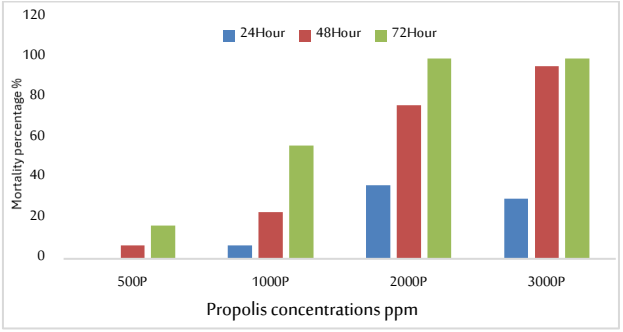

From Table 3 and Figure 3, it could be concluded that applying 3,000 ppm of bee venom concentration on wax moth larvae gave a 100% mortality percentage for the three tested times of 24, 48 and 72 hours. The mean mortality value was 9±0.57 of 2,000 ppm bee venom concentration with a 90% mortality percentage after 24 hours of applying. Then, the mean mortality value reached 10 with a 100% mortality percentage after 48 and 72 hours of using 2,000 ppm concentration. The mean mortality values of wax moths were 6.66±0.33 and 8.33±0.33 and 10 with mortality percentages of 66, 83.3 and 100% after 24, 48 and 72 hours with 1,000 ppm concentration, respectively. Data showed that applying 500 ppm of bee venom on wax moths gave the lowest mortality values after 24, 48 and 72 hours, giving 3.66±0.33, 7.33±0.33 and 9,66±0.33, with the lowest mortality percentages of 36, 73.3 and 96.6%, respectively.

Table 3. Mean mortality and percentages of the late wax moth stage treated with bee venom

Bee venom concentration(ppm)	24 hours	%	48 hours	%	72 hours	%
500	3.66b±0.33	36	7.33c±0.33	73.3	9.66a±0.33	96.6
1,000	6.66b±0.33	66	8.33b±0.33	83.3	10.0a	100
2,000	9.0a±0.57	90	10.0a	100	10.0a	100
3,000	10.0a	100	10.0a	100	10.0a	100
Control	0.0d	-	0.0d	-	0.0b	-
$LSD_{5\%}$	1.050		0.664		0.469	
F	150.3		387		886	
P	.0000***		.0000***		.0000***	

Figure 3. Mortality percentages of the wax moth larvae stage treated with bee venom

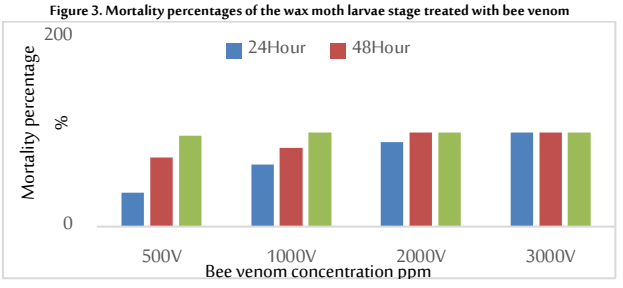

3.3. Effect of Bee Propolis and Venom Extracts During Post-embryonic Development of *G. mellonella* Larvae:

Table 4 shows the impact of four propolis concentrations of 500, 1,000, 2,000 and 3,000 ppm on the number of days experienced by larvae, pupae and adults after treatment. The shorter period of the larval stage with propolis at a 3,000-ppm concentration was followed by a concentration of 2,000 ppm and then 1,000 ppm with averages of 7.66, 11.33 and 18 days, respectively. The highest period of larval development for control was, on average, 24 days. Sanad and Mohany (2015) mentioned that the larval stage duration decreased by increasing the Egyptian propolis concentration, where it was 14.9±2.6 days at a 4% concentration, compared with 24.2±4.1 days at the control. The mean duration of the larval stage was decreased by increasing the Chinese propolis by a 4% concentration compared with 25.2±5.1 days at control.

A significant difference between the control and each of the tested four concentrations was observed. The lowest periods of pupa were 3,000 and 2,000, followed by 1,000 ppm. The average pupa stages were 6.66±0.33, 8.66±0.88 and 12.33±0.33 days. Sanad and Mohany (2015) described that as the Egyptian propolis concentration increased, the mean duration of the pupa stage decreased. It was 15.0±1.3 at 4% concentration, compared with 17.1±1.7 days for the control. The mean duration period of the pupal stage decreased by increasing the Chinese propolis concentration, giving 15.0±1.3 days at 4% concentration, compared with 16.1±1.8 days at control. At 3,000 and 2,000 ppm concentrations of propolis, the pupae were unable to develop for adults, where all the individuals died. On the other hand, with a 1,000-ppm concentration of propolis, all pupae were developed for adults. The average was 8.33±0.33 days, and the control was the highest average of 13±0.57 days. Sanad and Mohany (2015) mentioned that adult longevity was 10.1±1.7 days at 4% of the Egyptian propolis concentration compared with 14.2±2.3 days at the control.

Wax moth larvae are at the harmful stage that destroys wax combs with food and brood. Therefore, the longer the duration of the larvae stage, the greater the damage, and vice versa: the shorter the duration of the larvae stage, the lower the damage. Any substance that causes the wax moth eggs to not hatch or leads to a shorter duration of the larvae phase is important and can be included in the integrated control programmes of the greater wax moths (Ellis *et al.,* 2013). According to Garedew *et al.,* (2004), the wet weight of the larval instars increased drastically, from a mean value of 23±2.5 mg at L5 to 65.7±5.8 mg at L6 more than twice, achieving its maximum mean value of instars used in the investigation. Furthermore, the weight change during the entire larval developmental stage ranges from <1 mg at L1 to nearly 400 mg at L7.

Table 4. Effect of different propolis concentrations on the post-embryonic development period of wax moth larvae

Propolis concentration (ppm)	Period of stages (day)		Adult longevity
	Larval	Pupal	
500	21.33a±0.88	15.33a±0.66	11.66b±0.33
1,000	18.0b±1.15	12.33b±0.33	8.33c±0.33
2,000	11.33c±1.45	8.66c±0.88	0.0d
3,000	7.66d±0.33	6.66d±0.33	0.0d
Control	24.0a±0.57	16.0a±0.57	13a±0.57
$LSD_{5\%}$	3.044	1.878	1.050
F	49.976	46.812	352.7
P	0.0000***	0.0000***	0.0000***

In Table 5, the lowest period of larvae development was at the concentration of 3,000 followed by 2,000, and the least was 500 ppm of bee venom with averages of 3.0±0.57, 3.3±0.88 and 12.33±1.45 days, respectively. For the concentrations of 3,000 and 2,000 ppm, none of the larvae have succeeded in the development of pupa or adult insects. The concentrations of 500 and 1,000 ppm larvae evolved into pupa and did not succeed in reaching the adult stage. The study conducted by Ghoneim (2020) evaluated the effects of treating newly molted third-instar larvae of *G. mellonella* with scorpion L. *quinquestriatus* venom. The inability of *G. mellonella* larvae during ecdysis to shed their exocuticle (Linton *et al.*, 1997) or the suppression of chitin production (Adel, 2012) could be the reason for the larvae's death when exposed to the studied arthropod products.

Ghoneim *et al.*, (2000) mentioned that larval death may be attributed to the antifeedant impact of the venom and secretion, leading to persistent starvation in the larvae. The poison had a lethal effect on the pupae, as the severity effect was directly proportional to the dosage. In addition, the tested venom can induce pupal deaths in *G. mellonella* by interfering with important processes like suffocation, bleeding and desiccation (Possani *et al.,* 1999). In contrast, the venom did not have any impact on the survival of adult individuals. These deaths occur because the venom hinders proper exuviation and disrupts essential homeostatic mechanisms (Ghoneim *et al.*, 2000).

Table 5. Effect of different bee venom concentrations on the post-embryonic development period of wax moth larvae

Propolis concentration (ppm)	Period of stages (day)		Adult longevity
	Larval	Pupal	
500	12.33b±1.45	8.33b1.76	0.0 d
1,000	10.33b±2.60	7.66b±1.45	0.0 d
2,000	3.33c±0.88	0.0 c	0.0 d
3,000	3.0 c±0.57	0.0 c	0.0 d
Control	25.0a±1.15	17.0a±1.15	13.0a±1.20
$LSD_{5\%}$	4.744	3.608	1.627
F	35.38	38.025	126.75
P	0.0000***	0.0000***	0.0000***

3.4. Effect of Bee Propolis and Venom on Total Lipid, Protein and Carbohydrates of *G. mellonella* Larvae:

The present investigation indicates that all propolis concentrations impact lipids, protein and carbohydrates compared with control on wax moths. The data in Table 6a and Figure 4, the highest average of lipids, was achieved by propolis concentrations 2,000 and 1,000 ppm with mean values of 10.93±0.67 and 10.55±0.34, respectively. The lowest average of lipids was achieved by the control, giving a 3.16±0.26 value. Lipids are a vital energy source, precursors to hormones and structural components for insects. They are carried from their place of production of storage to the user organs by the hemolymph (Zhou and Miesfeld, 2009). However, the current findings partially align with previous studies that indicate an increase in lipids in different insect species following treatment with certain insect growth regulators during the larval stage (Bouaziz *et al.,* 2011). Protein had the highest average when a concentration of 3,000 ppm of propolis was used, with a mean value of 31.94±4.01. Control had the second-highest average, giving a mean value of 27.94±0.44. Protein metabolism is vital for generating energy and facilitating insect reproduction (Taskín and Aksoylar, 2011). It also plays a mandatory role in the development of adult structures in insects during their transformation from larvae and pupae to adults (Resmitha *et al.,* 2014). Through hormones, enzymes and nucleoproteins, proteins integrate and regulate a number of physiological and metabolic processes in the body of an insect (Chapman, 2012). For the carbohydrate analysis, the highest average rate was achieved by the control with a mean value of 2.59±0.006. A significant analysis was observed for all treatments compared with the control. During an insect's metamorphosis, carbohydrates are crucial to the composition and operation of every tissue. Furthermore, carbohydrates are necessary metabolites for the development of the embryo and the proper operation of the reproductive systems in both sexes. Carbohydrates are generally important for the physiology of insects exposed to external poisons (Kaufmann and Brown, 2008).

A wax moth larvicidal effect was observed when treated larvae with propolis and increased with the concentrations. In addition, higher concentrations of propolis extract accelerated the larvae and pupae

development in adults, which might lead to malformed and immature individuals. This higher rate of development requires more energy and feeds, which can be obtained by lipids and carbohydrate metabolic (Ararso and Legesse, 2016).

Table 6a. Total lipids, protein and carbohydrate values (mg/gram) for wax moths in different concentrations of propolis

Propolis concentration (ppm)	Lipids	Protein	Carbohydrates
500	7.88b±0.90	18.55b±0.28	1.11d±0.066
1,000	10.55a±0.34	19.82b±0.43	1.60c±0.04
2,000	10.93a±0.67	21.82b±0.30	1.74b±0.043
3,000	6.19b±0.58	31.94a±4.01	0.57e±0.01
Control	3.16c±0.267	27.94a±0.44	2.59a±0.006
$LSD_{5\%}$	1.89	5.758	0.127
F	28.598	9.770	342.67
P	0.0000***	0.0017***	0.0000***

Figure 4. Content of lipids, protein and carbohydrates of the wax moth larvae treated with propolis

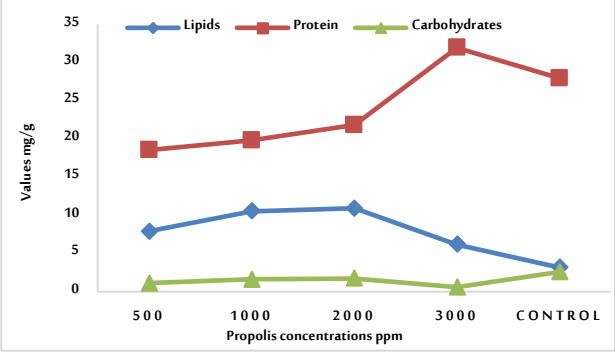

Table 6b and Figure 5 show the analysis of wax moths' lipids, protein and carbohydrates when extracting four concentrations of bee venom. The results are as follows: Wax moths' lipids were higher when treated with bee venom at a concentration of 1,000 ppm, followed by concentrations of 2,000 ppm and 500 ppm. The value of the lipids was lower in the control treatment.

According to Tanani *et al.,* (2021), in the fifth and seventh instars of normal larvae, respectively, the lipid content dropped steadily with instar (265.77±18.0 and 247.75 mg/g). This data demonstrates that all arthropod venoms have a shared impact of inducing larvae to amass a greater amount of lipids compared to control counterparts. Apitoxin had the lowest level of larval-boosting activity during their fifth instar. The scorpions' venom had the smallest enhancing impact on lipids in the seventh stage of larval development.

Lipids are a vital source of energy, precursors to hormones and structural components for insects. They are carried from their place of production of storage to the user organs by the haemolymph (Zhou and Miesfeld, 2009). According to Canavoso *et al.,* (2001), the reduction of lipids in wax moth larvae bodies treated with bee venom might be due to the venom's toxic compounds, which influence the synthesis of lipids in *G. mellonella* larvae and pupae bodies. In addition, bee venom disruptively affected physiology and subsequently deranged vital growth and reproduction functions (Bouaziz *et al.,* 2011).

The treatment with 2,000 ppm of bee venom had the highest protein content of the wax moth body, followed by the control and 3,000 ppm with negligible variations among them (27.39±0.48, 27±0.44 and 25.38±1.58). The treatment with 500 ppm of bee venom produced the lowest protein value (20.03±0.10, $\boldsymbol{P}$<0.0003). Tanani *et al.,* (2021) indicated that the treated larvae had significantly less total protein, irrespective of the venom amount or larval stage development. The effectiveness of the bee venom, observed in the larvae during their fifth instar with an inhibition rate of 19.80%, and wasp venom, observed in their seventh instar with a reduction rate of 34.77%, showed the most significant decline. Scorpion venom showed the least amount of strength loss (17.45% and 15.7% decreases in the fifth and seventh instar larvae, respectively).

Protein metabolism is critical for insect energy production and reproduction (Kong *et al.*, 2019), as well as for putting together adult structures when insects change from larvae or pupae to adults (Resmitha *et al.*, 2014). Proteins are essential for controlling and organising many of the body's natural and metabolic processes. This is achieved through the action of hormones, enzymes and nucleoproteins (Chapman, 2012). When it comes to analysing carbohydrates, the control group outperformed the others with an impressive average rate of 2.58±0.006. There was a noticeable analysis conducted for all treatments in comparison to the control. When *G. mellonella* larvae in their third instar were exposed to the LC_{50} value of each venom by Tanani *et al.,* (2021), there was a significant decrease in the amount of carbohydrates found in their bodily tissues during both their fifth and seventh instars. For regular larvae, there was a decrease in the amount of carbohydrates as they progressed through each instar. Specifically, in the fifth and seventh instars, the amount dropped to 0.0366±0.007 mg/g. When it comes to the impact on carbohydrates, it is interesting to note that the wasp venom had a minimal effect on the fifth larval instar. On the other hand, the scorpion venom had a similar effect on the seventh larval instar, resulting in reductions of 11.78% and 21.04%, respectively.

Carbohydrates are crucial for the development and functioning of various tissues during the process of metamorphosis in insects. In addition, carbohydrates initially support the proper functioning of the reproductive organs in both males and females, as well as in the development of embryos (Kaufmann and Brown, 2008). Carbohydrates significantly impact the physiology of insects exposed to foreign toxins, as highlighted by Kaufmann and Brown (2008).

The toxicity effect of bee venom on corn earworms, tobacco hornworms and lesser and greater wax moths was recorded (Ghoneim *et al.*, 2019a). In addition, Ghoneim *et al.,* (2019b) mentioned that bee venom causes reduced larval growth rate and weight and prevents adult emergence and fecundity for *G. mellonella* L.

Table 6b. Total lipids, protein and carbohydrate values (mg/gram) for wax moths in different concentrations of bee venom

Bee venom concentration(ppm)	Lipids	Protein	Carbohydrates
500	8.23ab±0.61	20.03c±0.10	0.14d±0.020
1,000	12.13a±0.285	24.04b±0.65	0.22d±0.003
2,000	11.75a±4.85	27.39a±0.48	1.40b±0.07
3,000	6.11ab±0.46	25.38ab±1.58	0.34c±0.003
Control	3.16b±0.26	27a±0.44	2.58a±0.006
$LSD_{5\%}$	6.948	2.586	0.103
F	2.969	14.886	105.177
P	0.0741(ns)	0.0003***	0.0000***

Figure 5. Content of lipids, protein and carbohydrates of wax moth larvae treated with bee venom

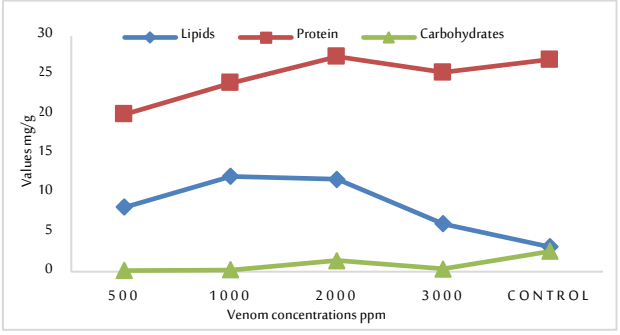

4. Conclusion

Based on the current findings, the applications of high concentrations of bee venom and propolis result in a complete reduction (100% reduction percentage) of wax moth larvae. At concentrations of 3,000 and 2,000 ppm of propolis, the pupal stage of the insect was unable to develop into the adult stage, resulting in the death of all individuals. At

concentrations of 3,000 and 2,000 ppm of bee venom, none of the larvae were able to reach the pupae or adult stage. At concentrations of 500 and 1,000 ppm, the bee larvae underwent metamorphosis into pupae but were unable to complete their development into adults. Accordingly, we recommend using bee venom with a concentration of 2,000 ppm and propolis with a concentration of 3,000 ppm to control the greater wax moth *Galleria mellonella* under laboratory conditions. However, bee venom and propolis can find their way into integrated pest management programmes to manage the greater wax moths in the foreseeable future.

Biographies

Amro Ahmed Taha

Research and Training Station, King Faisal University, 31982 Al-Ahsa, Saudi Arabia, 00966558054186, aaismail@kfu.edu.sa

Prof. Amro A. Taha is an Egyptian entomologist specialising in honey bees and currently working at the Research and Training Station of King Faisal University in Saudi Arabia. He holds a Ph.D. in Entomology (honey bees) from Egypt. He has conducted extensive training and lecturing on honey bee science for trainers across Egypt, Libya, Algeria, Sudan and Saudi Arabia. His international experience spans several countries, including Egypt, Libya, Algeria, Saudi Arabia, Cameroon and Zimbabwe. Prof. Taha has published 27 scientific papers, contributing significantly to the field of honey bee research.

ORCID: 0000-0002-0366-9645

Mohamed Samir Younis

Bee Research Department, Plant Protection Research Institute, Agricultural Research Center, Dokki, Giza, Egypt, 00201225415556, ms_younis@yahoo.com

Younis, an Egyptian associate professor, works at the Bee Research Department within the Plant Protection Research Institute of the Agricultural Research Center in Dokki, Giza. He graduated from the Faculty of Agriculture at Benha University, specialising in Economic Entomology, and holds both a master's degree from Benha University and a Ph.D. from Menoufia University. His research focuses on bee nutrition, pest and disease management in apiaries and the analysis of bee products, contributing valuable insights into sustainable beekeeping practices and honey bee health.

Heba A. Al-Ghanam

Pest Physiology Department, Plant Protection Research Institute, Agricultural Research Center, Dokki, Giza, Egypt, 00201099255170, drhebaalghanam20@gmail.com

Prof. Heba A. Al-Ghanam, an Egyptian scientist at the Plant Protection Research Institute in Dokki, Giza, specialises in pest physiology. A graduate of Mansoura University with a master's and Ph.D. in Agricultural Zoology (Nematology), her research focuses on pest management and nematology, particularly entomopathogenic and plant-parasitic nematodes, economic animal pests and biological control. She also studies physiology, biology and morphology of mites, emphasising sustainable agricultural pest control methods.

Doaa Abd El-Maksoud Abou El-Atta

Cotton and Crops Acarology Department, Plant Protection Research Institute, Agricultural Research Center, Dokki, Giza, Egypt, 00201020996519, doaaabouelatta@gmail.com

Prof. Doaa Abd El-Maksoud Abou El-Atta, an Egyptian scientist, works in the Cotton and Crops Acarology Department at the Plant Protection Research Institute, Agricultural Research Center, in Dokki, Giza. A graduate of the Faculty of Agriculture, Mansoura University, where she specialised in Agricultural Zoology (Acarology), she holds both a master's and a Ph.D. from the same institution. Her research focuses on soil mites, mite biology and control, plant-parasitic nematodes, entomopathogenic nematodes and biological control of economic pests in agriculture. ORCID: 0000-0003-1585-3244

References

Adel, M.M. (2012). Lufenuron impair the chitin synthesis and development of *Spodoptera littoralis* Bosid. (Lepidoptera: Noctuidae). *Journal of Applied Science Research*, **8**(5), 2766–2775.

Amany, S.M. Abou-Lila, Taha, A. A. and Younis, M. S. (2021). Evaluation of Dismate (PE) pheromone and its comparison by some chemicals control against wax moths under storage conditions at Menoufia Governorate, Egypt. *Egyptian Journal of Plant Protection Research Institute,* **4** (3), 409–414. DOI:10.21608/jppp.2015.75301

Ararso, Z. and Legesse, G. (2016). Insecticidal action of honeybees propolis extract against larvae of lesser wax moth. *Agric. Biol. JN Am*, **7**(6), 302–306. DOI:10.5251/abjna.2016.7.6.302.306

Assar, A.A., Abo El-Mahasen, M.M., Dahi, H.F. and Amin, H.S. (2016). Biochemical effects of some insect growth regulators and bioinsecticides against cotton leafworm, Spodoptera littoralis (Boisd.)(Lepidoptera Noctuidae). *Journal of Bioscience and Applied Research*, **2**(8), 587–594. DOI:10.21608/jbaar.2016.108937

Bouaziz, A., Boudjelida, H. and Soltani, N. (2011). Toxicity and perturbation of the metabolite contents by a chitin synthesis inhibitor in the mosquito larvae of Culiseta longiareolata. *Annals of biological research*, **2**(3), 134–142.

Bradbear, N. (2004). *Beekeeping and sustainable livelihoods*. Available at: https://openknowledge.fao.org/server/api/core/bitstreams/d968717a-7970-4e5a-b628-b837408c8985/content (*accessed on 02/11/2024*)

Bradford, M.M. (1976). A rapid and sensitive method for the quantitation of microgram quantities of protein utilizing the principle of protein-dye binding. *Analytical biochemistry*, **72**(1-2), 248–254. DOI:10.1006/abio. 1976.9999

Chapman, R.F. (2012). *The Insects: Structure and Function*. 5th edition. Cambridge, Cambridge University Press. DOI:10.1017/cbo9781139035460

CoStat Software (2004) *Microcomputer Program Analysis*, Version 6.303. CoHort Software, Monterey, CA. Available at: https://cohortsoftware.com/costat.html (*accessed on 30/10/2024*)

El-Kholy, E.M.S. and Mikhaiel, A.A. (2008). Scanning electron microscopy on the male antennae of the greater wax moth, *Galleria mellonella* (L.), treated with gamma radiation. *Isotope and Radiation Research,* **40**(3), 603–613.

Ellis, J.D., Graham, J.R. and Mortensen, A. (2013). Standard methods for wax moth research. *Journal of Apicultural Research*, **52**(1), 1–17. DOI:10.3896/IBRA.1.52.1.10

Garedew, A., Schmolz, E. and Lamprecht, I. (2004). Effect of the bee glue (propolis) on the calorimetrically measured metabolic rate and metamorphosis of the greater wax moth Galleria mellonella. *Thermochimica Acta*, **413**(1-2), 63–72.

Ghoneim, K. (2020). Toxicity and Deleterious Impacts of the Deathstalker Scorpion, Leiurus quinquestriatus, Venom on Development of the Greater Wax Moth, Galleria mellonella (Lepidoptera: Pyralidae). *Egyptian Academic Journal of Biological Sciences. A, Entomology*, **13**(4), 199–211. DOI:10.21608/ eajbsa.

Ghoneim, K.S., Mohamed, H.A. and Bream, A.S. (2000). Efficacy of the neem seed extract, neemazal, on growth and development of the Egyptian cotton leafworm, Spodoptera littoralis Boisd (Lepidoptera: Noctuidae). *Journal-Egyptian German Society Of Zoology*, **33**(E), 161–180.

Ghoneim, K., Hamadah, Kh., Tanani, M., Abdel-Khaliq, A., Emam, D. (2019a). Toxicity and Disruptive Impacts of the Honeybee Apitoxin on Growth and Development of The Greater Wax Moth, Galleria mellonella (Lepidoptera: Pyralidae). *Egyptian Academic Journal of Biological Sciences, F. Toxicology and Pest Control*, **11**(2), 97–106. DOI:10.21608/eajbsf.2019.45537

Ghoneim, K., Tanani, M., Hamadah, Kh.,Abdel-Khaliq, A. and Emam, D. (2019b). Deteriorated adult performance and reproduction of the greater wax moth Galleria mellonella (Lepidoptera: Pyralidae) by the honey bee Apitoxin. *Egyptian Academic Journal of Biological Sciences (A. Entomology).* **12**(4), 95–108. DOI:10.21608/eajbsa.2019.45828

Hussein, H.M., Hadi, M.H. and Hassoni, A.A. (2022). Evaluation of the efficiency of alcoholic propolis extract and *Bacillus thuringiensis* in the mortality rate of the third larval age of the great wax Moth *Galleria mellonella* (L.). *International Journal of Health Sciences,*

6(S2),11413–11419. DOI:10.53730/ ijhs.v6ns2.8273.

Izhar-ul-Haq, M., Muhammad, S. and Sohail, A. (2008). Effect of neem *Azadirachta indica* seed extracts against greater wax moth *Galleria mellonella* L. larvae. *Pakistan Entomological Society, Pakistan Entomologist*, **30**(2): 137–140.

James, R.R. (2011). Potential of ozone as a fumigant to control pests in honey bee (Hymenoptera: Apidae) hives. *Journal of Economic Entomology*, **104**(2), 353–359. DOI:10.1603/ec10385.

Joseph A.K., Shauna A., James M.R. (1972). Chemical basis of the sulfophospho-vanillin reaction for estimating total serum lipid. *Clinical Chemistry*, **18**(3), 198–201. DOI:10.1093/clinchem/18.3.199

Kaufmann, C. and Brown, M.R. (2008). Regulation of carbohydrate metabolism and flight performance by a hypertrehalosaemic hormone in the mosquito Anopheles gambiae. *Journal of insect physiology*, **54**(2), 367–377. DOI:10.1016/j.jinsphys.2007.10.007

Kong, H.G., Kim, H.H., Chung, J.H., Jun, J., Lee, S., Kim, H.M. and Ryu, C.M. (2019). The Galleria mellonella hologenome supports microbiota-independent metabolism of long-chain hydrocarbon beeswax. *Cell reports*, **26**(9), 2451–2464. DOI:10.1016/j.celrep.2019.02.018

Kosuge, T. (1969). The role of phenolics in host response to infection. *Annual Reviews,* **7**(n/a),195–222. DOI: 10.1146/annurev.py.07.090169.001211

Linton, Y.M., Nisbet, A.J. and Mordue, A.J. (1997). The effects of azadirachtin on the testes of the desert locust, Schistocerca gregaria (Forskål). *Journal of Insect Physiology*, **43**(11), 1077–1084. DOI:10.1016/s0022-1910(97)00060-7

Mahgoub, M.O., Lau, W.H., Omar, D.B. and El Naim, A.M. (2018). Evaluation the toxicity of honey bee venom on Achroia grisella developmental stages. *World Journal of Agricultural Research*, **6**(1), 5–9. DOI: 10.12691/wjar-6-1-2

Naqqash, M.N., Gökçe, A., Bakhsh, A. and Salim, M. (2016). Insecticide resistance and its molecular basis in urban insect pests. *Parasitology research*, **115**(n/a), 1363–1373. DOI:10.1007/s00436-015-4898-9

Netíková, L., Bogusch, P. and Heneberg, P. (2013). Czech ethanol-free propolis extract displays inhibitory activity against a broad spectrum of bacterial and fungal pathogens. *Journal of Food Science*, **78**(9), M1421–M1429. DOI:10.1111/1750-3841.12230

Owayss, A.A. and Abd-Elgayed, A.A. (2007). Potential efficacy of certain plant volatile oils and chemicals against greater wax moth *Galleria mellonella* (Lepidoptera: Pyralidae). *Entomological Society of Egypt (Economic Series),* **33**(n/a), 67–75.

Popova, M., Bankova, V., Butovska, D., Petkov, V., Nikolova-Damyanova, B., Sabatini, A. G. and Bogdanov, S. (2004). Validated methods for the quantification of biologically active constituents of poplar-type propolis. *Phytochemical Analysis: An International Journal of Plant Chemical and Biochemical Techniques*, **15**(4), 235-240. DOI:10.1002/pca.777

Possani, L.D., Becerril, B., Delepierre, M. and Tytgat, J. (1999). Scorpion toxins specific for Na+-channels. *European journal of biochemistry*, **264**(2), 287–300. DOI:10.1046/j.1432-1327.1999.00625.x

Resmitha, C., Reshma, R.M., Punathumparambath, B. and Vadakkadath Meethal, K. (2014). The ecdysone mimic, methoxyfenozide, alters the level of major haemolymph proteins in the larvae of Spodoptera mauritia Boisd.(Lepidoptera: Noctuidae). *Acta Biologica Indica*, **3**(2), 726–730.

Sanad, R.E. and Mohanny, K.M. (2015). Toxicological and biological effects of propolis and three plant extracts on the greater wax moth, *Galleria mellonella* L. *Egyptian Journal of Biological Pest Control*, **25**(1), 213–219.

Shimanuki, H., and Knox, D.A. (1997) Summary of control methods. In: Morse, R.A., and Flottum, K. (eds) *Honey Bee Pests, Predators and Diseases*. Medina, USA: Root company

Singh, N.B. and Sinha, R.N. (1977). Carbohydrates, lipids and protein in the developmental stages of Sitophillus oryzea and Sitophillus grannarius. *Annals of the Entomological Society of America*, **70**(1), 107–111. DOI:10.1093/aesa/70. 1.107

Snedecor, G.W. and Cochran, W.G. (1980). *Statistical Methods*. 7th ed. Iowa State, USA: University Press, Ames.

Tanani, M., Ghoneim, K., Hamadah, K. and Emam, D. (2021). Comparative impairing effects of selected arthropod venoms on the main body metabolites of Galleria mellonella (Lepidoptera: Pyralidae). *African Journal of Biological Sciences*, **3**(3), 64–79. DOI:10.33472/afjbs.3.3.2021.64-79

Tsegaye, A., Wubie, A.J., Eshetu, A.B. and Lemma, M. (2014). Evaluation of different non-chemical wax moth prevention methods in the backyards of rural beekeepers in the North West dry land areas of Ethiopia. *IOSR Journal of Agriculture and Veterinary Science*, **7**(3), 29–36. DOI:10.9790/2380-07312936

Wiesner, A. (1993). *Die Induktion der Immunabwehr eines Insekts (Galleria mellonella, Lepidoptera) durch synthetische Materialien und arteigne Haemolymphfaktoren.* "Induction of the immune defense of an insect (Galleria mellonella, Lepidoptera) by synthetic materials and species-specific haemolymph factors". Ph. D Thesis , Berline, Germany.

Zhou, G. and Miesfeld, R.L. (2009). Energy metabolism during diapause in Culex pipiens mosquitoes. *Journal of insect physiology*, **55**(1), 40–46. DOI:10.1016/j.jinsphys.2008.10.002

Scientific Journal of King Faisal University:
Basic and Applied Sciences

Characterising Optical Properties of Doped Metal Complex Nanocomposite Films with PVA/PVAC for Optoelectronics

Dawood Salman Abd Al-Kader [1] and Harakat Mohsin Roomy [2]

[1] Anbar Education Directorate, Ministry of Education, Anbar, Iraq
[2] Ministry of Education, Baghdad, Iraq

LINK	RECEIVED	ACCEPTED	PUBLISHED ONLINE	ASSIGNED TO AN ISSUE
https://doi.org/10.37575/b/med/240040	30/08/2024	27/11/2024	27/11/2024	01/12/2024
NO. OF WORDS	**NO. OF PAGES**	**YEAR**	**VOLUME**	**ISSUE**
5310	6	2024	25	2

ABSTRACT

This study investigates the optical properties of nanocomposite films made from polyvinyl alcohol (PVA), polyvinyl acetate (PVAC), and a 50/50 polyblend of PVA and PVAC, doped with varying concentrations 0, 3, 6, and 9 wt.% of the metal complex Fluoro pentaamine cobalt (III) fluoride $[Co(NH_3)_5F]F_2$ (FACF). The films were prepared using a solvent casting method and analysed with a computerised UV-VIS-IR spectrophotometer over the wavelength range of 250–850 nm. Key optical parameters, including the refractive index, extinction coefficient, and optical conductivity, were determined through absorption studies. The optical absorbance increased with higher FACF concentrations. UV-Vis spectra were used to estimate the band gap energies and investigate the electronic transitions from the valence band to the conduction band. A decrease in the band gap for allowed direct transitions was observed: from 4.0 eV to 2.55 eV for PVA, 4.1 eV to 2.6 eV for PVAC, and 4.35 eV to 2.6 eV for the polyblend as the FACF content increased. Additionally, both the extinction coefficient and refractive index increased with higher FACF concentrations. These nanocomposite films show potential for use in photovoltaic cells, optical sensors, LEDs, photodetectors and other luminescent devices, though further research is needed.

KEYWORDS

absorbance spectrum, casting method, energy gap, polyblend, polyvinyl acetate, polyvinyl alcohol

CITATION

Abd Al-Kader, D.S and Roomy, H.M. (2024). Characterising optical properties of doped metal complex nanocomposite films with PVA/PVAC for optoelectronics. *Scientific Journal of King Faisal University: Basic and Applied Sciences*, **25**(2), 57–62. DOI: 10.37575/b/med/240040

1. Introduction

Nowadays, polymers are widely diversified and play an important role in many aspects of human life due to their better features compared to traditional materials, such as low production costs, chemical stability, lightweight and ease of processing (Aziz *et al.*, 2017; Bhagyaraj *et al.*, 2020). Novel polymers and polymer composites have several unique qualities, including simple processing methods and optical characteristics that make them strong contenders for a variety of optoelectronic uses, including data processing, integrated optics, optical sensors, microlasers and Nanophotonics (Beckers *et al.*, 2017; Loste *et al.*, 2019). Moreover, polymers impregnated with noble metal nanoparticles exhibited unique and elevated features resulting from a distinct fusion of the intrinsic properties of the polymers and those of the metal nanoparticles (Hassan and Ah-yasari, 2019). By hydrolysing polyvinyl acetate in ethanol using potassium hydroxide, Haehnel and Hermann produced poly (vinyl alcohol) (PVA) for the first time in 1924 (Sharma *et al.*, 2023). PVA is a highly versatile material with several desirable properties, including high dielectric strength and excellent transparency and optical properties. These characteristics make it an attractive option for the preparation of electrolyte membranes, given its mechanical and chemical strength (Palanichamy *et al.*, 2023). PVA is synthetic, linear and semi-crystalline in nature. It contains a carbon chain and a hydroxyl functional group that acts as the backbone (Agrawal *et al.*, 2023). It is the most popular water-soluble polymer with the formula $(C_2H_4O)n$, and it is manufactured by saponification of poly 'vinyl ester' with sodium hydroxide (NaOH). PVA has an extremely high transmission of visible light, making it desirable in a variety of opto-electronic systems and applications and is economically and environmentally beneficial (Palanichamy *et al.*, 2023). Under acidic conditions, the OH groups in PVA tend to cross-link with aldehydes, forming hemiacetal or actual linkages chemically (Bulinski, 2021), (Zhong *et al.*, 2024).

In contrast, Poly (vinyl acetate) (PVAC) is referred to as 'white glue'. It is a clear, glassy substance that is transparent at ambient temperature, insoluble in water, odourless, colourless, and non-toxic. PVAC is a thermos-plastic polymer. In the presence of an alkali or acid, it can be alcoholysed to produce PVA. PVAC is highly stable in the presence of light and hardly ages under the influence of light. The term 'white latex' is commonly used to describe PVAC emulsion. It can be modified directly with a variety of additives. Its mechanical strength is good; specifically, it is a water-based adhesive and does not pollute the environment (Aruldass *et al.*, 2019). Since PVAC contains a COOH group, it can be amenable to the formation of safe and biocompatible films for application in both industrial and biomedical settings (Khalifa *et al.*, 2024).

Substances called metal complexes are frequently used in analytical chemistry. They can be produced to have specific molecular geometries, making it possible to use their unique spectroscopic, physical and electrochemical properties for analytical applications (Elattar *et al.*, 2024), (Yam and Lo, 1999). A metal complex or a 'coordination complex' is a type of chemical compound that consists of a coordination centre, which is usually a basic metal atom or ion, and a surrounding group of linked neutral molecules. Alternatively, they can be anions such as fluoride or chloride, also referred to as ligands or complex agents. These ligands can produce bonds by donating electrons to the orbitals of the metal ion (Kettle, 2013). Transition metals are distinguished by the multiple oxidation states (Chan and Wong, 2013). A paramagnetic compound Fluoro penta Amine Cobalt (III) Fluoride $[Co(NH_3)_5F]F_2$ (FACF) is the metal complex utilised in this work. FACF exhibits characteristic optical properties that are primarily influenced by the ligand field around the Co^{3+} ion, leading to the formation of distinct absorption bands in the UV-visible region. The observed colour is a consequence of these electronic transitions, and spectroscopic techniques like UV-Vis and IR spectroscopy are essential for studying these properties (Van Eldik *et al.*, 1978), (Schönherr, 2004). The purpose of this study is to examine the influence of incorporating metal complexes of FACF at

Corresponding Author: Dawood Salman Abd Al-Kader 009647813186439, dawodalany@gmail.com

varying concentrations on the optical behaviour of PVA and PVAC, both individually and in a poly blend of 50% PVA + 50% PVAC, using UV-visible radiation. The results of these measures have been subjected to investigation and discussion with regard to their potential applicability in a multitude of industrial applications.

2. Experimental Procedures

2.1. Prepared Fluoro Penta Amine Cobalt (III) Fluoride (FACF):

The preparation of FACF was conducted in accordance with the methodology described by Rabee *et al.* (2013). In a 400 ml container, (2 g) of ammonium fluoride NH_4F was dissolved totally in approximately 15 ml of pure NH_3^+ while stirring continuously. Then (3.5 g) of Cobalt fluoride (CoF_2) was added progressively to the mix. After obtaining a brown-coloured slurry, 2.5 mL of 33% Hydrogen Peroxide (H_2O_2) was gradually added. At the end of the effervescence, approximately 15 mL of concentrated hydrofluoric acid (HF) was gradually added. While stirring continuously on a hot plate, the mixture was heated to 85°C for 20 minutes, and then a Buchner funnel was used to filter out the FACF crystals after using ice to cool the mixture to room temperature.

2.2. Samples Preparation:

The polymers used in this work as the polymer matrix were poly (vinyl alcohol) (PVA), $(C_2H_4O)n$, and poly (vinyl acetate) (PVAC) $(C_4H_6O_2)n$. The PVA used was a fine white grain with a molecular weight ranging from 30,000 to 70,000 and a purity of 99.5%. PVAC is a solid polymer granule that is white to yellow with a molecular weight of 100,000 and 99.6% pure. All of the chemicals needed to make FACF were purchased from Sigma-Aldrich. Mothed of Solvent casting was used to create films of PVA, PVAC and 50% PVA + 50% PVAC doped with 0, 3, 6 and 9 wt% of metal complexes of FACF. First, distilled water was added to solid PVA $(C_2H_4O)n$ to produce a PVA solution. The distilled water was used to mix the PVA emulsion for ten hours, and then stirred it with a magnetic stirrer for two hours at 70°C. Using a magnetic stirrer, the required weight fractions of FACF were distributed in distilled water for one hour and then progressively added while stirring continuously into the polymeric emulsion, leaving it under string for two hours. Subsequently, the solution was transferred to clean Petri dishes and left to gradually evaporate at room temperature for a week. Following the drying process, the thin films were peeled from the Petri dishes and kept in vacuum desiccators until utilised. Using the same steps, the remaining PVAC samples and the combination solution of 50 % PVA + 50% PVAC were prepared. The produced films had a thickness between 100 and 120 nm. The optical characteristics of the sample's preparation films were examined using UV.VIS.IR spectroscopy in the submitted work.

3. Results and Discussions

3.1. Fourier Transform Infrared Spectroscopy (FTIR):

Fourier transform infrared (FTIR) spectroscopy is a significant analytical technique for examining the structural characteristics of polymers. It offers insights into the complex interactions and associations between the diverse components present in polymeric systems. Figure 1 illustrates the FTIR spectra of PVA, PVAC and a poly blend of 50% PVA + 50% PVAC doped with 0, 3, 6 and 9 wt. % of the metal complex of FACF. Below, Tables 1, 2 and 3 simulate common expected peaks based on typical FTIR responses for PVA and PVAC polymers doped with a cobalt complex. The tables present illustrative data regarding the absorption intensities at notable wavenumbers for each sample configuration. They comprise readings and typical peak regions observed for these materials in FTIR, encompassing prominent regions for PVA, PVAC and their doped blends.

Figure 1a. FTIR graph of PVA, PVAC and a poly blend of 50% PVA + 50% PVAC doped with 0, 3, 6 and 9 wt. % of the metal complex of FACF.

a

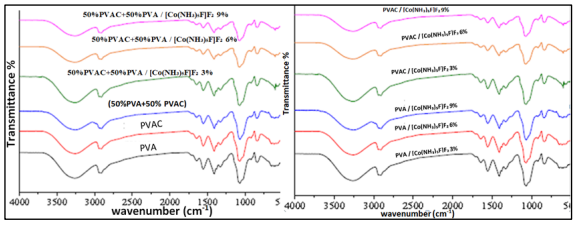

Figure1b. FTIR graph of 50% PVA + 50% PVAC thin film.

b

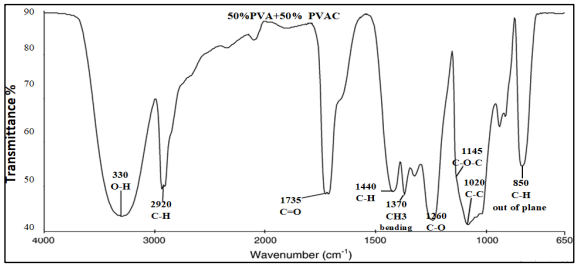

Table 1. Values of absorption peaks, peak assignments and transmission of PVA with 3, 6, 9 wt. % concentration of FACF composites; results based on FTIR analyses.

PVA			PVA / (3%) FACF			PVA / (6 %) FACF			PVA / (9 %) FACF		
Absorption Peak (cm^{-1})	Peak Assignment	Transmission (%)	Absorption Peak (cm^{-1})	Peak Assignment	Transmission (%)	Absorption Peak (cm^{-1})	Peak Assignment	Transmission (%)	Absorption Peak (cm^{-1})	Peak Assignment	Transmission (%)
3300	O-H stretching (hydroxyl groups)	60	3300	O-H stretching (hydroxyl groups in PVA)	57	3280	O-H stretching (hydroxyl groups in PVA)	55	3265	O-H stretching (hydroxyl groups in PVA)	53
2920	C-H stretching (asymmetric)	65	2920	C-H stretching (asymmetric)	63	2915	C-H stretching (asymmetric)	60	2910	C-H stretching (asymmetric)	57
1730	C=O stretching (carbonyl, minor)	60	1730	C=O stretching (carbonyl, minor in PVA)	58	1725	C=O stretching (carbonyl, minor in PVA)	55	1720	C=O stretching (carbonyl, minor in PVA)	53
1440	C-H bending	71	1440	C-H bending	67	1435	C-H bending	64	1430	C-H bending	61
1375	CH_3 bending	62	1370	CH_3 bending	59	1365	CH_3 bending	56	1360	CH_3 bending	54
1270	C-O stretching	50	1260	C-O stretching	52	1255	C-O stretching	50	1250	C-O stretching	47
1150	C-O-C stretching (ether linkages)	55	1140	C-O-C stretching (ether linkages)	48	1135	C-O-C stretching (ether linkages)	45	1130	C-O-C stretching (ether linkages)	42
950	C-F stretching	40	950	C-F stretching (from FACF)	43	940	C-F stretching (from FACF)	40	935	C-F stretching (from FACF)	37
			850	Co-N stretching	38	830	Co-N stretching	35	820	Co-N stretching	32
720	Out-of-plane bending vibrations	30	710	Out-of-plane bending vibrations	28	700	Out-of-plane bending vibrations	25	690	Out-of-plane bending vibrations	23

Table 2. Values of absorption peaks, peak assignments and transmission of PVAC with 3, 6, 9 wt. % concentration of FACF composites; results based on FTIR analyses.

PVAC			PVAC / (3%) FACF			PVAC / (6%) FACF			PVAC / (9%) FACF		
Absorption Peak (cm^{-1})	Peak Assignment	Transmission (%)	Absorption Peak (cm^{-1})	Peak Assignment	Transmission (%)	Absorption Peak (cm^{-1})	Peak Assignment	Transmission (%)	Absorption Peak (cm^{-1})	Peak Assignment	Transmission (%)
2920	C-H stretching (asymmetric)	70	2920	C-H stretching (asymmetric)	68	2925	C-H stretching (asymmetric)	65	2920	C-H stretching (asymmetric)	62
1735	C=O stretching (carbonyl)	65	1735	C=O stretching (carbonyl)	60	1730	C=O stretching (carbonyl)	58	1725	C=O stretching (carbonyl)	55
1440	C-H bending	70	1440	C-H bending	67	1445	C-H bending	64	1440	C-H bending	58
1375	CH_3 bending	67	1375	CH_3 bending	64	1370	CH_3 bending	62	1365	CH_3 bending	60
1260	C-O stretching	60	1260	C-O stretching	55	1265	C-O stretching	53	1260	C-O stretching	50
1150	C-O-C stretching	50	1150	C-O-C stretching	50	1150	C-O-C stretching	48	1145	C-O-C stretching	45
900	C-C stretching	45	950	C-F stretching (from FACF)	45	940	C-F stretching (from FACF)	42	900	C-F stretching (from FACF)	38
			850	Co-N stretching	40	860	Co-N stretching	38	840	Co-N stretching	35
730	Out-of-plane bending vibrations	30	720	Out-of-plane bending vibrations	30	710	Out-of-plane bending vibrations	32	700	Out-of-plane bending vibrations	28

Table 3. Values of absorption peaks, peak assignments and transmission of 50% PVA + 50% PVAC, with 3, 6, 9 wt. % concentration of FACF composites; results based on FTIR analyses

50%PVAC+50%PVA			50%PVAC+50%PVA / (3%) FACF			50%PVAC+50%PVA / (6%) FACF			50%PVAC+50%PVA / (9%) FACF		
Absorption Peak (cm^{-1})	Peak Assignment	Transmission (%)	Absorption Peak (cm^{-1})	Peak Assignment	Transmission (%)	Absorption Peak (cm^{-1})	Peak Assignment	Transmission (%)	Absorption Peak (cm^{-1})	Peak Assignment	Transmission (%)
3300	O-H stretching (hydroxyl groups in PVA)	53	3280	O-H stretching (hydroxyl groups in PVA)	51	3265	O-H stretching (hydroxyl groups in PVA)	49	3250	O-H stretching (hydroxyl groups in PVA)	58
29200	C-H stretching (asymmetric)	63	2915	C-H stretching (asymmetric)	61	2910	C-H stretching (asymmetric)	58	2905	C-H stretching (asymmetric)	55
1753	C=O stretching (carbonyl in PVAC)	60	1725	C=O stretching (carbonyl in PVAC)	56	1720	C=O stretching (carbonyl in PVAC)	54	1715	C=O stretching (carbonyl in PVAC)	52
1440	C-H bending (common to PVAC and PVA)	52	1440	C-H bending	49	1435	C-H bending	43	1430	C-H bending	62
1370	CH3 bending (PVAC)	48	1365	CH3 bending (PVAC)	44	1360	CH3 bending (PVAC)	40	1355	CH3 bending (PVAC)	66
1260	C-O stretching (common to PVAC and PVA)	55	1255	C-O stretching	52	1250	C-O stretching	50	1245	C-O stretching	48
1145	C-O-C stretching (ether linkages in PVA)	52	1135	C-O-C stretching (ether linkages in PVA)	50	1130	C-O-C stretching (ether linkages in PVA)	47	1125	C-O-C stretching (ether linkages in PVA)	45
1020	C-C stretching	45	935	C-F stretching (from FACF)	42	930	C-F stretching (from FACF	39	925	C-F stretching (from FACF)	36
850	C-H out-of-plane bending	55	840	Co-N stretching	51	830	Co-N stretching	48	820	Co-N stretching	30
690	Out-of-plane bending vibrations	30	695	Out-of-plane bending vibrations	28	690	Out-of-plane bending vibrations	25	680	Out-of-plane bending vibrations	22

3.2. UV-VIS Spectra:

The spectra of absorbance for wavelengths of samples ranging from 200 to 900 nm are indicated in Figure 1 for samples of PVA, PVAC and 50 % PVA + 50% PVAC with different concentrations of 0, 3, 6, and 9 wt.% FACF. It is possible that multiple electron transitions can happen in polymers. Optical absorption measurements are used to determine the band structure, absorption edge and optical energy band gaps. Pure polymers show no signs of absorption, but by increasing the doping concentration of the FACF, the absorption gradually increases, as indicated in this figure. In other words, absorption increases with the proportion of absorbed molecules, and this rise can be explained by the minute structural distortion found in both PVA and PVAC (Abdelaziz, 2012). The FACF compound enhances the absorbance spectra of the PVA and PVAC host materials. Furthermore, as the concentration of FACF increases, the wavelength corresponding to the aforementioned shoulder-like absorption band also increases. The addition of FACF resulted in the appearance of unique peaks that could be attributed to the formation of charge transfer complexes in the polymer due to the presence of halogens (Gadhave and Dhawale, 2022). These peaks broaden when the concentration of FACF increases due to the high binding between the additive and the host poly. The complexation between PVA, PVAC and FACF is indicated by the red-shift behaviour observed in the composite films and could potentially result from a shift in crystal structure caused by additives (Abdelrazek and Elashmawi, 2008). Furthermore, Figure 1 illustrates how absorbance rises with the percentages of absorbed particles. From the graph, it is evident that maximum absorption is found at 9% for all samples in this study.

Figure 2. Optical absorption versus wavelength of (a) PVA, (b)PVAC and (c) 50 %PVA+50% PVAC, with 0, 3, 6, and 9 wt. % concentration of FACF composites.

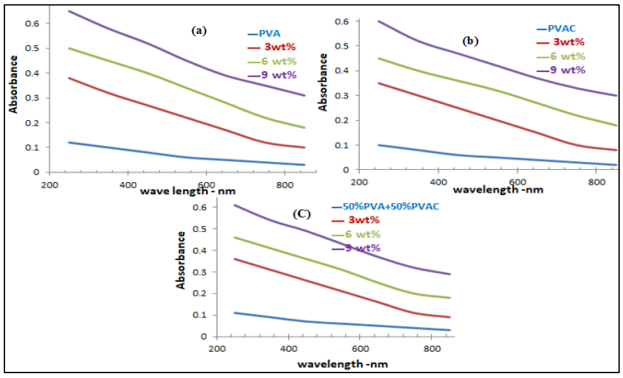

Due to the exceptional importance of the optical band gap and the energy values of the materials being studied, there have been numerous attempts to analyse and calculate the energy required for the electronic transition from the valence-band level to the conduction-band level. Based on the following experimental relationship, these models and assumptions are based on the value of the absorption coefficient α, which appears as an exponential function of the photon energy near the band edge in the semiconductor (Mohammed *et al.*, 2022):

$$\alpha h\nu = \beta\,(h\nu - Eopt.)^{y} \quad \ldots\ldots\ldots\ldots (1)$$

where β is a constant named the band tailing parameter, E_{op} is the energy of the optical band gap, and y is the power factor of the transition mode, which depends on the type of material being studied – whether it is direct or indirect, allowed or forbidden. The energy of the band gap is determined from the graph of $(\alpha h\upsilon)^{1/y}$ vs photon energy ($h\upsilon$). The plots of the band gap energy values obtained from Figures 3 a, b and c illustrate the allowed direct transition y=1/2. As seen in Figures 3 a, b and c, a reasonable linear fit is obtained for $(\alpha h\upsilon)^2$ vs $h\upsilon$. The respective values of E_{op} are obtained by extrapolating to $(\alpha h\upsilon)^2 = 0$ for allowed and direct transition. In the current investigation, a band gap of 4 eV was gained for pure PVA, while 4.1 eV was obtained for pure PVAC, as shown in table 4. It can be observed that across all three material systems, higher doping concentrations (in particular, the 9 wt% sample) result in a markedly elevated absorption coefficient at a given photon energy. This trend suggests that the addition of FACF enhances the material's capacity to absorb light, potentially due to an increase in electronic states that facilitate photon absorption. In each case, the absorption rate rises markedly at a particular threshold energy level. This point frequently correlates with the material's band gap energy, wherein electronic transitions from the valence to the conduction band become feasible. The figures indicate that the absorption onset occurs at approximately 2 to 3 eV, which suggests that this range may be close to the band gap energies for these doped polymers, PVA vs PVAC vs mixed (50% PVA + 50% PVAC). Each polymer matrix (PVA, PVAC and

the blend) displays distinctive absorption characteristics in the presence of the dopant. In general, the absorption coefficient for the mixed system (50% PVA + 50% PVAC) appears to increase in a more gradual manner with increasing doping concentration. In contrast, the pure PVAC and PVA systems exhibit more pronounced changes in slope with each doping level. The slope of the absorption curves undergoes a change with the level of doping, particularly at higher doping concentrations. For example, the 9 wt% doped samples exhibit a steeper curve, indicating a higher rate of increase in absorption with photon energy. This finding may be attributed to an enhanced interaction between photons and the electronic states introduced by the FACF dopant. The interaction between each polymer matrix and the dopant is unique, influencing the absorption behaviour in a manner that can be tailored by modifying the dopant concentration and polymer composition. The observed reduction in the optical energy gap with increasing doping ratio can be attributed primarily to the introduction of impurity-induced states (band tails), enhanced carrier interactions and disorder effects that modify the band structure. At lower doping levels, the optical energy gap may initially appear constant or even increase slightly due to the Burstein-Moss shift. However, as doping intensifies, the cumulative effects of band gap renormalisation, carrier-phonon interactions and localised states in the band tails result in a narrowed optical energy gap. This behaviour is highly relevant in applications such as solar cells and LEDs, where tuning the band gap by doping can improve device performance and efficiency (Zidan *et al.*, 2003). Table 4 presents the obtained values of the energy band gaps.

Figure 3. Energy gaps of allowed direct transition $(\alpha h\upsilon)^2$ against photon energy for PVA, PVAC and 50% PVA+50% PVAC, with 0, 3, 6, and 9 wt. % concentration of FACF composites

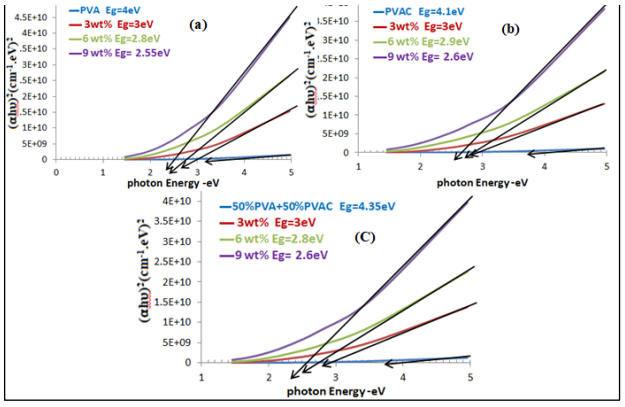

The variation in the coefficient of excitation k with wavelength provides confirmation of the interaction between the energy of the medium and the photon. The value of K was determined by applying the following formula (Balkanski, 1980):

$$\kappa = \alpha\lambda / 4\pi \ldots\ldots\ldots(2)$$

The dependence of κ on the wavelength 190–800 nm of pure for both PVA, PVAC and 50% PVA+50% PVAC / 0, 3, 6, 9 wt% of FACF compound samples is illustrated in Figure 4 a, b and c. The graph shows a decline in the coefficient of excitation values for the pure PVA, PVAC and 50% PVA+50% PVAC samples across 290–800 nm wavelengths, while there is an increase in the coefficient of excitation values for the 3, 6, and 9 wt%. As the concentration of FACF increased, the coefficient of excitation also increased due to the higher concentration of the additive, resulting in a greater coefficient of absorbance.

Figure 4. Extinction coefficient versus wavelength for (a) PVA, (b)PVAC, and (c) 50% PVA+50% PVAC, with 0, 3, 6, and 9 wt. % concentration of FACF composites.

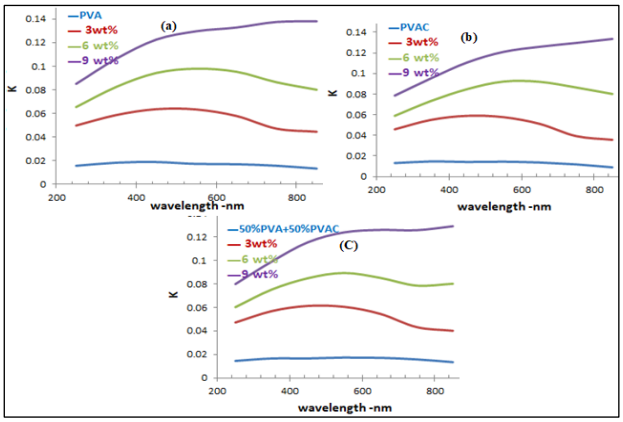

The refractive index (n) is an essential optical characteristic of every polymer. It is closely linked to a material's optical, magnetic and electrical characteristics, making it valuable for researching the chemical, physical and molecular features of a polymer using optical methods. The index of refraction is calculated according to the following formula (Salman *et al.*, 2015):

$$n = \sqrt{\frac{4R - \kappa^2}{(R-i)^2}} - \frac{(R+1)}{(R-1)} \ldots\ldots\ldots(3)$$

where R is reflectance. The plans are shown in Figures 5 a, b and c, which represent the variations of the refraction index of PVA, PVAC and 50% PVA+50% PVAC, with different doping concentrations of 0, 3, 6, and 9 wt.% FACF thin films, respectively, in the investigated range of wavelengths at room temperature. In Figure 5, it is evident that for all prepared samples, the index of refraction decreases as the wavelength increases. Conversely, the figure demonstrates that the index of refraction (n) increases with the addition of the additive percentage FACF, which is in line with the growth in packing density due to the rise in FACF content (Rabee *et al.*, 2013). In other words, this result can be attributed to the occurrence of additional atomic refractions as a consequence of the growth linear polarisation, which is consistent with the Lorentz formula (Ahmad *et al.*, 2007).

Figure 5. The refraction of the index vs wavelength for (a) PVA, (b)PVAC, and (c) 50% PVA+50% PVAC, with 0, 3, 6, and 9 wt.% concentration of FACF composites.

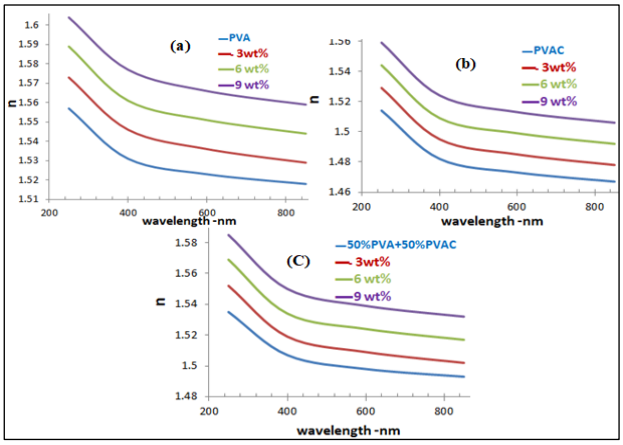

Figure 6 shows the deviation of optical conductivity σ as a function of photon energy for PVA, PVAC and 50% PVA+ 50% PVAC, with different doped concentrations of 0, 3, 6, and 9 wt.% FACF thin films. It can be observed that pure PVA and PVAC have nearly constant

conductivity σ up to about 5.6 eV of photon energy, then it rises as the photon energy increases. The higher absorption behavior of the polymer composite films, resulting from the increased concentration of FACF, leads to an enhancement in optical conductivity. The band gap energy decreases while optical conductance increases due to an increase in the FACF concentration caused by a growth in the total of mobile charge carriers and an increase in the amorphous nature of the host polymer.

Figure 6. Optical conductivity σ as a function of photon energy for (a) PVA, (b)PVAC and (c) 50%PVA+50%PVAC, with 0, 3, 6, and 9 wt.% concentration of FACF composites.

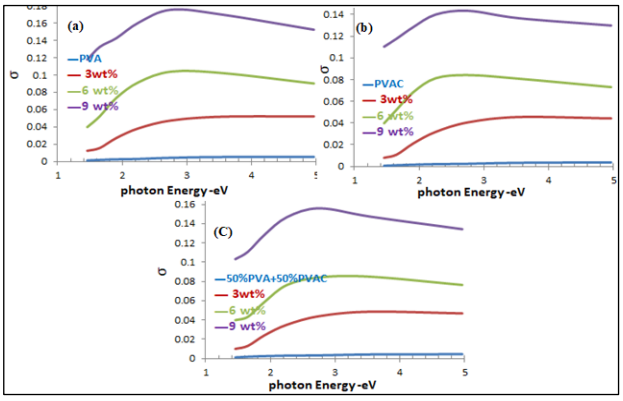

Table 4. Energy gap values of the allowed direct transition of PVA, PVAC and 50% PVA+50% PVAC, with 0, 3, 6, and 9 wt.% concentration of FACF composites.

Additive concentrate %	PVA/$[Co(NH_3)5F]F_2$	PVAC/$[Co(NH_3)5F]F_2$	50%PVA+50%PVc/$[Co(NH3)5F]F_2$
	E_g(ev) of allowed direct transitions	E_g(ev) of allowed direct transitions	E_g(ev) of allowed direct transitions
0	4	4.1	4.35
3	3	3	3
6	2.8	2.9	2.8
9	2.55	2.6	2.6

4. Conclusions

Polymer films based on PVA, PVAC and 50% PVA+50% PVAC, with different concentrations; 0, 3, 6, and 9 wt.% FACF, were prepared using a solvent casting procedure. The optical characteristics were analysed depending on the additive concentrations. The UV outcomes demonstrated that FACF is an effective additive for improving the optical characteristics of both PVA and PVAC, whether used individually or in combination. The absorbance of the PVA and PVAC increased as the weight percentages of FACF increased. The optical properties also show that as the concentration of FACF increases, the band gap energy of the host polymer matrix decreases. This is thought to be due to a higher level of disorder as a result of the increase in the local state within the optical band gap for both PVA and PVAC films. The appearance of the overlap corresponds to the increase in doping concentrations for all samples, which is caused by additional complexation with the polymer matrix. These overlaps confirm that the energy band gap decreases with increasing FACF content in the polymer matrix. The optimal optical characteristics were achieved at 9 wt.% FACF for all prepared samples. The impact of varying concentrations of FACF on the optical performance of nanocomposite films has been studied, with a particular focus on the coefficients of extinction, optical conductivity, and index of refraction. Finally, the field of metal-doped PVA research is still open. Owing to its significance in novel high-tech uses, its effectiveness in optoelectronics has been a significant focus of scientific investigation.

Biographies

Dawood Salman Abd Al-Kader

Anbar Education Directorate, Ministry of Education, Anbar, Iraq, 009647813186439, dawodalany@gmail.com

Abd Al-Kader, an Iraqi, holds a PhD in physics, specialising in thin films, from Anbar University, College of Science. His research, published in Scopus-indexed journals, focuses on light-matter interactions in various materials, particularly in optics and plasmas. He is currently a physics teacher at the Anbar Education Directorate and has experience as a research evaluator for several academic journals. He is also deeply interested in green synthesis and nanomaterials, exploring sustainable methods for material development.

ORCID: 0009-0008-7776-8313.

Harakat Mohsin Roomy

Department of Physics, College of Open Education, Ministry of Education, Baghdad, Iraq, +9647717660139, hrkatm37@gmail.com

Harakat, an Iraqi PhD in laser and optics from the University of Baghdad, specialises in optical systems fabrication using plasma technology. She is a faculty member at the College of Open Education and a researcher affiliated with the Ministries of Science and Technology and Higher Education. Harakat has also worked as a nanotechnology researcher at the Ministry of Industry and as a research reviewer for its journals. She has published both domestic and international studies on optics and plasma, with articles indexed in Scopus.

ORCID: 0000-0002-7919-4463.

References

Abdelaziz, M. (2012). Optical and dielectric properties of poly (vinylacetate)/lead oxide composites. *Journal of Materials Science: Materials in Electronics*, **23**(n/a), 1378–86. DOI: 10.1007/s10854-011-0602-8

Abdelrazek, E.M. and Elashmawi, I.S. (2008). Characterisation and physical properties of CoCl2 filled polyethyl-methacrylate films. *Polymer Composites*, **29**(9), 1036–43. DOI: 10.1002/pc.20481

Agrawal, P.K., Sharma, P., Singh, V.K. and Chauhan, S. (2023). A comprehensive review on the engineering of biocompatible polyvinyl alcohol composites with enhanced properties using carbonaceous fillers. *Journal of Materials and Environmental Science*, **14**(5), 560–81.

Ahmad, A.H., Awatif A.M, Zeid and Abdul-Majied N. (2007). Dopping effect on optical constants of polymethylmethacrylate (PMMA). *Engineering and Technology Journal*, **25**(4), 558–68

Aruldass, S., Mathivanan, V., Mohamed, A.R. and Tye, C.T. (2019). Factors affecting hydrolysis of polyvinyl acetate to polyvinyl alcohol. *Journal of Environmental Chemical Engineering*, **7**(5), 103238. DOI: 10.1016/j.jece.2019.103238

Aziz, S.B., Mamand, S.M., Saed, S.R., Abdullah, R.M. and Hussein, S.A. (2017). New method for the development of plasmonic metal-semiconductor interface layer: polymer composites with reduced energy band gap. *Journal of Nanomaterials*, **2017**(1), 8140693. DOI: 10.1155/2017/8140693

Balkanski, M. (1980). Optical properties of solids. *Crystal Research and Technology*, **15**(10)1122. DOI: 10.1002/crat.19800151004

Beckers, M., Schlüter, T., Gries, T., Seide, G. and Bunge, C.A. (2017). Fabrication techniques for polymer optical fibres. In: C.A. Bunge, T. Gries, M. Beckers (eds.) *Polymer Optical Fibres*, pp.187–199. Elsevier: Woodhead Publishing. DOI: 10.1016/B978-0-08-100039-7.00006-3

Bhagyaraj, S., Oluwafemi, O.S. and Krupa, I. (2020). Polymers in optics. In: M.A.A., AlMaadeed, D., Ponnamma and M.A., Carignano (eds.) *Polymer Science and Innovative Applications: Materials, Techniques, and Future Developments*. Elsevier. pp. 423–55. Elsevier. DOI:10.1016/B978-0-12-816808-0.00013-5

Bulinski, M. (2021). Metal doped PVA films for opto-electronics-optical and electronic properties, an overview. *Molecules*, **26**(10), 2886. DOI: 10.3390/molecules26102886

Chan, W.T.K. and Wong, W.T. (2013). A brief introduction to transition metals in unusual oxidation states. *Polyhedron*, **52**(n/a), 43–61. DOI: 10.1016/j.poly.2012.09.004

Elattar, R.H., El-Malla, S.F., Kamal, A.H. and Mansour, F.R. (2024). Applications of metal complexes in analytical chemistry: A review article. *Coordination Chemistry Reviews*, **501**(n/a), 215568. DOI: 10.1016/j.ccr.2023.215568

Gadhave, R.V.I. and Dhawale, P.V. (2022). State of research and trends in the development of polyvinyl acetate-based wood adhesive. *Open Journal of Polymer Chemistry*, **12**(1), 13–42. DOI: 10.4236/ojpchem.2022.121002.

Hassan, D. and Ah-yasari, A.H. (2019). Fabrication and studying the dielectric properties of (polystyrene-copper oxide) nanocomposites for piezoelectric application. *Bulletin of Electrical Engineering and Informatics*, **8**(1), 52–7. DOI:10.11591/eei.v8i1.1019

Kettle, S.F.A. (2013). *Physical Inorganic Chemistry: A coordination Chemistry Approach*. Springer.

Khalifa, M., El Sayed, A.M., Kassem, S.M. and Tarek, E. (2024). Synthesis, structural, optical, and thermal properties of LaFeO3/Poly (methyl methacrylate)/Poly (vinyl acetate) nanocomposites for radiation shielding. *Scientific Reports*, **14**(1), 3672. DOI: 10.1038/s41598-024-54207-5

Loste, J., Lopez-Cuesta, J.M., Billon, L., Garay, H. and Save, M. (2019). Transparent polymer nanocomposites: An overview on their synthesis and advanced properties. *Progress in Polymer Science*, **89**(n/a), 133–58. DOI: 10.1016/j.progpolymsci.2018.10.003

Mohammed, M.K., Abbas, M.H., Hashim, A., Rabee, R.H., Habeeb, M.A. and Hamid, N. (2022). Enhancement of optical parameters for PVA/PEG/Cr2O3 nanocomposites for photonics fields. *Revue des Composites et des Matériaux Avancés-Journal of Composite and Advanced Materials*, **32**(4), 205–9. DOI: 10.18280/rcma.320406

Palanichamy, K., Anandan, M., Sridhar, J., Natarajan, V. and Dhandapani, A. (2023). PVA and PMMA nano-composites: A review on strategies, applications and future prospects. *Materials Research Express*, **10**(2), 022002. DOI: 10.1088/2053-1591/acb527.

Rabee, B.H., Hashim, A., Salman, S.R., Abbas, A.K., Rashid, F.L. and Ahmed, H. (2013). Preparation of [Co (NH3) 5Cl] Cl2 complexes and characterization of (PVA-[Co (NH3) 5Cl] Cl2]) composites. *Chemistry and Materials Research*, **3**(7), 50–4.

Salman, S.A., Khodair, Z.T. and Abed, S.J. (2015). Study the effect of substrate temperature on the optical properties of cofe2o4 films prepared by chemical spray pyrolysis method. *International Letters of Chemistry, Physics and Astronomy*, **61**(n/a), 118–27. DOI: 10.56431/p-5agw6p

Schönherr, T. (Ed.). (2004). *Optical Spectra and Chemical Bonding in Transition Metal Complexes: Special Volume II, Dedicated to Professor Jørgensen*, (Vol. 107). Springer.

Sharma, P., Agrawal, P.K., Singh, V.K., Chauhan, S. and Bhaskar, J. (2023). A comprehensive review on properties of polyvinyl alcohol (PVA) crosslinked with carboxylic acid. *Journal of Materials and Environmental Science,* **14**(10), 1236–52.

Van Eldik, R., Palmer, D.A. and Kelm, H. (1978). Mechanistic information from the effects of pressure on the kinetics of the reduction of Co (NH3) 5F2+, Co (NH3) 5Cl2+ and Co (NH3) 5Br2+ by iron (II) in dimethylsulphoxide. *Inorganica Chimica Acta*, **29**(n/a), 253–9. DOI:10.1016/S0020-1693(00)89657-7

Yam, V.W.W. and Lo, K.K.W. (1999). Recent advances in utilisation of transition metal complexes and lanthanides as diagnostic tools. *Coordination Chemistry Reviews*, **184**(1), 157–240. DOI: 10.1016/S0010-8545(98)00262-8

Zhong, Y., Lin, Q., Yu, H., Shao, L., Cui, X., Pang, Q. and Hou, R. (2024). Construction methods and biomedical applications of PVA-based hydrogels. *Frontiers in Chemistry*, **12**(n/a), 1376799. DOI: 10.3389/fchem.2024.1376799

Zidan, H.M., Tawansi, A. and Abu-Elnader, M. (2003). Miscibility, optical and dielectric properties of UV-irradiated poly (vinylacetate)/poly (methylmethacrylate) blends. Physica B: Condensed Matter, 339(2-3), 78–86. DOI: 10.1016/j.physb.2003.08.054.

Scientific Journal of King Faisal University:
Basic and Applied Sciences

Perfect Roman and Perfect Italian Domination of Cartesian Product Graphs

Ahlam Almulhim
Department of Mathematics and Statistics, College of Science, King Faisal University, Al-Ahsa, Saudi Arabia

LINK	RECEIVED	ACCEPTED	PUBLISHED ONLINE	ASSIGNED TO AN ISSUE
https://doi.org/10.37575/b/sci/240037	29/08/2024	28/11/2024	28/11/2024	01/12/2024
NO. OF WORDS	**NO. OF PAGES**	**YEAR**	**VOLUME**	**ISSUE**
4871	6	2024	25	2

ABSTRACT

For a graph $G = (V, E)$, a function $f: V \to \{0,1,2\}$ is a perfect Roman dominating function (PRDF) on G if every $v \in V$ with $f(v) = 0$ is adjacent to exactly one vertex u with $f(u) = 2$. The sum $\sum_{v \in V} f(v)$ is the weight $w(f)$ of f. The perfect Roman domination number $\gamma_R^p(G)$ of G is least positive integer k such that there is a PRDF f on G with $w(f) \leq k$. A function $f: V \to \{0,1,2\}$ is a perfect Italian dominating function (PIDF) on G if for every $v \in V$ with $f(v) = 0$, $\sum_{u \in N(v)} f(u) = 2$. The sum $\sum_{v \in V} f(v)$ is the weight $w(f)$. The perfect Italian domination number $\gamma_I^p(G)$ of G is least positive integer k such that there is a PIDF f on G with $w(f) \leq k$. Perfect Roman domination and perfect Italian domination are variants of Roman domination, which was originally introduced as a defensive strategy of the Roman Empire. In this article, we prove that the perfect Roman domination and perfect Italian domination problems for Cartesian product graphs are NP-complete. We also give an upper bound for $\gamma_I^p(G)$, where G is the Cartesian product of paths and cycles.

KEYWORDS
graph domination, graph operations, graph theory, np-completeness, problem complexity, simple graphs

CITATION
Almulhim, A. (2024). Perfect Roman and Perfect Italian Domination of Cartesian Product Graphs. *Scientific Journal of King Faisal University: Basic and Applied Sciences*, **25**(2), 63–8. DOI: 10.37575/b/sci/240037

1. Introduction and Preliminaries

In this paper, we consider finite, simple and undirected graphs $G = (V, E)$, with vertex set V and edge set E. We denote the number of vertices in a graph G by $|G|$. Two vertices, u and v, in G are *adjacent* or *neighbours* if $uv \in E$. The set of neighbours of a vertex v in G is denoted by $N_G(v)$ or by $N(v)$ if G is known from the context. The number of edges in a path is its *length*. We denote a path with k vertices by P_k. A cycle graph with k vertices is denoted by C_k.

Roman domination was first introduced by Cockayne *et al.,* (2004) after a series of papers on strategies used to defend the ancient Roman Empire (ReVelle, 1997; Stewart, 1999; Revelle and Rosing, 2000). The Roman domination notion was inspired by Emperor Constantine's (272–337 AD) defence plan to protect the Roman Empire. The approach was as follows: (i) any city in the empire could have no more than two legions stationed there, and (ii) every city without a legion had to be near a city with two armies. Therefore, if an attack were launched against a city without an army, a city with two armies could send one of its armies to defend the former. Roman domination and its variants have been the subject of more than 100 academic articles. Even though the original strategy focused on army distribution, it can now be applied to any distribution problem, such as service centre distribution. Perfect Roman domination introduced in (Henning *et al.,* 2018), Italian domination introduced as Roman $\{2\}$-domination in (Chellali *et al.,* 2016) and perfect Italian domination introduced in (Haynes and Henning, 2019) are variants of Roman domination. In the current paper, we continue the study of perfect Roman and perfect Italian dominations.

For a graph $G = (V, E)$, every function $f: V \to A$, where $A \subset \mathbb{Z}$, corresponds to the partition $\left(V_i^f \middle| V_i^f := \{v \in V | f(v) = i\}, i \in A\right)$. The weight of f is $w(f) := \sum_{v \in V} f(v)$. If H is a subgraph of G, then $w(f(H)) := \sum_{v \in V(H)} f(v)$. A Roman dominating function (RDF) is a function $f: V \to \{0,1,2\}$ such that every $v \in V_0^f$ is adjacent to at least one vertex in V_2^f. The Roman domination number of G, denoted by $\gamma_R(G)$, is the minimum weight of an RDF f on G. For recent work in Roman domination, we refer the reader to Luiz (2024). A function $f: V(G) \to \{0,1,2\}$ is a *perfect RDF* (PRDF) on G if every $v \in V_0^f$ is adjacent to exactly one vertex $u \in V_2^f$. The *perfect Roman domination number* of a graph G, denoted by $\gamma_R^p(G)$, is the minimum weight of a PRDF on G. It is clear that any PRDF on G is also an RDF, so $\gamma_R(G) \leq \gamma_R^p(G)$ for every graph G. We refer the reader to (Henning and Klostermeyer, 2018; Darkooti *et al.*, 2019 and Cabrera Martínez, 2022) for further work in perfect Roman domination.

We now provide a simple example to illustrate the concept of perfect Roman domination: Let $P_5 := v_1v_2v_3v_4v_5$ be a path with five vertices. Let $f: V(P_5) \to \{0,1,2\}$ be a function defined as $f(v_1) = 0$, $f(v_2) = 2$, $f(v_3) = 2, f(v_4) = 0, f(v_5) = 1$ is a PRDF, as every vertex with weight equal to 0 (namely, v_1 and v_4) is adjacent to a vertex with weight equal to 2. Observe that $w(f) = 5$ but that $\gamma_R^p(G) \neq 5$, as we can find another PRDF with a weight less than 5. Define a function $g: V(P_5) \to \{0,1,2\}$ such that $g(v_1) = 2$, $g(v_2) = 0$, $g(v_3) = 0, g(v_4) = 2$ and $g(v_5) = 0$. Then, g is a PRDF on P_5 with $w(g) = 4$. It is not difficult to check that there is no PRDF on P_5 with a weight less than 4. So, $\gamma_R^p(P_5) = 4$.

An *Italian dominating function* (IDF) on G is a function $f: V(G) \to \{0,1,2\}$ such that if $v \in V_0^f$, $\sum_{u \in N(v)} f(u) \geq 2$. The minimum weight of an IDF on G is called the *Italian domination number* of G, denoted by $\gamma_I(G)$. Observe that every RDF on a graph G is also an IDF, so $\gamma_I(G) \leq \gamma_R(G) \leq \gamma_R^p(G)$. Italian domination is also called Roman $\{2\}$-domination in the literature. We refer the reader to (Almulhim *et al.*, 2024) for a recent survey paper on Roman $\{2\}$-domination.

A function $f: V(G) \to \{0,1,2\}$ is a *perfect IDF* (PIDF) on G if for every $v \in V_0^f$, $\sum_{u \in N(v)} f(u) = 2$. The *perfect Italian domination number* of G, denoted by $\gamma_I^p(G)$, is the minimum weight of a PIDF on G. Clearly, every PIDF on G is also an IDF, so $\gamma_I(G) \leq \gamma_I^p(G)$. To read more about perfect Italian domination, we refer the reader to (Nazari-Moghaddam and Chellali, 2022; Banerjee *et al.*, 2021; Pradhan *et al.*, 2022).

To illustrate the concept of perfect Italian domination, let $f: V(P_5) \to \{0,1,2\}$ be a function on P_5 such that $f(v_1) = 1$, $f(v_2) = 0$, $f(v_3) = 1, f(v_4) = 0$ and $f(v_5) = 1$. Then, $V_0^f = \{v_2, v_4\}$, $\sum_{u \in N(v_2)} f(u) = \mathrm{f(v_1)} + f(v_3) = 2$ and $\sum_{u \in N(v_4)} f(u) = \mathrm{f(v_3)} + f(v_5) = 2$. So f is a PIDF on P_5 with $w(f) = 3$. It is not

Corresponding Author: Ahlam Almulhim 00966506923348, ahmulhem@kfu.edu.sa

difficult to check that there is no PIDF on P_5 with a weight less than 3. So, $\gamma_I^p(P_5) = 3$.

In general, none of the numbers $\gamma_R(G)$ and $\gamma_I^p(G)$ is bound for the other. Let $G = K_{n_1,n_2,\cdots,n_m}$ be the complete m-partite graph where $n_i \geq 3$ for each $i \in [m]$. If $m \geq 4$, $\gamma_I^p(G) = n_1 + n_2 + \cdots + n_m$ (Lauri and Mitillos, 2020); while, $\gamma_R(G) \leq 4$, as we can label one vertex from the first partite and one vertex from the second partite with 2 and label the rest of the vertices with 0. If $m = 3$, $\gamma_I^p(G) = 3$ (Lauri and Mitillos, 2020), while $\gamma_R(G) = 4$ (Cockayne *et al.*, 2004). As $\gamma_R(G) \leq \gamma_R^p(G)$, the latest example yields a graph G with $\gamma_I^p(G) \leq \gamma_R^p(G)$. Generally, none of the numbers $\gamma_R^p(G)$ and $\gamma_I^p(G)$ is bound for the other. If $m \geq 4$, $\gamma_R^p(G) \leq n_\alpha + 1$, where $n_\alpha = \min_{i\in[m]}\{n_i\}$, as we can label one vertex in the n_α-partite with 2, label the rest of vertices in the same partite with 1 and label the rest of vertices in G with 0. So, $\gamma_R^p(G) \leq \gamma_I^p(G)$.

This paper aims to increase the list of NP-complete problems. In mathematics, the NP-completeness theory is used to determine how difficult it is to find a polynomial time algorithm to solve a decision problem. More than 3,000 problems in graph theory and computer science have proven to be NP-complete problems when expressed as decision problems. This list is growing rapidly. All NP-complete problems are thought to have similar hardness. So, if one of those problems is solved in polynomial time, all other NP-complete problems can be solved in polynomial time. This observation hints at the usefulness of having a large list of NP-complete problems.

Darkooti *et al.,* (2019) proved that perfect Roman domination is an NP-complete problem for bipartite graphs. In the current paper, similar methods are used to prove that the perfect Roman domination problem is NP-complete for Cartesian product graphs.

Lauri and Mitillos (2020) proved that perfect Italian domination is NP-complete even if G is a bipartite planar graph. In this paper, we follow the technique they used and prove that perfect Italian domination is NP-complete even if G is a Cartesian product graph.

In the last section of this paper, we discuss perfect Italian domination of the Cartesian product graph of the paths P_r and P_s, or of the path P_r and the cycle C_s, or of the cycles C_r and C_s, where $r, s \geq 6$. We also give un upper bound for $\gamma_I^p(G)$, where G is a Cartesian product of graphs. For perfect Roman domination of the Cartesian product of cycles and paths, we refer the readers to Almulhim *et al.,* (2022).

Let G_1 and G_2 be two graphs. The *Cartesian product graph* of G_1 and G_2, denoted by $G_1 \boxtimes G_2$, is a graph with the Cartesian product $V(G_1) \times V(G_2)$ as its set of vertices. Two vertices $(v, u), (v', u') \in G_1 \boxtimes G_2$ are adjacent if either

$v = v'$ and $uu' \in G_2$ or

$u = u'$ and $vv' \in G_1$.

To prove our results, we must first introduce several graphs. Let $H_{x,l} := \left(V(H_{x,l}), E(H_{x,l})\right)$, $l \geq 1$, where $V(H_{x,l}) := \{x, y, u_1, \cdots, u_l, v_1, \cdots, v_l\}$ and $E(H_{x,l}) := \{xu_i, yu_i, yv_i \mid i \in [l]\}$. The graph $H_{x,3}$ is shown in Figure 1. Let $H_c := \left(V(H_c), E(H_c)\right)$, where $V(H_c) := \{c, c', c''\}$ and $E(H_c) := \{cc', cc''\}$, so H_c is a path of length two. Let $O_c := \left(V(O_c), E(O_c)\right)$, where $V(O_c) := \{c, c', c'', d', d''\}$ and $E(O_c) := \{cc', cc'', cd', cd'', c'c'', d'd''\}$. Let K_2 be a clique of size two with the vertex set $\{w_1, w_2\}$. Let $F_{x,l} := H_{x,l} \boxtimes K_2$, $F_c := H_c \boxtimes K_2$ and $Q_c := O_c \boxtimes K_2$.

Figure 1. The graph $\mathbf{H_{x,3}}$.

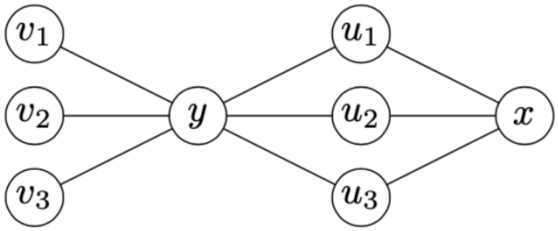

2. The Complexity of Perfect Roman Domination of Cartesian Product Graphs

In this section, we prove that the perfect Roman domination problem for Cartesian product graphs is NP-complete.

To begin, we write the problem as a decision problem, that is, a problem for which the answer to its instances is either yes or no. So, instead of asking, 'Let G be a graph. Find a PRDF on G of minimum weight', we let PERFECT ROMAN DOMINATION be the decision problem where a graph G and an integer k are given. The goal is to decide whether G has a PRDF of weight at most k.

If a function $f: V(G) \to \{0,1,2\}$ is given, we can check in polynomial time (with respect to the number of vertices in the graph) whether the function is PRDF of weight less than or equal to k. We need to check only the weight of the neighbours of each vertex and whether the sum of all vertices' weight is at most k. Thus, the problem is NP. We proceed by providing a polynomial-time reduction from the decision problem EXACT 3-COVER (X3C). (X3C). What we mean by a polynomial-time reduction is that if there is a polynomial algorithm to solve the PERFECT ROMAN DOMINATION problem, then there is a polynomial algorithm to solve the X3C problem. So, the PERFECT ROMAN DOMINATION problem is not more difficult than the X3C problem.

In the X3C problem, a set X with $|X| = 3q$ and a collection C of 3-element subsets of X are given. The question is, does C contain a subset C' such that every element $x \in X$ is in precisely one element of C'? If the answer is yes, we say (X, C) has an *exact cover*. The X3C problem is known to be NP-complete (Johnson and Garey, 1979).

Proposition 1. Let f be a PRDF on G containing $F_{x,l}$ as a subgraph, with $\{(x, w_1), (x, w_2)\}$ as a vertex cut. If $f(x, w_1) = 2$, then $w\left(f(F_{x,l})\right) \geq l + 2$.

Proof. Assume that $f(y, w_1) = 2$. Therefore, for all $i \in [l]$, the vertex (u_i, w_1) is adjacent to two vertices labelled 2. So, we must have $f(u_i, w_1) \geq 1$ for all $i \in [l]$. This implies that $w\left(f(F_{x,l})\right) \geq l + 4$. So, the statement holds. We may assume that $f(y, w_1) \neq 2$. If $f(v_i, w_1) = 0$ for some $i \in [l]$, then we must have $f(v_i, w_2) = 2$. So, for all $i \in [l]$, either $f(v_i, w_1) \geq 1$ or $f(v_i, w_2) \geq 1$. This implies that $w\left(f(F_{x,l})\right) \geq l + 2$. Thus, the statement holds. ■

Remark 1. *Due to the symmetry between the vertices* (x, w_1) *and* (x, w_2)*, the result of Proposition 1 holds if we write* '$f(x, w_2) = 2$' *instead of* '$f(x, w_1) = 2$'.

Proposition 2. *Let* f *be a PRDF on a graph* G *containing* $F_{x,l}$, $l \geq 3$ *as a subgraph, with* $\{(x, w_1), (x, w_2)\}$ *as a vertex cut. If* $f(x, w_1) = 1$, *then* $w\left(f(F_{x,l})\right) \geq 5$.

Proof. We prove by discussing all possibilities of $f(x, w_2)$. If $f(x, w_2) = 2$, the result follows by Proposition 1 and Remark 1. If $f(x, w_2) = 1$, then clearly $w\left(f(F_{x,l})\right) \geq 6$. If $f(x, w_2) = 0$, it is clear that $w\left(f(F_{x,l})\right) \geq 5$. ■

Proposition 3. *Let f be a PRDF on a graph G containing $F_{x,l}$, $l \geq 3$ as a subgraph, with $\{(x,w_1),(x,w_2)\}$ as a vertex cut.*

If $f(x,w_1)=0$ and $f(x,w_2)=1$, then $w\left(f\left(F_{x,l}\right)\right) \geq 5$.

If $f(x,w_1)=0$ and $f(x,w_2)=0$, then $w\left(f\left(F_{x,l}\right)\right) \geq 4$.

If $w\left(f\left(F_{x,l}\right)\right)=4$, then $f(y,w_1)=f(y,w_2)=2$.

The following proposition is not difficult to check.

Proposition 4. *Let G be a graph containing F_c as a subgraph, with $\{(c,w_1),(c,w_2)\}$ as a vertex cut. If f is a PRDF on G, then f has allocated labels of weight greater than or equal to 4 to F_c.*

Theorem 1. PERFECT ROMAN DOMINATION *is NP-complete for Cartesian product graphs.*

Proof. Let (X,C) be an instance of $X3C$ such that $X=\{x_1,x_2,\cdots,x_{3q}\}$ and $C=\{C_1,C_2,\cdots,C_t\}$. We describe a polynomial-time reduction from the X3C instance to a PERFECT ROMAN DOMINATION instance.

Let H be the graph with vertex set $V(H)=\{x_1,x_2,\cdots,x_{3q}\}\cup\{c_1,c_2,\cdots,c_t\}$ such that $x_ic_j\in E(H)$ if and only if $x_i\in C_j$. Let $k=12q+4t$. Let Q be the graph obtained from H by identifying x_i for $i\in[3q]$ with x in $H_{x,k}$ (informally, for each $i\in[3q]$, attach a copy of $H_{x,k}$ to x_i) and attaching to c_i for $i\in[t]$ two pendants c'_i,c''_i (i.e. c_i is identified with c in H_c). We denote the vertex y in the graph $H_{x,k}$ that corresponds to x_i by y_i. Let G be the Cartesian product of Q and K_2 (with $\{w_1,w_2\}$ as the vertex set of K_2). We prove (X,C) has an exact cover if and only if G has a PRDF f with $w(f)\leq k$.

Let C' be an exact cover of (X,C). Define a function $f:V(G)\to\{0,1,2\}$ as follows: set $f(y_i,w_1)=f(y_i,w_2)=2$ for all $i\in[3q]$; set $f(c_i,w_1)=f(c_i,w_2)=2$ if $C_i\in C'$; set $f(c'_i,w_1)=f(c''_i,w_2)=2$ if $C_i\in C\setminus C'$; and all the remaining vertices are labelled 0. As $|X|=3q$ and $|C|=t$, then $w(f)=4(3q)+4t=12q+4t=k$. Since C' is an exact cover, every x_i is in exactly one 3-element subset $C_j\in C'$, so (x_i,w_1) is adjacent to exactly one vertex, namely (c_j,w_1), labelled 2. Similarly, (x_i,w_2) is adjacent to exactly one vertex, namely (c_j,w_2), labelled 2. It is not hard to see that any other vertex labelled 0 is adjacent to exactly one vertex labelled 2. Thus, f is a PRDF.

Conversely, assume that there exists a PRDF f on G such that $w(f)\leq k$. Note that G contains $3q$ copies of $F_{x,k}$. Observe also that for any $i\in[3q]$, $E\left(F_{x_i,k}-\{(x_i,w_1),(x_i,w_2)\},G-F_{x_i,k}\right)=\phi$; informally, if $F_{x_i,k}$ is connected to $G-F_{x_i,k}$, it is connected only through the vertices (x_i,w_1) and (x_i,w_2). From Propositions 1, 2 and 3, f has allocated labels of weight greater than or equal to $12q$ to $\cup_{i\in[3q]}V\left(F_{x_i,k}\right)$. Note that G contains t copies of F_c. By Proposition 4, the function f has allocated labels of weight greater than or equal to $4t$ to $\cup_{i\in[t]}V\left(F_{c_i}\right)$. Therefore, f allocates labels of weight exactly $12q$ to $\cup_{i\in[3q]}V\left(F_{x_i,k}\right)$ and exactly $4t$ to $\cup_{i\in[t]}V\left(F_{c_i}\right)$. By Proposition 3, we must have $f(x_i,w_1)=f(x_i,w_2)=0$ and $f(y_i,w_1)=f(y_i,w_2)=2$ for all $i\in[3q]$. This also means that all neighbours of (x_i,w_1) in $F_{x_i,k}$ are labelled 0. Since f is a PRDF, (x_i,w_1) is adjacent to exactly one neighbour of the form (c_j,w_1) such that $f(c_j,w_1)=2$. Thus $C'=\{C_j\mid f(c_j,w_1)=2\}$ is an exact cover of (X,C). ■

3. The Complexity of Perfect Italian Domination of Cartesian Product Graphs

In this section, we prove that the perfect Italian domination problem of Cartesian product graphs is NP-complete.

Let the PERFECT ITALIAN DOMINATION be the decision problem where a graph G and an integer k are given and the goal is to decide whether G has a PIDF of weight at most k.

If a function $f:V(G)\to\{0,1,2\}$ is given, we can check in polynomial time whether the function is a PIDF with $w(f)\leq k$. Thus, the problem is in NP class. To proceed, a polynomial-time reduction from X3C will be given. We need some propositions before describing the reduction.

Proposition 5. *Let f be a PIDF on a graph G containing $F_{x,l}$ as subgraph, with $\{(x,w_1),(x,w_2)\}$ as a vertex cut. If $f(x,w_1)\neq 0$, then $w\left(f\left(F_{x,l}\right)\right)>l$.*

Proof. Assume that $f(x,w_1)=2$. If $f(u_i,w_1)>0$ for all $i\in[l]$, *then* $w\left(f\left(F_{x,l}\right)\right)\geq l+2$, and we are done. So, assume $f(u_i,w_1)=0$ for some $i\in[l]$. Then, $f(y,w_1)=0$. Let $Q:=\{i\mid f(v_i,w_1)=0\}$. Then, $f(v_i,w_2)=2$ for all $i\in Q$. Thus, for every $i\in[l]$, either $f(v_i,w_1)\geq 1$ or $f(v_i,w_2)\geq 1$. *Then,* $w\left(f\left(F_{x,l}\right)\right)\geq l+2$, and we are done.

Assume $f(x,w_1)=1$. If $f(y,w_1)=2$, then $f(u_i,w_1)>0$ for all $i\in[l]$; so, $w\left(f\left(F_{x,l}\right)\right)\geq l+3$, and we are done. If $f(y,w_1)=1$, then for every $i\in[l]$, either $f(v_i,w_1)\geq 1$ or $f(v_i,w_2)\geq 1$. So, $w\left(f\left(F_{x,l}\right)\right)\geq l+2$, and we are done. If $f(y,w_1)=0$, then for every $i\in[l]$, either $f(u_i,w_1)>0$ or $f(u_i,w_2)>0$. So, $w\left(f\left(F_{x,l}\right)\right)\geq l+1$, and we are done. ■

Remark 2. *Due to the symmetry between (x,w_1) and (x,w_2), the result of Proposition 5 holds if we write '$f(x,w_2)\neq 0$' instead of '$f(x,w_1)\neq 0$'.*

Let $u\in G$ and f be a PIDF on G. We say that u is *satisfied* if either $f(u)\neq 0$ or $\sum_{v\in N(u)}f(v)=2$. Let $u\in H\subseteq G$ with $f(u)=0$. We say that u is *in-satisfied* with respect to H if u is satisfied and $\sum_{v\in N(u)\cap H}f(v)=2$; we say that u is *out-satisfied* with respect to H if u is satisfied and $\sum_{v\in N(u)\setminus H}f(v)=2$.

Proposition 6. Let G be a graph *containing $F_{x,l}$, $l\geq 3$ as a subgraph, with $\{(x,w_1),(x,w_2)\}$ as a vertex cut. Let f be a PIDF on G. If $f(x,w_1)=0$ and $f(x,w_2)=0$, f has allocated labels of weight at least 4 to $F_{x,l}$, with equality if and only if $f(y,w_1)=f(y,w_2)=2$.*

Proposition 7. *Let G be a graph containing Q_c as a subgraph, with $\{(c,w_1),(c,w_2)\}$ as a vertex cut. Let f be a PIDF on G. Then, $w\left(f(Q_c)\right)\geq 4$. In addition, if $w\left(f(Q_c)\right)=4$, then either $f(c,w_1)=f(c,w_2)=0$ or $f(c,w_1)=f(c,w_2)=2$.*

Proof. If each vertex in the set $\{(c',w_1),(c'',w_1),(c',w_2),(c'',w_2)\}$ is labelled 1 or 2, *then* $w\left(f(Q_c)\right)\geq 4$, *and* we are done. So, assume without losing generality that $f(c',w_1)=0$. Since $N\left((c',w_1)\right)=\{(c,w_1),(c'',w_1),(c',w_2)\}$, the weight assigned to those vertices combined is 2. Note that no vertex in $N\left((c',w_1)\right)$ is adjacent to a vertex in $\{(d',w_2),(d'',w_2)\}$. If each vertex in $\{(d',w_2),(d'',w_2)\}$ is labelled 1 or 2, we are done. Without losing generality, suppose $f(d',w_2)=0$. Since $N\left((d',w_2)\right)=\{(c,w_2),(d'',w_2),(d',w_1)\}$, the weight assigned to those vertices combined is 2. Thus, the first claim is true. The second claim is not difficult to check. ■

Theorem 2. *PERFECT ITALIAN DOMINATION is NP-complete for Cartesian product graphs.*

Proof. Let (X,C) be an instance of $X3C$ such that $X=\{x_1,x_2,\cdots,x_{3q}\}$ and $C=\{C_1,C_2,\cdots,C_t\}$ is a collection of 3-element subsets of X. We describe a polynomial-time reduction to *PERFECT ITALIAN DOMINATION*.

Let H be the graph with vertex set $V(H)=\{x_1,x_2,\cdots,x_{3q}\}\cup\{c_1,c_2,\cdots,c_t\}$, where $x_ic_j\in E(H)$ if and only if $x_i\in C_j$. Let $k=12q+4t$. Let Q be the graph acquired from H by identifying x_i for $i\in[3q]$ with x in $H_{x,k}$ (informally, for each $i\in[3q]$, attach a copy of $H_{x,k}$ to x_i) and identifying c_i with c in O_c (informally, for each $i\in[t]$, attach a copy of O_c to c_i). Let $G:=Q\boxtimes K_2$, that is, G is the Cartesian product of Q and K_2. We prove that (X,C) has an exact

cover if and only if G admits a PIDF f such that $w(f) \leq k$.

Assume that (X, C) has an exact cover C'. Define a function $f: V(G) \to \{0,1,2\}$ as follows: set $f(y_i, w_1) = f(y_i, w_2) = 2$ for all $i \in [k]$. If $C_i \in C'$, set $f(c_i, w_1) = f(c_i, w_2) = 2$. If $C_i \in C \setminus C'$, set $f(c'_i, w_1) = f(d'_i, w_1) = f(c''_i, w_2) = f(d''_i, w_2) = 1$. Label the remaining vertices with 0. See Figure 2. Since C' is an exact cover, every $x_i \in X$ is in exactly one element of C'. So, (x_i, w_1) and (x_i, w_2) are satisfied, and it is simple to check that the rest of vertices of G are satisfied. Thus, f is a PIDF with $w(f) = 4(3q) + 4t = k$.

Conversely, assume that there exists a PIDF f on G such that $w(f) \leq k$. By Proposition 5 and Remark 2, $f(x_i, w_1) = f(x_i, w_2) = 0$ for every $i \in [3q]$; otherwise, we would have $w(f) > k$. By Proposition 6, $w\left(f\left(F_{x,k}\right)\right) \geq 4$. Observe that G contains $3q$ copies of $F_{x,k}$. By Proposition 7, $w\left(f(\mathrm{Q_c})\right) \geq 4$. Note that G contains t copies of Q_c. Since $w(f) \leq k$, we must have $w\left(f\left(F_{x,k}\right)\right) = 4$ for all the $3q$ copies of $F_{x,k}$, and $w\left(f(\mathrm{Q_c})\right) = 4$ for all the t copies of $\mathrm{Q_c}$. By Proposition 7, for every $i \in [t]$, either $f(c_i, w_1) = f(c_i, w_2) = 0$ or $f(c_i, w_1) = f(c_i, w_2) = 2$. Construct the subset $C' \subseteq C$ as follows: let $C_i \in C'$ if and only if $f(c_i, w_1) = 2$. By Proposition 6, for every $i \in [3q]$, (x_i, w_1) is out-satisfied with respect to $F_{x_i,k}$. So, for every $i \in [3q]$, (x_i, w_1) is adjacent to exactly one (c_j, w_1) with $f(c_j, w_1) = 2$. Thus, every $x_i \in X$ is in exactly one element in C'. Thus, C' is an exact cover. ■

Figure 2. The restriction of f on Q_{c_i}.

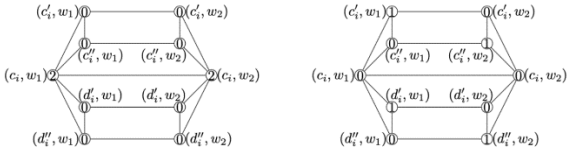

4. Bounds on $\gamma_I^p(G)$ of the Cartesian Product of Graphs

In this section, we show that if $G \in \{P_r \boxtimes P_s, C_r \boxtimes C_s\}$, where $r, s \geq 6$, $\gamma_I^p(G) \leq \frac{1}{2}|G| + \frac{1}{2}\min\{r, s\}$, and if $G = P_r \boxtimes C_s$, where $r \geq 6$, $\gamma_I^p(G) \leq \frac{1}{2}|G| + \frac{1}{2}r$. We also give an upper bound for $\gamma_I^p(G)$, where G is the Cartesian product of graphs. Then, we end this section with an open problem.

The graph $P_r \boxtimes P_s$ is a grid graph, $P_r \boxtimes C_s$ is a cylinder grid graph, and $C_r \boxtimes C_s$ is a torus grid graph with r rows and s columns. We denote the vertex in row i and column j by $a_{i,j}$; see Figure 3.

Figure 3. Cartesian products of paths and cycles.

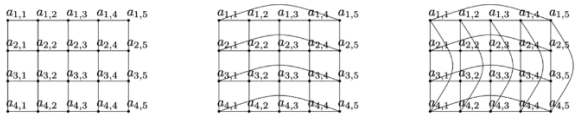

Let $G \in \{P_r \boxtimes P_s, P_r \boxtimes C_s, C_r \boxtimes C_s\}$. Let $f: V(G) \to \{0,1,2\}$ be a function defined by

$$f(a_{i,j}) = \begin{cases} 1, & \text{if } j \text{ even}, \\ 1, & \text{if } j \in \{1, s\} \text{ and } i \equiv 1 \bmod 3, \\ 0, & \text{otherwise.} \end{cases}$$

To begin, assume that $G = P_r \boxtimes P_s$. We could presume that $r \leq s$.

Lemma 1. *If* $r \equiv 0 \bmod 3$, $\gamma_I^p(G) \leq \frac{1}{2}|G| + \frac{1}{2}r$.

Proof. Define a function $f': V(G) \to \{0,1,2\}$ by

$$f'(a_{i,j}) = \begin{cases} 1, & \text{if } j \in \{1, s\} \text{ and } i = r - 1, \\ f(a_{i,j}), & \text{otherwise.} \end{cases}$$

See Figure 4; we use red to highlight the vertices $a_{i,j}$ for which $f'(a_{i,j}) \neq f(a_{i,j})$.

Clearly, f' is a PIDF on G. If s is odd,

$$\begin{aligned} w(f') &= \frac{r(s-3)}{2} + r + \frac{2r}{3} + 2 \\ &= \frac{rs}{2} + \frac{r}{6} + 2 \\ &\underset{(1)}{\leq} \frac{|G|}{2} + \frac{r}{2}. \end{aligned}$$

Inequality (1) holds as $r \geq 6$. If s is even,

$$\begin{aligned} w(f') &= \frac{r(s-2)}{2} + r + \frac{r}{3} + 1 \\ &= \frac{rs}{2} + \frac{r}{3} + 1 \\ &\underset{(2)}{\leq} \frac{|G|}{2} + \frac{r}{2}. \end{aligned}$$

Inequality (2) holds as $r \geq 6$. Thus, the statement holds. ■

Figure 4. The function f' when $r \equiv 0 \bmod 3$.

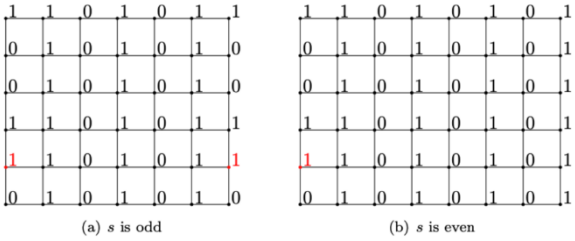

Lemma 2. *If* $r \equiv 1 \bmod 3$, $\gamma_I^p(G) \leq \frac{1}{2}|G| + \frac{1}{2}r$.

Proof. It is not difficult to see that f is a PIDF on G.

If s is odd,

$$\begin{aligned} w(f) &= \frac{r}{2}(s-3) + r + \frac{2(r-1)}{3} + 2 \\ &= \frac{rs}{2} + \frac{r}{6} + \frac{4}{3} \\ &< \frac{rs}{2} + \frac{r}{2} \\ &= \frac{|G|}{2} + \frac{r}{2}. \end{aligned}$$

If s is even,

$$\begin{aligned} w(f) &= \frac{r(s-2)}{2} + r + \frac{r-1}{3} + 1 \\ &= \frac{rs}{2} + \frac{r}{3} + \frac{2}{3} \\ &< \frac{rs}{2} + \frac{r}{2}. \end{aligned}$$

Thus, the statement holds. ■

Remark 3. *Observe that if* $G \in \{P_r \boxtimes C_s, C_r \boxtimes C_s\}$, $r \equiv 1 \bmod 3$ *and* s *is odd, then* f *is a PIDF on* G. *From the above proof,* $\gamma_I^p(G) < \frac{|G|}{2} + \frac{r}{2}$.

Lemma 3. *If* $r \equiv 2 \bmod 3$, $\gamma_I^p(G) \leq \frac{1}{2}|G| + \frac{1}{2}r$.

Proof. Checking that f is a PIDF on G is simple, see Figure 5.

If s is odd,

$$\begin{aligned} w(f) &= \frac{r(s-3)}{2} + r + \frac{2(r-2)}{3} + 2 \\ &= \frac{rs}{2} + \frac{r}{6} + \frac{2}{3} \\ &< \frac{rs}{2} + \frac{r}{2}. \end{aligned}$$

If s is even,

$$\begin{aligned} w(f) &= \frac{r(s-2)}{2} + r + \frac{r-2}{3} + 1 \\ &= \frac{rs}{2} + \frac{r}{3} + \frac{1}{3} \\ &< \frac{rs}{2} + \frac{r}{2}. \end{aligned}$$

So, the statements hold. ■

Figure 5. The function f when $r \equiv 2 \ mod \ 3$.

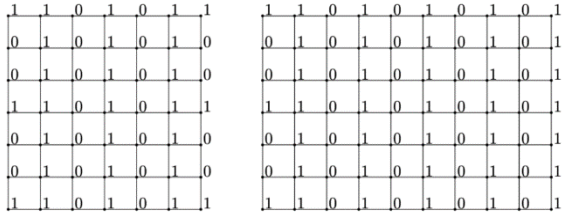

(a) s is odd (b) s is even

Remark 4. If $G = P_r \boxtimes C_s$, $r \equiv 2 \mod 3$ and s is odd, then f is a PIDF on G. So, $\gamma_I^p(G) < \frac{|G|}{2} + \frac{r}{2}$.

Theorem 3. If $G = P_r \boxtimes P_s$, where $r, s \geq 6$, $\gamma_I^p(G) \leq \frac{1}{2}|G| + \frac{1}{2}\min\{r, s\}$.

Proof. Follows by Lemmas 1, 2 and 3. ■

Now, assume $G \in \{P_r \boxtimes C_s, C_r \boxtimes C_s\}$.

Lemma 4. If s is even, $\gamma_I^p(G) \leq \frac{1}{2}|G|$.

Proof. Let $g: V(G) \to \{0,1,2\}$ be a function defined by

$$g\left(a_{i,j}\right) = \begin{cases} 1, & \text{if } j \text{ is even,} \\ 0, & \text{if } j \text{ is odd.} \end{cases}$$

The function g is a PIDF on G with weight equal to $\frac{1}{2}|G|$. ■

Lemma 5. If s is odd and $r \equiv 0 \mod 3$, $\gamma_I^p(G) \leq \frac{1}{2}|G| + \frac{1}{2}r$.

Proof. If $G = P_r \boxtimes C_s$, we slightly modify the function f by labelling $a_{i,j}$ with 1 if $j \in \{1, s\}$ and $i = r - 1$, keeping the rest of the labels without any change. This is the labelling used in Lemma 1 (the function f'), and we showed that the sum of all labellings is at most $\frac{1}{2}|G| + \frac{1}{2}r$.

If $G = C_r \boxtimes C_s$, then f is PIDF on G, and $w(f) < w(f')$. So, the statement holds. ■

Lemma 6. If s is odd and $r \equiv 2 \mod 3$, $\gamma_I^p(G) \leq \frac{1}{2}|G| + \frac{1}{2}r$.

Proof. For $G = P_r \boxtimes C_s$, see Remark 4. For $G = C_r \boxtimes C_s$, define a function $f': V(G) \to \{0,1,2\}$ by

$$f'\left(a_{i,j}\right) = \begin{cases} 1, & \text{if } j \in \{1, s\} \text{ and } i = r, \\ f\left(a_{i,j}\right), & \text{otherwise.} \end{cases}$$

Checking that f' is a PIDF is simple, in addition,

$$\begin{aligned} w(f') &= \frac{r(s-3)}{2} + r + \frac{2(r-2)}{3} + 4 \\ &= \frac{rs}{2} + \frac{r}{6} + \frac{8}{3} \\ &\leq \frac{rs}{2} + \frac{r}{2}. \end{aligned}$$

The last inequality follows from the fact that $r \equiv 2 \mod 3$ and $r \geq 6$. ■

Theorem 4. Let $r, s \geq 6$. If $G = P_r \boxtimes C_s$, $\gamma_I^p(G) \leq \frac{1}{2}|G| + \frac{1}{2}r$. If $G = C_r \boxtimes C_s$, $\gamma_I^p(G) \leq \frac{1}{2}|G| + \frac{1}{2}\min\{r, s\}$.

Proof. Follows by Lemmas 4–6, Remarks 3 and 4, and the symmetry between s and r when $G = C_r \boxtimes C_s$. ■

Looking at Theorems 3 and 4 and knowing that $\gamma_I^p(H) \leq \frac{1}{2}|H| + 1$ if H is a path or a cycle, it is natural to ask whether we can always drive an upper bound for $\gamma_I^p(G_1 \boxtimes G_2)$ in terms of $\gamma_I^p(G_1)$ or $\gamma_I^p(G_2)$. The following theorem answers this question.

Theorem 5. Let G_1 and G_2 be graphs and $G = G_1 \boxtimes G_2$. Assume $\gamma_I^p(G_1) = m_1$ and $\gamma_I^p(G_2) = m_2$. Then, $\gamma_I^p(G) \leq \min\{m_1|G_2|, m_2|G_1|\}$.

Proof. We can assume that $\min\{m_1|G_2|, m_2|G_1|\} = m_1|G_2|$. Let g be a PIDF witnessing that $\gamma_I^p(G_1) = m_1$. Define a function h on G as follows: for every $(v, u) \in G_1 \boxtimes G_2$, set $h(v, u) = g(v)$. Let (v, u) be any vertex in G. If $h(v, u) \neq 0$, it is done. So, assume $h(v, u) = 0$. Let $A := \{(v, u') \mid uu' \in E(G_2)\}$ and $B := \{(v', u) \mid vv' \in E(G_1)\}$; then, $N(v, u) = A \cup B$. Every vertex in A is labelled 0 as $h(v, u') = g(v) = h(v, u) = 0$. Since g is a PIDF on G_1, $\sum_{(v',u)\in B} h(v', u) = \sum_{v' \in N_{G_1}(v)} g(v') = 2$. Thus, h is PIDF on G and $w(h) \leq m_1|G_2|$. ■

Haynes and Henning (2019) showed that if T is a tree with $|T| \geq 3$, then $\gamma_I^p(T) \leq \frac{4}{5}|T|$. The following is a direct result of the previous theorem.

Corollary 1. If T_1 and T_2 are trees with $|T_1|, |T_2| \geq 3$, then $\gamma_I^p(T_1 \boxtimes T_2) \leq \frac{4}{5}|T_1 \boxtimes T_2|$.

Haynes and Henning (2019) proved that their result is tight. They showed that if n is a multiple of 5, there exists a tree T with $|T| = n$ such that $\gamma_I^p(T) = \frac{4}{5}n$. For example, let T' be the graph obtained from the star graph S_4 by adding an extra vertex adjacent to one of the leaves; then, $|T'| = 5$ and $\gamma_I^p(T') = \frac{4}{5}|T'|$. However, $\gamma_I^p(T' \boxtimes T') \leq 17$. We end this paper with the following open question.

Question. Is the bound in Corollary 1 tight?

5. Conclusions

In this paper, we proved that the perfect Roman domination and perfect Italian domination problems of the Cartesian product graphs are NP-complete. We also provided an upper bound for the perfect Italian domination number for the Cartesian product of a path and a path, a path and a cycle, a cycle and a cycle, and a tree and a tree. For future work, we suggest studying the complexity of the perfect Roman domination and perfect Italian domination of the Cartesian product of specific types of graphs. We also suggest finding the tight upper bound of the perfect Italian domination number of the Cartesian product of paths and cycles and investigating the perfect Roman and perfect Italian domination numbers of the Cartesian product of other types of graphs.

Biography

Ahlam Almulhim

Department of Mathematics and Statistics, College of Science, King Faisal University, Al-Ahsa, Saudi Arabia, 00966506923348, ahmulhem@kfu.edu.sa

Ahlam Almulhim is an assistant professor in the Department of Mathematics and Statistics at King Faisal University, Saudi Arabia. She earned her PhD in Mathematics from Arizona State University in 2020. Doctor Almulhim has chaired and participated in several academic committees at the department, college and university levels. She currently leads the Development and Quality Assurance Office at the College of Science. Her research focuses on graph theory, including domination theory, its applications and the complexity of

related problems.

ORCID: 0000-0001-9131-044X

Acknowledgement

We thank the reviewers and editors for their comments, which significantly enhanced the manuscript.

References

Almulhim, A., Akwu, A.D. and AlSubaiei, B. (2022). The perfect Roman domination number of the Cartesian product of some graphs. *Journal of Mathematics,* **2022**(1), 1957027. DOI:10.1155/2022/1957027

Almulhim, A., AlSubaiei, B. and Monda, S.R. (2024). Survey on Roman $\{2\}$-domination. *Mathematics*, **12**(17), 2771. DOI:10.3390/math12172771

Banerjee, S., Henning, M.A. and Pradhan, D. (2021). Perfect Italian domination in cographs. *Applied Mathematics and Computation*, **391**(n/a), 125703. DOI:10.1016/j.amc.2020.125703

Cabrera Martínez, A., García-Gómez, C. and Rodríguez-Velázquez, J.A. (2022). Perfect domination, Roman domination and perfect Roman Domination in lexicographic product graphs. *Fundamenta Informaticae*, **185**(3), 201–20. DOI:10.3233/FI-222108

Chellali, M., Haynes, T.W., Hedetniemi, S.T. and McRae, A.A. (2016). Roman 2-domination. *Discrete Applied Mathematics,* **204**(n/a), 22–8. DOI:10.1016/j.dam.2015.11.013

Cockayne, E.J., Dreyer Jr, P.A., Hedetniemi, S.M. and Hedetniemi, S.T. (2004). Roman domination in graphs. *Discrete Mathematics*, **278**(1-3), 11–22. DOI:10.1016/j.disc.2003.06.004

Darkooti, M., Alhevaz, A., Rahimi, S. and Rahbani, H. (2019). On perfect Roman domination number in trees: Complexity and bounds. *Journal of Combinatorial Optimization*, **38**(n/a), 712–20. DOI:10.1007/s10878-019-00408-y

Johnson, D. S. and Garey, M. R. (1979). *Computers and Intractability: A Guide to the Theory of NP-Completeness*. USA, New York City: W. H. Freeman.

Haynes, T.W. and Henning, M.A. (2019). Perfect Italian domination in trees. *Discrete Applied Mathematics,* **260**(n/a), 164–77. DOI:10.1016/j.dam.2019.01.038

Henning, M.A. and Klostermeyer, W.F. (2018). Perfect Roman domination in regular graphs. *Applicable Analysis and Discrete Mathematics,* **12**(1), 143–52. DOI:10.2298/AADM1801143H

Henning, M.A., Klostermeyer, W.F. and MacGillivray, G. (2018). Perfect Roman domination in trees. *Discrete Applied Mathematics,* **236**(n/a), 235–45. DOI:10.1016/j.dam.2017.10.027

Lauri, J. and Mitillos, C. (2020). Perfect Italian domination on planar and regular graphs. *Discrete Applied Mathematics,* **285**(n/a), 676–87. DOI:10.1016/j.dam.2020.05.024

Luiz, A.G. (2024). Roman domination and independent Roman domination on graphs with maximum degree three. *Discrete Applied Mathematics,* **348**(n/a), 260–78. DOI:10.1016/j.dam.2024.02.006

Nazari-Moghaddam, S. and Chellali, M. (2022). A new upper bound for the perfect Italian domination number of a tree. *Discussiones Mathematicae Graph Theory*, **42**(n/a), 1005–22. DOI:10.7151/dmgt.2324

Pradhan, D., Banerjee, S. and Liu, J. B. (2022). Perfect Italian domination in graphs: Complexity and algorithms. *Discrete Applied Mathematics*, **319**(n/a), 271–95. DOI:10.1016/j.dam.2021.08.020

ReVelle, C. S. (1997). Can you protect the Roman Empire. *Johns Hopkins Magazine*, **49**(2), 40.

Revelle, C. and Rosing, K.E. (2000). Defendens Imperium Romanum: A classical problem in military strategy. *American Mathematical Monthly,* **107**(7), 585–94. DOI:10.2307/2589113

Stewart, I. (1999). Defend the Roman Empire! *Scientific American,* **281**(6), 136–8. DOI:10.1038/scientificamerican1299-136

إرشادات التسليم (المجلة العلمية لجامعة الملك فيصل)

Submission Guidelines (The Scientific Journal of King Faisal University)

1. General Information

- The Journal publishes in English and Arabic.
- There are no submission or publication fees.
- It takes up to 100 days from submission to publication.
- Manuscripts must be submitted to the appropriate managing editor:
  - The Managing Editor of Basic and Applied Sciences: secretary-b@kfu.edu.sa. The associate editor will check if the author has followed the Submission Instructions. If not, the manuscript will be sent back to the author. If the instructions are followed, the associate editor will create an account and send the author the username and password to log in using our online submission system (ScholarOne): https://mc04.manuscriptcentral.com/sjkfub.
  - The Managing Editor of Humanities and Management Sciences (educational manuscripts only): sjkfu-assed@kfu.edu.sa. The associate editor will check if the author has followed the Submission Instructions. If not, the manuscript will be returned to the author. If followed, the associate editor will create an account and send the author the username and password to log in using our online submission system (ScholarOne): https://mc04.manuscriptcentral.com/sjkfuh.
  - The Managing Editor of Humanities and Management Sciences (non-educational manuscripts): sjkfu-hm@kfu.edu.sa. The associate editor will check if the author has followed the Submission Instructions. If not, the manuscript will be returned to the author. If followed, the associate editor will create an account and send the author the username and password to log in using our online submission system (ScholarOne): https://mc04.manuscriptcentral.com/sjkfuh.

2. Pre-Submission Guidelines

- **Content**: Authors must ensure a clearly articulated academic contribution to the field, clarity of abstracts, quality of and conformity to the stated aims and scope of the Journal and readability of their manuscripts.
- **Manuscript Word Limit**: Manuscripts must not exceed 8,000 words, considering all inclusions (e.g. references, tables, figures).
- **Abstract Word Limit**: Abstracts must not exceed 200 words.
- **Title Word Limit**: Manuscript titles must not exceed 15 words.
- **Keyword Limit**: Keywords must not exceed six words and must not be used in the manuscript title.
- **Number of Tables and Figures**: Tables, figures, abbreviations and footnotes must be kept to a minimum. Tables and figures must not exceed six, each.
- **Reference Limit**: There must be no more than 40 references unless the manuscript is a review article or equivalent.
- **Quotations**: A quotation must not exceed 50 words. Longer quotations required due to the nature of the academic field must be justified in the cover letter.
- **Appendixes**: Appendixes are not allowed. If readers would like to access appendixes, they can reach out to corresponding authors.
- **Linguistic Quality**: Manuscripts must be written at an acceptable language level.
- **Plagiarism**: The Journal maintains a strict plagiarism policy.
- **Reviewers**: Authors must suggest five reviewers, who are specialised in the field of the manuscript, are not affiliated with authors' institutions, are at least associate professors and have not worked on joint projects with authors. Reviewers' names, phone numbers, email addresses, academic field, academic rank and institutions must be provided.
- **Documents Required**: Title page (with author details) and main document (without author details):
  - **Title Page**: It must consist of the following: the manuscript title, author details, minor and major field of the topic, 80-word bio and acknowledgements (optional). Below are explanations of how the author details and bio are written.
  - **Main Manuscript**: It must be submitted in MSWord format. It must consist of the following: manuscript title, abstract, keywords, main body and references.
- **Author Details**: Author details must be included in the following order: full name, department, college, university, city and country (or the equivalent). In the absence of an employer, one may write 'Independent Researcher'. Ranks (e.g. Dr and Prof.) must not be included. A star '*' should be placed next to the corresponding author's name. Below is an example:

  Abdulrahman Essa Al Lily*
  Department of Curriculum and Teaching Methods, College of Education, King Faisal University, Al Ahsa, Saudi Arabia
- **Bio**: The bio must be in the following format: the author's name, under which is written the author's department, college, university, city, country (or equivalent), the author's contact number and email address, under which is written an 80-word description of the author. Author's names and affiliations are not part of the 80-word count. If the author has an ORCID number or personal website, this can be included at the end of the description. Below is an example:

  Abdulrahman Essa Al Lily
  Department of Curriculum and Teaching Methods, College of Education, King Faisal University, Al Ahsa, Saudi Arabia, 00966000000000, scijkfu@kfu.edu.sa
  Prof. Al Lily is an Oxford graduate, Saudi professor, a former national-centre director, editor-in-chief (Scopes) and bestselling author (Amazon). He has coined 4 theories (e.g. 'Multiple Stupidities', "Retroactivism' and 'On-the-Go Sourcing') and 3 notions ('Crowd-Authoring', 'Crowd-Reflecting' and 'Door-Knocking'). His work is translated into 7 languages (including Spanish, Filipino, Indonesian, Chinese and Italian). His interviews is in 5 languages (including, French, Spanish and German). He has published 24 ISI/Scopus-indexed articles with the globally largest publishers (Elsevier, Springer, Taylor & Francis, Wiley, SAGE, Cogent, Palgrave, Nature Research & Oxford). His work is cited by 35 countries (Including Hungary, Serbia, Russia, Peru, Korea, Colombia, Switzerland, Netherlands, Sweden, Finland and Latvia) in 6 languages (including Turkish and Lithuanian). He has worked as a consultant for such institutions as Wikipedia and the University of Hanover. He worked during the summer in New Zealand and Italy. He has participated in conferences in Singapore, Greece, Spain, US, Japan & Bulgaria.
  ORCID: 0000-0002-5116-422X.
  Website: https://abdulallily.wordpress.com/

3. Post-Reviewing Guidelines

- **Page Settings**: Page size is A4. Margins are 2.5 cm, each side. Any standard font is acceptable.
- **Headings**: There must be no more than three levels of headings. The first level of headings must be numbered: 1., 2., 3., etc. The second level of headings must be numbered: 1.1., 1.2., 1.3., etc. The third level of headings must be numbered: 1.1.1., 1.1.2., 1.1.3, etc. The headings for abstracts, bios and references must not be numbered.
- **Tables and Figures**: Captions must be above tables and figures. In the body, 'see above' or 'see below' must not be used. Instead, use 'see Table 1' or 'see Figure 1'.
- **Measuring Units**: In the case of using local measuring units in the manuscript, the equivalent of international units must be included. Scientific rather than provincial terms must be used. Currencies must be in U.S. dollars.
- **Footnotes**: Footnotes must be kept to a minimum. They must be referred to in the text in uppercase numbers. Footnotes must appear at the bottom of the page on which they are introduced.
- **References**: Authors must follow the APA style of referencing. References must be arranged alphabetically. The reference list must not be numbered. Non-English references must be "romanised" into English.
- **Digital Object Identifier (DOI)**: If a reference has a DOI, it must be included.

Proofreading Certificates: Once accepted, manuscripts must be sent by authors to an accredited proofreading company. A proofreading certificate must be submitted to the Journal. A suggested company is: proofreadmyessay.co.uk

1. معلومات عامة

- **أخلاقيات البحث**: لا تقبل المجلة استلام أي ورقة أو تحكيم يتضمن أي نوع من أنواع التحامل أو العدوانية أو التطرف أو التشدق الأيديولوجي (سواء كان ذلك موجها لشخص، أو مدرسة فكرية، أو طائفة، أو جنس، أو أيديولوجية بعينها). كما لا تقبل استلام الأبحاث أو تقييمات المحكمين التي تحمل أفكاراً تناهض الأمن الفكري والمجتمعي، أو تُعزز الإرهاب والأفكار المتطرفة، أو تحضّ عليها تصريحاً أو تلميحاً.
- **أوقات العمل**: تقوم المجلة بمهمة استلام الأوراق العلمية على مدار العام، وفي حالة وجود توقف سيتم وضع رد تلقائي على البريد الإلكتروني.
- **رسوم النشر**: المجلة لا تتقاضى أي أجر أو رسوم مالية مقابل عملية النشر العلمي وإجراءاته (النشر مجانًا لجميع الباحثين).
- **لغة النشر**: تقبل المجلة أبحاثاً مكتوبة باللغة العربية أو اللغة الإنجليزية.
- **مدة النشر**: بعد انضمام المجلة إلى المعرف الرقمي العالمي الموحد (DOI) أصبح بإمكان أي بحث جديد مرسل للمجلة أن ينشر على الموقع الإلكتروني للمجلة برقم المعرف الرقمي (DOI) في غضون فترة لا تزيد عن 100 يوم عمل منذ تسليمه للمجلة وأعطائه رقم قيد.
- **آلية تسليم الورقة**: يجب تسليم الورقة للمحرر المناسب، وفقاً للآتي:
  - تسلم أوراق العلوم الأساسية والتطبيقية إلى سعادة محرر فرع العلوم الأساسية والتطبيقية: secretary-b@kfu.edu.sa. سيقوم المحرر بتدقيق الورقة للتأكد من اتباعها لـ "تعليمات النشر". في حال عدم اتباع التعليمات، فستعاد الورقة للمؤلف. في حال اتباع التعليمات، فسيقوم المحرر بإنشاء حساب للمؤلف وتزويده باسم المستخدم وكلمة السر لتسليم ورقته من خلال نظام التسليم الإلكتروني (ScholarOne): https://mc04.manuscriptcentral.com/sjkfub.
  - تسلم أوراق العلوم الإنسانية والإدارية (الأبحاث التربوية فقط) إلى سعادة محرر فرع العلوم الإنسانية والإدارية للقضايا التربوية: sjkfu-assed@kfu.edu.sa. سيقوم المحرر بتدقيق الورقة للتأكد من اتباعها لـ "تعليمات النشر". في حال عدم اتباع التعليمات، فستعاد الورقة للمؤلف. في حال اتباع التعليمات، فسيقوم المحرر بإنشاء حساب للمؤلف وتزويده باسم المستخدم وكلمة السر لتسليم ورقته من خلال نظام التسليم الإلكتروني (ScholarOne): https://mc04.manuscriptcentral.com/sjkfuh.
  - تسلم أوراق العلوم الإنسانية والإدارية (الأبحاث غير التربوية) إلى سعادة محرر فرع العلوم الإنسانية والإدارية للقضايا غير التربوية: sjkfu-hm@kfu.edu.sa. سيقوم المحرر بتدقيق الورقة للتأكد من اتباعها لـ "تعليمات النشر". في حال عدم اتباع التعليمات، فستعاد الورقة للمؤلف. في حال اتباع التعليمات، فسيقوم المحرر بإنشاء حساب للمؤلف وتزويده باسم المستخدم وكلمة السر لتسليم ورقته من خلال نظام التسليم الإلكتروني (ScholarOne): https://mc04.manuscriptcentral.com/sjkfuh.
- **الرسائل العلمية**: تقبل المجلة الأوراق المستلة من الرسائل العلمية، على أن يتم النص على ذلك.
- **الحقوق الفكرية**: جميع حقوق الطبع والنشر محفوظة للمجلة، ولا يسمح بإعادة طبع أو نشر أي جزء من المجلة أو نسخه بأي شكل وبأي وسيلة كانت إلكترونية أو آلية بما في ذلك التصوير والتسجيل والإدخال في أي نظام حفظ معلومات أو استعادتها دون الحصول على موافقة كتابية من رئيس هيئة التحرير.
- **آراء المؤلفين**: الآراء المضمنة في الأوراق المنشورة تعبر عن وجهات نظر كتابها ولا تعبر بالضرورة عن وجهة نظر المجلة.
- **فلسفة الأوراق العلمية**: لا تستقبل المجلة الأوراق العلمية التي لا تراعي المحاور الآتية ولا تحقق مدى عاليا في كل محور:
  - مدى احتمالية اقتباس الورقة من قبل بحوث أخرى في كلاريفيت وسكوبس خلال عامين قادمين؛ حيث إن هذا يعد أحد المتطلبات المهمة لتصنيف المجلة في قاعدة بيانات سكوبس.
  - مدى فائدة الورقة للقارئ الدولي ومدى اتساع جمهور الورقة خارج نطاق المكان والزمان واللغة. يُعرف القارئ الدولي هنا بأنه "شخصية اعتبارية محايدة (سواء شخص، مجموعة، جهة، مؤسسة أو مُنظمة) لا تشترك مع المؤلف في الحدود الزمانية والمكانية واللغوية التي كُتبت بها الورقة".
- **ضرورة اتباع الإرشادات**: وفقاً لسياسة المجلة، فإنه يتوجب على أصحاب السعادة الباحثين ضبط ورقتهم وفقاً لملف "إرشادات التسليم"، واتباعها حرفياً وبدقة متناهية وعالية جداً، حيث إن عدم الالتزام بها بأي وجه من الأوجه سيمثل عائقاً لنشر الورقة. نؤكد الضرورة القصوى للاتباع الحرفي والدقيق لهذه الإرشادات. إن المجلة تسعى جاهدة أن تكون مصنفة في عدد من قواعد البيانات المتميزة عالمياً مما يتطلب دقة عالية في ضبط الورقة، وعليه وجب توخي الحذر التام في كيفية ضبط الورقة وفقاً للمطلوب، حيث إن آلية صياغة المراجع، على سبيل المثال، هي العنصر الأهم لقواعد البيانات العالمية. في حالة قيام المؤلف بإرسال الورقة إلى المجلة، وتبين لهيئة التحرير وجود بعض الإرشادات لم يتم اتباعها، فإنه سيتم إرجاع الورقة للمؤلف، وسيتم إخباره بعدم اتباعه للإرشادات، بدون تحديد أي من الإرشادات لم يتم اتباعها، وذلك لأن الوقت للأسف لا يتسع للمجلة لأن تزود كل مؤلف بتغذية فردية عن أي من الإرشادات لم يتم مراعاتها، كما أنه بناء على سياسة المجلة فإن السادة الباحثين هم المعنيون بالدرجة الأولى من التأكد من اتباع كافة الإرشادات. ولذلك ننصح سعادة المؤلف الرئيس، بعد الانتهاء من ضبط الورقة، بأن يقوم بإرسال الورقة للمؤلفين الآخرين (وأيضاً لزميل من غير المؤلفين) للتأكد من أن جميع الإرشادات قد اتبعت. كما ننصح أصحاب السعادة المؤلفين أن يقوموا أيضاً بالاستعانة بطرق واستراتيجيات أخرى يرون أنها قد تساعدهم في التأكد من اتباع كافة الإرشادات؛ فعلى سبيل المثال، القيام بطباعة ملف "إرشادات التسليم"، ثم وضع علامة "صح" بجانب كل فقرة من الإرشادات للتأكد من تغطية جميع الإرشادات. تؤكد المجلة لأصحاب السعادة المؤلفين أنها من خلال خطتها الاستراتيجية الحالية تسعى لأن تكون منار التميز في العالم العربي (بجميع ما يتطلبه التميز من عمل شاق ودقة)، وهذا قد يزيد العبء على المجلة والمؤلف والمحكمين وجميع "أصحاب الشأن" على حد سواء. سيمنح المؤلف فرصين كحد أعلى لاتباع التعليمات، وفي حالة عدم قيامه بذلك، فإن هيئة التحرير ستقوم بطي قيد البحث، حتى وإن أوصى المحكمين بقبول البحث. اتباع التعليمات تحمل نفس الماهية التي تحملها القيمة العلمية للورقة.
- **متعارضات**: في حالة تضارب توصيات المحكمين مع إرشادات النشر، فيتم استبعاد توصيات المحكمين وتعتمد إرشادات النشر، مع ضرورة إعلام المحرر بهذا التضارب.

2. شروط لا يتم استلام الورقة دونها

- **المستندات المطلوبة**: يجب تسليم ملفين على صيغة الوورد (DOC)، وهما كالتالي:
  - الملف الأول تحت مسمى "بيانات الباحث" (Title Page): يجب ترتيب هذا الملف كالتالي:
    - عنوان الورقة بالعربي (غير مطلوب إذا كانت الورقة باللغة الإنجليزية).
    - بيانات المؤلف بالعربي (على أن يتضمن اسم المؤلف، اسم القسم، اسم الكلية، اسم الجامعة، اسم المدينة، واسم الدولة، البريد الإلكتروني، رقم الواتساب). في حالة عدم وجود قسم أو كلية أو جامعة، يكتب ما يعادلها. في حالة عدم الانتساب لجامعة، يكتب "باحث مستقل" (غير مطلوب إذا كانت الورقة باللغة الإنجليزية).
    - عنوان الورقة بالإنجليزي.
    - بيانات المؤلف بالإنجليزي (على أن يتضمن اسم المؤلف، اسم القسم، اسم الكلية، اسم الجامعة، اسم المدينة، واسم الدولة، البريد الإلكتروني، رقم الواتساب). في حالة عدم الانتساب لجامعة، يكتب "Independent Researcher".
    - تحديد تخصص الورقة: 1) التخصص العام، 2) التخصص الدقيق ، 3) التخصص الأدق من الدقيق.
    - نبذة من 80 كلمة عن كل مؤلف. أدناه توضيح عن كيفية كتابة النبذ (إذا كانت الورقة بالعربي فتكتب النبذة بالعربي، وإذا كانت الورقة بالإنجليزي، فتكتب النبذة بالإنجليزي).
    - شكر وتقدير (اختياري).

- الملف الثاني تحت عنوان "ملف البحث" (Main Document): تتبع المجلة سياسة التحكيم المزدوج مجهول الهوية، وعليه يجب على المؤلف عدم تضمين ما يكشف هويته في "ملف البحث"، حيث ان "ملف البحث" سيرسل كما هو للمحكمين. يجب ترتيب الملف كالتالي:
  - عنوان الورقة بالعربي (غير مطلوب إذا كانت الورقة باللغة الإنجليزية).
  - ملخص الورقة بالعربي (غير مطلوب إذا كانت الورقة باللغة الإنجليزية).
  - الكلمات المفتاحية بالعربي (غير مطلوب إذا كانت الورقة باللغة الإنجليزية).
  - عنوان الورقة بالإنجليزي.
  - ملخص البحث بالإنجليزي.
  - الكلمات المفتاحية بالإنجليزي.
  - مضمون البحث.
  - المراجع.

- **"نبذة عن المؤلف"**: يجب تزويد نبذة عن كل مشارك في البحث. تتضمن النبذة الاسم، ثم أدناه اسم القسم، الكلية، الجامعة، المدينة، الدولة (أو ما يوازيه)، رقم الواتساب مع فتح الخط الدولي، البريد الإلكتروني، ثم أدناه نبذة عن الباحث (من 80 كلمة لكل باحث، علماً أن اسم الباحث و مكان العمل لا يحسب من هذه الـ 80 كلمة). إذا كان لدى الباحث رقم أوركيد و/أو صفحة شخصية، فيدرج في نهاية النبذة. يجب أن تتضمن النبذة جنسية المؤلف، وأعلى درجة علمية حصل عليها (مثلاً، ماجستير، دكتوراه) واسم الجامعة التي حصل منها على هذه الدرجة. يمكن للمؤلف الكتابة في النبذة عن نشاطه البحثي واهتماماته البحثية ومدى التأثير الوطني والعالمي الذي حققه ومدى قدرته على التواصل خارج نطاق مكان عمله وشيء من نشاطه في المؤتمرات والدورات التدريبية. النبذة هي وسيلة مهمة يستطيع الباحث من خلالها التعريف بنفسه وتسويق ذاته؛ فينبغي أن تحظى باهتمام عال من قبل المؤلف. ترتب النبذ وفقاً لترتيب المؤلفين. أدناه مثال على ذلك:

  عبدالرحمن عيسى الليلي
  قسم المناهج وطرق التدريس، كلية التربية، جامعة الملك فيصل، الأحساء، المملكة العربية السعودية، 00966000000000، scijkfu@kfu.edu.sa
  أ.د. الليلي دكتوراه (أكسفورد)، سعودي، أستاذ دكتور، مدير مركز وطني، رئيس هيئة تحرير (سكوبس)، أعماله في 7 لغات (منها، إسباني، فلبيني، إندونيسي، صيني، إيطالي)، مقابلاته في 5 لغات (منها، فرنسي، إسباني، ألماني)، مؤسس 4 نظريات (منها، "Multiple Stupidities" و"Retroactivism" و"On-the-Go Sourcing") و 3 منهجيات ("Crowd-Authoring" و"Crowd-Reflecting" و"Door-Knocking")، أكثر مبيعاً (أمازون)، نشر مع أكبر دور نشر (Nature Research, Cogent, Palgrave, Elsevier, Springer, Taylor & Francis, Wiley, Sage, Oxford)، نشر 24 ورقة في ISI و/أو سكوبس، أبحاثه مقتبسة من قبل 35 دولة (منها المجر، صربيا، روسيا، بيرو، كوريا، كولومبيا، سويسرا، هولندا، السويد، فنلندا، لاتفيا) في 6 لغات (منها، التركية و الليتوانية)، عمل خلال الصيف في نيوزلندا وايطاليا. شارك بأوراق في مؤتمرات سنغافورة، اليونان، اليابان، بلغاريا وغيرها. عمل مستشاراً لمؤسسات منها الويكيبيديا و جامعة هانوفر.
  رقم الأوركيد (ORCID): 0000-0002-5116-422x
  الموقع الشخصي: https://abdulrahmanallily.wordpress.com

- **عدد كلمات الورقة**: ألا يتجاوز عدد كلمات الورقة 8000 كلمة في أي حال من الأحوال (شاملة كل شيء، بما في ذلك المراجع والجداول والأشكال والملخص وبيانات المؤلفين والهوامش والرومنة وكل شيء).
- **الملخص**: ألا يزيد الملخص عن 200 كلمة. لا يسمح بإدراج مراجع أو اقتباسات في الملخص.
- **عدد كلمات العنوان**: ألا يزيد عنوان الورقة عن 15 كلمة.
- **عدد الكلمات المفتاحية**: أن تحتوي الورقة على ست كلمات مفتاحية باللغة العربية وترجمتها بالإنجليزية، ويجب ألا يكون قد سبق ذكرها في العنوان، كما يجب ألا تزيد كل كلمة مفتاحية عن كلمتين.
- **عدد الجداول والرسومات**: ينبغي تقليص عدد الجداول والرسومات والاختصارات والحواشي السفلية، قدر المستطاع. يجب ألا تتضمن الورقة أكثر من (6) جداول و (6) صور/أشكال. علماً أن عدم وجود أشكال بالورقة لا يعني أن عدد الجداول يمكن أن يزيد عن (6)، وعدم وجود جداول بالورقة لا يعني أن عدد الأشكال يمكن أن يزيد عن (6). يجب ألا يزيد عدد السطور عن 20 وعدد الأعمدة عن 7 في كل جدول من الجداول.
- **الجودة اللغوية**: يجب أن يكون البحث مكتوبًا بمستوى لغوي صحيح مقبول. كما يجب على المؤلف الضغط على أيقونة "المراجعة اللغوية" في ملف الوورد للتأكد من عدم وجود أخطاء لغوية.
- **عدد المراجع**: يجب ألا يزيد عدد المراجع عن 40 مرجعًا (إلا في حالة كون الورقة "مراجعة أدبية").
- **الاقتباس**: يجب أن تكون نسبة الاقتباس غير المشروع 0%.
  - يسري ذلك على نوعي الاقتباس: الاقتباس الذاتي و الاقتباس من الآخرين. ويقصد بالاقتباس الذاتي أن ينقل الباحث من عمل آخر له قام بنشره من قبل دون أن يشير إلى النقل.
  - يستثنى من الاقتباس غير المشروع تلك العبارات والجمل المتداولة التي لا تُمثل انتهاكا لحقوق الآخرين، ولا تطعن في الأصالة العلمية؛ مثل عبارة:
    والجدول يُوضح معاملات متغيرات الدراسة التي وضعت في قائمة الاستقصاء التي اعتمد عليها الباحث في تجميع البيانات الأولية.
  - في حالة الاقتباس الحرفي ولجعل الاقتباس مشروعاً، فيجب ألا يزيد عن 30 كلمة، وتوضع في علامة تنصيص، ويذكر اسم المرجع ورقم الصفحة. مثال على ذلك:
    ويجدر الإشارة إلى أنه "يعد التعليم عن بعد في زمن الكورونا مختلفاً بشكل أساسي وجوهري عن "التعليم عن بعد" التقليدي من عدة أوجه، أولها كونه مفاجئا وغير مخطط له مسبقاً" (العلي، 2020: 15).
  - غير مسموح بالاقتباس الحرفي إلا في حالة الضرورة القصوى والمبررة؛ حيث مفترض من المؤلف أن يعيد صياغة أي اقتباس بأسلوبه الشخصي.
  - في حالة كون أن طبيعة التخصص تتطلب اقتباسات مطولة، فيجب تبرير ذلك في الخطاب الموجه للمجلة أثناء التسليم.
- **العبارات غير الأكاديمية**: يجب أن تكون اللغة المكتوب بها الورقة لغة علمية أكاديمية مباشرة تبتعد عن الإسهاب الذي لا علاقة له بالورقة من الناحية العلمية، وأيضا تبتعد عن تكرار الجمل والمعاني المعلومة بالضرورة؛ ومن الأمثلة على ذلك ما يرد في مقدمة البحث وخاتمته لدى بعض الباحثين: (فإن أكن أصبت فمن الله وحده وله المنة على ذلك، وإن تكن الثانية فمن نفسي ومن الشيطان، والله الهادي إلى سواء السبيل..)، (أحمد الله أن أعانني ويسر لي إتمام هذا البحث بعدما لاقيت فيه من عناء وجهد طيلة شهور متتابعة، فإن أصبت فإمساك بمعروف، وإن تكن الأخرى فتسريح بإحسان..)، (حفظه الله ورعاه وسدد على طريق الخير خطاه..)، (رحمه الله وطيب ثراه..)، ونحو ذلك، ويستثنى من ذلك ما يتعلق بالأنبياء والمرسلين: (صلى الله عليه وسلم)، (عليه السلام).
- **المرفقات/الملاحق**: ألا تتضمن الورقة مرفقات، وفي حال ضرورة المرفقات فإنها توضع في المتن، أو يتم وضع رابط للمرفقات على الإنترنت (يتم تزويد الملحقات فقط في حالة طلب المحكمين لها).

3. إجراءات يطلب من المؤلف عملها فقط بعد صدور قرار المحكمين

- **مقاس الصفحة**: يكون مقاس الصفحة A4، على عمود واحد، الهوامش 2.5 سم من جميع الجهات، ويكون نوع الخط من الخطوط الدارج استخدامها، ويكون حجم الخط مقبولا.
- **جودة اللغة**: يجب التأكد من الخلو التام من وجود أي ملاحظات لغوية.
- **العناوين**:
  - لا يزيد عدد مستويات العناوين عن ثلاثة. أي يسمح فقط بعناوين أساسية، وفرعية وفرعية فرعية فقط. أي كون هناك عناوين فرعية فرعية فرعية غير مسموح لتجاوزها ثلاثة مستويات. الأساسية والفرعية. يجب ترقيمها كالتالي: 1.، 2.، 3.، وتحت 1. يكون 1.1.، 1.2.، 1.3.، وتحت 1.1. يكون 1.1.1.، 1.1.2.، 1.1.3.، وهكذا. يجب ألا يتم ترقيم عنوان الملخص، والنبذة عن المؤلف والمراجع.

- المجلة لا تستقبل عناوين الأبحاث التي تدور حول فرد بعينه أو قصيدة بعينها أو كتاب بعينه؛ مثل: "المفارقة الشعرية في شعر أبي الحسن القيرواني"، "حجيّة المنجز الكلامي في مقدّمة دلائل الإعجاز لعبد القاهر الجرجاني"، "هرمية المصطلح البلاغي والنقدي عند الجاحظ"، "النسق البنيوي في قصيدة أبي ذؤيب الهذلي في رثاء أولاده الخمسة".
- نظراً لكون المجلة العلمية لجامعة الملك فيصل مجلة متعددة التخصصات تندرج ضمن المنصات العالمية للبحث العلمي فإن هذا يتطلب من الباحثين كتابة عنوان الورقة وملخصها باللغة العلمية المباشرة بصياغة سهلة بعيدة عن التعقيد مما ييسر لكل قارئ في مختلف التخصصات فهم مضمون الورقة وعنوانها وملخصها.
- لا تنشر المجلة الأوراق التي تتحدد بذكر مدينة أو محافظة بعينها في العنوان البحثي (يمكن الاكتفاء بذكر اسم الدولة فقط إذا لزم الأمر)، وذلك لأن تخصيص اسم مدينة بعينها يحدد من نسبة الاستشهادات للورقة بعد نشرها، لأنه غالباً ما تكون هذه المدينة غير معلومة أو غير ذات اهتمام من القراء، وهذا يتعارض مع سياسة المجلة في استقطاب الأوراق ذات العمومية والانتشار الواسع. وإذا أراد الباحث أن يخصص محافظة أو مدينة ما، فيمكنه الإشارة لذلك في ملخص الورقة وحدودها المكانية وليس في العنوان.

- **التواريخ والأرقام**: يجب أن تكون جميع تواريخ الورقة بالميلادي وبأرقام إنجليزية (سواء في المتن أو المراجع).
- **الجداول**: يتم كتابة رقم وعنوان الشكل أو الجدول أعلاه. في المتن، يتم الإشارة إلى الجدول أو الشكل دائماً برقمه سواءً قبل أو بعد وضعه، وترقم الجداول تسلسليا حسب تسلسل ذكرها في المتن.
- **العملات**: يجب كتابة القيمة بالدولار بين قوسين، بعد أي قيمة مذكورة بالريال السعودي أو أي عملة أخرى.
- **الاختصارات**: عند استخدام رموز لاختصار مصطلح، فيجب أن يذكر نص المصطلح كاملا في أول مرة يرد فيها في نص البحث. علما أن المسموح به ثلاث اختصارات على الأكثر.
- **المقاييس الرياضية**: يجب استخدام الاختصارات المقننة دوليا بدلا من كتابة الكلمة كاملة مثل سم، ملم، كلم و% (لكل من سنتمتر، مليمتر، كيلومتر والنسبة المئوية، على الترتيب). يفضل استخدام المقاييس المترية وفي حالة استخدام وحدات أخرى يكتب المعادل المتري لها بين أقواس مربعة. في حالة ذكر وحدات قياس أو أسماء دارجة إقليميا للكائنات الحية في المتن يذكر عقبها مباشرة المقابل لها بالوحدات القياسية أو الاسم اللاتيني للكائن. يجب أن تكون جميع العملات بالدولار الأمريكي.
- **الحواشي**: يفضل تقليص الحواشي، ولكن في حالة الحاجة لها، فيشار إلى الحاشية في المتن بأرقام بين قوسين مرتفعة عن السطر، ترقم الحواشي داخل المتن وتكتب حواشي كل صفحة أسفلها مفصولة عن المتن بخط ولا تجمع في نهاية المتن. يعاد ترقيم الحواشي ابتداءً من الرقم 1 مع بداية كل صفحة جديدة.
- **الهوامش السفلية**: تأخذ المراجع المدرجة في الحواشي السفلية ترقيماً متسلسلاً لكل صفحة بحيث يوضع رقم الحاشية بين قوسين علويين ()، وتكون جميع العناصر الببليوجرافية لكل مرجع مرتبة وفقا للترتيب المذكور في قائمة المراجع، سواء ذكرت البيانات كاملة أو مختصرة، كما يجب التأكد من أن جميع المراجع الواردة في المتن والحواشي مذكورة في قائمة المراجع، كما يجب ألا تكون هنالك مراجع بالقائمة لم يشر إليها في المتن.
- **روابط المراجع**:
  - **للمراجع العربية**: في حالة الرغبة في إدراج رابط لمرجع عربي، فيكتب بعد المرجع "متوفر بموقع:" ثم يدرج الرابط، وبعد الرابط يفتح قوس ويكتب "تاريخ الاسترجاع:" ثم يدرج التاريخ على هذه الصيغة "2020/07/27"، ثم يغلق القوس.
  - **للمراجع الإنجليزية**: في حالة الرغبة في إدراج رابط لمرجع إنجليزي، فيكتب بعد المرجع "Available at:" ثم يدرج الرابط، وبعد الرابط يفتح قوس ويكتب "accessed on" ثم يدرج التاريخ على هذه الصيغة "2020/07/27"، ثم يغلق القوس.
- **ترتيب قائمة المراجع**: يجب ترتيب المراجع هجائياً. ويجب عدم ترقيم قائمة المراجع.
- **مرجعان لمؤلف في سنة واحدة**: في حالة وجود مرجعين لمؤلف واحد في سنة واحدة، فللتمييز بينهما يكتب حرف بجانب التاريخ كالآتي: (2020أ)، (2020ب)، وبالإنجليزي (2020a)، (2020b)
- **DOI للمرجع**: عند استعمال مراجع لها رقم DOI، يجب ذكر هذا الرقم.
- **المراجع داخل المتن**: بخصوص آلية كتابة المراجع داخل المتن:
  - إذا كان المرجع في بداية الجملة، يكتب اسم عائلة الباحث/الباحثين يليها تاريخ النشر بين قوسين. مثال: "ذكر الصالح والأحمد (2020) بأن..."
  - إذا كان المرجع في نهاية الجملة، فيكتب بين قوسين اسم عائلة الباحث/الباحثين، ثم فاصلة، ثم تاريخ النشر. مثال: "وهذا هو أساس المشكلة (الصالح والأحمد، 2020)."
  - في حالة كون المرجع لأكثر من باحثين فيكتب اسم عائلة الباحث الأول متبوعا بكلمة "وآخرون". مثال: "ذكر المحمد وآخرون (2020) بأن..." أو "وهذا ما يسمى بالتعليم المدمج (العلي وآخرون، 2020)."
  - يجب تدوين رقم الصفحة المقتبس منها داخل المتن. أدناه أمثلة على كيفية عمل هذا التدوين:
    - "وهذه من القضايا الأساسية التي ستساهم في تطور التعليم العالي" (المحمد، 2020: 15).
    - ذكر المحمد (2020: 15) أن هذه "من القضايا الأساسية التي ستساهم في تطور التعليم العالي".
    - ذكر المحمد (2020) أن هذه "من القضايا الأساسية التي ستساهم في تطور التعليم العالي" (ص. 15).
- **المراجع في قائمة المراجع**: لا يتم استخدام كلمة "وآخرون" (. et al) في قائمة المراجع.
- **صفحات الويكيبيديا**: لا يسمح باقتباس صفحات الويكيبيديا.
- **تعريف الرومنة**: يجب رومنة/ترجمة قائمة المراجع العربية. يقصد بالرومنة النقل الصوتي للحروف إلى الإنجليزية، أي تحويل منطوق الحروف العربية إلى حروف إنجليزية. تتم الرومنة عن طريق مترجم قوقل (http://translate.google.com)، حيث إن في كتابة أي جملة في مترجم قوقل (مثلاً: " إنجازات جامعة الملك فيصل منذ تأسيسها")، فستكون رومنة هذه الجملة متوفرة بأسفل النص " iinjazat jamieat almalik faysal mundh tasisiha"، وترجمتها متوفرة على الجنب (Achievements of King Faisal University since its foundation). رومنة المراجع العربية لا يعني حذف المراجع العربية. فالمراجع العربية والمرومنة تبقى سوياً. توضع أولاً المراجع العربية، يليها المراجع المرومنة والإنجليزية. تدمج المراجع المرومنة والإنجليزية سوياً وترتب هجائياً.
- **تعديلات هيئة التحرير على عنوان الورقة**: يحقّ لهيئة التحرير إعادة صياغة عنوان الورقة في المرحلة الأخيرة للنشر (قبل الإحالة لعدد)، وذلك وفقاً لمقتضيات التوجه التطويري العام للمجلة حالياً، والذي يتطلب الاقتصار على نشر العناوين: "الموجزة، والبسيطة، والواضحة، والعامة التي لا تشتمل على صف دراسي بعينه أو جامعة أو محافظة أو مدينة بعينها في العنوان" وبالتالي سيتم استبعاد أية كلمة غير ضرورية من العنوان لأن هذه المصطلحات تحدّ من نسبة انتشار البحث، وشموليته، وتقلل من نسبة اقتباسه واستشهاداته من قبل الباحثين.
- **شهادة مراجعة لغوية**: في حالة قبول الورقة للنشر، فإنه سيطلب من المؤلف إرسال ورقته لشركة معتمدة لمراجعة الورقة من قبل متحدثي اللغة الإنجليزية كلغة أم، وموافاة المجلة بشهادة إثبات مراجعة لغوية من قبل الشركة. إذا كانت الورقة باللغة العربية، فإن المراجعة تكون لعنوان الورقة والملخص باللغة الإنجليزية. وإذا كانت الورقة باللغة الإنجليزية، فإن المراجعة تكون على الورقة كاملة. تكون هذه المراجعة اللغوية كمرحلة أخيرة قبل نشر الورقة وبعد إدخال كامل ملاحظات المحكمين والمحررين وهيئة التحرير. أدناه إحدى هذه الشركات والتي تقوم بالمراجعة اللغوية خلال 24 ساعة:
https://proofreadmyessay.co.uk

4. آلية كتابة الدوريات والمجلات في المراجع (يطلب عملها فقط في حالة قبول الورقة للنشر)

4.1. كتابة الدوريات والمجلات العربية في قائمة المراجع

يبدأ كل مرجع باسم العائلة للمؤلف الأول، ثم فاصلة، ثم الاسم الأول واسم الأب للمؤلف الأول، ثم فاصلة، ثم اسم العائلة للمؤلف الثاني، ثم فاصلة، ثم الاسم الأول واسم الأب للمؤلف الثاني، ثم حرف العطف "و" ثم اسم العائلة للمؤلف الثالث، ثم فاصلة، ثم الاسم الأول واسم الأب للمؤلف الثالث، ثم نقطة، ثم فتح قوس، ثم التاريخ، ثم إغلاق القوس، ثم نقطة، ثم عنوان البحث، ثم نقطة، ثم اسم المجلة يكون مكتوبا بشكل مائل، ثم فاصلة، ثم رقم المجلد مكتوبا بشكل عريض، ثم فتح قوس، ثم

يكتب رقم العدد، ثم يغلق القوس، علماً أنه لا يوجد مسافة بين رقم المجلد ورقم العدد، ثم فاصلة، ثم رقم أول صفحة للبحث، ثم علامة "-" ثم رقم آخر صفحة للبحث. (مع مراعاة أن حرف العطف "و" يوضع دائما قبل المؤلف الأخير أيًّا كان عدد المؤلفين). أدناه مثال على ذلك:

الأحمد، محمد عبدالرحمن، العلي، إسماعيل صلاح والصالح، أحمد محمد. (2020). إنجازات جامعة الملك فيصل منذ تأسيسها. *المجلة العلمية لجامعة الملك فيصل: فرع العلوم الإنسانية والإدارية*، **13**(2)، 213-223.

في حالة عدم وجود تاريخ، فتكتب العبارة التالية "د.ت." في مكان التاريخ، سواء في المتن أو المرجع. على سبيل المثال:

الأحمد، محمد عبدالرحمن، العلي، إسماعيل صلاح والصالح، أحمد محمد. (د.ت.). إنجازات جامعة الملك فيصل منذ تأسيسها. *المجلة العلمية لجامعة الملك فيصل: فرع العلوم الإنسانية والإدارية*، **13**(2)، 213-223.

في حالة عدم وجود رقم مجلد، فتكتب العبارة التالية "بدون رقم مجلد" في مكان رقم المجلد. على سبيل المثال:

الأحمد، محمد عبدالرحمن، العلي، إسماعيل صلاح والصالح، أحمد محمد. (2020). إنجازات جامعة الملك فيصل منذ تأسيسها. *المجلة العلمية لجامعة الملك فيصل: فرع العلوم الإنسانية والإدارية*، **بدون رقم مجلد** (2)، 213-223.

في حالة عدم وجود رقم عدد، فتكتب العبارة التالية "بدون رقم عدد" في مكان رقم العدد. على سبيل المثال:

الأحمد، محمد عبدالرحمن، العلي، إسماعيل صلاح والصالح، أحمد محمد. (2020). إنجازات جامعة الملك فيصل منذ تأسيسها. *المجلة العلمية لجامعة الملك فيصل: فرع العلوم الإنسانية والإدارية*، **13**(بدون رقم عدد)، 213-223.

في حالة عدم وجود أرقام صفحات، فتكتب العبارة التالية "بدون أرقام صفحات" في مكان أرقام الصفحات، أو رقم مسلسل البحث في مجلات الأونلاين. على سبيل المثال:

الأحمد، محمد عبدالرحمن، العلي، إسماعيل صلاح والصالح، أحمد محمد. (2020). إنجازات جامعة الملك فيصل منذ تأسيسها. *المجلة العلمية لجامعة الملك فيصل: فرع العلوم الإنسانية والإدارية*، **13**(2)، بدون أرقام صفحات.

4.2. كتابة الدوريات والمجلات الإنجليزية في قائمة المراجع

يبدأ كل مرجع باسم العائلة للمؤلف الأول، ثم فاصلة، ثم الحرف الأول من الاسم الأول للمؤلف الأول، ثم نقطة، ثم الحرف الأول لاسم الأب للمؤلف الأول، ثم نقطة، ثم فاصلة، ثم اسم العائلة للمؤلف الثاني، ثم فاصلة، ثم الحرف الأول من الاسم الأول للمؤلف الثاني، ثم نقطة، ثم الحرف الأول لاسم الأب للمؤلف الثاني، ثم نقطة، ثم حرف العطف "and" (وليس "&") ثم اسم العائلة للمؤلف الثالث، ثم فاصلة، ثم الحرف الأول من الاسم الأول للمؤلف الثالث، ثم نقطة، ثم الحرف الأول لاسم الأب للمؤلف الثالث، ثم نقطة، ثم فتح قوس، ثم التاريخ بالميلادي، ثم إغلاق القوس، ثم نقطة، ثم عنوان البحث بحروف صغيرة (صمول small)، ثم فتح علامة تنصيص واحدة، ثم عنوان البحث مترجما بحروف صغيرة (صمول small؛ يستثنى من ذلك الكلمة الأولى وأسماء الأشخاص وأسماء الأماكن وأسماء الجنسيات واللغات والأسابيع والشهور فيبقى الحرف الأول منها بحروف كبيرة، كابتل capital)، ثم إغلاق علامة التنصيص، ثم نقطة، ثم اسم المجلة مترجما (أو مرومن) يكون مكتوبا بشكل مائل والحرف الأول من كل كلمة يكون كبيرا (كابتل capital؛ يستثنى من ذلك أدوات التنكير والتعريف مثل "a" و "an" و "the" وحروف الجر مثل "to" و "of" و "in" وأدوات الربط "and" و "but" و "or" فيبقى الحرف الأول منها بحروف صغيرة، إلا إذا كانوا في بداية اسم المجلة فيكون الحرف الأول منها بحروف كبيرة)، ثم فاصلة، ثم رقم المجلد مكتوبا بشكل عريض، ثم فتح قوس، ثم يكتب رقم العدد، ثم يغلق القوس، علماً أنه لا يوجد مسافة بين رقم المجلد ورقم العدد، ثم رقم أول صفحة للبحث، ثم علامة "-" ثم رقم آخر صفحة للبحث، ثم نقطة، ثم تكتب "[in Arabic]" أدناه مثال على رومنة المرجع العربي:

Al Ahmed, M.A., Al Ali, I.S. and Al Salah, A.M. (2020). Iinjazat jamieat almalik faysal mundh tasisiha 'Achievements of King Faisal University since its foundations'. *The Scientific Journal of King Faisal University: Humanities and Management Sciences,* **13**(2), 213-223. [in Arabic]

في حالة كون المرجع بلغة غير العربية وغير الإنجليزية، وهذه اللغة تستخدم حروف غير إنجليزية، فتتم رومنة العنوان بالطريقة نفسها التي تتم بها رومنة العناوين العربية. ولكن، في حالة كون الدورية بلغة غير العربية وغير الإنجليزية، ولكن هذه اللغة تستخدم الحروف الإنجليزية نفسها، فلا حاجة لرومنة عنوان البحث، ويكتفى بإبقاء العنوان في لغته الأصل ووضع الترجمة في علامة تنصيص. فعلى سبيل المثال، في حالة كون الدورية باللغة

Al Ahmed, K.A., Al Muhammed, S.F. and Al Saleh, A.F. (2020). The history of agriculture in Al Ahsa. *The Scientific Journal of King Faisal University: Humanities and Management Sciences*, **13**(2), 213-222.

في حالة عدم وجود تاريخ، فيكتب "n/a". على سبيل المثال:

Al Ahmed, K.A., Al Muhammed, S.F. and Al Saleh, A.F. (n/a). The history of agriculture in Al Ahsa. *The Scientific Journal of King Faisal University: Humanities and Management Sciences*, **13**(2), 213-222.

في حالة عدم وجود رقم مجلد، فيكتب "n/a". على سبيل المثال:

Al Ahmed, K.A., Al Muhammed, S.F. and Al Saleh, A.F. (2020). The history of agriculture in Al Ahsa. *The Scientific Journal of King Faisal University: Humanities and Management Sciences*, **n/a**(2), 213-222.

في حالة عدم وجود رقم عدد، فيكتب "n/a". على سبيل المثال:

Al Ahmed, K.A., Al Muhammed, S.F. and Al Saleh, A.F. (2020). The history of agriculture in Al Ahsa. *The Scientific Journal of King Faisal University: Humanities and Management Sciences*, **13**(n/a), 213-222.

في حالة عدم وجود أرقام صفحات، فيكتب "n/a". على سبيل المثال:

Al Ahmed, K.A., Al Muhammed, S.F. and Al Saleh, A.F. (2020). The history of agriculture in Al Ahsa. *The Scientific Journal of King Faisal University: Humanities and Management Sciences*, **13**(2), n/a.

4.3. رومنة/ترجمة الدوريات والمجلات غير الإنجليزية في قائمة المراجع

يبدأ كل مرجع باسم العائلة للمؤلف الأول، ثم فاصلة، ثم الحرف الأول من الاسم الأول للمؤلف الأول، ثم نقطة، ثم الحرف الأول لاسم الأب للمؤلف الأول، ثم نقطة، ثم فاصلة، ثم اسم العائلة للمؤلف الثاني، ثم فاصلة، ثم الحرف الأول من الاسم الأول للمؤلف الثاني، ثم نقطة، ثم الحرف الأول لاسم الأب للمؤلف الثاني، ثم نقطة، ثم حرف العطف "and" (وليس "&") ثم اسم العائلة للمؤلف الثالث، ثم فاصلة، ثم الحرف الأول من الاسم الأول للمؤلف الثالث، ثم نقطة، ثم الحرف الأول لاسم الأب للمؤلف الثالث، ثم نقطة، ثم فتح قوس، ثم التاريخ بالميلادي، ثم إغلاق القوس، ثم نقطة، ثم عنوان البحث (مرومن) بحروف صغيرة (صمول small)، ثم فتح علامة تنصيص واحدة، ثم عنوان البحث مترجما بحروف صغيرة (صمول small؛ يستثنى من ذلك الكلمة الأولى وأسماء الأشخاص وأسماء الأماكن وأسماء الجنسيات واللغات والأسابيع والشهور فيبقى الحرف الأول منها بحروف كبيرة، كابتل capital)، ثم إغلاق علامة التنصيص، ثم نقطة، ثم اسم المجلة مترجما (أو مرومن) يكون مكتوبا بشكل مائل والحرف الأول من كل كلمة يكون كبيرا (كابتل capital؛ يستثنى من ذلك أدوات التنكير والتعريف مثل "a" و "an" و "the" وحروف الجر مثل "to" و "of" و "in" وأدوات الربط "and" و "but" و "or" فيبقى الحرف الأول منها بحروف صغيرة، إلا إذا كانوا في بداية اسم المجلة فيكون الحرف الأول منها بحروف كبيرة)، ثم فاصلة، ثم رقم المجلد مكتوبا بشكل عريض، ثم فتح قوس، ثم يكتب رقم العدد، ثم يغلق القوس، علماً أنه لا يوجد مسافة بين رقم المجلد ورقم العدد، ثم فاصلة، ثم رقم أول صفحة للبحث، ثم علامة "-" ثم رقم آخر صفحة للبحث. أدناه مثال على ذلك:

الألمانية، فيبدأ المرجع باسم العائلة للمؤلف الأول، ثم فاصلة، ثم الحرف الأول من الاسم الأول للمؤلف الأول، ثم نقطة، ثم الحرف الأول لاسم الأب للمؤلف الأول، ثم نقطة، ثم فاصلة، ثم اسم العائلة للمؤلف الثاني، ثم فاصلة، ثم الحرف الأول من الاسم الأول للمؤلف الثاني، ثم نقطة، ثم الحرف الأول لاسم الأب للمؤلف الثاني، ثم نقطة، ثم حرف العطف "and" (وليس "&") ثم اسم العائلة للمؤلف الثالث، ثم فاصلة، ثم الحرف الأول من الاسم الأول للمؤلف الثالث، ثم نقطة، ثم الحرف الأول لاسم الأب للمؤلف الثالث، ثم نقطة، ثم فتح قوس، ثم التاريخ بالميلادي، ثم إغلاق القوس، ثم نقطة، ثم عنوان البحث باللغة الألمانية (صمول small)، ثم فتح علامة تنصيص واحدة، ثم عنوان البحث مترجما بحروف صغيرة (صمول small؛ يستثنى من ذلك الكلمة الأولى وأسماء الأشخاص وأسماء الأماكن وأسماء الجنسيات واللغات والأسابيع والشهور فيبقى الحرف الأول منها بحروف كبيرة، كابتل capital)، ثم إغلاق علامة التنصيص، ثم نقطة، ثم اسم المجلة مترجما يكون مكتوبا بشكل مائل والحرف الأول من كل كلمة يكون كبيرا (كابتل capital؛ يستثنى من ذلك أدوات التنكير والتعريف مثل "a" و "an" و "the" وحروف الجر مثل "to" و "of" و "in" وأدوات الربط "and" و "but" و "or" فيبقى الحرف الأول منها بحروف صغيرة، إلا إذا كانوا في بداية اسم المجلة فيكون الحرف الأول منها بحروف كبيرة)، ثم فاصلة، ثم رقم المجلد بحروف كبيرة)، ثم فاصلة، ثم رقم العدد، ثم يغلق القوس، علماً أنه لا يوجد مسافة بين رقم المجلد ورقم العدد، ثم رقم أول صفحة للبحث، ثم علامة "-" ثم رقم آخر صفحة للبحث، ثم نقطة، ثم تكتب "[in German]" أدناه مثال على ذلك:

Al Ahmed, M.A., Al Ali, I.S. and Al Salah, A.M. (2020). Erfolge der King Faisal University seit ihrer gründung 'Achievements of King Faisal University since its foundations'. *The Scientific Journal of King Faisal University: Humanities and Management Sciences*, **13**(2), 213-223. [in German]

5. آلية كتابة المؤتمرات والندوات والملتقيات في المراجع (يطلب عملها فقط في حالة قبول الورقة للنشر)

5.1. كتابة المؤتمرات والندوات والملتقيات العربية في قائمة المراجع

يبدأ كل مرجع باسم العائلة للمؤلف الأول، ثم فاصلة، ثم الاسم الأول واسم الأب للمؤلف الأول، ثم فاصلة، ثم اسم العائلة للمؤلف الثاني، ثم فاصلة، ثم الاسم الأول واسم الأب للمؤلف الثاني، ثم حرف العطف "و" ثم اسم العائلة للمؤلف الثالث، ثم فاصلة، ثم الاسم الأول واسم الأب للمؤلف الثالث، ثم نقطة، ثم فتح قوس، ثم التاريخ، ثم إغلاق القوس، ثم نقطة، ثم عنوان البحث، ثم نقطة، ثم يكتب "في:" ثم يكتب اسم المؤتمر بشكل مائل، ثم فاصلة، ثم اسم مكان انعقاد المؤتمر، ثم فاصلة، ثم اسم مدينة المؤتمر، ثم فاصلة، ثم اسم دولة المؤتمر، ثم فاصلة، ثم تاريخ انعقاد المؤتمر، ثم نقطة. (مع مراعاة أن حرف العطف "و" يوضع دائما قبل المؤلف الأخير أيًّا كان عدد المؤلفين). أدناه مثال على ذلك:

الأحمد، محمد عبدالرحمن، العلي، إسماعيل صلاح والصالح، أحمد محمد. (2020). الموهبة في التعليم العالي. في: *الملتقى الوطني الأولى لمنسقي الموهوبين، جامعة الملك فيصل*، الأحساء، المملكة العربية السعودية، 2020/03/05-03.

5.2. كتابة المؤتمرات والندوات والملتقيات الإنجليزية في قائمة المراجع

يبدأ كل مرجع باسم العائلة للمؤلف الأول، ثم فاصلة، ثم الحرف الأول من الاسم الأول للمؤلف الأول، ثم نقطة، ثم الحرف الأول لاسم الأب للمؤلف الأول، ثم نقطة، ثم فاصلة، ثم اسم العائلة للمؤلف الثاني، ثم فاصلة، ثم الحرف الأول من الاسم الأول للمؤلف الثاني، ثم نقطة، ثم الحرف الأول لاسم الأب للمؤلف الثاني، ثم نقطة، ثم حرف العطف "and" (وليس "&") ثم اسم العائلة للمؤلف الثالث، ثم فاصلة، ثم الحرف الأول من الاسم الأول للمؤلف الثالث، ثم نقطة، ثم الحرف الأول لاسم الأب للمؤلف الثالث، ثم نقطة. ثم فتح قوس، ثم التاريخ بالميلادي، ثم إغلاق القوس، ثم نقطة، ثم عنوان البحث بحروف صغيرة (صمول small)، ثم فتح علامة تنصيص واحدة، ثم عنوان البحث مترجما بحروف صغيرة (صمول small؛ يستثنى من ذلك الكلمة الأولى وأسماء الأشخاص وأسماء الأماكن وأسماء الجنسيات واللغات والأسابيع والشهور فيبقى الحرف الأول منها بحروف كبيرة، كابتل capital)، ثم إغلاق علامة التنصيص، ثم نقطة، ثم يكتب اسم المؤتمر مترجما (أو مرومن) يكون مكتوبا بشكل مائل والحرف الأول من كل كلمة يكون كبيرا (كابتل capital؛ يستثنى من ذلك أدوات التنكير والتعريف مثل "a" و "an" و "the" وحروف الجر مثل "to" و "of" و "in" وأدوات الربط "and" و "but" و "or" فيبقى الحرف الأول منها بحروف صغيرة، إلا إذا كانوا في بداية اسم المجلة فيكون الحرف الأول منها بحروف كبيرة)، ثم فاصلة، ثم اسم مكان المؤتمر مترجما (أو مرومن)، ثم فاصلة، ثم يكتب اسم مدينة المؤتمر بالإنجليزي، ثم فاصلة، ثم اسم دولة المؤتمر بالإنجليزي، ثم فاصلة، ثم تاريخ انعقاد المؤتمر، ثم نقطة، ثم يكتب "[in Arabic]" أدناه مثال على رومنة المرجع العربي:

Al Ahmed, K.A., Al Muhammed, S.F. and Al Saleh, A.F. (2020). Al'iibdae fi altaelim aleali 'Creativity in higher education'. In: *The First National Symposium for the Coordinators of the Gifted*, King Faisal University, Al Ahsa, Saudi Arabia, 03-05/03/2020. [in Arabic]

في حالة كون المرجع بلغة غير العربية وغير الإنجليزية، وهذه اللغة تستخدم حروف غير إنجليزية، فتتم رومنة العنوان بالطريقة نفسها التي تتم بها رومنة العناوين العربية. أما في حالة كون المرجع بلغة غير العربية وغير الإنجليزية، ولكن هذه اللغة تستخدم الحروف الإنجليزية، فلا حاجة لرومنة عنوان البحث، ويكتفى بإبقاء العنوان في لغته الأصل ووضع الترجمة في علامة تنصيص. فعلى سبيل المثال، في حالة كون المرجع باللغة الفرنسية، فيبدأ المرجع باسم العائلة للمؤلف الأول، ثم فاصلة، ثم الحرف الأول من الاسم الأول للمؤلف الأول، ثم نقطة، ثم الحرف الأول لاسم الأب للمؤلف الأول، ثم نقطة، ثم فاصلة، ثم اسم العائلة للمؤلف الثاني، ثم فاصلة، ثم الحرف الأول من الاسم الأول للمؤلف الثاني، ثم نقطة، ثم الحرف الأول لاسم الأب للمؤلف الثاني، ثم نقطة، ثم حرف العطف "and" ثم اسم العائلة للمؤلف الثالث، ثم فاصلة، ثم الحرف الأول من الاسم الأول للمؤلف الثالث، ثم نقطة، ثم الحرف الأول لاسم الأب للمؤلف الثالث، ثم نقطة. ثم فتح قوس، ثم التاريخ بالميلادي، ثم إغلاق القوس، ثم نقطة، ثم عنوان البحث بحروف صغيرة (صمول small)، ثم فتح علامة تنصيص واحدة، ثم عنوان البحث مترجما بحروف صغيرة (صمول small؛ يستثنى من ذلك الكلمة الأولى وأسماء الأشخاص وأسماء الأماكن وأسماء الجنسيات واللغات والأسابيع والشهور فيبقى الحرف الأول منها بحروف كبيرة، كابتل capital)، ثم إغلاق علامة التنصيص، ثم نقطة، ثم يكتب اسم المؤتمر مترجما (أو مرومن) يكون مكتوبا بشكل مائل والحرف الأول من كل كلمة يكون كبيرا (كابتل capital؛ يستثنى من ذلك أدوات التنكير والتعريف مثل "a" و "an" و "the" وحروف الجر مثل "to" و "of" و "in" وأدوات الربط "and" و "but" و "or" فيبقى الحرف الأول منها بحروف صغيرة، إلا إذا كانوا في بداية اسم المجلة فيكون الحرف الأول منها بحروف كبيرة)، ثم فاصلة، ثم اسم مكان المؤتمر مترجما (أو مرومن)، ثم فاصلة، ثم يكتب اسم مدينة المؤتمر بالإنجليزي، ثم فاصلة، ثم اسم دولة المؤتمر بالإنجليزي، ثم فاصلة، ثم تاريخ انعقاد المؤتمر، ثم نقطة، ثم يكتب "[in Arabic]" أدناه مثال على رومنة المرجع العربي:

Al Ahmed, K.A., Al Muhammed, S.F. and Al Saleh, A.F. (2020). Al'iibdae fi altaelim aleali 'Creativity in higher education'. In: *The First National Symposium for the Coordinators of the Gifted*, King Faisal University, Al Ahsa, Saudi Arabia, 03-05/03/2020. [in Arabic]

5.3. رومنة/ترجمة المؤتمرات والندوات والملتقيات غير الإنجليزية في قائمة المراجع

يبدأ كل مرجع باسم العائلة للمؤلف الأول، ثم فاصلة، ثم الحرف الأول من الاسم الأول للمؤلف الأول، ثم نقطة، ثم الحرف الأول لاسم الأب للمؤلف الأول، ثم نقطة، ثم فاصلة، ثم اسم العائلة للمؤلف الثاني، ثم فاصلة، ثم الحرف الأول من الاسم الأول للمؤلف الثاني، ثم نقطة، ثم الحرف الأول لاسم الأب للمؤلف الثاني، ثم نقطة، ثم حرف العطف "and" ثم اسم العائلة للمؤلف الثالث، ثم فاصلة، ثم الحرف الأول من الاسم الأول للمؤلف الثالث، ثم نقطة، ثم الحرف الأول لاسم الأب للمؤلف الثالث، ثم نقطة. ثم فتح قوس، ثم التاريخ بالميلادي، ثم إغلاق القوس، ثم نقطة، ثم عنوان البحث بحروف صغيرة (صمول small؛ يستثنى من ذلك الكلمة الأولى وأسماء الأشخاص وأسماء الأماكن وأسماء الجنسيات واللغات والأسابيع والشهور فيبقى الحرف الأول منها بحروف كبيرة، كابتل capital)، ثم يكتب بحروف صغيرة (صمول small؛ يستثنى من ذلك الكلمة الأولى وأسماء الأشخاص وأسماء الأماكن وأسماء الجنسيات واللغات والأسابيع والشهور فيبقى الحرف الأول منها بحروف كبيرة، كابتل capital)، ثم نقطة، ثم يكتب "In:"، ثم يكتب اسم المؤتمر يكون مكتوبا بشكل مائل والحرف الأول من كل كلمة يكون كبيرا (كابتل capital؛ يستثنى من ذلك أدوات التنكير والتعريف مثل "a" و "an" و "the" وحروف الجر مثل "to" و "of" و "in" وأدوات الربط "and" و "but" و "or" فيبقى الحرف الأول منها بحروف صغيرة، إلا إذا كانوا في بداية اسم المجلة فيكون الحرف الأول منها بحروف كبيرة)، ثم فاصلة، ثم اسم مكان المؤتمر، ثم فاصلة، ثم اسم مدينة المؤتمر، ثم فاصلة، ثم اسم دولة المؤتمر، ثم فاصلة، ثم تاريخ انعقاد المؤتمر، ثم نقطة. أدناه مثال على ذلك:

Al Ahmed, K.A., Al Muhammed, S.F. and Al Saleh, A.F. (2020). Giftedness and creativity. In: *The First National Symposium for the Coordinators of the Gifted*, King Faisal University, Al Ahsa, Saudi Arabia, 03-05/03/2020.

الثالث، ثم نقطة. ثم فتح قوس، ثم التاريخ بالميلادي، ثم إغلاق القوس، ثم نقطة، ثم عنوان البحث باللغة الفرنسية (صمول small)، ثم فتح علامة تنصيص واحدة، ثم عنوان البحث مترجما بحروف صغيرة (صمول small؛ يستثنى من ذلك الكلمة الأولى وأسماء الأشخاص وأسماء الأماكن وأسماء الجنسيات واللغات والأسابيع والشهور فيبقى الحرف الأول منها بحروف كبيرة، كابتل capital)، ثم إغلاق علامة التنصيص، ثم نقطة، ثم يكتب "In:"، ثم يكتب اسم المؤتمر مترجما يكون مكتوبا بشكل مائل والحرف الأول من كل كلمة يكون كبيرا (كابتل capital؛ يستثنى من ذلك أدوات التنكير والتعريف مثل "a" و "an" و "the" وحروف الجر مثل "to" و "of" و "in" وأدوات الربط "and" و "but" و "or" فيبقى الحرف الأول منها بحروف صغيرة، إلا إذا كانوا في بداية اسم المجلة فيكون الحرف الأول منها بحروف كبيرة)، ثم فاصلة، ثم اسم مكان المؤتمر مترجما، ثم فاصلة، ثم يكتب اسم مدينة المؤتمر بالإنجليزي، ثم فاصلة، ثم اسم دولة المؤتمر بالإنجليزي، ثم فاصلة، ثم تاريخ انعقاد المؤتمر، ثم نقطة، ثم يكتب "[in French]". أدناه مثال على رومنة المرجع الفرنسي:

Al Ahmed, K.A., Al Muhammed, S.F. and Al Saleh, A.F. (2020). Créativité dans l'enseignement supérieur 'Creativity in higher education'. In: *The First National Symposium for the Coordinators of the Gifted*, King Faisal University, Al Ahsa, Saudi Arabia, 03-05/03/2020. [in French]

6. آلية كتابة الكتب في قائمة المراجع (يطلب عملها فقط في حالة قبول الورقة للنشر)

ملاحظات:

- إذا كانت طبعة الكتاب هي الطبعة الأولى، فلا يكتب أي شيء بخصوص رقم الطبعة.
- تصاغ مراجع التقارير والدراسات الصادرة عن وزارات ومؤسسات حكومية وغير حكومية بالطريقة نفسها التي تصاغ بها الكتب.

6.1. كتابة الكتب العربية في قائمة المراجع

يبدأ كل مرجع باسم العائلة للمؤلف الأول، ثم فاصلة، ثم الاسم الأول واسم الأب للمؤلف الأول، ثم فاصلة، ثم اسم العائلة للمؤلف الثاني، ثم فاصلة، ثم الاسم الأول واسم الأب للمؤلف الثاني، ثم حرف العطف "و" ثم اسم العائلة للمؤلف الثالث، ثم فاصلة، ثم الاسم الأول واسم الأب للمؤلف الثالث، ثم نقطة، ثم فتح قوس، ثم التاريخ، ثم إغلاق القوس، ثم نقطة، ثم عنوان الكتاب بخط مائل، ثم نقطة، ثم اسم مدينة الناشر، ثم فاصلة، ثم اسم دولة الناشر، ثم نقطتين رأسيتين، ثم اسم الناشر. (مع مراعاة أن حرف العطف "و" يوضع دائما قبل المؤلف الأخير أيًا كان عدد المؤلفين). أدناه مثال على ذلك:

الأحمد، محمد عبدالرحمن، العلي، إسماعيل صلاح والصالح، أحمد محمد. (2020). *إنجازات جامعة الملك فيصل منذ تأسيسها*. السعودية: مكتبة جرير.

في حالة وجود رقم طبعة، فيكتب التالي:

الأحمد، محمد عبدالرحمن، العلي، إسماعيل صلاح والصالح، أحمد محمد. (2020). *إنجازات جامعة الملك فيصل منذ تأسيسها*. الطبعة الثانية. الرياض، السعودية: مكتبة جرير.

في حالة كون الكتاب مترجمًا، فيكتب بعد اسم المؤلف: "ترجمة: اسم العائلة، الاسم الأول اسم الأب". أدناه مثال على ذلك:

وايت، جولي. ترجمة: الأحمد، محمد عبدالرحمن، العلي، إسماعيل صلاح والصالح، أحمد محمد. (2020). *إنجازات جامعة الملك فيصل منذ تأسيسها*. الطبعة الثانية. الرياض، السعودية: مكتبة جرير.

في حالة كون الكتاب محققاً، فيكتب بعد اسم المؤلف: "تحقيق: اسم العائلة، الاسم الأول اسم الأب". أدناه مثال على ذلك:

الخالد، محمد. تحقيق: الأحمد، محمد عبدالرحمن. (2020). *إنجازات جامعة الملك فيصل منذ تأسيسها*. الطبعة الثانية. الرياض، السعودية: مكتبة جرير.

6.2. كتابة الكتب الإنجليزية في قائمة المراجع

يبدأ كل مرجع باسم العائلة للمؤلف الأول، ثم فاصلة، ثم الحرف الأول من الاسم الأول للمؤلف الأول، ثم نقطة، ثم الحرف الأول لاسم الأب للمؤلف الأول، ثم نقطة، ثم فاصلة، ثم اسم العائلة للمؤلف الثاني، ثم فاصلة، ثم الحرف الأول من الاسم الأول للمؤلف الثاني، ثم نقطة، ثم الحرف الأول لاسم الأب للمؤلف الثاني، ثم نقطة، ثم حرف العطف "and" (وليس "&") ثم اسم العائلة للمؤلف الثالث، ثم فاصلة، ثم الحرف الأول من الاسم الأول للمؤلف الثالث، ثم نقطة، ثم الحرف الأول لاسم الأب للمؤلف الثالث، ثم نقطة، ثم فتح قوس، ثم التاريخ بالميلادي، ثم إغلاق القوس، ثم نقطة، ثم عنوان الكتاب بحروف مائلة والحرف الأول من كل كلمة يكون كبيرا (كابتل capital؛ يستثنى من ذلك أدوات التنكير والتعريف مثل "a" و "an" و "the" وحروف الجر مثل "to" و "of" و "in" وأدوات الربط "and" و "but" و "or" فيبقى الحرف الأول منها بحروف صغيرة، إلا إذا كانوا في بداية اسم المجلة فيكون الحرف الأول منها بحروف كبيرة)، ثم نقطة، ثم اسم مدينة الناشر، ثم فاصلة، ثم اسم دولة الناشر، ثم نقطتين رأسيتين، ثم اسم الناشر، ثم نقطة. أدناه مثال على ذلك:

Al Ahmed, K.A., Al Muhammed, S.F. and Al Saleh, A.F. (2020). *The History of Agriculture in Al Ahsa*. Saudi Arabia: Jarir Bookstore.

في حالة وجود رقم طبعة، فيكتب التالي:

Al Ahmed, K.A., Al Muhammed, S.F. and Al Saleh, A.F. (2020). *The History of Agriculture in Al Ahsa*. 2nd edition. Riyadh, Saudi Arabia: Jarir Bookstore.

6.3. رومنة/ترجمة الكتب غير الإنجليزية في قائمة المراجع

ملاحظة: عند رومنة/ترجمة مراجع الكتب العربية فإنه لا يكتب اسم المحقق.

يبدأ كل مرجع باسم العائلة للمؤلف الأول، ثم فاصلة، ثم الحرف الأول من الاسم الأول للمؤلف الأول، ثم نقطة، ثم الحرف الأول لاسم الأب للمؤلف الأول، ثم نقطة، ثم فاصلة، ثم اسم العائلة للمؤلف الثاني، ثم فاصلة، ثم الحرف الأول من الاسم الأول للمؤلف الثاني، ثم نقطة، ثم الحرف الأول لاسم الأب للمؤلف الثاني، ثم نقطة، ثم حرف العطف "and" (وليس "&") ثم اسم العائلة للمؤلف الثالث، ثم فاصلة، ثم الحرف الأول من الاسم الأول للمؤلف الثالث، ثم نقطة، ثم الحرف الأول لاسم الأب للمؤلف الثالث، ثم نقطة، ثم فتح قوس، ثم التاريخ بالميلادي، ثم إغلاق القوس، ثم نقطة، ثم عنوان الكتاب (مرومن) بحروف مائلة والحرف الأول من كل كلمة يكون كبيرا (كابتل capital)، ثم فتح علامة تنصيص واحدة، ثم عنوان الكتاب مترجما والحرف الأول من كل كلمة يكون كبيرا (كابتل capital؛ يستثنى من ذلك أدوات التنكير والتعريف مثل "a" و "an" و "the" وحروف الجر مثل "to" و "of" و "in" وأدوات الربط "and" و "but" و "or" فيبقى الحرف الأول منها بحروف صغيرة، إلا إذا كانوا في بداية اسم المجلة فيكون الحرف الأول منها بحروف كبيرة) والكلمة غير مائلة، ثم إغلاق علامة التنصيص، ثم نقطة، ثم اسم مدينة الناشر مترجمة، ثم فاصلة، ثم اسم دولة الناشر مترجمة، ثم نقطتين رأسيتين، ثم اسم الناشر مترجما (أو مرومن)، ثم نقطة، ثم تكتب "[in Arabic]" أدناه مثال على رومنة المرجع العربي:

Al Ahmed, M.A., Al Ali, I.S. and Al Salah, A.M. (2020). *Iinjazat Jamieat Almalik Faysal Mundh Tasisiha* 'Achievements of King Faisal University since its Foundations'. Riyadh, Saudi Arabia: Jarir Bookstore. [in Arabic]

في حالة كون الكتاب بلغة غير العربية وغير الإنجليزية، ولكن هذه اللغة تستخدم حروف غير إنجليزية، فتتم رومنة العنوان بالطريقة نفسها التي تتم بها رومنة العناوين العربية. ولكن، في حالة كون الكتاب بلغة غير العربية وغير الإنجليزية، ولكن هذه اللغة تستخدم الحروف الإنجليزية

نفسها، فلا حاجة لرومنة عنوان الكتاب، ويكتفى بإبقاء العنوان في لغته الأصل ووضع الترجمة في علامة تنصيص. فعلى سبيل المثال، في حالة كون الكتاب باللغة الألمانية، فيبدأ المرجع باسم العائلة للمؤلف الأول، ثم فاصلة، ثم الحرف الأول من الاسم الأول للمؤلف الأول، ثم نقطة، ثم الحرف الأول لاسم الأب للمؤلف الأول، ثم نقطة، ثم فاصلة، ثم اسم العائلة للمؤلف الثاني، ثم فاصلة، ثم الحرف الأول من الاسم الأول للمؤلف الثاني، ثم نقطة، ثم الحرف الأول لاسم الأب للمؤلف الثاني، ثم نقطة، ثم حرف العطف "and" (وليس "&") ثم اسم العائلة للمؤلف الثالث، ثم فاصلة، ثم الحرف الأول من الاسم الأول للمؤلف الثالث، ثم نقطة، ثم الحرف الأول لاسم الأب للمؤلف الثالث، ثم نقطة، ثم فتح قوس، ثم التاريخ بالميلادي، ثم إغلاق القوس، ثم نقطة، ثم عنوان الكتاب باللغة الألمانية بحروف مائلة والحرف الأول من كل كلمة يكون كبيرا (كابتل capital)، ثم فتح علامة تنصيص واحدة، ثم عنوان الكتاب مترجما والحرف الأول من كل كلمة يكون كبيرا (كابتل capital؛ يستثنى من ذلك أدوات التنكير والتعريف مثل "a" و "an" و "the" وحروف الجر مثل "to" و "of" و "in" وأدوات الربط "and" و "but" و "or" فيبقى الحرف الأول منها بحروف صغيرة، إلا إذا كانوا في بداية اسم المجلة فيكون الحرف الأول منها بحروف كبيرة) والكلمة غير مائلة، ثم إغلاق علامة التنصيص، ثم نقطة، ثم اسم مدينة الناشر مترجمة للإنجليزي، ثم فاصلة، ثم اسم دولة الناشر مترجمة للإنجليزي، ثم نقطتين رأسيتين، ثم اسم الناشر مترجما للإنجليزي، ثم نقطة، ثم تكتب "[in German]" أدناه مثال على رومنة المرجع الألماني:

Al Ahmed, M.A., Al Ali, I.S. and Al Salah, A.M. (2020). *Erfolge der King Faisal University seit ihrer Gründung'* Achievements of King Faisal University since its Foundations'. Riyadh, Saudi Arabia: Jarir Bookstore. [in German]

7. آلية كتابة فصل من كتاب في قائمة المراجع (يطلب عملها فقط في حالة قبول الورقة للنشر)

7.1. كتابة فصل في كتاب عربي في قائمة المراجع

يبدأ كل مرجع باسم العائلة للمؤلف الأول، ثم فاصلة، ثم الاسم الأول واسم الأب للمؤلف الأول، ثم فاصلة، ثم اسم العائلة للمؤلف الثاني، ثم فاصلة، ثم الاسم الأول واسم الأب للمؤلف الثاني، ثم حرف العطف "و" ثم اسم العائلة للمؤلف الثالث، ثم فاصلة، ثم الاسم الأول واسم الأب للمؤلف الثالث، ثم نقطة، ثم فتح قوس، ثم التاريخ، ثم إغلاق القوس، ثم نقطة، ثم عنوان الفصل، ثم نقطة، ثم يكتب "في:" ثم يكتب الاسم الأول، ثم اسم الأب، ثم اسم العائلة للمؤلف الأول، ثم فاصلة، ثم يكتب الاسم الأول، ثم اسم الأب، ثم اسم العائلة للمؤلف الثاني، ثم حرف العطف "و"، ثم يكتب الاسم الأول، ثم اسم الأب، ثم اسم العائلة للمؤلف الثالث، ثم يفتح قوس ويكتب "محررون" (أو محرر إذا كان مفردا)، ثم يغلق القوس، ثم اسم الكتاب بخط مائل، ثم نقطة، ثم اسم مدينة الناشر، ثم فاصلة، ثم اسم دولة الناشر، ثم نقطتين رأسيتين، ثم اسم الناشر. (مع مراعاة أن حرف العطف "و" يوضع دائما قبل المؤلف الأخير أيًّا كان عدد المؤلفين). أدناه مثال على ذلك:

الأحمد، محمد عبدالرحمن، العلي، إسماعيل صلاح والصالح، أحمد محمد. (2020). الموهبة في التعليم العالي. في: محمد الصالح، إبراهيم العبدالرحمن وصلاح الخالد (محررون) *الإبداع في العالم العربي*. الرياض، السعودية: مكتبة العبيكان.

7.2. كتابة فصل في كتاب إنجليزي في قائمة المراجع

يبدأ كل مرجع باسم العائلة للمؤلف الأول، ثم فاصلة، ثم الحرف الأول من الاسم الأول للمؤلف الأول، ثم نقطة، ثم الحرف الأول لاسم الأب للمؤلف الأول، ثم نقطة، ثم فاصلة، ثم اسم العائلة للمؤلف الثاني، ثم فاصلة، ثم الحرف الأول من الاسم الأول للمؤلف الثاني، ثم نقطة، ثم الحرف الأول لاسم الأب للمؤلف الثاني، ثم نقطة، ثم حرف العطف "and" (وليس "&") ثم اسم العائلة للمؤلف الثالث، ثم فاصلة، ثم الحرف الأول من الاسم الأول للمؤلف الثالث، ثم نقطة، ثم الحرف الأول لاسم الأب للمؤلف الثالث، ثم نقطة، ثم فتح قوس، ثم التاريخ بالميلادي، ثم إغلاق القوس، ثم نقطة، ثم عنوان الفصل، ثم نقطة، ثم اسم العائلة للمؤلف الثاني، ثم فاصلة، ثم الحرف الأول من الاسم الأول للمؤلف الثاني، ثم نقطة، ثم الحرف الأول لاسم الأب للمؤلف الثاني، ثم نقطة، ثم اسم العائلة كاملاً للمؤلف الثاني، ثم حرف العطف "and" (وليس "&")، ثم يكتب الحرف الأول من الاسم الأول للمؤلف الثالث، ثم نقطة، ثم الحرف الأول لاسم الأب للمؤلف الثالث، ثم نقطة، ثم اسم العائلة كاملاً للمؤلف الثالث، ثم يفتح قوس ويكتب "eds." (أو "ed." إذا كان مفردا)، ثم يغلق القوس، ثم اسم الكتاب بخط مائل والحرف الأول من كل كلمة يكون كبيرا (كابتل capital)، ثم فتح علامة تنصيص واحدة، ثم عنوان الكتاب مترجما والحرف الأول من كل كلمة يكون كبيرا (كابتل capital؛ يستثنى من ذلك أدوات التنكير والتعريف مثل "a" و "an" و "the" وحروف الجر مثل "to" و "of" و "in" وأدوات الربط "and" و "but" و "or" فيبقى الحرف الأول منها بحروف صغيرة، إلا إذا كانوا في بداية اسم المجلة فيكون الحرف الأول منها بحروف كبيرة)، ثم نقطة، ثم اسم مدينة الناشر، ثم فاصلة، ثم اسم دولة الناشر، ثم نقطتين رأسيتين، ثم اسم الناشر. أدناه مثال على ذلك:

Al Ahmed, K.A., Al Muhammed, S.F. and Al Saleh, A.F. (2020). Giftedness and creativity. In: A.E. Al Ibrahim, A.L. Al Salim and R.E. Al Rashid (eds.) *Creativity in the Arab World*. Riyadh, Saudi Arabia: Obeikan Bookstore.

7.3. رومنة/ترجمة فصل في كتاب غير إنجليزي في قائمة المراجع

يبدأ كل مرجع باسم العائلة للمؤلف الأول، ثم فاصلة، ثم الحرف الأول من الاسم الأول للمؤلف الأول، ثم نقطة، ثم الحرف الأول لاسم الأب للمؤلف الأول، ثم نقطة، ثم فاصلة، ثم اسم العائلة للمؤلف الثاني، ثم فاصلة، ثم الحرف الأول من الاسم الأول للمؤلف الثاني، ثم نقطة، ثم الحرف الأول لاسم الأب للمؤلف الثاني، ثم نقطة، ثم حرف العطف "and" (وليس "&") ثم اسم العائلة للمؤلف الثالث، ثم فاصلة، ثم الحرف الأول من الاسم الأول للمؤلف الثالث، ثم نقطة، ثم الحرف الأول لاسم الأب للمؤلف الثالث، ثم نقطة، ثم فتح قوس، ثم التاريخ بالميلادي، ثم إغلاق القوس، ثم نقطة، ثم عنوان الفصل (مرومن) بحروف صغيرة (صمول small)، ثم فتح علامة تنصيص واحدة، ثم عنوان الفصل مترجما بحروف صغيرة (صمول small؛ يستثنى من ذلك الكلمة الأولى وأسماء الأشخاص وأسماء الأماكن وأسماء الجنسيات واللغات والأسابيع والشهور فيبقى الحرف الأول منها بحروف كبيرة، كابتل capital)، ثم إغلاق علامة التنصيص، ثم نقطة، ثم يكتب "In:"، ثم يكتب الحرف الأول من الاسم الأول للمؤلف الأول، ثم نقطة، ثم الحرف الأول لاسم الأب للمؤلف الأول، ثم نقطة، ثم اسم العائلة كاملاً للمؤلف الأول، ، ثم فاصلة، ثم يكتب الحرف الأول من الاسم الأول للمؤلف الثاني، ثم نقطة، ثم الحرف الأول لاسم الأب للمؤلف الثاني، ثم نقطة، ثم اسم العائلة كاملاً للمؤلف الثاني، ثم حرف العطف "and" (وليس "&")، ثم يكتب الحرف الأول من الاسم الأول للمؤلف الثالث، ثم نقطة، ثم الحرف الأول لاسم الأب للمؤلف الثالث، ثم نقطة، ثم اسم العائلة كاملاً للمؤلف الثالث، ثم يفتح قوس ويكتب "eds." (أو "ed." إذا كان مفردا)، ثم يغلق القوس، ثم اسم الكتاب (مرومن) بخط مائل والحرف الأول من كل كلمة يكون كبيرا (كابتل capital)، ثم فتح علامة تنصيص واحدة، ثم عنوان الكتاب مترجما والحرف الأول من كل كلمة يكون كبيرا (كابتل capital؛ يستثنى من ذلك أدوات التنكير والتعريف مثل "a" و "an" و "the" وحروف الجر مثل "to" و "of" و "in" وأدوات الربط "and" و "but" و "or" فيبقى الحرف الأول منها بحروف صغيرة، إلا إذا كانوا في بداية اسم المجلة فيكون الحرف الأول منها بحروف كبيرة)، ثم نقطة، ثم اسم مدينة الناشر مترجمة، ثم فاصلة، ثم اسم دولة الناشر مترجما، ثم نقطتين رأسيتين، ثم اسم الناشر مترجما (أو مرومن)، ثم نقطة، ثم تكتب "[in Arabic]" أدناه مثال على رومنة المرجع العربي:

Al Ahmed, K.A., Al Muhammed, S.F. and Al Saleh, A.F. (2020). Al'iibdae fi altaelim aleali 'Creativity in higher education'. In: M. Al Saleh, I. Al

Abdulrahman and S. Al Khalid (eds.) *Al'iibdae Fi Alealam Alearabii'* Creativity in the Arab World'. Riyadh, Saudi Arabia: Obeikan Bookstore. [in Arabic]

في حالة كون الفصل بلغة غير العربية وغير الإنجليزية، ولكن هذه اللغة تستخدم حروف غير إنجليزية، فتتم رومنة العنوان بالطريقة نفسها التي تتم بها رومنة العناوين العربية. ولكن، في حالة كون الفصل بلغة غير العربية وغير الإنجليزية، ولكن هذه اللغة تستخدم الحروف الإنجليزية نفسها، فلا حاجة لرومنة عنوان الفصل والكتاب، ويكتفى بإبقاء العنوان في لغته الأصل ووضع الترجمة في علامة تنصيص. فعلى سبيل المثال، في حالة كون الفصل باللغة الألمانية، فيبدأ المرجع باسم العائلة للمؤلف الأول، ثم فاصلة، ثم الحرف الأول من الاسم الأول للمؤلف الأول، ثم نقطة، ثم الحرف الأول لاسم الأب للمؤلف الأول، ثم نقطة، ثم فاصلة، ثم اسم العائلة للمؤلف الثاني، ثم فاصلة، ثم الحرف الأول من الاسم الأول للمؤلف الثاني، ثم نقطة، ثم الحرف الأول لاسم الأب للمؤلف الثاني، ثم نقطة، ثم حرف العطف "and" (وليس "&") ثم اسم العائلة للمؤلف الثالث، ثم فاصلة، ثم الحرف الأول من الاسم الأول للمؤلف الثالث، ثم نقطة، ثم الحرف الأول لاسم الأب للمؤلف الثالث، ثم نقطة، ثم فتح قوس، ثم التاريخ بالميلادي، ثم إغلاق القوس، ثم نقطة، ثم فتح علامة تنصيص واحدة، ثم عنوان الفصل مترجما للإنجليزية بحروف صغيرة (صمول small؛ يستثنى من ذلك الكلمة الأولى وأسماء الأشخاص وأسماء الأماكن وأسماء الجنسيات واللغات والأسابيع والشهور فيبقى الحرف الأول منها بحروف كبيرة، كابتل capital)، ثم إغلاق علامة التنصيص، ثم نقطة، ثم يكتب "In:"، ثم يكتب الحرف الأول من الاسم الأول للمؤلف الأول، ثم نقطة، ثم الحرف الأول لاسم الأب للمؤلف الأول، ثم نقطة، ثم اسم العائلة كاملاً للمؤلف الأول، ، ثم فاصلة، ثم يكتب الحرف الأول من الاسم الأول للمؤلف الثاني، ثم نقطة، ثم الحرف الأول لاسم الأب للمؤلف الثاني، ثم نقطة، ثم اسم العائلة كاملاً للمؤلف الثاني، ثم حرف العطف "and" (وليس "&")، ثم يكتب الحرف الأول من الاسم الأول للمؤلف الثالث، ثم نقطة، ثم الحرف الأول لاسم الأب للمؤلف الثالث، ثم نقطة، ثم اسم العائلة كاملاً للمؤلف الثالث، ثم يفتح قوس ويكتب "eds." (أو "ed." إذا كان مفردا)، ثم يغلق القوس، ثم اسم الكتاب باللغة الألمانية بخط مائل والحرف الأول من كل كلمة يكون كبيرا (كابتل capital)، ثم فتح علامة تنصيص واحدة، ثم عنوان الكتاب مترجما للإنجليزية والحرف الأول من كل كلمة يكون كبيرا (كابتل capital؛ يستثنى من ذلك أدوات التنكير والتعريف مثل "a" و "an" و "the" وحروف الجر مثل "to" و "of" و "in" وأدوات الربط "and" و "but" و "or" فيبقى الحرف الأول منها بحروف صغيرة، إلا إذا كانوا في بداية اسم المجلة فيكون الحرف الأول منها بحروف كبيرة)، ثم فتح قوس، ثم اسم مدينة الناشر مترجمة للإنجليزية، ثم فاصلة، ثم اسم دولة الناشر مترجما للإنجليزية، ثم نقطتين رأسيتين، ثم اسم الناشر مترجما للإنجليزية، ثم نقطة، ثم تكتب "[in German]" أدناه مثال على رومنة المرجع الألماني:

Al Ahmed, K.A., Al Muhammed, S.F. and Al Saleh, A.F. (2020). Kreativität in der hochschulbildung 'Creativity in higher education'. In: M. Al Saleh, I. Al Abdulrahman and S. Al Khalid (eds.) *Kreativität in der Arabischen Welt* 'Creativity in the Arab World'. Riyadh, Saudi Arabia: Obeikan Bookstore. [in German]

8. آلية كتابة رسائل الماجستير والدكتوراه في قائمة المراجع (يطلب عملها فقط في حالة قبول الورقة للنشر)

8.1. كتابة رسائل الماجستير والدكتوراه العربية في قائمة المراجع

يبدأ كل مرجع باسم العائلة للمؤلف، ثم فاصلة، ثم الاسم الأول واسم الأب للمؤلف، ثم نقطة، ثم فتح قوس، ثم التاريخ، ثم إغلاق القوس، ثم نقطة، ثم عنوان الرسالة بخط مائل، ثم نقطة، ثم يكتب "رسالة ماجستير" أو "رسالة دكتوراه"، ثم فاصلة، ثم اسم الجامعة، ثم فاصلة، ثم اسم المدينة، ثم فاصلة، ثم اسم الدولة، ثم نقطة. أدناه مثال على ذلك:

الأحمد، محمد عبدالرحمن. (2020). *تأملات في الإبداع*. رسالة دكتوراه، جامعة الملك فيصل، الأحساء، السعودية.

8.2. كتابة رسائل الماجستير والدكتوراه الإنجليزية في قائمة المراجع

يبدأ كل مرجع باسم العائلة للمؤلف، ثم فاصلة، ثم الحرف الأول من الاسم الأول للمؤلف، ثم نقطة، ثم الحرف الأول لاسم الأب للمؤلف، ثم نقطة، ثم فتح قوس، ثم التاريخ بالميلادي، ثم إغلاق القوس، ثم نقطة، ثم عنوان الرسالة بحروف مائلة والحرف الأول من كل كلمة يكون كبيرا (كابتل capital؛ يستثنى من ذلك أدوات التنكير والتعريف مثل "a" و "an" و "the" وحروف الجر مثل "to" و "of" و "in" وأدوات الربط "and" و "but" و "or" فيبقى الحرف الأول منها بحروف صغيرة، إلا إذا كانوا في بداية اسم المجلة فيكون الحرف الأول منها بحروف كبيرة)، ثم نقطة، ثم يكتب " Master's Dissertation" إذا كانت رسالة ماجستير أو "PhD Thesis" إذا كانت رسالة دكتوراه، ثم فاصلة، ثم اسم الجامعة، ثم فاصلة، ثم اسم المدينة، ثم فاصلة، ثم اسم الدولة، ثم نقطة. أدناه مثال على ذلك:

Al Ahmed, K.A. (2020). *The History of Agriculture in Al Ahsa*. PhD Thesis, King Faisal University, Al Ahsa, Saudi Arabia.

8.3. رومنة/ترجمة رسائل الماجستير والدكتوراه غير الإنجليزية في قائمة المراجع

يبدأ كل مرجع باسم العائلة للمؤلف الأول، ثم فاصلة، ثم الحرف الأول من الاسم الأول للمؤلف الأول، ثم نقطة، ثم الحرف الأول لاسم الأب للمؤلف الأول، ثم نقطة، ثم فتح قوس، ثم التاريخ بالميلادي، ثم إغلاق القوس، ثم نقطة، ثم عنوان الرسالة (مرومن) بحروف مائلة والحرف الأول من كل كلمة يكون كبيرا (كابتل capital)، ثم فتح علامة تنصيص واحدة، ثم عنوان الرسالة مترجما والحرف الأول من كل كلمة يكون كبيرا (كابتل capital؛ يستثنى من ذلك أدوات التنكير والتعريف مثل "a" و "an" و "the" وحروف الجر مثل "to" و "of" و "in" وأدوات الربط "and" و "but" و "or" فيبقى الحرف الأول منها بحروف صغيرة، إلا إذا كانوا في بداية اسم المجلة فيكون الحرف الأول منها بحروف كبيرة) والكلمة غير مائلة، ثم إغلاق علامة التنصيص، ثم نقطة، ثم يكتب "Master's Dissertation" إذا كانت رسالة ماجستير أو "PhD Thesis" إذا كانت رسالة دكتوراه، ثم فاصلة، ثم اسم الجامعة، ثم فاصلة، ثم اسم المدينة، ثم فاصلة، ثم اسم الدولة، ثم نقطة، ثم تكتب "[in Arabic]" أدناه مثال على رومنة المرجع العربي:

Al Ahmed, M.A. (2020). *Tamalat Fi Al'iibdae* 'Reflections on Creativity'. PhD Thesis, King Faisal University, Al Ahsa, Saudi Arabia. [in Arabic]

في حالة كون الرسالة بلغة غير العربية وغير الإنجليزية، ولكن هذه اللغة تستخدم حروف غير إنجليزية، فتتم رومنة العنوان بالطريقة نفسها التي تتم بها رومنة العناوين العربية. ولكن، في حالة كون الرسالة بلغة غير العربية وغير الإنجليزية، ولكن هذه اللغة تستخدم الحروف الإنجليزية نفسها، فلا حاجة لرومنة عنوان الرسالة، ويكتفى بإبقاء العنوان في لغته الأصل ووضع الترجمة في علامة تنصيص. فعلى سبيل المثال، في حالة كون الرسالة باللغة الألمانية، فيبدأ المرجع باسم العائلة للمؤلف الأول، ثم فاصلة، ثم الحرف الأول من الاسم الأول للمؤلف الأول، ثم نقطة، ثم الحرف الأول لاسم الأب للمؤلف الأول، ثم نقطة، ثم فتح قوس، ثم التاريخ بالميلادي، ثم إغلاق القوس، ثم نقطة، ثم عنوان الرسالة باللغة الألمانية بحروف مائلة والحرف الأول من كل كلمة يكون كبيرا (كابتل capital)، ثم فتح علامة تنصيص واحدة، ثم عنوان الرسالة مترجما والحرف الأول من كل كلمة يكون كبيرا (كابتل capital؛ يستثنى من ذلك أدوات التنكير والتعريف مثل "a" و "an" و "the" وحروف الجر مثل "to" و "of" و "in" وأدوات الربط "and" و "but" و "or" فيبقى الحرف الأول منها بحروف صغيرة، إلا إذا كانوا في بداية اسم المجلة فيكون الحرف الأول منها بحروف كبيرة) والكلمة غير مائلة، ثم إغلاق علامة التنصيص، ثم نقطة، ثم يكتب "Master's Dissertation" إذا كانت رسالة ماجستير أو "PhD Thesis" إذا كانت رسالة دكتوراه، ثم فاصلة، ثم اسم الجامعة بالإنجليزي، ثم فاصلة، ثم اسم المدينة بالإنجليزي، ثم فاصلة، ثم اسم الدولة بالإنجليزي، ثم نقطة،

ثم تكتب "[in German]" أدناه مثال على ذلك:

Al Ahmed, M.A. (2020). *Überlegungen zur Kreativität* 'Reflections on Creativity'. PhD Thesis, King Faisal University, Al Ahsa, Saudi Arabia. [in German]

9. آلية كتابة موقع إلكتروني في قائمة المراجع (يطلب عملها فقط في حالة قبول الورقة للنشر)

ملاحظة: المراجع المأخوذة من شبكة المعلومات يلزم فيها كتابة العنوان التفصيلي الذي يفتح الصفحة الخاصة بالمرجع مباشرة وليست الصفحة العامة للموقع. يجب ألا يزيد عدد حروف الرابط عن 120 حرف.

9.1. كتابة موقع إلكتروني عربي في قائمة المراجع

يبدأ كل مرجع باسم العائلة للمؤلف الأول، ثم فاصلة، ثم الاسم الأول واسم الأب للمؤلف الأول، ثم فاصلة، ثم اسم العائلة للمؤلف الثاني، ثم فاصلة، ثم الاسم الأول واسم الأب للمؤلف الثاني، ثم حرف العطف "و" ثم اسم العائلة للمؤلف الثالث، ثم فاصلة، ثم الاسم الأول واسم الأب للمؤلف الثالث، ثم نقطة، ثم فتح قوس، ثم التاريخ، ثم إغلاق القوس، ثم نقطة، ثم العنوان بخط مائل، ثم نقطة، ثم يكتب "متوفر بموقع:" ثم يدرج الرابط، وبعد الرابط يفتح قوس ويكتب "تاريخ الاسترجاع:" ثم يدرج التاريخ على هذه الصيغة "2020/07/27"، ثم يغلق القوس. (مع مراعاة أن حرف العطف "و" يوضع دائما قبل المؤلف الأخير أيًا كان عدد المؤلفين). أدناه مثال على ذلك:

الأحمد، محمد عبدالرحمن، العلي، إسماعيل صلاح والصالح، أحمد محمد. (2020). *إنجازات جامعة الملك فيصل منذ تأسيسها*. متوفر بموقع: https://www.kfu.edu.sa/ar/Departments/Sjournal/Pages/home.aspx (تاريخ الاسترجاع: 2020/07/27)

9.2. كتابة موقع إلكتروني إنجليزي في قائمة المراجع

يبدأ كل مرجع باسم العائلة للمؤلف الأول، ثم فاصلة، ثم الحرف الأول من الاسم الأول للمؤلف الأول، ثم نقطة، ثم الحرف الأول لاسم الأب للمؤلف الأول، ثم نقطة، ثم فاصلة، ثم اسم العائلة للمؤلف الثاني، ثم فاصلة، ثم الحرف الأول من الاسم الأول للمؤلف الثاني، ثم نقطة، ثم الحرف الأول لاسم الأب للمؤلف الثاني، ثم نقطة، ثم حرف العطف "and" (وليس "&") ثم اسم العائلة للمؤلف الثالث، ثم فاصلة، ثم الحرف الأول من الاسم الأول للمؤلف الثالث، ثم نقطة، ثم الحرف الأول لاسم الأب للمؤلف الثالث، ثم نقطة، ثم فتح قوس، ثم التاريخ بالميلادي، ثم إغلاق القوس، ثم نقطة، ثم العنوان بحروف مائلة والحرف الأول من كل كلمة يكون كبيرا (كابتل capital؛ يستثنى من ذلك أدوات التنكير والتعريف مثل "a" و "an" و "the" وحروف الجر مثل "to" و "of" و "in" وأدوات الربط "and" و "but" و "or" فيبقى الحرف الأول منها بحروف صغيرة، إلا إذا كانوا في بداية اسم المجلة فيكون الحرف الأول منها بحروف كبيرة) والكلمة غير مائلة، ثم إغلاق علامة التنصيص، ثم نقطة، ثم يكتب "Available at:" ثم يدرج الرابط، وبعد الرابط يفتح قوس ويكتب "accessed on" ثم يدرج التاريخ على هذه الصيغة "2020/07/27"، ثم يغلق القوس. أدناه مثال على ذلك:

Al Ahmed, K.A., Al Muhammed, S.F. and Al Saleh, A.F. (2020). *The History of Agriculture in Al Ahsa*. Available at: https://www.kfu.edu.sa/ar/Departments/Sjournal/Pages/home.aspx (accessed on 10/12/2020)

9.3. رومنة/ترجمة موقع إلكتروني غير إنجليزي في قائمة المراجع

يبدأ كل مرجع باسم العائلة للمؤلف الأول، ثم فاصلة، ثم الحرف الأول من الاسم الأول للمؤلف الأول، ثم نقطة، ثم الحرف الأول لاسم الأب للمؤلف الأول، ثم نقطة، ثم فاصلة، ثم اسم العائلة للمؤلف الثاني، ثم فاصلة، ثم الحرف الأول من الاسم الأول للمؤلف الثاني، ثم نقطة، ثم الحرف الأول لاسم الأب للمؤلف الثاني، ثم نقطة، ثم حرف العطف "and" (وليس "&") ثم اسم العائلة للمؤلف الثالث، ثم فاصلة، ثم الحرف الأول من الاسم الأول للمؤلف الثالث، ثم نقطة، ثم الحرف الأول لاسم الأب للمؤلف الثالث، ثم نقطة، ثم فتح قوس، ثم التاريخ بالميلادي، ثم إغلاق القوس، ثم نقطة، ثم العنوان (مرومن) بحروف مائلة والحرف الأول من كل كلمة يكون كبيرا (كابتل capital)، ثم فتح علامة تنصيص واحدة، ثم العنوان مترجما والحرف الأول من كل كلمة يكون كبيرا (كابتل capital؛ يستثنى من ذلك أدوات التنكير والتعريف مثل "a" و "an" و "the" وحروف الجر مثل "to" و "of" و "in" وأدوات الربط "and" و "but" و "or" فيبقى الحرف الأول منها بحروف صغيرة، إلا إذا كانوا في بداية اسم المجلة فيكون الحرف الأول منها بحروف كبيرة) والكلمة غير مائلة، ثم إغلاق علامة التنصيص، ثم نقطة، ثم يكتب "Available at:" ثم يدرج الرابط، وبعد الرابط يفتح قوس ويكتب "accessed on" ثم يدرج التاريخ على هذه الصيغة "2020/07/27"، ثم يغلق القوس، ثم تكتب "[in Arabic]". أدناه مثال على رومنة المرجع العربي:

Al Ahmed, M.A., Al Ali, I.S. and Al Salah, A.M. (2020). *Iinjazat Jamieat Almalik Faysal Mundh Tasisiha* 'Achievements of King Faisal University since its Foundations'. Available at: https://www.kfu.edu.sa/ar/Departments/Sjournal/Pages/home.aspx (accessed on 10/12/2020) [in Arabic]

في حالة كون الموقع بلغة غير العربية وغير الإنجليزية، ولكن هذه اللغة تستخدم حروف غير إنجليزية، فتتم رومنة العنوان بالطريقة نفسها التي تتم بها رومنة العناوين العربية. ولكن، في حالة كون الموقع بلغة غير العربية وغير الإنجليزية، ولكن هذه اللغة تستخدم الحروف الإنجليزية نفسها، فلا حاجة لرومنة عنوان الموقع، ويكتفى بإبقاء العنوان في لغته الأصل ووضع الترجمة في علامة تنصيص. فعلى سبيل المثال، في حالة كون الموقع باللغة الألمانية، فيبدأ المرجع باسم العائلة للمؤلف الأول، ثم فاصلة، ثم الحرف الأول من الاسم الأول للمؤلف الأول، ثم نقطة، ثم الحرف الأول لاسم الأب للمؤلف الأول، ثم نقطة، ثم فاصلة، ثم اسم العائلة للمؤلف الثاني، ثم فاصلة، ثم الحرف الأول من الاسم الأول للمؤلف الثاني، ثم نقطة، ثم الحرف الأول لاسم الأب للمؤلف الثاني، ثم نقطة، ثم حرف العطف "and" (وليس "&") ثم اسم العائلة للمؤلف الثالث، ثم فاصلة، ثم الحرف الأول من الاسم الأول للمؤلف الثالث، ثم نقطة، ثم الحرف الأول لاسم الأب للمؤلف الثالث، ثم نقطة، ثم فتح قوس، ثم التاريخ بالميلادي، ثم إغلاق القوس، ثم نقطة، ثم العنوان باللغة الألمانية بحروف مائلة والحرف الأول من كل كلمة يكون كبيرا (كابتل capital)، ثم فتح علامة تنصيص واحدة، ثم العنوان مترجما للإنجليزية والحرف الأول من كل كلمة يكون كبيرا (كابتل capital؛ يستثنى من ذلك أدوات التنكير والتعريف مثل "a" و "an" و "the" وحروف الجر مثل "to" و "of" و "in" وأدوات الربط "and" و "but" و "or" فيبقى الحرف الأول منها بحروف صغيرة، إلا إذا كانوا في بداية اسم المجلة فيكون الحرف الأول منها بحروف كبيرة) والكلمة غير مائلة، ثم إغلاق علامة التنصيص، ثم نقطة، ثم يكتب "Available at:" ثم يدرج الرابط، وبعد الرابط يفتح قوس ويكتب "accessed on" ثم يدرج التاريخ على هذه الصيغة "2020/07/27"، ثم يغلق القوس، ثم تكتب "[in German]". أدناه مثال على ذلك:

Al Ahmed, M.A., Al Ali, I.S. and Al Salah, A.M. (2020). *Erfolge der King Faisal University seit ihrer Gründung* 'Achievements of King Faisal University since its Foundations'. Available at: https://www.kfu.edu.sa/ar/Departments/Sjournal/Pages/home.aspx (accessed on 10/12/2020) [in German]